Design and Synthesis of a 3-D Fragment Library

Thomas Downes

Doctor of Philosophy

University of York

Chemistry

October 2019

Abstract

This thesis describes the design and synthesis of a library of novel 3-D fragments for use in drug discovery. Chapter 1 explains the process of fragment based drug discovery in detail, as well as why the synthesis of novel 3-D fragments is needed and the previous work carried out in the group to design and select 33 initial 3-D fragments. These fragments were designed to fit industry-recommended guidelines on physicochemical properties and their 3-D shape was analysed using principal moments of inertia (PMI) plots to demonstrate that they occupied under-explored areas of 3-D space. Chapter 2 describes synthetic efforts towards four of these fragments, **A**-**D**. Fragments **A** and **B** were successfully synthesised using a 1,3-dipolar cycloaddition with an alkyne followed by hydrogenation to introduce the desired stereochemistry. Fragments **C** and **D** could only be synthesised as a mixture of diastereomers. However, while exploring a new approach to synthesise fragment **D**, four analogues, fragments **E**-**H** were prepared.

Chapter 3 details a new approach that was devised in order to synthesise 3-D fragments that contained greater functional group variation. This route focussed on the triflation, Suzuki-Miyaura cross-coupling, hydrogenation and derivatisation of β-ketoesters to give 3-D fragments. Using this route, 24 novel 3-D fragments were synthesised.

Finally, Chapter 4 contains an analysis of both the physicochemical properties and the 3-D shapes of the 1st and 2nd generation 3-D fragments. These properties are compared to both industry-recommended guidelines and commercially available fragment libraries.

Acknowledgements

I would first like to thank Professor Peter O'Brien for his help and support over the last four years. His guidance and patience have made this thesis possible and I will be forever grateful. I would also like to thank all the people who collaborated on this project. These include Professor Rod Hubbard and our industrial partners, whose contributions to this project have been invaluable, and Mary Wheldon, Paul Bond and Masakazu Atobe, who got this project off the ground and helped train me.

I would also like to thank all the members of POB group, past and present, for keeping me (almost) sane during my PhD with their excellent company. Particular thanks must go to Paul and James, who have helped shape this project and push it forward. I could not have asked for two better partners in crime.

This thesis has been a long road, and I owe a great debt of gratitutde to all of those who helped support me along the way. Particularly in the last year of my PhD thanks go to Niall, Rhod, Theo and all the other friends who did their best to keep me on track. Thanks also must go to Nick for getting me back on that track.

Finally, the biggest thanks must go to my family, who have been unfailingly supportive in all my endeavours, and to Elena, who has been my rock for as long as I have known her. Getting to this point has taken a lot of patience and support and I cannot thank you enough.

Declaration of Authorship

I declare that this thesis is a presentation of original work and I am the sole author. This work has not previously been presented for an award at this, or any other, University. All sources are acknowledged as References.

Contents

List of Tables

Abbreviations and Conventions

aq	Aqueous		ESI	Electrospray Ionization
Ar	Aryl		Et	Ethyl
ATR	Attenuated total reflectance		EtOAc	Ethyl Acetate
Boc	*tert*-Butyloxycarbonyl		FBDD	Fragment based drug discovery
br	Broad		h	Hour(s)
Bu	Butyl		HMQC	Heteronuclear Multiple-Quantum Coherence
cat.	Catalytic			
Cbz	Carboxybenzyl		HRMS	High Resolution Mass Spectrometry
cm^{-1}	Wavelength (in IR)		HTS	High Throughput Screening
d	Doublet (in NMR)			
δ_C	^{13}C NMR chemical shift		Hz	Hertz
DBU	1,8-Diazabicyclo-[5.4.0]undec-7-ene		*i*	iso
			IR	Infrared
DPPA	Diphenylphosphorylazide		*J*	Coupling Constant
DEPT	Distortionless Enhancement by Polarisation Transfer		m	Multiplet (in NMR)
			M	Molar
δ_H	^1H NMR chemical shift		Me	Methyl
DMAP	*N,N*-dimethylaminopyridine		mg	Milligram
			MHz	Megahertz
DMSO	dimethyl sulphoxide		min	Minute(s)
eq.	equivalent(s)			

mL	Millilitre		q	quartet (in NMR)
mmol	Millimole		quint	quintet (in NMR)
mp	Melting point		R	alkyl, unless otherwise specified
MS	Mass spectrometry			
MW	Molecular weight		R_F	Retention Factor (in TLC)
m/z	mass:charge ratio		rt	room temperature
nM	Nanomolar		s	singlet (in NMR)
μl	microlitre		SMILES	Simplified molecular-input line-entry system
NMR	Nuclear Magnetic Resonance			
			t	triplet (in NMR)
NMR	Nuclear Magnetic Resonance		*t* (*tert*)	tertiary
			THF	tetrahydrofuran
NPR	Normalised PMI ratio		TLC	Thin Layer Chromatography
o-	*ortho*			
OMe	methoxy			
PAINS	Pan-assay interference compounds			
PBF	Plane of best fit			
PMI inertia	Principal moment of			
Ph	Phenyl			
ppm	parts per million			
Pr	Propyl			

CHAPTER 1: INTRODUCTION

Drug discovery is a huge and many-faceted industry, with different companies using different approaches at every stage of the process. Within the initial screening process, a variety of techniques including high throughput screening, DNA encoded libraries, and target-focussed libraries are used. All of these offer their own pros and cons and all have led to drug discovery programmes. The idea of screening smaller molecules than those used in the techniques listed above in order to start the drug discovery process with highly efficient hits started in the early 1980s,[1] but the technology required for the detection of weakly-binding molecules meant that the concept was not used practically until the late 1990s. In 1996, work by Fesik *et al*. kickstarted the field of fragment based drug discovery (FBDD). Since its inception 23 years ago, FBDD has resulted in three FDA approved drugs (Figure 1.1) and dozens of clinical candidates, proving it to be a valuable technique.
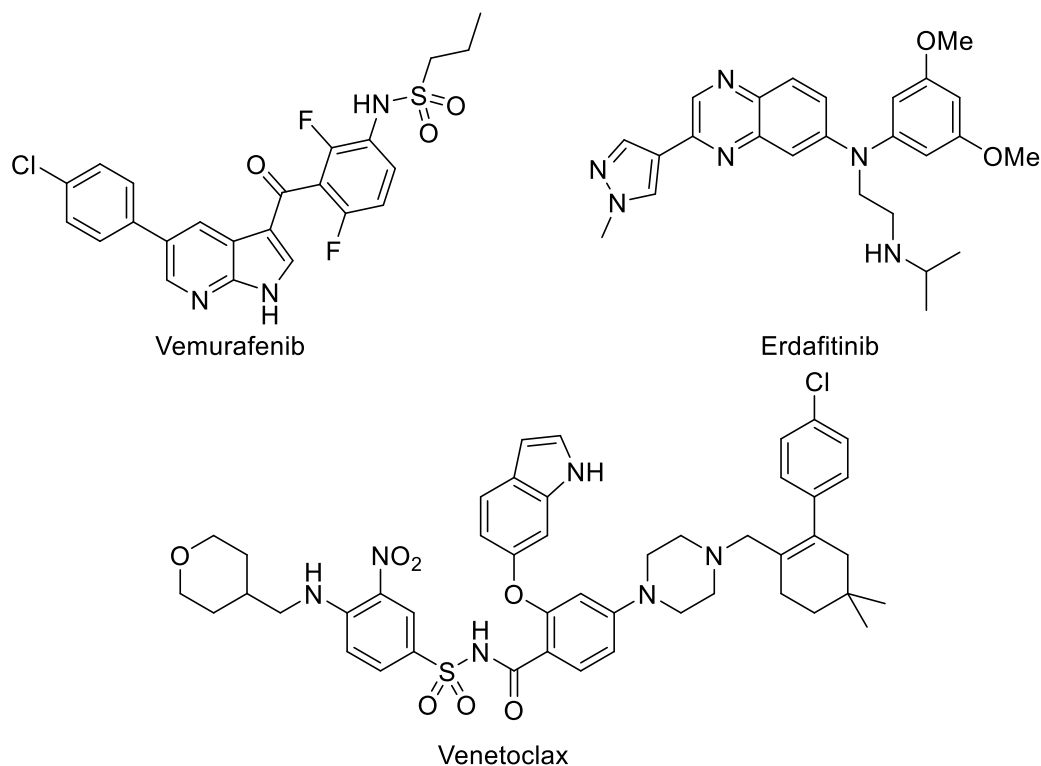
Figure 1.1: Current FDA-approved drugs derived from fragment based drug discovery

Since the publication of the landmark paper 'Escape from Flatland' in 2007, attention has turned to the synthesis of 3-D fragment libraries, the topic of this thesis. This Chapter includes an overview of FBDD (Section 1.1), explanation of methods used to quantify 3-D shape (Section 1.2), a review of recent literature on the synthesis of 3-D fragments (Section 1.3) and previous work in the group on this topic (Section 1.4) before describing the aims of this project (Section 1.5).

1.1 Fragment Based Drug Discovery

1.1.1 Overview of Fragment Based Drug Discovery

Fragment based drug discovery (FBDD) is a method of drug discovery which screens smaller molecules than other approaches in order to provide small, highly efficient starting points for drug discovery programmes. Screening smaller molecules gives a number of important advantages including greater hit rates, better sampling of chemical space and increased ligand efficiency. These advantages have allowed the field of FBDD to grow rapidly, from its first empirical use in 1996 by Fesik *et al.*[2] to providing three clinically approved drugs and numerous clinical candidates just over twenty years later.[3–5] A representation of the FBDD process is shown in Scheme 1.1, demonstrating how the reduced complexity of fragments results in increased hit rate compared to HTS compounds.
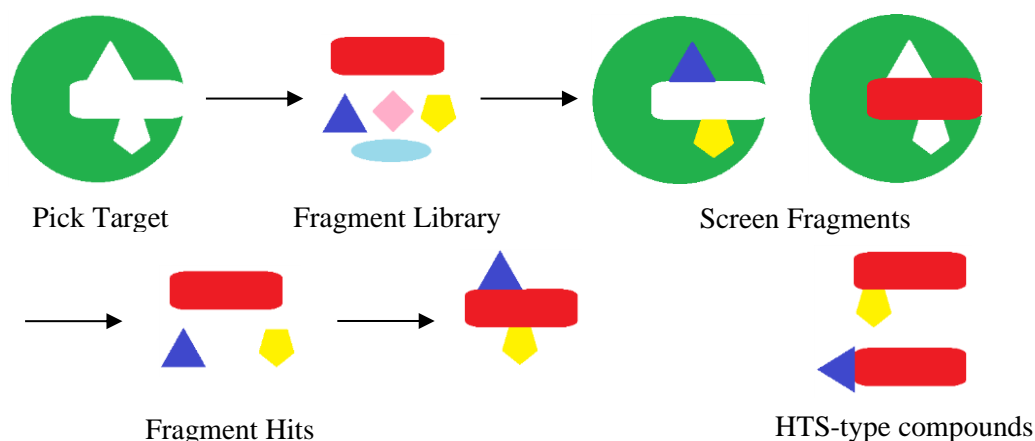

Scheme 1.1: Schematic representation of the FBDD process

Fragment libraries are relatively small, with libraries typically numbering 1,000-20,000 compounds. The small size of the library is made possible by the fact that these smaller compounds better sample chemical space. Consider Scheme 1.1, where the HTS-type compounds possess the requisite groups to bind but are unable to do so. As molecules become more complex, the chance that those groups are all correctly oriented decreases exponentially, hence the need to screen larger collections. Once the fragment hits are obtained, there are three possible strategies for developing a hit compound: growing, linking and merging. Should multiple hits be obtained in close but not identical binding locations then either merging or building a linker between two or more different fragments offers a very attractive way to increase potency quickly. Often though, this cannot be performed as multiple sites are not found, in which case fragment growing is used. The aim of all three of

these techniques is to identify a molecule that has both high enough potency and good enough physicochemical properties to function as a starting point for a full drug discovery programme.

Fragment based drug discovery is a relatively new field, with the first key theoretical contribution published in 1981 and no breakthroughs until 1996. In 1981, Jencks detailed the factors involved in the binding of small molecules and the potential for merging initial small molecule hits into larger compounds.[1] The idea of the binding of small molecules was then further explored[6,7] before the first practical results were reported in 1996 by Fesik *et al.*[2] Fesik's group describes the screening of a relatively small compound library (around 10,000 compounds) with an average molecular weight of just 213 Da. Two hits were identified that bound in close but separate locations in the target protein. Optimisation of these two fragments led to ligands **1** and **2**, with mM and μM potencies. The two ligands were then linked to give ligand **3** which displayed substantially improved affinity over its two constituent ligands (Scheme 1.2).
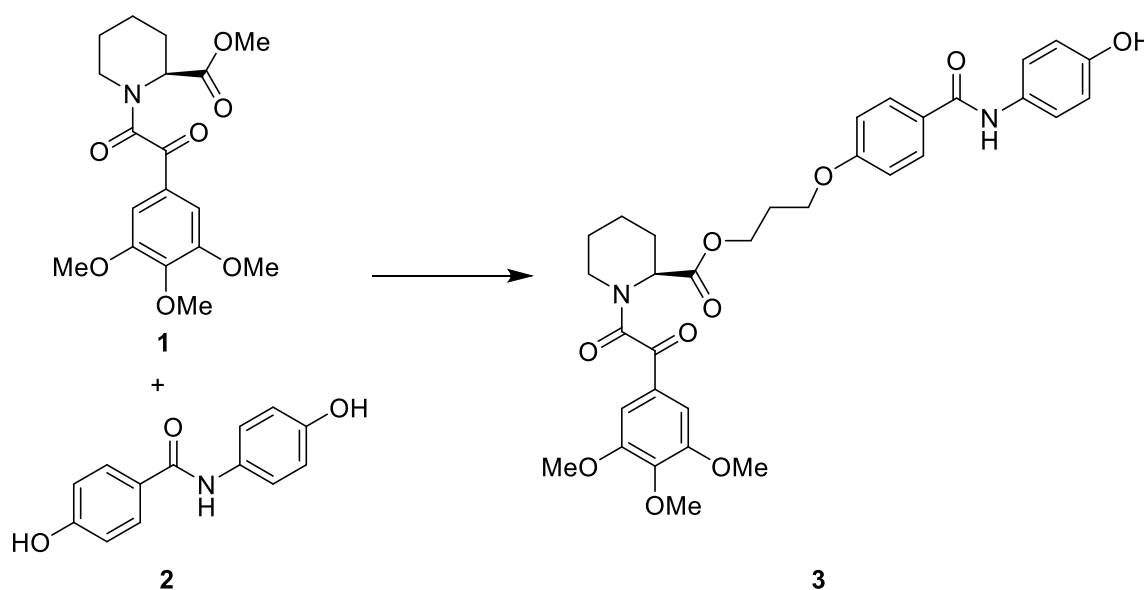
Scheme 1.2

This ability to synthesise a low nM affinity ligand for the target protein from a library of 10,000 small molecules initiated the field of FBDD. Since its inception, improvement in the sensitivity of various screening methods has made hit detection easier. Hit detection has always been a significant issue with FBDD, as such small molecules typically only bind very weakly to target proteins. However, over the past two decades, new methods have evolved for the screening of fragments and other methods, such as NMR screening techniques, have

improved to the point where FBDD is now a substantial part of the drug discovery landscape. Key advances include work from Nienaber *et al.*[8] on the use of X-ray crystallography as a screening technique as well as the development of techniques such as weak affinity chromatography (WAC),[9] surface plasmon resonance (SPR)[10] and isothermal titration calorimetry (ITC).[11]

1.1.2 Properties of Fragments

Although the concept of FBDD had been around for more than twenty years, there were initially no criteria set to define what a fragment actually was. The understanding was that fragments were smaller than lead-like compounds used in typical HTS programmes, but it took until 2003 for fragment space to be defined. Congreve *et al*. from Astex proposed a fragment 'rule of three',[12] based on Lipinski's 'rule of five' for orally-available drugs.[13] It contained five criteria: molecular weight (MW) ≤ 300, three or fewer rotatable bonds, H-bond donors and H-bond acceptors and values of cLogP ≤ 3. This rule remains popular today, in part because of its simplicity and the broadness of its criteria.

In 2015, researchers from Astex aimed to streamline the 'rule of three' into tighter guidelines based on their own successes and experience in FBDD programmes. Table 1.1 shows a comparison of the initial 'rule of three' and the more recent updated guidelines for X-ray screening. Although Astex proposed other criteria which are more difficult to quantify, such as the importance of multiple synthetically accessible vectors to allow for fragment growth, the most notable guidelines were the tight range of desired molecular weight and cLogP. These were in part due to Astex's focus on X-ray crystallography as a primary screening technique with molecules adhering to these criteria providing a greater chance of progressible hits.

Property	'Rule of Three'	Updated Guidelines
Molecular Weight (Da.)	≤ 300	140-230
Heavy Atom Count (HAC)	N/A	10-16
cLogP	≤ 3	0-2
Rotatable Bonds	≤ 3	≤ 3
H-Bond Donors	≤ 3	N/A
H-Bond Acceptors	≤ 3	N/A

Table 1.1: Fragment space guidelines

1.1.3 Fragment Based Drug Discovery *versus* High Throughput Screening

FBDD is most commonly compared to the technique from which it evolved, high throughput screening (HTS). HTS functions very similarly to FBDD but both the molecules (MW 300-500) and the libraries in HTS tend to be significantly larger. In particular, HTS focusses on lead-like compounds, which have less strict guidelines and tend to aim for properties within Lipinski's 'rule of five'.[13] The difference in size between these two classes of compounds causes some marked differences during screening, including hit rate, ease of screening, ligand efficiency and library size. A review of recent literature on FBDD programmes performed by Johnson *et al*.[14] compared the properties of fragment hits reported in 2015-2017 with the lead compounds that resulted from those hits (Figure 1.2). The differences between compounds that are considered 'lead-like' and 'fragment-like' were evident, particularly in terms of molecular weight. For the purpose of the analysis, fragments were defined as having MW ≤ 300, but they did not have to comply with other 'rule of three' criteria. The spread in cLogP values is particularly notable given that 5% of fragment hits disobeyed the 'rule of three' based on cLogP while only 60% conformed to the more stringent updated guidelines.
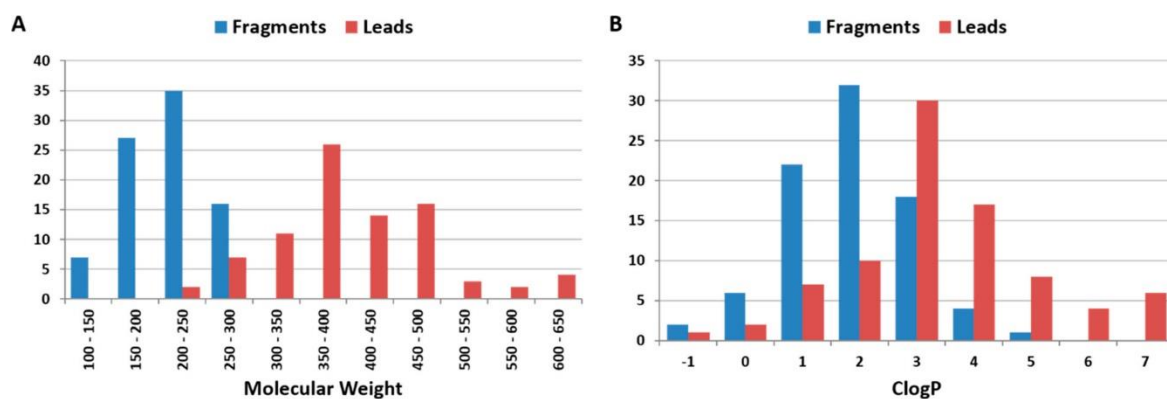

Figure 1.2: Figure from Johnson *et al*. comparing fragment hits and the resulting lead compounds[14]

The differences in potency, hit rate and ease of screening between fragments and lead-like compounds are inextricably linked. Lead-like compounds, being both larger and typically more lipophilic, usually form several key interactions with a target during a binding event. This results in strong binding with the protein, particularly when compared to a smaller molecule that may only have one or two interactions. However, the binding groups must be in a near-perfect alignment for the interactions to take place, otherwise the lead-like compound cannot bind properly and the enthalpy of one binding interaction would be

counteracted by the significant entropy loss of binding a large molecule. Furthermore, even if all the binding groups are perfectly oriented, a single group out of place elsewhere in the molecule may cause steric clashing that prevents the molecule from binding. Hit rates in HTS are therefore very low, with libraries numbering hundreds of thousands or even millions of compounds being screened in order to provide serviceable leads for drug discovery programmes. In contrast, FBDD focusses on using typically one or two binding groups in a molecule. This gives a much better chance for binding, as the groups are more likely to be correctly oriented to bind, and the small molecule means that there is much less chance of steric clashing. The size of the molecule also reduces the entropy cost on binding. However, even this lower cost can be difficult to overcome with only one or two binding interactions with the target protein. Fragments therefore tend to have a better hit rate, with 2% often the expectation, but the hits obtained are of substantially lower potency. Indeed, it was the low potency of the hits that caused FBDD to only become a viable process within the last 25 years. This has now been overcome though with the wealth of screening techniques that are now available.

Whereas HTS libraries feature hundreds of thousands of compounds, fragment libraries typically contain only a few thousand compounds. This is due to both the greater hit rate with fragments and the ability of smaller molecules to more effectively sample chemical space. Reymond has done extensive work on enumerating the number of possible molecules that contain a certain number of medicinally relevant heavy atoms (carbon, oxygen, nitrogen, and fluorine).[15,16] In work with Fink, it was shown that there are approximately 26.4 million realistic compounds consisting of 11 or fewer carbon, oxygen, nitrogen and fluorine atoms (plus hydrogen).[15] This does not take into account other medicinally relevant but less common atoms such as sulfur and chlorine. Of these 26.4 million compounds, almost exactly half (13.2 million) were 'rule of three' compliant. When this paper was published in 2007, the authors lacked the computational power to move beyond 11 heavy atoms. However, in 2015, Reymond detailed the enumeration of all possible realistic structures of molecules up to 17 heavy atoms containing carbon, nitrogen, oxygen, sulfur and the halogens. The number of possible structures was a staggering 166.4 billion. For comparison, there are only 977 million possible structures with up to 13 heavy atoms using the same parameters. Although still a huge number, and far beyond any current synthetic capabilities, this library is just 0.6% of the size of the 17 heavy atom library. Hence, a library of 10,000 lead-like compounds consisting of 17 heavy atoms would cover the same percentage of chemical space as a library of only 60 fragments. This, combined with the higher hit rate that also

allows for the synthesis and screening of fewer compounds, is part of what makes FBDD such a promising area, and also what makes it so well suited for academic collaborations.

The last key advantage that FBDD has over HTS is the versatility of fragment hits. As shown in Figure 1.3 from Churcher *et al.*,[17] molecular weight and cLogP tend to increase as a hit is developed into a viable clinical candidate. By starting with smaller, more hydrophilic compounds, there is more room during the optimisation process to improve potency without compromising lipophilicity. Increasing lipophilicity has been shown to correlate with increased chance of failure during development due to off-target effects,[18,19] meaning that starting with hit compounds that have low cLogP is very attractive to pharmaceutical companies.
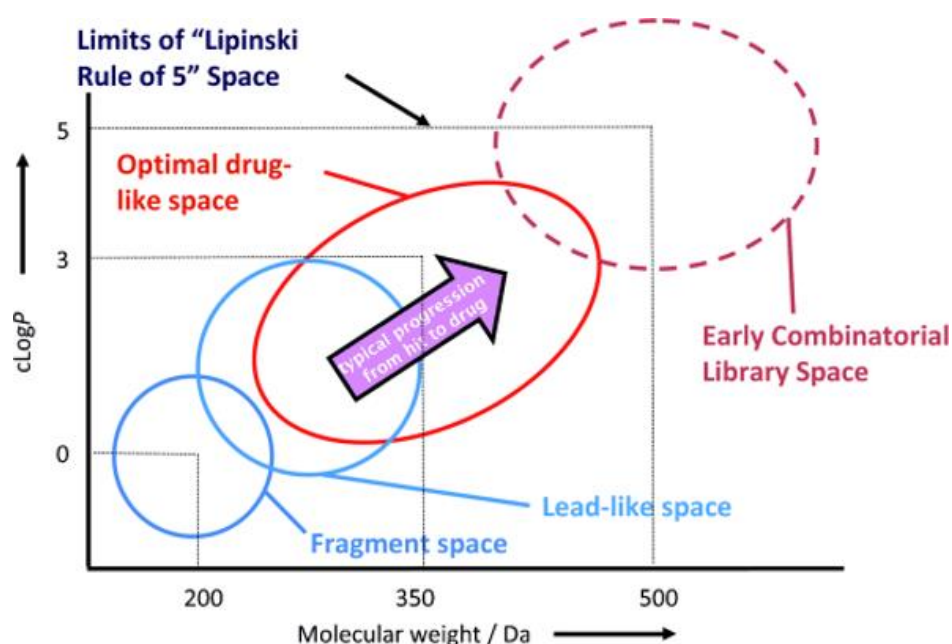

Figure 1.3: Figure from Churcher *et al*. showing the progression towards drug-like space[17]

1.1.4 Fragment Based Drug Discovery Successes

Since its inception in 1996, FBDD has resulted in over 30 clinical candidates[20] and three of these have gone on to become approved drugs: Vemurafenib, Venetoclax and Erdafitinib (see Figure 1.1).[3–5] All three are anti-cancer drugs, targeting melanoma, lymphoma and bladder cancer respectively. As is evident from the size of their structures, the approved drugs derived from FBDD have grown significantly from the fragments they were likely derived from. An abbreviated scheme showing the discovery process for Vemurafenib is shown in Scheme 1.3. The initial hit, fragment **4**, was a simple aza-indole, with early optimisation focussing on the linker and the linked phenyl ring. The additional methoxy group in the evolved fragment **5** formed a key hydrogen bonding interaction that improved

potency 100-fold as well as the selectivity. Further optimisation of the same aromatic ring lead to another 100-fold potency increase in the clinical candidate **6** before a chlorophenyl group was added to the azaindole to give the final compound, Vemurafenib. The structure of the initial fragment hit has been almost entirely preserved in the final compound in order to maintain the key binding interactions and the shape of the compound in the binding pocket.
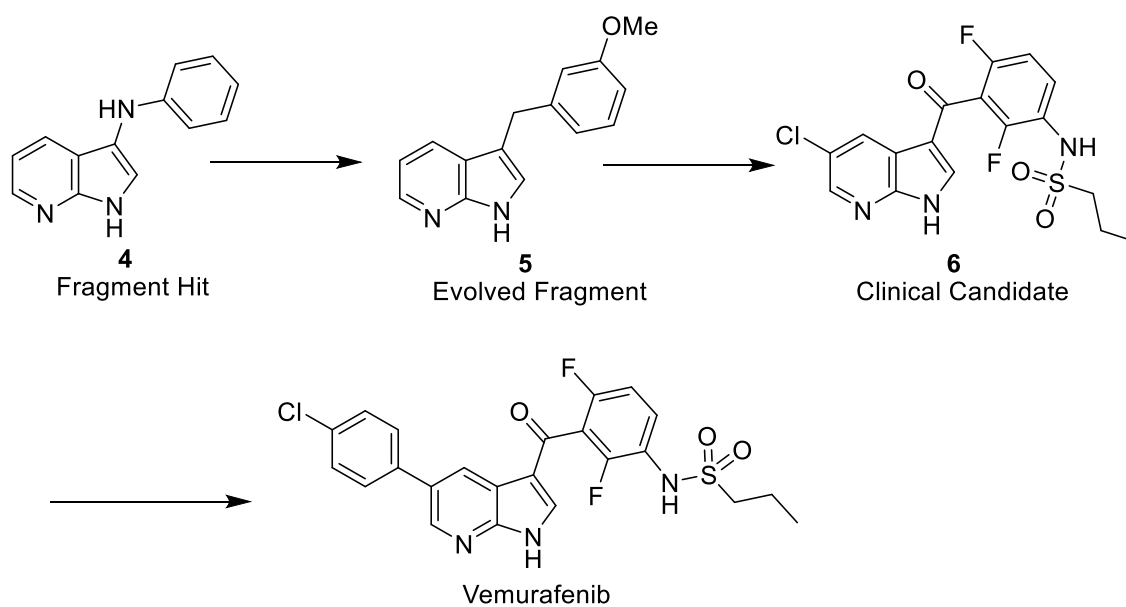
Scheme 1.3: The discovery process of Vemurafenib

1.2 Quantifying 3-D Shape

Although comparing the 3-D shape of different molecules is relatively easy to do qualitatively, it is much more difficult to do quantitatively. A number of methods have been developed in an attempt to do so, each with their own pros and cons. As such, no one method has been agreed upon universally as the best method for quantifying 3-D shape, although several are commonly used. Four of the most common techniques are described in this Section.

The simplest method is to calculate the fraction of sp^3 carbons (Fsp^3) which is the number of sp^3 hybridised carbons divided by the total number of carbons (Equation 1). This gives a number between 0 and 1. Despite being created as recently as 2009 by Lovering *et al*.,[21] Fsp^3 has already become one of the most popular methods for assessing 3-D character.

$$Fsp^3 = \frac{number\ of\ sp^3\ hybridised\ carbons}{total\ number\ of\ carbons} \qquad (1)$$

Fsp^3 has proved popular for two main reasons: its ease of calculation and its proven usefulness. Unlike other methods, Fsp^3 is quick to calculate and gives a single number value that can be easily compared to other libraries. Furthermore, in the seminal paper 'Escape from Flatland' that proposed the use of Fsp^3, Lovering *et al*. showed that increasing Fsp^3 correlated with reduced clinical attrition rate. As shown in Figure 1.4, the average Fsp^3 values increased at every stage in the process since compounds with lower Fsp^3 were more likely to fail. Drugs failing in the clinic cost pharmaceutical companies huge amounts of money every year, so finding a molecular property that correlates with clinical success was seen as a major breakthrough.
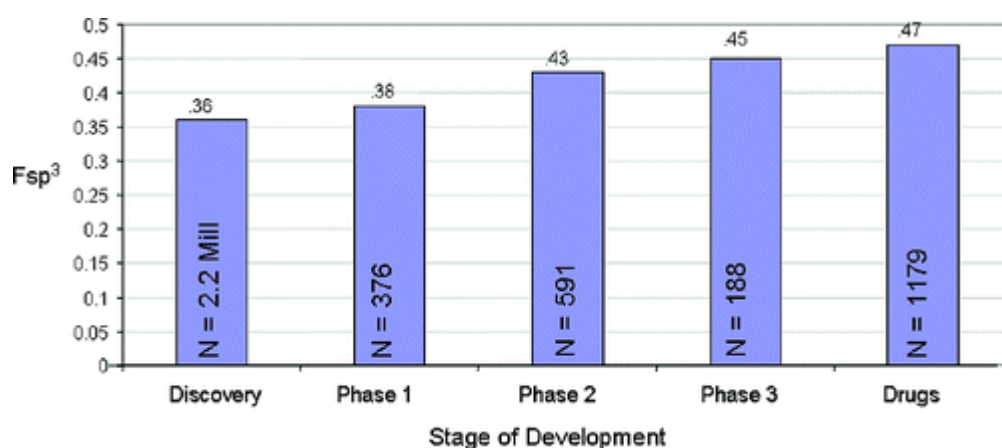

Figure 1.4: Graph showing the average Fsp^3 of molecules at each stage of the drug discovery process from Lovering *et al*.[21]

However, Fsp^3 does have some drawbacks. Chief among these is its use as a measure of 3-D shape. Although being easy to calculate is a significant advantage, Blagg *et al*. pointed

out in 2012 that two molecules with the same Fsp^3 value can have vastly different shapes. They used the example of molecules **7** and **8**, both of which have $Fsp^3 = 0$. However, whereas diazo compound **7** is flat, imide **8** shows significant 3-D character (Figure 1.5).
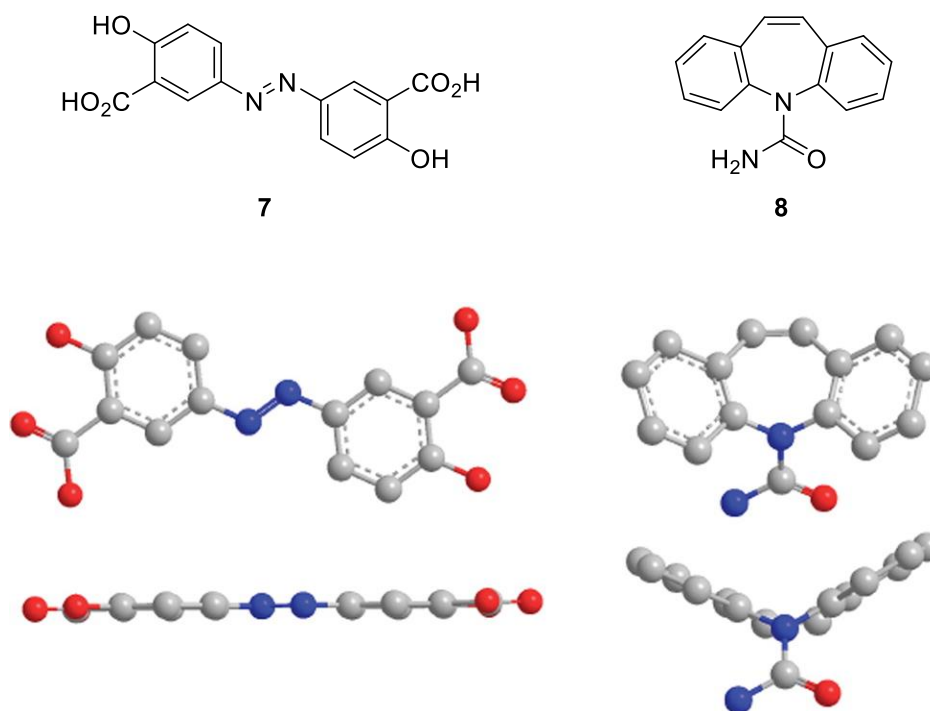

7   **8**

Figure 1.5: Demonstration of the limited correlation between Fsp^3 and 3-D shape from Blagg *et al*.[22]

Fsp^3 is therefore useful as an easy to calculate figure that gives some indication of 3-D shape and allows for rapid comparison of different libraries. It is important to note though that it only gives an indication of 3-D character – a library of compounds with an Fsp^3 value of 0.5 is highly likely to be more 3-D than one with an average Fsp^3 of 0.1.

In 1986, Meyer[23] described a number of ways to quantify 3-D shape using a concept he called 'globularity' after a term first used by Timmermans in 1954.[24] Two of these methods could be deemed as forerunners to plane of best fit (PBF) and principal moments of inertia (PMI) plots: one method measured the cross-sectional area of a molecule along a plane whereas the other compared the ratios of the moments of inertia along each axis. These will not be described here as they have been improved upon since by Blagg *et al*. (PBF)[22] and Sauer and Schwarz (PMI).[25] The third method is substantially different and compares the computationally generated surface area of a molecule with the surface area of a sphere with the same volume. First, the lowest energy conformation of a molecule is computationally generated. Then, the van der Waals radius sphere is traced around each atom to give the shape of the molecule. The surface area of this shape is then calculated to give the actual

surface area, A_{act}. Then, the ideal surface area is calculated by using the total van der Waals volume of all the atoms using Equation 2.

$$A_{vdw} = 4\pi\left(\frac{3V_{vdw}}{4\pi}\right)^{\frac{2}{3}} \approx 4.84 V_{vdw}^{\frac{2}{3}} \tag{2}$$

With the actual and the van der Waals surface area calculated, the ratio of the two is taken. Dividing the van der Waals area by the actual surface area then gives a number between 0 and 1. A value of 1 indicates that both surface areas are identical and the molecule is therefore spherical, whereas a value closer to 0 indicates a flatter molecule.

This method of calculating globularity shares some of the same benefits as Fsp^3, namely that the process gives out a single value between 0 and 1 that allows for quick and easy comparison between compounds and libraries. It is a better quantifier of 3-D shape than Fsp^3 as the data uses the conformation of the molecule. However, this process has several drawbacks. Since it focusses on surface area, atoms with large van der Waals radii cause significant distortion. In addition, a molecule with several planar sections will have the same globularity value irrespective of the orientation of those planar sections. Biphenyl **9**, for example, could have the two rings in-plane or twisted 90° to each other (Figure 1.6). These planar sections will have minimal overlap, and both conformations will have similar globularity values despite one being planar and the other not.
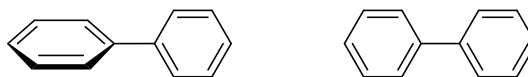
9

Figure 1.6: Conformations of biphenyl

Since its introduction in 2012, plane of best fit (PBF) has proved to be a very popular method for quantifying 3-D shape. Conceptually simple, PBF fits a 2-D plane through a 3-D molecule. The method involves initial calculation of the lowest energy conformation. The plane is then computationally optimised to ensure that it has the smallest possible deviation from the atoms of the calculated conformation (Figure 1.7). The average deviation of the heavy atoms from that plane is then given as the deviation from planarity (DFP) value.

Figure 1.7: Figure from Blagg *et al*. showing the PBF for cyclohexane and its deviations from planarity[22]

The higher the DFP value, the further a molecule is from being 2-D and thus the more 3-D it is. Although in theory the DFP value has no upper limit, in practise Blagg *et al*. showed that drug-like molecules rarely exceed a DFP value of 2 and proteins have an upper limit of around 10. PBF should therefore not be used to compare molecules of significantly different size, but this is not an issue for fragment libraries where fragments are typically capped at a MW of 300 Da. Blagg *et al*.[22] compared the PBF values for a given set of compounds with other methods of quantifying 3-D shape. They showed a clear correlation between PBF and globularity, but no correlation with Fsp^3, confirming that Fsp^3 is not a good measure of 3-D shape.

The final method for quantifying 3-D shape described here is principal moments of inertia (PMI), which is represented graphically by PMI plots. PMI focusses on the moments of inertia of a molecule along three principal axes and requires the computational calculation of the ground state conformation of a molecule. Then, the moments of inertia in the x, y and z axes are calculated. The calculated moments of inertia are then sorted in ascending order from I_1 to I_3. These three moments of inertia are then normalised using Equations 3 and 4 to give the normalised values NPR1 (normalised PMI ratio 1) and NPR2.

$$NPR1 = \frac{I_1}{I_3} \tag{3}$$

$$NPR2 = \frac{I_2}{I_3} \tag{4}$$

The NPR values are then plotted on a graph which gives a representation of their 3-D shape. Figure 1.8 shows an example PMI plot. If all three moments of inertia of a compound's conformation are equal ($I_1 = I_2 = I_3$) then the compound will have NPR values of (1,1) and it will be spherical. An example of this is as adamantane. A compound that is disc-like such as benzene will have NPR values of (0.5,0.5) and be located at the bottom of the plot. Finally, a rod-like compound such as a polyalkyne will have NPR values of (0,1) and be located at the top left corner. One of the key advantages of PMI plots is that the data are very easy to visualise. Compounds that are more spherical are closer to the top-right corner of the plot whereas flatter compounds are closer to the 'rod-disc axis', the term used for the left-hand side of the triangle. Another advantage is that PMI can be used to generate a single value for each conformation of a compound that describes its 3-D character, enabling easy comparison of compounds and libraries.
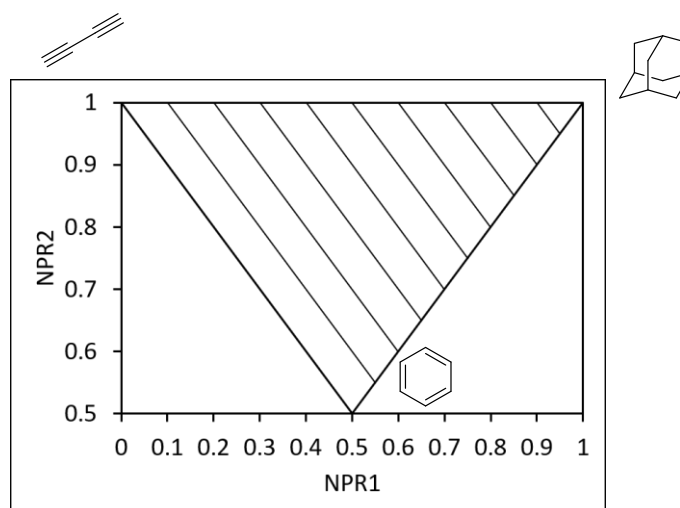
Figure 1.8: Example PMI plot with structures of 1-D, 2-D and 3-D compounds and ∑NPR values added

In order to help assess 3-D shape further, the plot can be divided into the ten sections shown in Figure 1.8. Each section is delineated by a line corresponding to a single ∑NPR value. ∑NPR, simply calculated by adding the NPR1 and NPR2 values, is a number between 1 and 2 where 1 is the rod-disc axis and 2 is spherical. These ∑NPR values are shown along the top of the PMI plot in Figure 1.8. Blagg *et al* compared PBF with PMI plots to see if the two methods correlated.[22] PBF value was plotted against ∑NPR for a library of ~4 million compounds, using ∑NPR > 1.07 and PBF > 0.6 to define a compound as being 3-D. Importantly, the two methods clearly correlated well, with increasing PBF score corresponding to increasing ∑NPR, although there were a significant number of compounds that were deemed 3-D by one method but not by the other.

Overall, Fsp^3 remains the most popular metric, but it is important to recognise that Fsp^3 does not correlate with other 3-D shape metrics and so should not be used to classify a molecule as 3-D or not.[22] Of the other three methods, PBF and PMI plots are by far the most popular and the strong correlation between the two shows that either can be used, although PMI plots provide more information by giving points on a 2-D plot rather than a single value.

**1.3 Recent Approaches to the Generation or Synthesis of 3-D Fragments**

Since Lovering *et al*. published 'Escape from Flatland' in 2009, there has been significant interest in the synthesis of 3-D fragments from both academia and industry. A number of different approaches have been taken to synthesise libraries of 3-D fragments, including:

- Diversity-oriented synthesis (DOS), in which one or two poised and versatile intermediates are transformed using a range of reactions to give a library of compounds containing a variety of different scaffolds

- Computational generation of shape-diverse libraries based on lists of commercially available compounds followed by purchasing a representative set. This is often carried out to start a library before synthesis of other fragments which are added to the library.

- Degradation of natural products to give their constituent fragments. This can either be done computationally, breaking natural products down to their constituent parts and then purchasing or synthesising these parts, or chemically, where natural products are reacted in order to obtain constituent fragments.

- Diversification of specific scaffolds to give a fragment set. Unlike DOS, where multiple scaffolds are synthesised, a popular approach is to synthesise a limited number of scaffolds featuring several synthetic handles and then to use these handles to diversify the scaffolds into a library of fragments.

- Use of a single piece of synthetic methodology in order to access a range of fragments. Here, the diversity comes from being able to use a range of substrates in a single key reaction to give good variation in the fragments formed. This can overlap with the previous method, where some variation is introduced in the key reaction then further diversification is carried out.

All of these methods have led to the successful creation of 3-D fragment libraries. In this section, examples where these methods have been employed to obtain 3-D fragments will be summarised.

1.3.1 Diversity-Oriented Synthesis

The first example where diversity-oriented synthesis (DOS) was used to create a small library of 3-D fragments was reported by Young *et al.*[26] The aim was to create a library of fragments featuring diverse scaffolds and high 3-D character as quantified by PMI plots. Previously, DOS and FBDD had been seen as two opposing methods due to the relatively large molecules that are typically produced by DOS.[27] However, in this study, DOS was used to synthesise molecules with MW ≤ 300. Using a build/couple/pair (B/C/P) approach starting with either 2,4- or 2,2-disubstituted pyrrolidines, a variety of fused bicyclic and spirocyclic fragments were synthesised. Scheme 1.4 shows one example where pyrrolidine **10** was 'built', then a group containing a terminal alkene was 'coupled' on to the pyrrolidine nitrogen to give sulfonamide **11** and finally the two alkenes were 'paired' using Grubbs metathesis. Subsequent transformations gave fragment **12**. Using this method, 35 fragments containing a variety of ring sizes were synthesised.
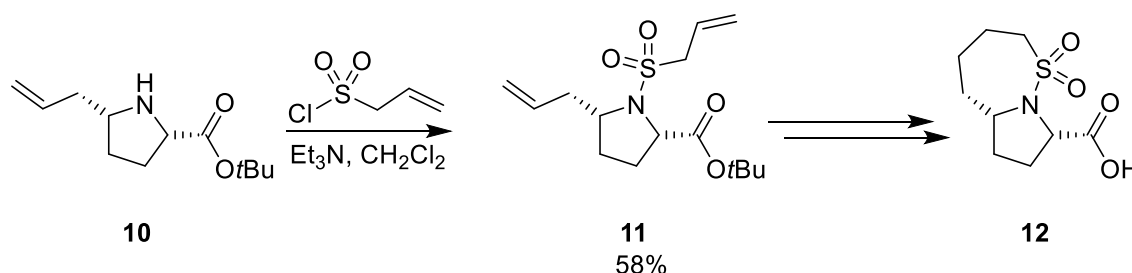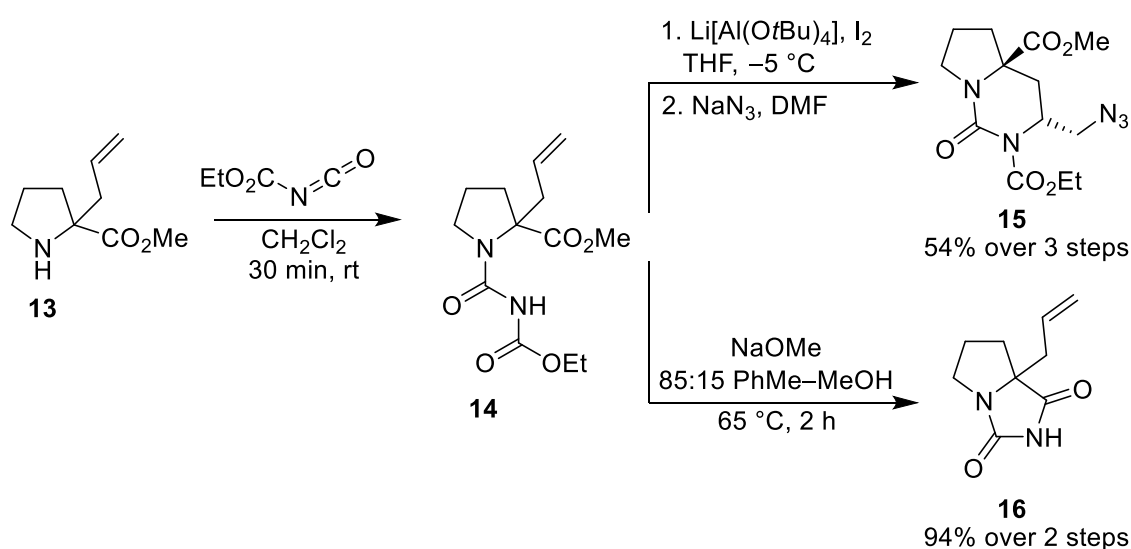

Scheme 1.4

3-D shape analysis was performed on the 35 fragments and compared to an analysis of 18,534 fragments from the ZINC database. Figure 1.9 shows the resulting PMI plot with the synthesised compounds shown in red and a selection of fragment structures shown alongside. The blue shaded area represents a ∑NPR value approximately ≤ 1.2 and 75% of the ZINC database compounds are in this region.
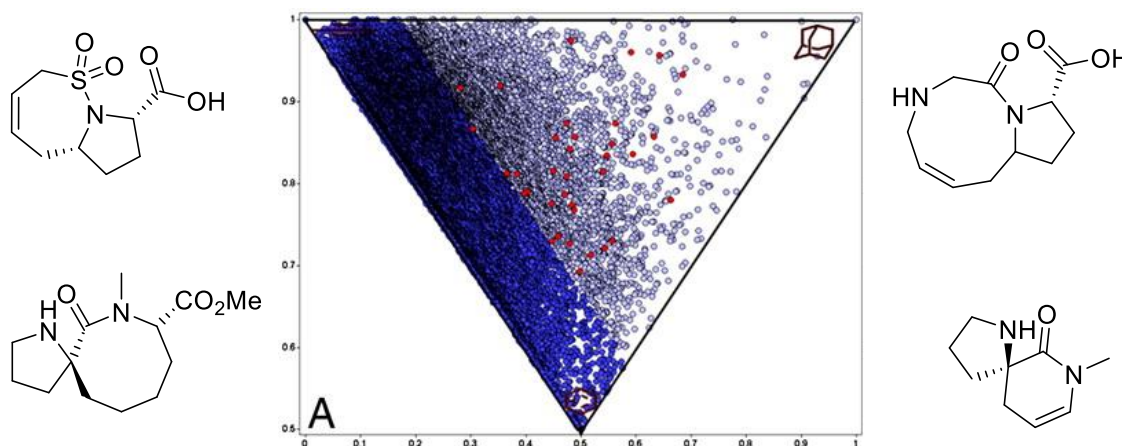

Figure 1.9: PMI plot and example fragments from Hung *et al.*[26]

This strategy was also used by Nelson, Marsden *et al.* in 2015 to synthesise compounds based on disubstituted amino acids. Although the paper focussed on the synthesis of scaffolds which could be turned into a large library of lead-like compounds, the scaffolds themselves would all be interesting 3-D fragments if deprotected. Starting with allyl substituted proline methyl ester **13**, phenylalanine or the azetidine and piperazine analogues, a wide variety of scaffolds were prepared. First, a variety of groups were attached to the nitrogen, for example the acyl urea in **14** (Scheme 1.5). These attached groups were then either coupled with the allyl group (as in compound **15**) or with the ester (compound **16**) to give the different scaffolds. In total, 22 scaffolds were synthesised this way, all with very high Fsp^3 values, appropriate fragment properties (if deprotected) and a high level of novelty.


Scheme 1.5

The use of DOS to synthesise a fragment library was described by Spring *et al.* in 2018.[28] Starting with the versatile, functionalised amine **17**, each of the three synthetic handles (amine, alkyne and ester) were either further functionalised or coupled with each other in a variety of combinations. Ultimately, 25 different scaffolds were synthesised using this process with good variation of ring size, functionality and binding vectors (Scheme 1.6).
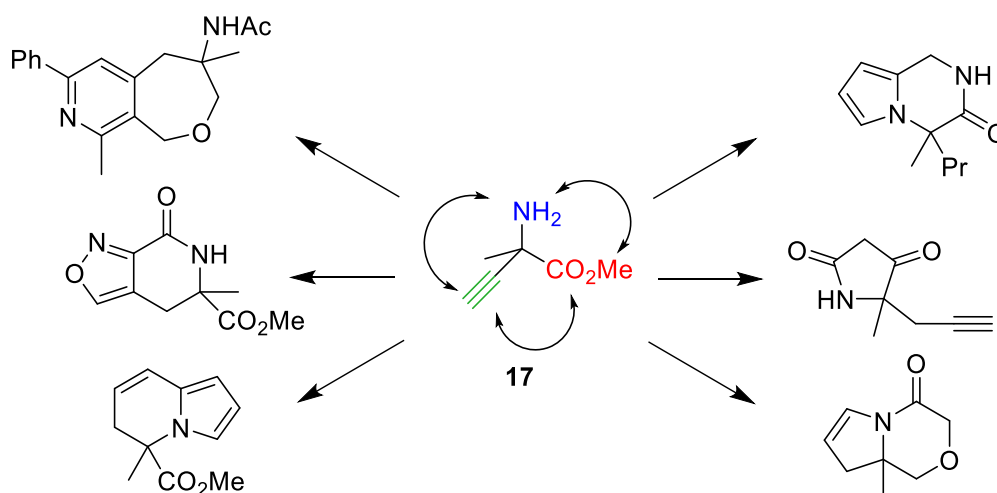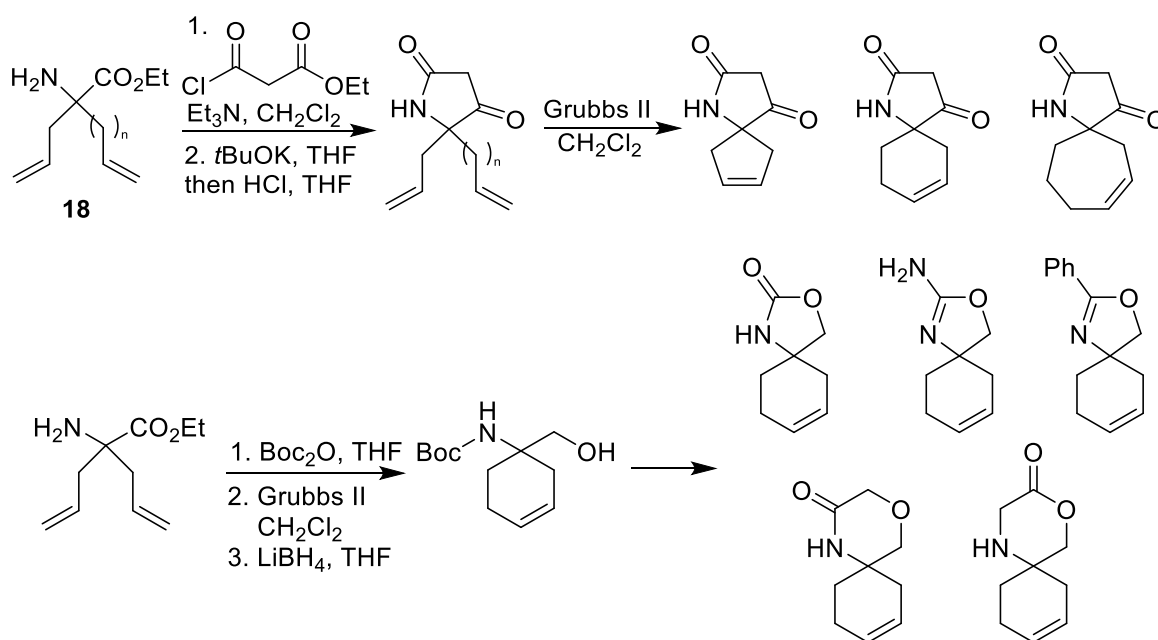
Scheme 1.6

A library of 40 fragments was synthesised from the different scaffolds and their 3-D shape was assessed using PMI analysis (Figure 1.10). As well as these 40 fragments, the PMI plot also shows a virtual library of phenyl derivatives of the 40 fragments and a commercially available 1000 fragment library (from Maybridge). Using $\sum$NPR > 1.1 as their criteria for classifying a compound as 3-D, 37 of the 40 synthesised compounds were deemed to be 3-D as opposed to only 28% of the Maybridge library.
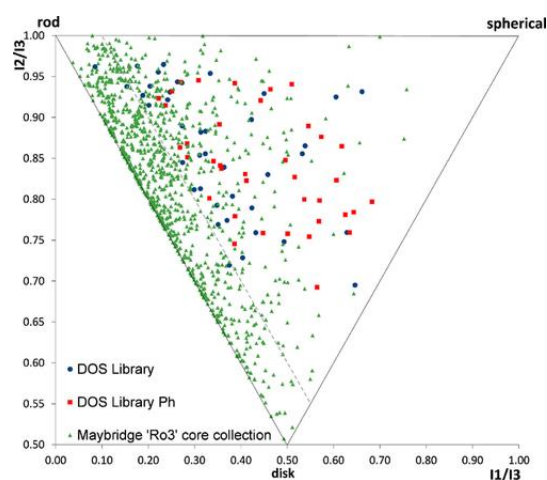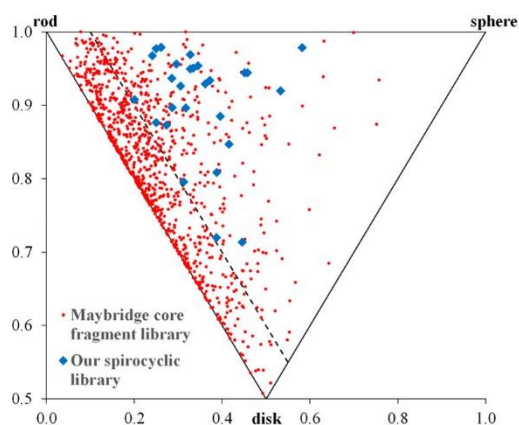

Figure 1.10: PMI plot of compounds from Spring *et al.*[28]

A similar approach was taken by the same group in 2019 using amines **18** as the starting point.[29] This time the focus was on building a library of spirocyclic compounds. For example, a series of tetramic acid spirocycles with various ring sizes of cycloalkene were synthesised (Scheme 1.7). The ability to synthesise a range of alternatives to the tetramic acid ring was also demonstrated. Oxazolidones, oxazolines and morpholinones were formed in one or two steps from a key *N*-Boc amino alcohol intermediate (Scheme 1.7).

Scheme 1.7

The alkenes in the scaffolds in Scheme 1.7 were then diversified to add alcohol, epoxide, aziridine, difluorocyclopropane, ketone and dibromo functionality to the fragments. In total, 28 fragments were synthesised with attractive physicochemical properties that fitted within the updated fragment guidelines. Furthermore, PMI analysis showed that the compounds exhibited substantially higher average $\sum$NPR values than a library of 1000 commercially available fragments from Maybridge, including no compounds with $\sum$NPR < 1.1 (Figure 1.11).

Figure 1.11: PMI plot of compounds from Spring's 2019 work[29]

1.3.2 Computational Generation of Shape-Diverse Libraries

In 2013, work was published by a consortium of academic and industrial collaborators on the creation of a library of 3-D fragments.[30] Industry partners in the consortium had identified a lack of compounds with good 3-D shape in their libraries and sought to rectify this through this project. The PMI plot in Figure 1.12 (left) shows a collection of 1000 fragments belonging to one of the industrial collaborators and is notable for the high concentration of compounds along the rod-disc axis. To kick-start the project, a process was devised to take an initial list of 13.4 million compounds available from e-molecules or the ZINC database and narrow it down to a library of just 200 fragments that were highly shape diverse, had good physicochemical properties and would be available for purchase. Initial filters to remove compounds which did not fit typical fragment properties (9-18 heavy atoms, XlogP < 3, total polar surface area < 3, number of rotatable bonds < 4) and/or contained PAINS motifs (functional groups likely to cause false hits) left 180,000 potential compounds. These were then passed through an algorithm to select a set of 5,000 compounds which covered 3-D space (based on PMI analysis) as evenly as possible. Finally, each compound within this set was reviewed by medicinal chemists in industry to assess the attractiveness of each compound as an addition to their fragment libraries to give a set of 200 compounds. Of these, 20 were unavailable, 10 failed QC and the remaining 170 fragments formed the initial library. The PMI plot in Figure 1.12 (right) shows these 170 fragments and their even coverage of 3-D space, a clear improvement on the industry fragment collection. However, it is worth noting that in attempting to cover 3-D space evenly, a substantial number of these fragments have a $\sum$NPR value < 1.1 despite this area already being well populated by other libraries.
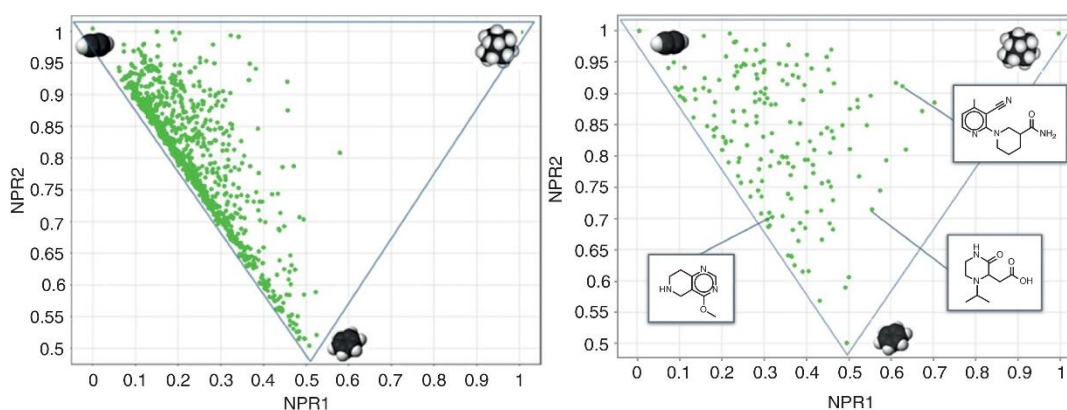

Figure 1.12: PMI plots of 1,000 fragments from an industry collection (left) and the 170 fragments from the 3-D fragment consortium library (right)[30]

Another example of computationally generating a library of compounds which could then be purchased was described by Nelson, Marsden *et al*.[31] They sought to combine 60 purchased fragments with 20 synthesised fragments (based on a few synthetic routes) to give a library of 80 fragments that covered 3-D space as evenly as possible. Four routes were selected for syntheses, giving 63 potential scaffolds and, after decoration, a total of 66,000 potential compounds. Both these and the 12.7 million compound ZINC database were first put through a filter to ensure that heavy atom count (HAC) was between 18 and 22. This is an interesting choice since typical fragment libraries have a lower average HAC. The authors comment that this allowed them to select more of their potential scaffolds, but it did result in around 40% of the compounds after the HAC filter having a MW > 300, which are not 'rule of three' compliant fragments. Selection of 100,000 of the successful ZINC fragments at random followed by further filtering for AlogP between –1 and 3 narrowed the field down to approximately 9,000 synthesisable fragments and 67,000 ZINC fragments. These were then passed through an algorithm to select a shape-diverse set of fragments which resulted in 20 synthesisable fragments and 60 ZINC fragments. The PMI plot of the resulting library, as well as the structures of some of the synthesised fragments, is shown in Figure 1.13.
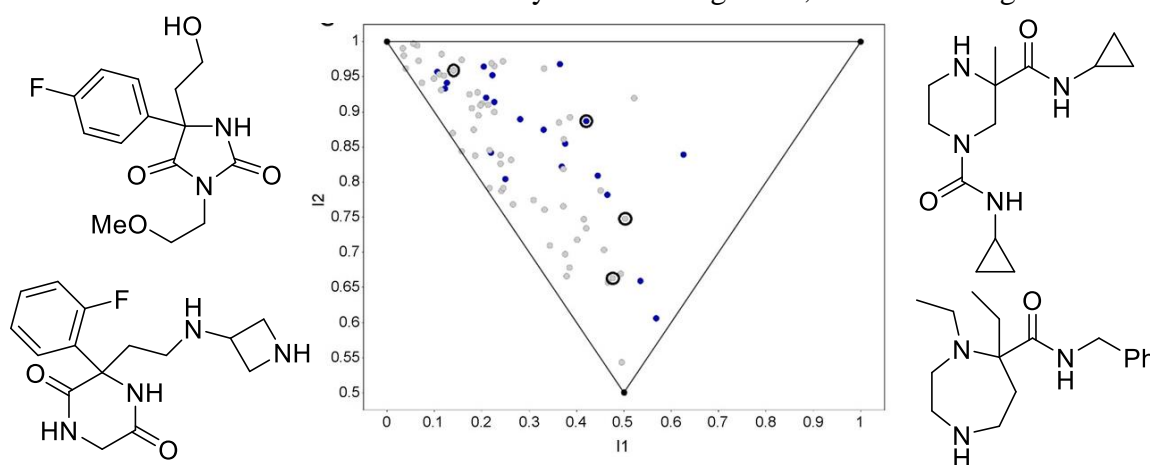

Figure 1.13: PMI plot of the library from Nelson, Marsden *et al*. with synthesised fragments in blue, ZINC fragments in grey and successful hits circled[32]

As evidenced by the structures in Figure 1.13, one criticism of this fragment library would be the high levels of complexity in these fragments, with multiple binding groups within each fragment. The library was tested against Aurora-A kinase using high-throughput X-ray crystallography screening. Four of the 80 fragments were hits, all with highly diverse shapes (see the four circled points, Figure 1.13).

1.3.3 Degradation of Natural Products

Natural products have historically been an excellent source of drug and drug-like molecules.[33] One approach to harnessing some of the potential of natural products is to break down natural products into their constituent fragments and then screen these fragments against targets. With typically high Fsp^3 values and number of stereogenic centres, natural product-based fragments have shown promise in their ability to generate highly shape-diverse libraries. Two key approaches have been taken towards natural product-based fragment libraries. Natural products can either be deconstructed computationally into their constituent fragments, which are then purchased or synthesised, or they can be degraded chemically to give fragments directly.

In 2014, Waldmann *et al.*[34] published their work on the computational deconstruction of natural products into their constituent fragments, which were then purchased in order to form a fragment library. Starting from a set of 180,000 natural products, an algorithm that sequentially removed sections of the natural product was used to generate 750,000 potential fragments. After filtering using various criteria, namely Alog $P < 3.5$, MW 120–350 Da, ≤ 3 hydrogen bond donors, ≤ 6 hydrogen bond acceptors and ≤ 6 rotatable bonds in addition to PAINS filters, 160,000 potential fragments were identified. Although these criteria are more generous than those typically used for fragments, it has previously been noted that a higher proportion of successful natural product-like fragments are non'rule of three' compliant .[35] Further filtering to remove macrocycles and structures with a high number of rings or bridged carbons reduced the count to 110,000 fragments. From these, a set of 2,000 with representative pharmacophores were then selected. Scheme 1.8 shows an example of the potential fragments resulting from a natural product using this methodology. In this case, each individual ring of the pentacyclic natural product is a valid fragment.
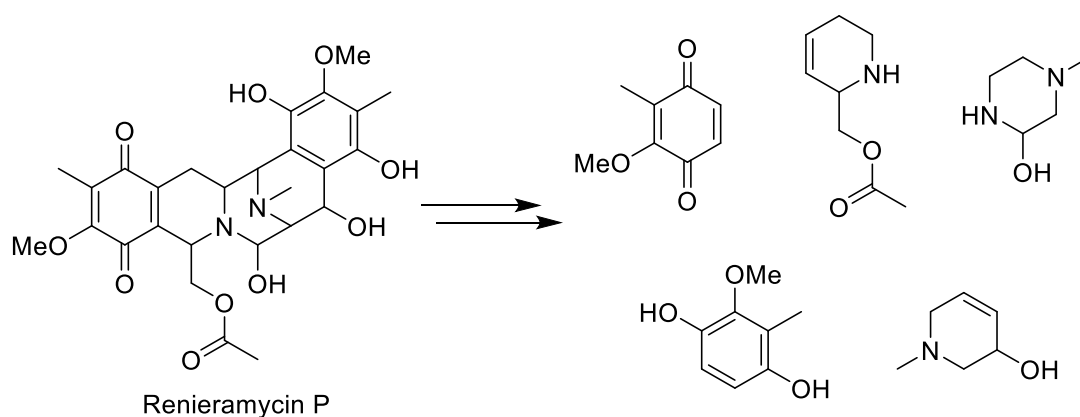
Scheme 1.8

The group then tested this virtual library of 2,000 fragments in a screening programme. From this screen, 193 compounds that were either identical or very similar to compounds in the virtual library were purchased and screened against p38α MAP kinase. Crystal structures were obtained for 9 of these compounds bound with the kinase and, interestingly, several different binding locations were observed. Notably, two compounds bound in an allosteric site. Synthesis of further related fragments resulted in two fragments that formed a novel class of inhibitor for this protein, stabilising its inactive form and showing the value of sp³-rich natural product-like fragments.

Lizos *et al*. took an alternative approach to natural product-derived fragments in their 2017 work,[36] focussing on direct chemical reactions of natural products in order to either fragment large natural products or modify smaller natural products. First, computational analysis of a library of 17,000 natural products was used to select suitable compounds which could easily be chemically degraded to give fragments. Of the 66,000 possible degradation products, 9,000 passed fragment property filters (MW 150-300 and cLogP < 3). A PMI plot of these 9,000 potential fragments showed almost complete coverage of the plot, demonstrating the value of natural product-like structures in exploring 3-D space. The 9,000 potential fragments were then assessed for their availability, functional groups, similarity to Novartis' current fragment library and 3-D shape before being purchased or synthesised for addition to the library. An example of the degradation approach is shown in Scheme 1.9. TBS protection of the alcohols in Tacrolimus followed by ozonolysis gave access to the top two fragments after deprotection and oxidation/reduction. Alternatively, retro-aldol reactions caused fragmentation to give access to the bottom two fragments. Although these fragments contain more stereogenic centres than typical fragments, the unique method of their synthesis means that they are easily accessible as single enantiomers.
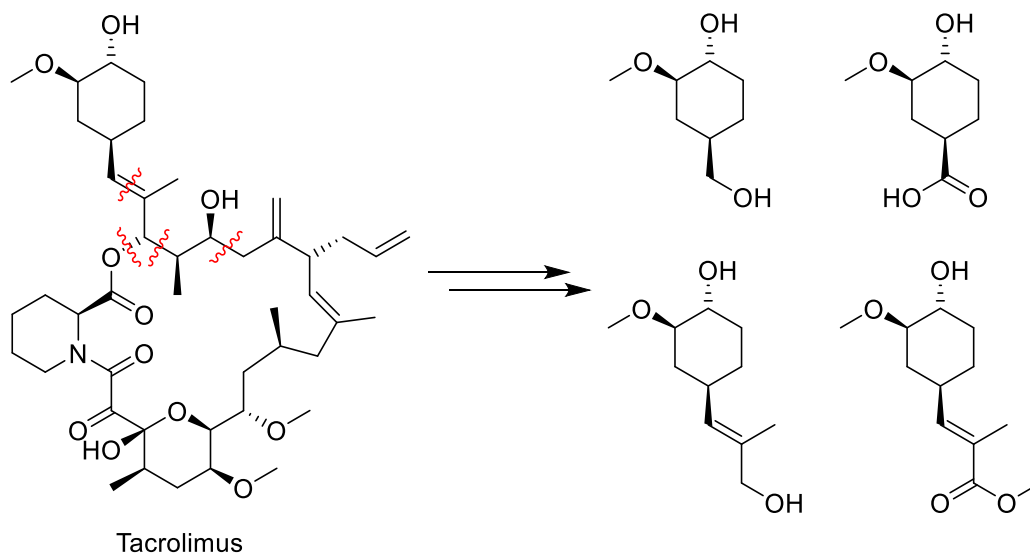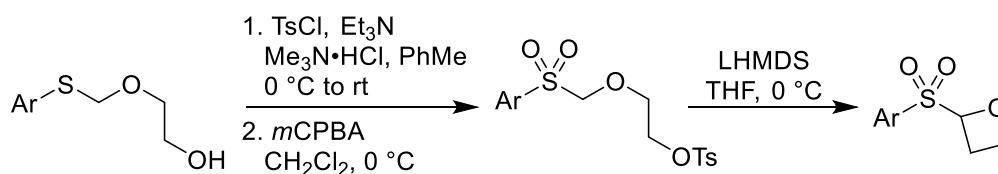
Scheme 1.9

At the time of publishing, 150 fragments generated by this approach had been added to the Novartis collection, filling underrepresented space in their library both in terms of fragments with high natural product-likeness and high Fsp^3 values (most fragments from this methodology had $Fsp^3 > 0.7$).

### 1.3.4 Scaffold Diversification

One of the most popular routes for library design is the synthesis of a limited number of scaffolds which can then be diversified using a toolkit of well-known reactions. This approach is attractive for a number of reasons including its ability to develop large numbers of fragments very quickly and its use to showcase novel methodology by using it to produce a library of medicinally-relevant compounds.

Two examples of this approach were reported by Bull *et al.*[37,38] In both, a small scaffold was produced in just a few steps using new methodology and the scaffolds were diversified at multiple points to create a library of fragments. For example, the synthesis of 2-(aryl-sulfonyl)oxetane scaffold was achieved as shown in Scheme 1.10. The aryl group was varied to include additional synthetic handles such as halogens and esters that allowed for further diversification.
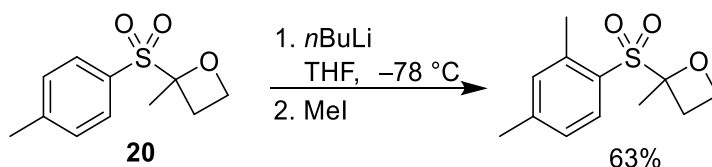

Scheme 1.10

Three different approaches for diversification are shown in Scheme 1.11. Oxetane **19** was synthesised with a 4-chlorophenyl group, with the chlorine then able to take part in coupling reactions. Both alkyl and aryl groups were able to be attached, using either iron-mediated cross-coupling or classical Suzuki-Miyaura cross-coupling. Alternatively, a variety of groups in the position α to the sulfone and oxetane could be attached using lithiation/trapping methodology (Scheme 1.11).
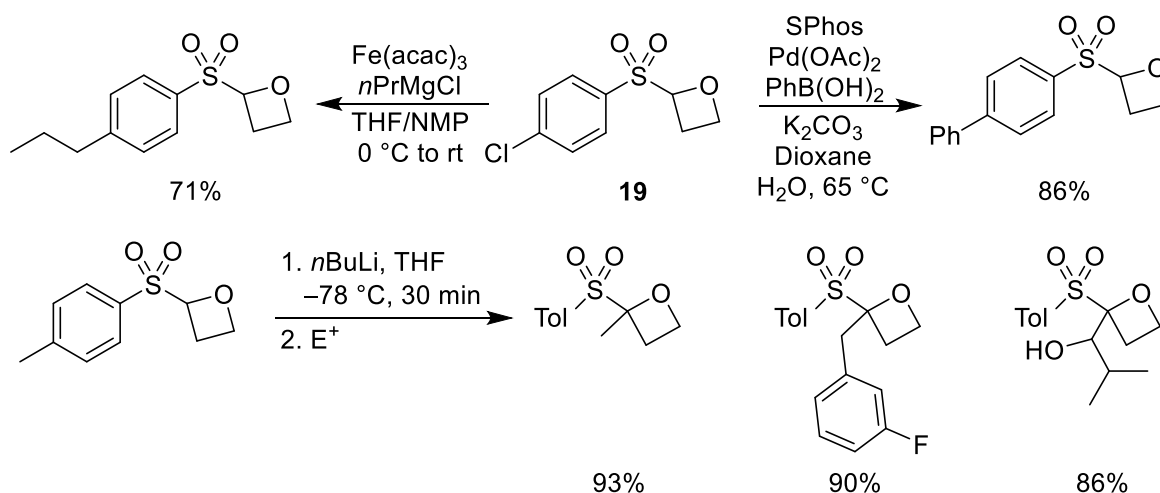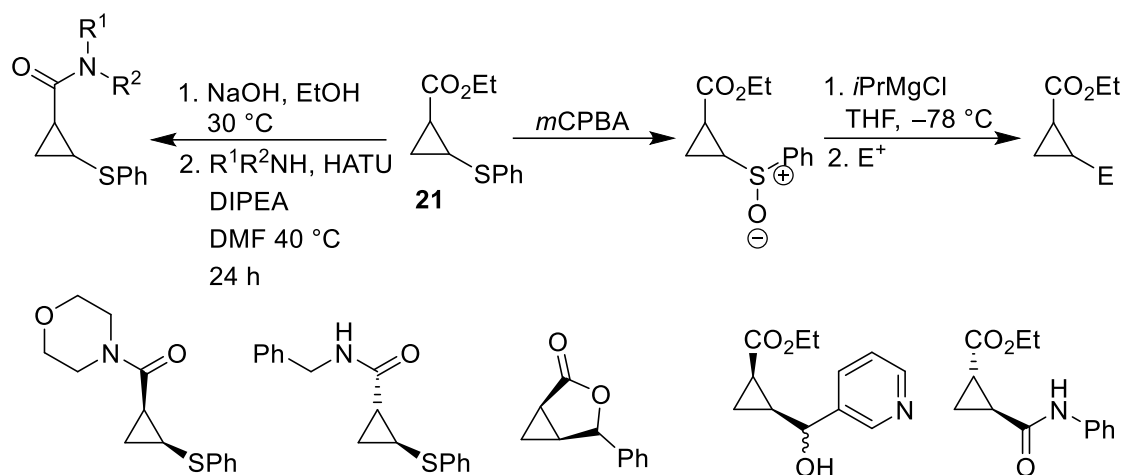

Scheme 1.11

In addition, disubstituted oxetanes such as **20** were subjected to sulfone-directed *ortho-*metallation. This resulted in the addition of a methyl group in the *ortho-* position of the aromatic ring (Scheme 1.12).
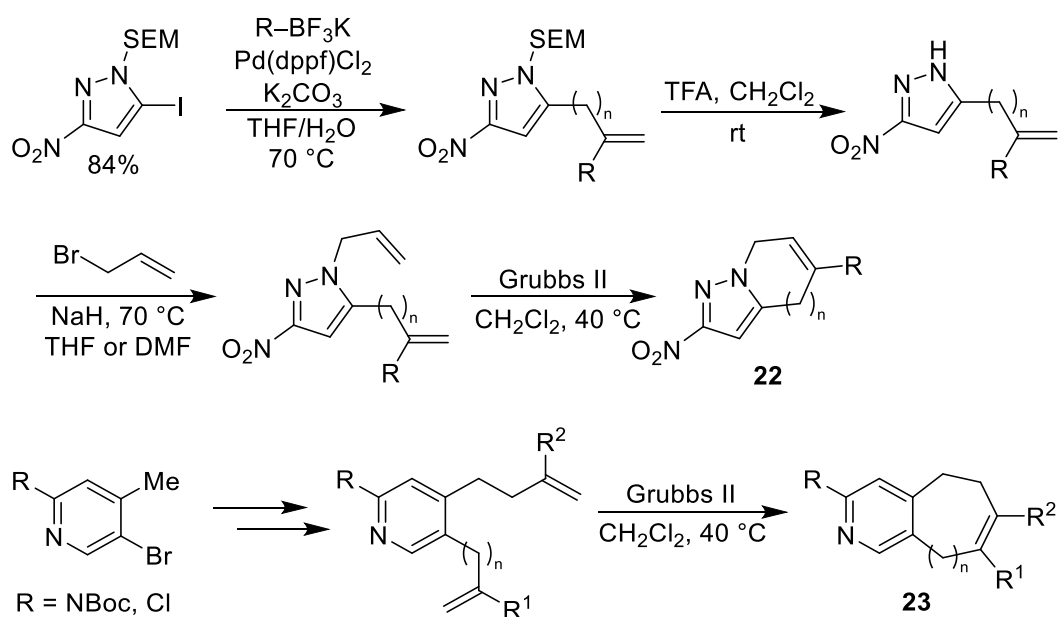

Scheme 1.12

Bull *et al*. used a similar approach to synthesise a library of disubstituted cyclopropanes.[38] A variety of different cyclopropanes were synthesised, including potential fragments, larger lead-like compounds and building blocks that contained key groups including boronic acids. The work focussed on cyclopropanes **21**. After extensive investigation, a cobalt-catalysed reaction was used to give large amounts of both *cis*-**21** and *trans*-**21**. Cyclopropanes **21** were then diversified either *via* the ester or the sulfide. Hydrolysis of the ester followed by amide couplings resulted in the synthesis of a wide variety of amides, whereas oxidation of the sulfide to the sulfoxide allowed for the sulfoxide to then be turned into a Grignard reagent. This Grignard reagent could then be reacted with a range of electrophiles to give fragments including those shown in Scheme 1.13.

Scheme 1.13

In 2016, Spring *et al.* reported a scaffold diversification approach that focussed on partially saturated heteroaromatic bicyclic fragments.[39] Two key scaffolds were developed based on either bicyclic pyrazoles or pyridines (Scheme 1.14). Synthesis of pyrazole scaffold **22** involved the attachment of two alkene-containing groups to a pyrazole ring followed by the use of metathesis to join the alkenes and synthesise the second ring. By varying the chain length of the second alkene-containing substituent either 5-, 6- or 7-membered rings could be fused with the initial pyrazole. Synthesis of the pyridine scaffold involved a very similar approach. Two alkenes, the second of which contained a variable chain length linker, were attached to the pyridine using Suzuki-Miyaura coupling and a benzylic lithiation reaction. Subsequent metathesis resulted in bicyclic scaffolds **23**.

Scheme 1.14

Importantly, both bicyclic scaffolds **22** and **23** contained an alkene in the second ring. This alkene was functionalised using either one, two or three steps to create a library of fragments (examples shown in Figure 1.14). In total, 42 fragments were synthesised, all of which showed excellent physicochemical properties. Fraction of aromatic carbons and number of stereogenic centres were calculated instead of the more common Fsp^3 values. In these categories, the library compared unfavourably with the reference commercially-available libraries, although this does not necessarily mean that the fragments are less 3-D.
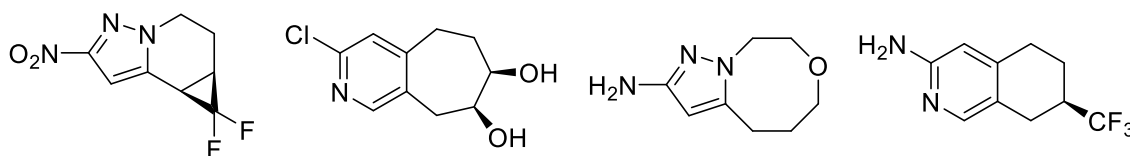

Figure 1.14: Example fragment structures from Spring *et al.*[39]

1.3.5 Versatile Methodology for Fragment Synthesis

The final approach to 3-D fragments is the use of a single, versatile reaction in which various substrates can be used to give a diverse range of products. In the previously described strategy, a significant number of synthetic steps from starting material to fragment is often needed due to the need to synthesise a core scaffold and then perform further reactions on it. In contrast, the examples in this Section show a selection of different synthetic routes that turn relatively simple molecules into a more complex fragment in a few steps, often in a one-pot process.

An example of this strategy, using C-H activation to synthesise small bicyclic compounds, was described by Fagnou *et al.*[40] Rees *et al.* refer to it as an example of an approach that demonstrates ideal characteristics of fragment synthesis.[41] Key points in favour of this approach included its use of new chemistry (rhodium-mediated C-H activation), the ability to elaborate the fragment in all positions and vectors, the mix of aromatic and unsaturated carbons and the potential to include heterocycles. The key reaction involves the activation of an *ortho* C-H bond in the aromatic ring of **24** using rhodium. An alkene group was then attached between the aryl ring and the amide nitrogen (Scheme 1.15).
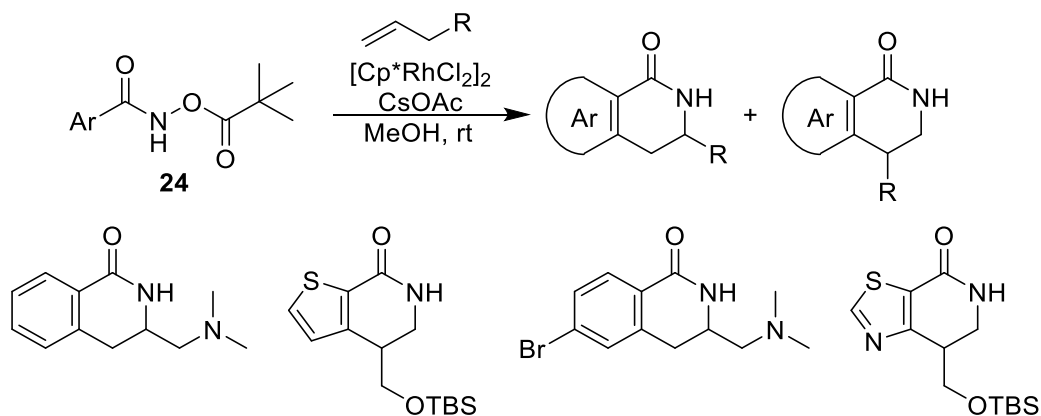
Scheme 1.15

By varying the alkene, groups could be added at either end to add diversity. Furthermore, a variety of aromatic groups were used including heteroaromatics and aromatics with synthetic handles to allow for further derivatisation. However, a number of less desirable properties of this approach were noted. Polar groups were not well tolerated and substantially lower yields were obtained with pyridine or free amine groups. Also, the reaction could not be performed in water as the solvent. However, it is important to consider the properties detailed when designing a new fragment synthesis.

The Willand group have published two papers using the versatile methodology approach to synthesise fragments.[42,43] The use of 1,3-dipolar cycloadditions to prepare isoxazoline fragments was described in 2015.[42] An aldoxime was first chlorinated and the desired alkene then added. A wide variety of alkenes were used, particularly exocyclic alkenes as these would generate spirocycles. Addition of base caused the chloro-oxime to collapse, generating the desired 1,3-dipole, a nitrile oxide. Subsequent cycloaddition gave the target fragments directly after purification (Scheme 1.16). Using this method, 21 fragments were synthesised including 5,4- 5,5- 5,6- and 5,7-spirocycles as well as some monocyclic compounds. A good variety of functional groups were tolerated on the alkene, allowing for the inclusion of amines, nitriles, esters and aromatics.
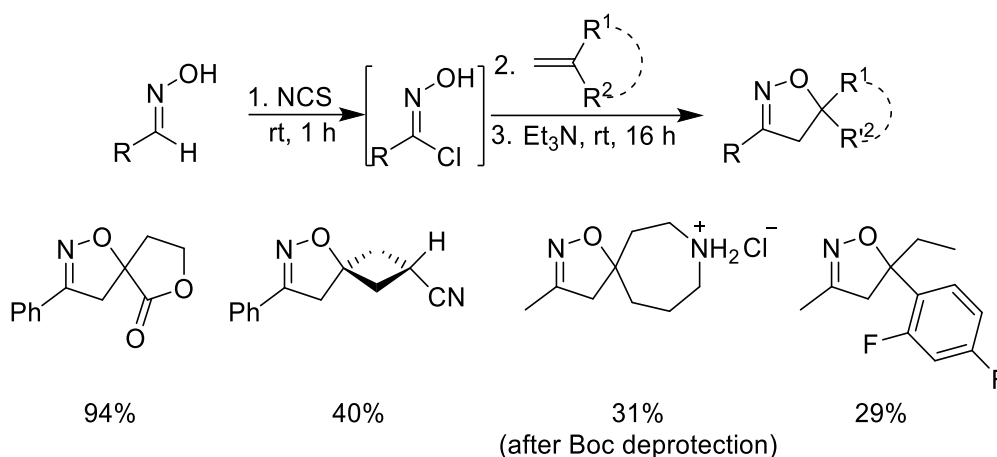
Scheme 1.16

As well as ensuring that the fragments were appropriately sized (MW range of 140-291), the fragments also showed good solubility in buffer solution and high Fsp^3 values (0.25-0.92). The 3-D shape of the fragments was determined using PMI analysis. The 21 isoxazoline fragments had an average $\sum NPR = 1.19 \pm 0.08$, substantially better than the figure of 1.09 ± 0.07 that the group calculated for their library of commercially available fragments. The compounds clustered slightly in the top left corner of the PMI plot, which is to be expected for a library containing a common framework, but the spread was still enough to ensure that a significant amount of 3-D space was covered.

The other work published by Willand *et al.* in this area focussed on the synthesis of spirohydantoin fragments.[43] Similar methodology had been developed previously for the synthesis of hydantoins,[44] but the reaction required large amounts of potassium cyanide to work, which was highly undesirable. By performing the reaction in a microwave, the group were able to reduce the amount of cyanide required to 1.5 equivalents and the reaction was complete in just ten minutes. A variety of cyclic ketones could be used to deliver a diverse set of fragments, including spirocyclic tetrahydropyrans, piperidines and azepanes (Scheme 1.17).
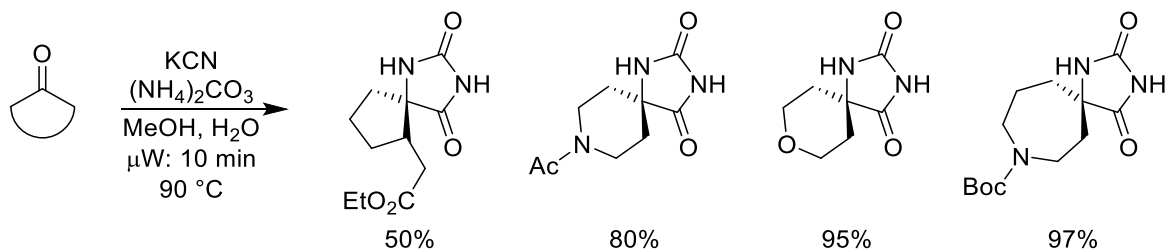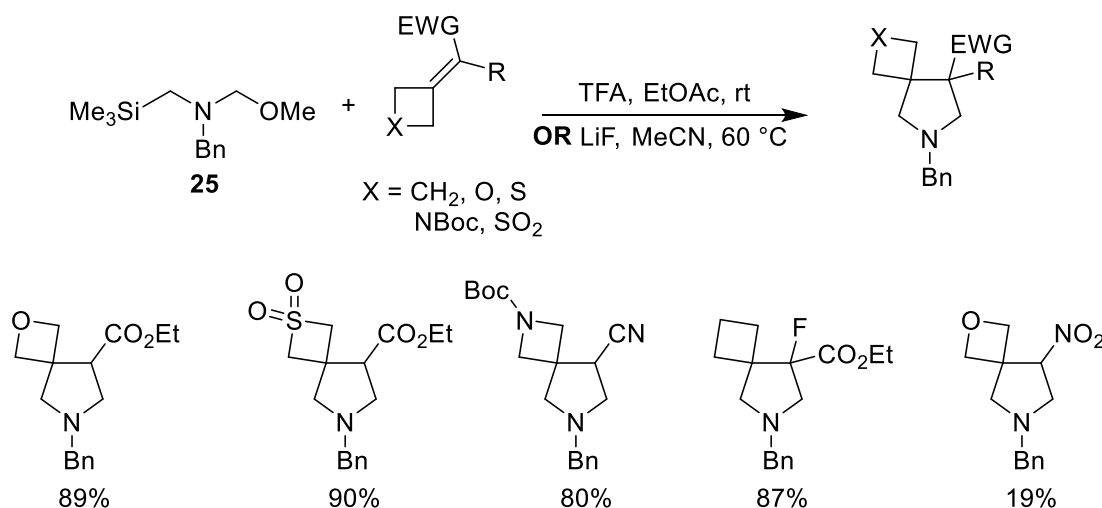
Scheme 1.17

In total, 27 fragments were synthesised using this methodology. PMI analysis was used to assess the 3-D character of the synthesised compounds. These compounds showed a similar

level of 3-D character to those from the group's previous work. There was a small amount of clustering in the top left corner but these fragments were better spread overall and made a valuable addition to the group's fragment library.

Cycloaddition reactions work well as a method to synthesise fragment libraries due to the ease of varying the substrates and their ability to create complex molecules from simple starting materials. Mykhailiuk *et al.* leveraged these advantages to synthesise a library of spirocyclic pyrrolidine fragments.[45] Amine **25**, a well-known ylid precursor,[46] was reacted with a variety of electron-deficient alkenes featuring a 4-membered ring to synthesise fragments quickly. Two sets of conditions were used to ensure the best yields for the target fragments (Scheme 1.18). In total, 20 cycloaddition products were synthesised using this methodology with good variation of both the electron-withdrawing group and the four-membered ring.

Scheme 1.18

The potential of these cycloaddition products was then demonstrated by derivatising both the ester and nitrogen. Furthermore, they were able to obtain single enantiomers of the products using either HPLC, kinetic resolution or chiral auxiliaries. Although fragments are typically screened as racemates to increase the potential for hits, chiral fragments will have to be synthesised as single enantiomers at some point in the process. Thus, demonstrating that this is possible makes these fragments more attractive.

Erdman *et al.* also designed a library of 3-D pyrrolidine fragments based on a cycloaddition strategy.[47] Chiral amine **27** was reacted with aromatic aldehydes **26** to give an iminium ion. This then formed a metallo-azomethine ylid with either copper or silver and this ylid underwent a cycloaddition with the cyanoalkene to give trisubstituted pyrrolidines (Scheme 1.19). A variety of heteroaromatics including pyridines, pyrazoles, imidazoles and indoles

were used and the directing camphorsultam group could easily be converted into either the ester or alcohol. In total, 48 Fragments were synthesised using this methodology and both PBF and PMI analysis was performed. The fragments showed an even spread of $\sum$NPR values from $\sum$NPR = 1.06-1.37 and these correlated well with the PBF scores.
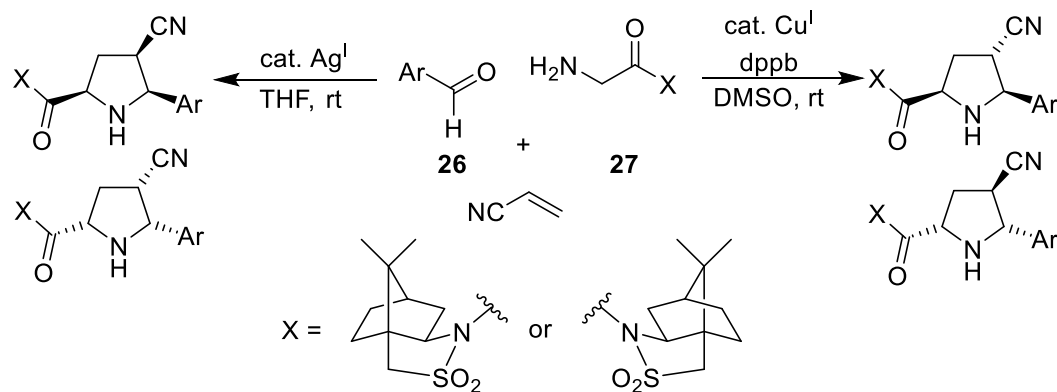
Scheme 1.19

Marsden, Nelson *et al.*[48] synthesised a library of fragments based on twisted bicyclic lactams. The key reaction, shown in Scheme 1.20, used dibutyltin oxide to close the ring, resulting in the bicyclic lactams shown. This reaction gives fragments directly, although lactam **28** is a versatile intermediate which could be further diversified. The four fragments shown in Scheme 1.20 are all derived from lactam **28**, by either reduction of the ketone, chlorination then Suzuki-Miyaura coupling of the amide or annulation of an aromatic ring. The result was a library of 22 diverse fragments all based on a bicyclic lactam core.

Scheme 1.20
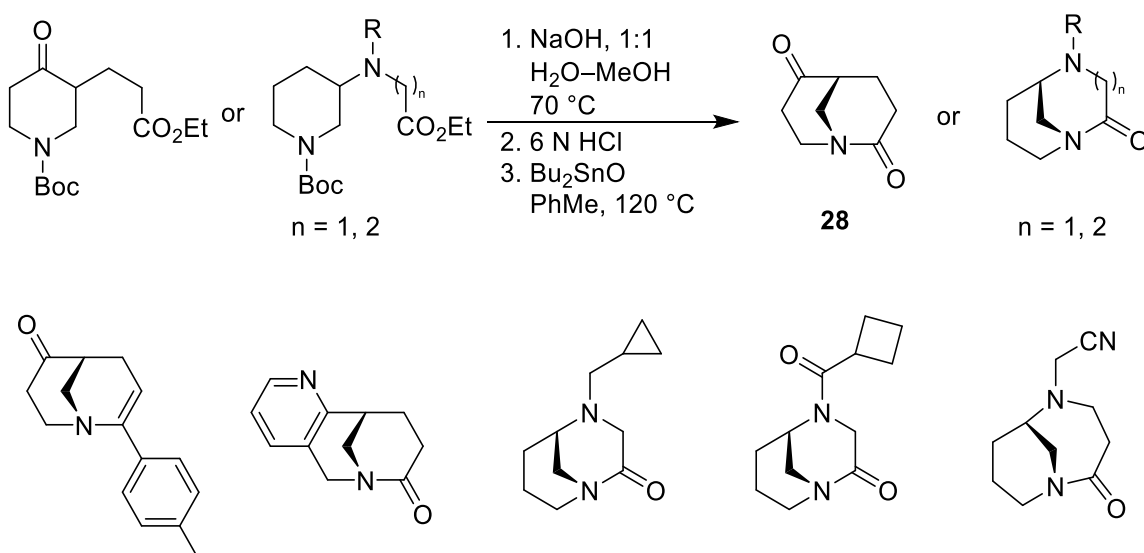
3-D Shape analysis was performed on the 22 fragments, with the resulting PMI plot shown in Figure 1.15. The fragments demonstrated excellent 3-D shape with no compounds on the rod-disc axis and a good spread across 3-D space
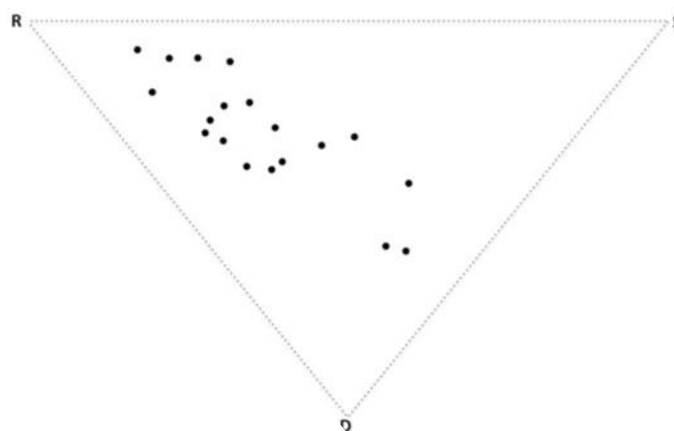
Figure 1.15: PMI plot of 22 fragments from Marsden, Nelson *et al.*[48]

Recently, Grainger *et al.* reported the synthesis of α-substituted saturated nitrogen heterocycle fragments using C-H activation methodology.[49] Aryl C-H bonds and C-H bonds α- to *N*-Boc groups were activated using an iridium photocatalyst. A wide variety of saturated nitrogen heterocycles and heteroaromatic groups were coupled in this way to give 23 polycyclic compounds in generally good yields (Scheme 1.21). The reaction was shown to work on gram-scale and is attractive both for building and elaborating fragments.
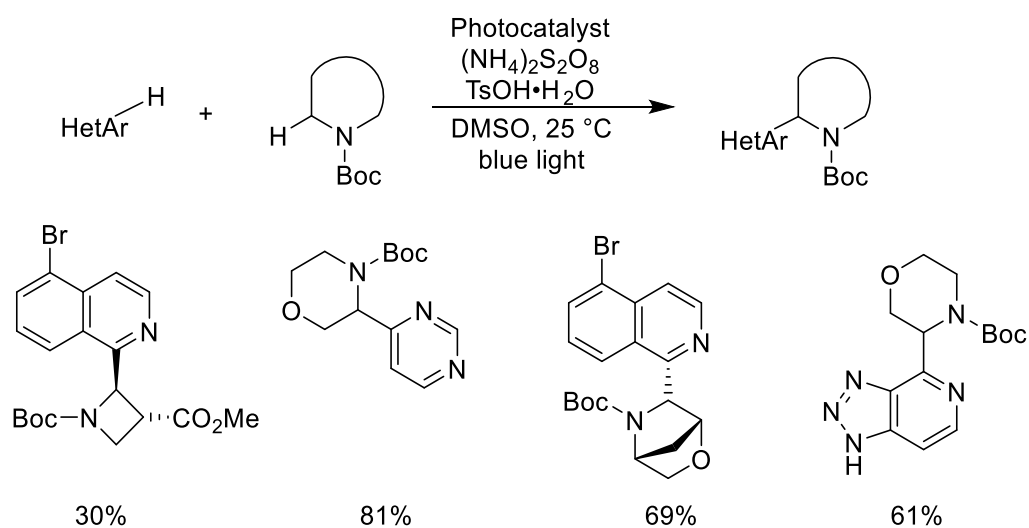
Scheme 1.21

1.4 Previous Group Work towards the Creation of a 3-D Fragment Library

In 2012, the O'Brien group embarked on a project to design and synthesise a library of 3-D fragments based on saturated heterocycles. The project, led by PhD student Mary Wheldon, focussed on the design of families of disubstituted heterocyclic fragments, from which the most 3-D would be selected and synthesised. This Section describes the design and selection of the 3-D fragments.

1.4.1 3-D Shape Analysis

A reliable protocol was required for the generation of molecular conformations and the analysis of their 3-D shape. As demonstrated in Section 1.2, there are several methods of quantifying 3-D shape including globularity,[23] plane of best fit (PBF)[22] and principal moments of inertia (PMI) plots.[25] From these, PMI plots were selected as the primary method of 3-D shape quantification, due to their ease of use, their prevalence in the literature and the easy visualisation of the data.[26,32,36,50] The conformational generation protocol was developed using Pipeline Pilot. Pipeline Pilot is a tool that allows for the streamlining of several processes and contains features including computational conformer generation, effectively using a 'ball and springs' model. Molecules submitted to the Pipeline Pilot protocol were ionised to physiological pH (pH 7.4) and then passed into the conformation generation software. The BEST method algorithm was used for the computational generation of conformers, with all conformations up to 20.0 kcal mol^{-1} above the energy of the ground state conformation being calculated. The data outputted by Pipeline Pilot included molecular properties such as heavy atom count, rotatable bond count and polar surface area for each conformation as well as 3-D shape.

1.4.2 PMI Analysis of a Commercially Available Fragment Library

A commercially available library was run through the Pipeline Pilot protocol to provide a point of comparison for the proposed structures. A sample library of 1000 commercially available fragments from Maybridge was selected. Although all of the conformations up to 20 kcalmol^{-1} were calculated, only the ground state energies were plotted due to the high number of conformations. As shown by the PMI plot in Figure 1.16, the library is dominated by compounds along or near to the rod-disc axis (the line that corresponds to $\sum$NPR = 1.0). Using $\sum$NPR values, shown by the diagonal lines in Figure 1.16, it can be seen that the majority of molecules in the Maybridge fragment library exhibit ground state conformations with $\sum$NPR ≤ 1.1 and a large amount of compounds lie directly on the rod-disc axis.
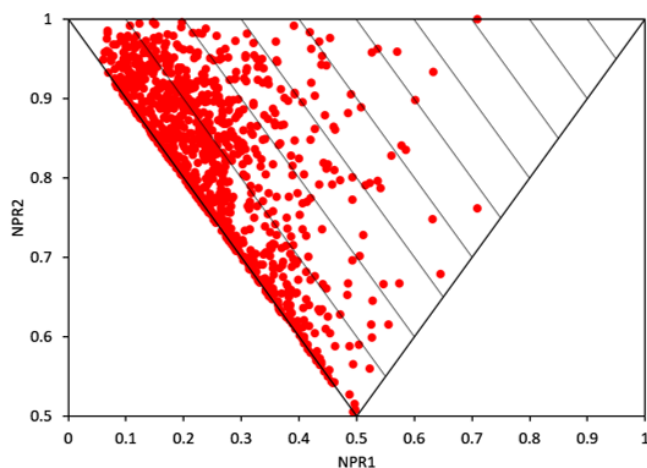
Figure 1.16: PMI plot of 1,000 fragments from the Maybridge Library

This result was encouraging since it emphasised how under-explored the more 3-D region of the PMI plot was ($\sum$NPR >1.3). The target of the project was therefore to synthesise fragments with high $\sum$NPR values and thus contribute to this under-used area.

1.4.3 Fragment Design and Selection

Initially, the group decided to focus on fragments containing saturated nitrogen-based heterocycles. Piperidines and pyrrolidines are the second and seventh most common rings found in drug molecules.[51] This, combined with the group's experience in the synthesis of nitrogen-based heterocycles, made it a logical place to start construction of the York 3-D fragment library.[52–57] It was anticipated that disubstituted compounds would give interesting 3-D shapes whilst not providing too large an entropic barrier on binding. To prevent the fragments from having too many pharmacophores, which would reduce the hit rate by increasing the potential for unfavourable interactions, or becoming too polar, one of these groups was selected to be a methyl group. The methyl group would change the 3-D shape of the molecule while having minimal impact on the MW, rotatable bond count or lipophilicity. The other group was selected to be either an ester or an alcohol. Both were simple pharmacophores that are frequently found in drug molecules. Furthermore, one is a hydrogen bond acceptor and the other a hydrogen bond donor, giving more variety in the library. Two families of compounds were therefore selected: a disubstituted pyrrolidine scaffold **29** and a disubstituted piperidine scaffold **30** (Figure 1.17). The proposed compounds would all be synthesised as racemates. It was envisioned that synthesising the racemates would be easier and it provides two potentially active compounds. Should any fragments be hits, synthesis of single enantiomers would then be considered.
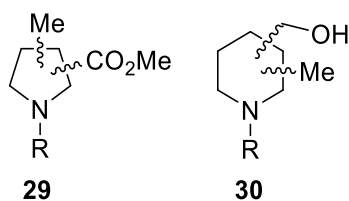
Figure 1.17: Proposed Fragment Structures

The final decision in compound design was then to decide on the capping groups for the nitrogen. NH, methyl, acetyl and methanesulfonyl groups were selected due to their low molecular weight, their prevalence in medicinal chemistry and the different hybridisation states of the nitrogen atom. It was anticipated that the *N*-acetyl and sulfonyl groups would cause the nitrogen to form a flat sp^2 centre, giving a different shape. The steric bulk of the sulfonyl group would also potentially force substituents on the neighbouring carbons into an axial position, again changing the shapes of the molecules. With the two families of fragments designed, all the possible isomers and compounds were then enumerated. This gave 14 possible isomers of the pyrrolidine system (Figure 1.18), resulting in 56 possible compounds.
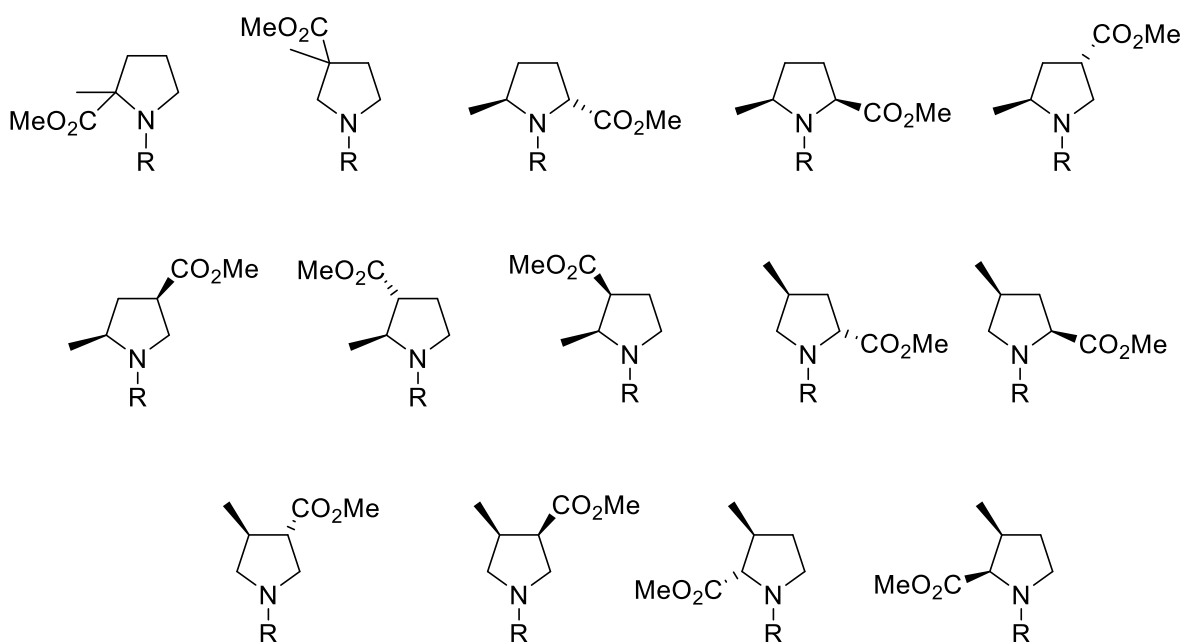
Figure 1.18: The 14 proposed pyrrolidine isomers

The piperidines were then also enumerated to give 23 isomers and 92 potential compounds after the capping groups were attached (Figure 1.19).
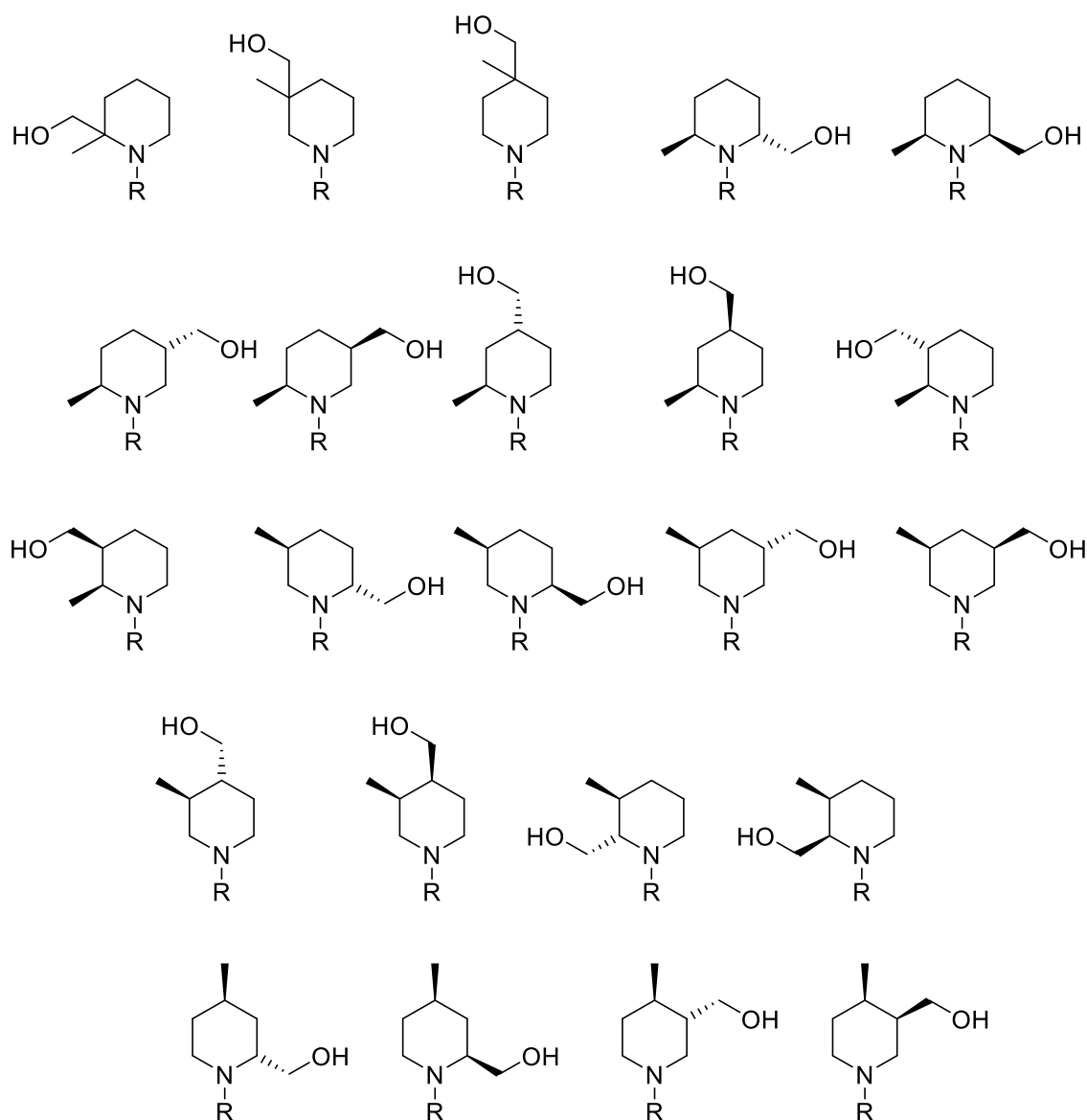
Figure 1.19: The 23 isomers of the proposed piperidine system

Before moving on to 3-D shape analysis, the physicochemical properties of these compounds were calculated computationally, and their properties compared to fragment guidelines from the literature. Table 1.1 shows the properties of the proposed fragments alongside the two well-known sets of guidelines (see Section 1.1.2). As shown in Table 1.1, the proposed fragments fitted very well with the fragment guidelines. All proposed fragments fitted completely with the 'rule of three', while all except the NH piperidines fitted the updated guidelines on molecular weight and HAC due to having MW < 140. The calculated lipophilicity values were slightly lower than the updated guidelines recommended, although the two were measured using different metrics (cLogP *vs* AlogP) and later calculations showed that the cLogP values fell almost entirely within the updated guidelines. The

properties of the library were therefore deemed to fit sufficiently within both sets of guidelines and were taken forward on to selection and synthesis.

Property	'Rule of Three'	Updated Guidelines	Our Fragments
Molecular Weight (Da.)	≤ 300	140-230	129-221
Heavy Atom Count (HAC)	N/A	10-16	9-14
logP[a]	≤ 3	0-2	–1.18-0.36
Rotatable Bonds	≤ 3	N/A	1-2

[a]Both sets of guidelines are reported as cLogP values but initially only AlogP values were available for the York fragments. Later calculations showed that the cLogP values for the York fragments were –0.18-1.32

Table 1.2: Comparison of Proposed Fragment Properties with Literature Guidelines

1.4.4 Fragment Selection

With the structures of the potential pyrrolidine and piperidine fragments set, fragments were selected for synthesis. The compounds were run through Pipeline Pilot to check them for 3-D shape. All conformations up to 20 kcal mol^{-1} were initially calculated in the process, but compounds so high in energy above the ground state would be very unlikely to be binding conformations as they would be almost completely unpopulated. Most examples of PMI plots in the literature use only the ground state conformations,[26,32,36,50] but this is also problematic as other low energy conformations will be significantly populated and compounds do not always bind in their ground state conformations. It was therefore decided to implement a limit of 1.5 kcal mol^{-1} above the ground state, with all conformations ≤ 1.5 kcal mol^{-1} above the ground state being plotted. This corresponds to approximately a 12:1 occupation ratio of the ground state to the higher energy state and seemed an appropriate limit to ensure that most of the possible binding conformations would be included without diluting the dataset with unlikely conformations. The PMI plots of the 92 piperidine compounds with just the ground states (left) and all conformations up to 1.5 kcal mol^{-1} (right) are shown in Figure 1.20.
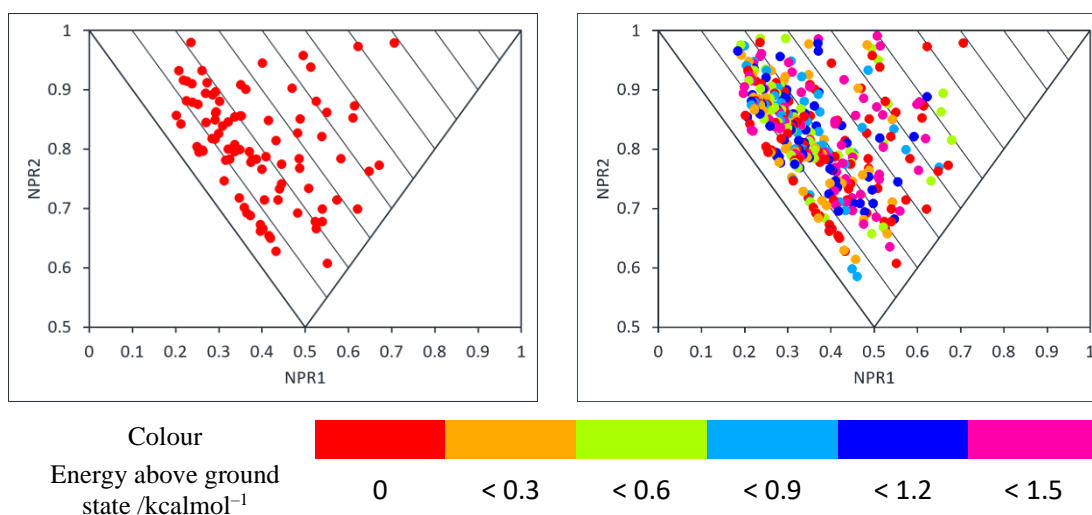
Figure 1.20: PMI plots of the ground state (left) and low energy (right) conformations of the 92 piperidines

The PMI plot of all the low energy conformations in Figure 1.20 showed that these piperidines had a significant number of conformations with interesting 3-D shape, and no conformations on the rod-disc axis. It was then considered how to select which of these piperidines should be synthesised. A cut-off at a particular ∑NPR value was decided on, where all compounds with at least one conformation above that ∑NPR value would be synthesised. The cut-off was set at a level to select an appropriate number of compounds for synthesis while also maintaining good 3-D shape. For the piperidines, this cut-off was set at ∑NPR = 1.38, and 19 of the 92 possible piperidines were selected (Figure 1.21).
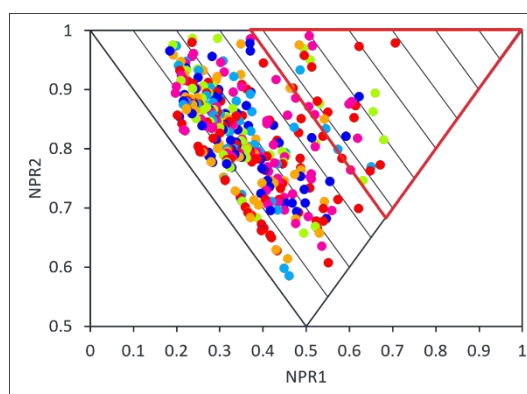
Figure 1.21: PMI plot of the proposed piperidines with the cut-off at ∑NPR = 1.38 shown

The PMI plot of the 19 selected compounds is shown in Figure 1.22. The PMI plot showed an excellent spread of conformations across 3D space, with conformers reaching as far as ∑NPR = 1.68. Only one conformation exists below ∑NPR = 1.1 and the conformations show minimal clustering, which was pleasing given the structural similarities of these piperidines.
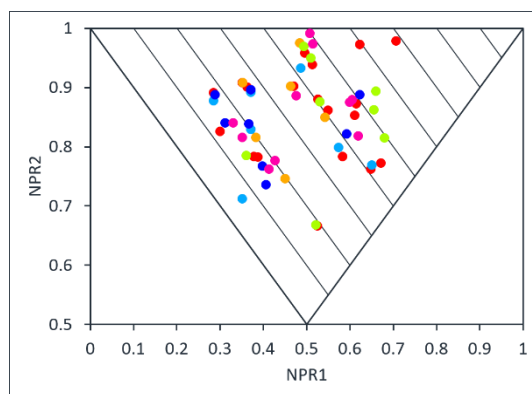
Figure 1.22: PMI plot of the selected 19 piperidines

The structures of the selected piperidines are shown in Figure 1.23. Despite being selected purely by shape, the piperidines showed a good variety of substitution patterns. The compounds selected also contained all four nitrogen groups, giving good diversity within the target fragments.
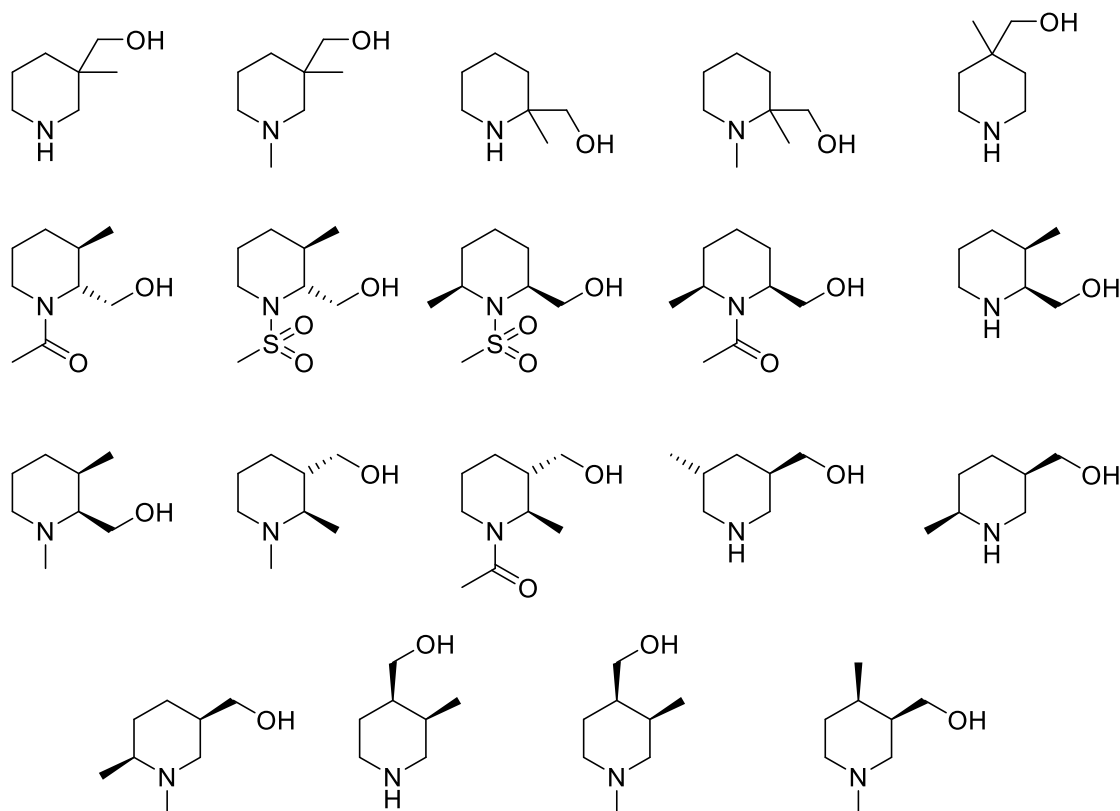
Figure 1.23: Structures of the 19 selected piperidines

With the 19 piperidines selected, the same process was applied to the pyrrolidines. Both the ground state and low energy conformation PMI plots of the pyrrolidines displayed a wide range of 3-D conformations. The ground state (Figure 1.24, left) conformations showed almost no clustering, while the low energy conformations (Figure 1.24, right) did display

some clustering in the upper right corner. However, it was expected that once the less 3-D compounds were removed, the clustering would become significantly less.
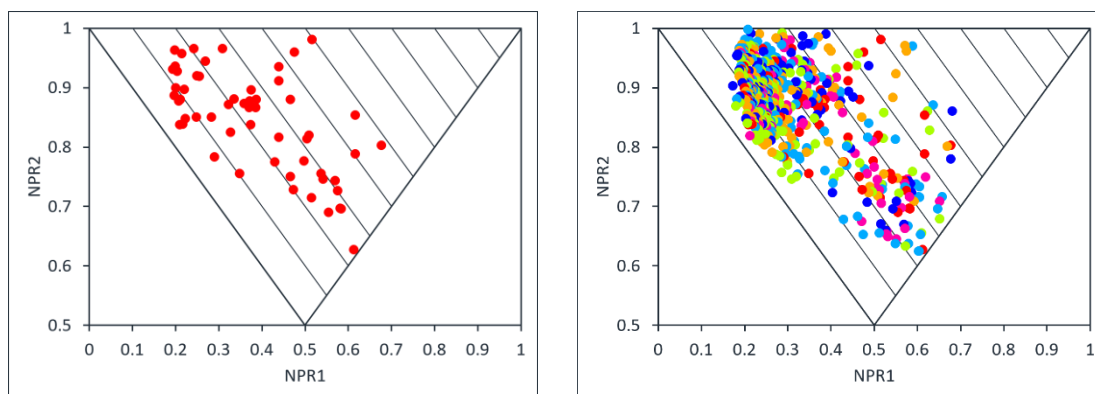
Figure 1.24: PMI plots of the ground state (left) and low energy (right) conformations of the 56 proposed pyrrolidines

The ∑NPR cut-off for the pyrrolidine fragments was set at ∑NPR ≥ 1.36 (Figure 1.25, left). 14 Of the possible 56 pyrrolidines were selected for synthesis. As the PMI plot of the selected pyrrolidines shows, the clustering was no longer an issue and the selected compounds displayed an excellent spread of conformations over the PMI plot (Figure 1.25, right).
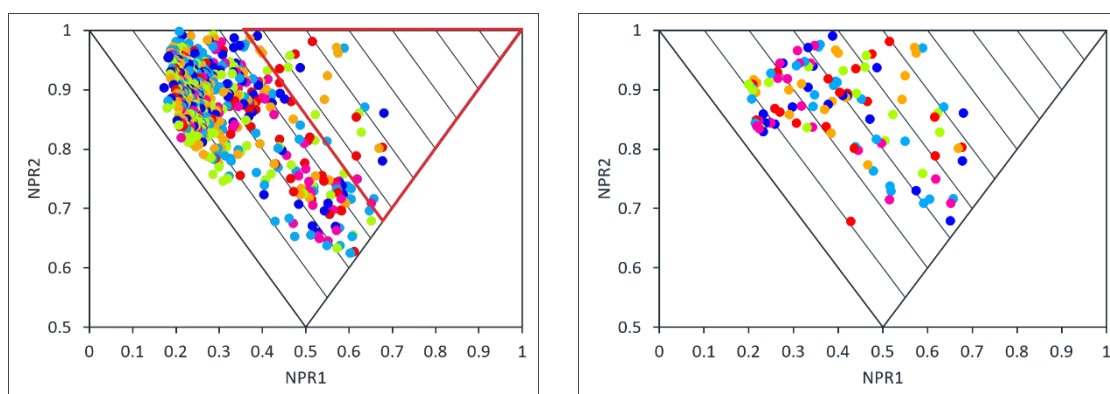
Figure 1.25: PMI plots of the 56 pyrrolidines showing the ∑NPR cut-off (left) and the 14 selected pyrrolidines (right)

The structures of the 14 selected pyrrolidines are shown in Figure 1.26. Pleasingly, a wide variety of structures was chosen, including 8 of the possible 14 isomers and examples of each of the nitrogen groups. This gave a total of 33 pyrrolidine and piperidine 3-D fragments.
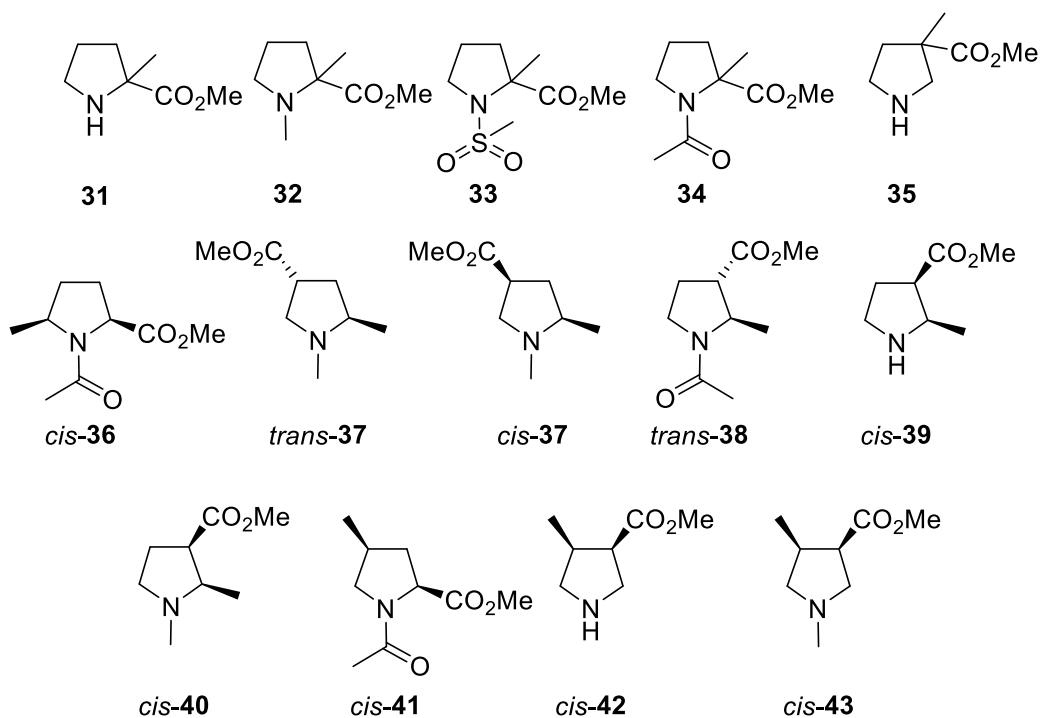
Figure 1.26: Structures of the 14 pyrrolidine fragments

With the compounds selected, synthetic efforts towards these 33 fragments began. Initial work from two members of the group resulted in the synthesis of a few pyrrolidine and piperidine fragments before more researchers joined the project. When more people, including myself, joined the project the fragments were divided among the group for synthesis. Chapter 2 of this thesis will deal with the synthesis of the fragments I was tasked with making, *trans*-**37** and *cis*-**37** and *cis*-**42** and *cis*-**43**.

1.5 Project Outline

The primary aim of the project was to aid in the completion of the synthesis of the 33 pyrrolidine and piperidine 3-D fragments selected as described in the previous Section. My contribution to this would be to synthesise four of the pyrrolidine fragments: *trans*-**37**, *cis*-**37**, *cis*-**42** and *cis*-**43** (Figure 1.27). Our efforts on the synthesis of these 3-D fragments is detailed in Chapter 2.
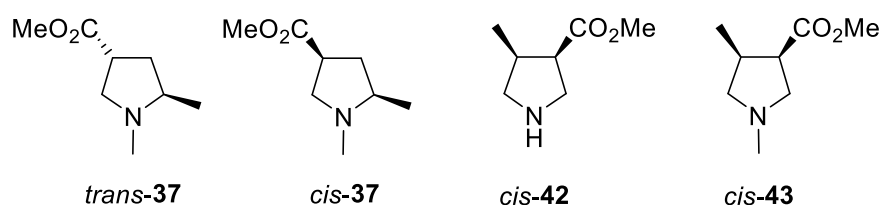
Figure 1.27: Structures of the four pyrrolidine fragments for synthesis

Once synthetic efforts towards these four fragments was completed, the plan was to design and synthesise a 2nd generation of fragments with good 3-D shape to add to the library. As the synthesis of the first-generation shape-selected fragments proved difficult, an alternative approach to fragment synthesis was sought. Focussing on the versatile methodology approach, a synthetic route was designed that could use a variety of β-ketoesters and aryl boronic acids to synthesise *cis*-3,4-disubstituted 5- and 6- membered ring fragments *cis*-**44** (Scheme 1.22). Diversification of the ester group would allow for three different points of diversification and/or further growth. The design and synthesis of these new, 2nd generation 3-D fragments is discussed in Chapter 3.
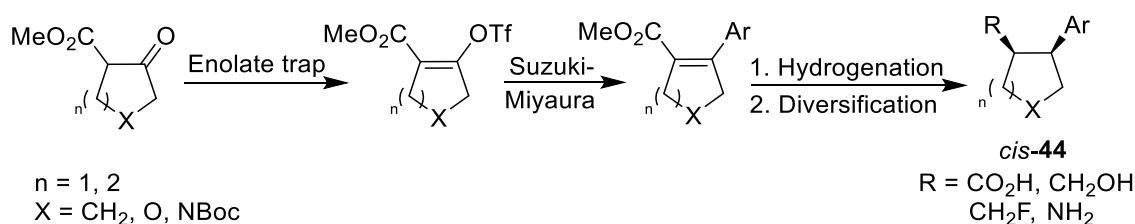
Scheme 1.22

Finally, Chapter 4 contains a detailed analysis of both the physicochemical and 3-D shape properties of all of the synthesised fragments in the York 3-D fragment library. Separate analysis of the 1st generation and 2nd generation fragments as well as the whole library is included. In addition, the 3-D shape properties were compared to a selection of other available 3-D fragment libraries.

CHAPTER 2: SYNTHESIS OF PYRROLIDINE 3-D FRAGMENTS

In this Chapter, the synthetic work towards 3-D fragments *cis*-**42**, *cis*-**43**, *trans*-**37** and *cis*-**37** (Figure 2.1) is detailed. Section 2.1 covers the synthesis of the two 3,4-disubstituted pyrrolidines ci*s*-**42** and *cis*-**43**. This includes a literature survey on the synthesis of similar molecules before describing the different routes that were explored. Similarly, the relevant literature background on the synthesis of the two 2,4-disubstituted pyrrolidines *trans*-**37** and *cis*-**37** and our synthetic efforts are described in Section 2.2.
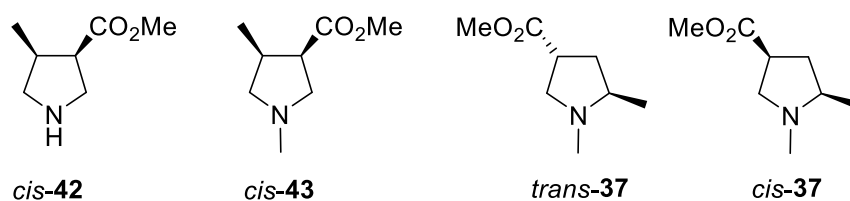
Figure 2.1: Structures of the four target fragments

During the development of routes to 2,4-disubstituted pyrrolidines *trans*-**37** and *cis*-**37**, a highly diastereoselective approach to *cis*-2,4-disubstituted pyrrolidines was optimised. Thus, the synthesis of four *t*-butyl ester-substituted *cis*-2,4-disubstituted pyrrolidine fragments, namely *cis*-**45**, *cis*-**46**, *cis*-**47** and *cis*-**48** (Figure 2.2), is described (Section 2.3).
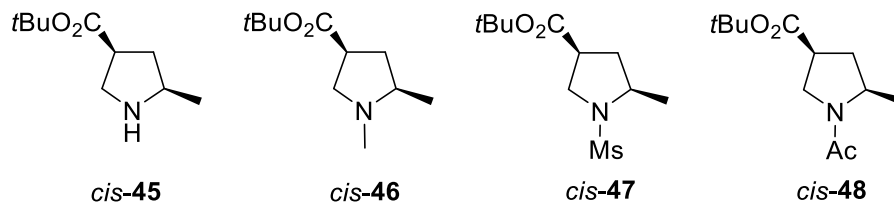
Figure 2.2: Structures of the four *t*-butyl ester fragments

2.1 Synthesis of 3,4-Disubstituted Pyrrolidine Fragments

This Section describes our efforts towards the synthesis of 3,4-disubstituted pyrrolidines *cis*-**42** and *cis*-**43**. The selection of these 3-D fragments as targets was described in Section 1.4. The PMI plots for each fragment *cis*-**42** and *cis*-**43** are shown in Figure 2.3. Given that the two fragments only differ at the *N*-substituent, the same route would be used to prepare both fragments.
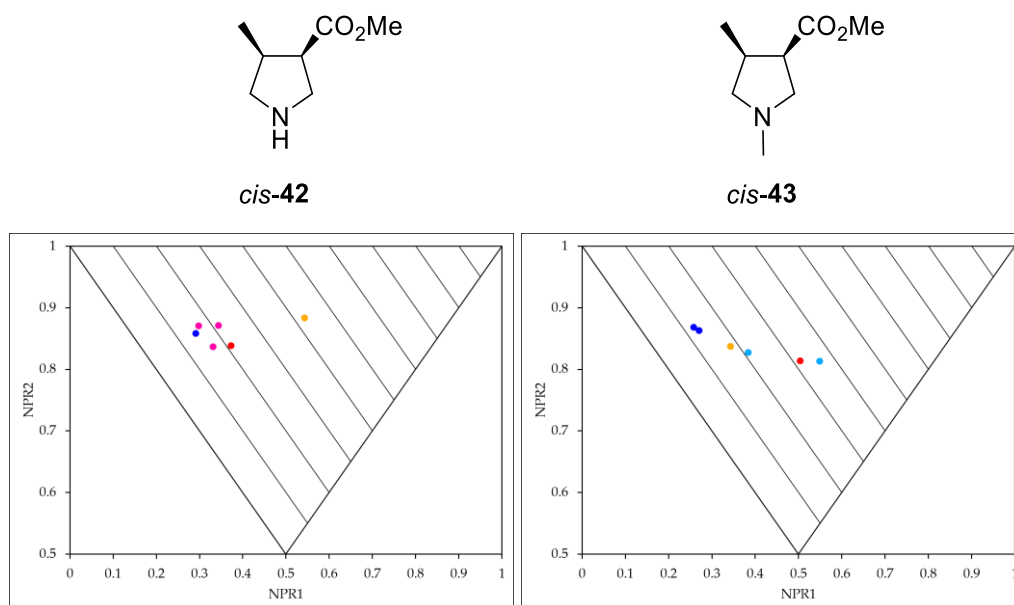
Figure 2.3: Structures and PMI plots of fragments *cis*-**42** and *cis*-**43**

2.1.1 Overview of Previous Synthetic Routes to 3,4-Disubstituted Pyrrolidines

The synthesis of *cis*-3,4-disubstituted monocyclic pyrrolidines is relatively uncommon and there are few synthetic routes available to access them. There are many examples of the synthesis of *cis*-3,4-pyrrolidines which are part of bicyclic systems but there are fewer examples if the substituents are separate. *trans*-3,4-Pyrrolidines are more common in the literature due to the increased number of synthetic routes available.

The most common route to 3,4-disubstituted pyrrolidines was pioneered by Achiwa *et al.* in 1985,[46] where an azomethine ylid was generated *in situ* from easily accessible ylid precursor **25**.[58] The ylid can react with alkenes to give a range of pyrrolidines. For example, treatment of ylid precursor **25** with catalytic TFA in the presence of dimethyl maleate *cis*-**49** gave pyrrolidine *cis*-**50** in 94% yield (Scheme 2.1). TFA converts the hemiaminal in **25** into an iminium and the resulting methoxide can then attack the trimethylsilyl group. This generates the azomethine ylid which undergoes the 1,3-dipolar cycloaddition. One of the key advantages of 1,3-dipolar cycloadditions is that the pericyclic nature of the reaction means

that the pyrrolidine generated is a single diastereomer, retaining the stereochemistry of the alkene.
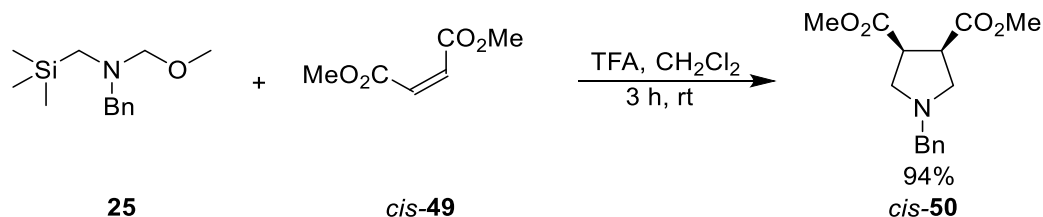
Scheme 2.1

This strategy has been widely employed since the initial report with a variety of electron poor alkenes being utilised. Aromatic groups on the alkene are popular. For example, the use of *p*-bromophenyl alkene *trans*-**51** gave pyrrolidine *trans*-**52** in 85% yield (Scheme 2.2).[59] The cycloaddition is typically performed using alkenes with two electron withdrawing groups attached. However, it can be performed on alkenes with an alkyl group and an electron withdrawing group. Under standard TFA conditions, alkene *cis*-**53** reacted with ylid precursor **25** to give pyrrolidine *cis*-**54** in 41% yield (Scheme 2.2), a significantly lower yield than those reactions involving an alkene with two electron withdrawing groups.
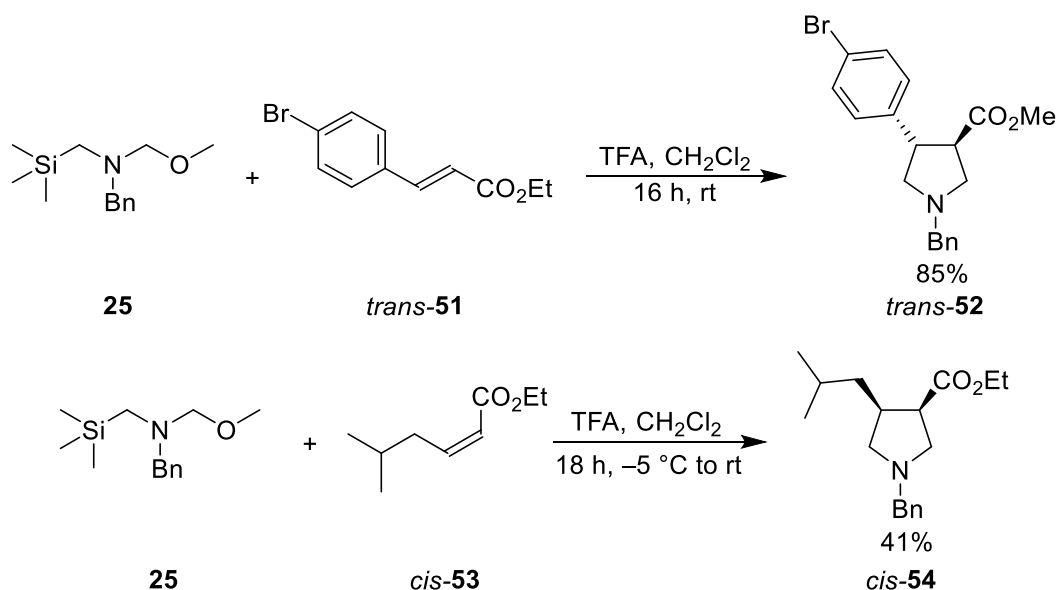
Scheme 2.2

Catalytic TFA with CH_2Cl_2 as solvent has remained the most popular method for 1,3-dipolar cycloadditions using precursor **25**, although others have used fluoride to activate ylid precursor **25**. This was first reported by Dent *et al.* in 1987,[60] where LiF or CsF in MeCN were used. Fluoride caused the decomposition of precursor **25** into the ylid which underwent the 1,3-dipolar cycloaddition with dimethyl maleate *cis*-**49** to give pyrrolidine *cis*-**50** (Scheme 2.3).
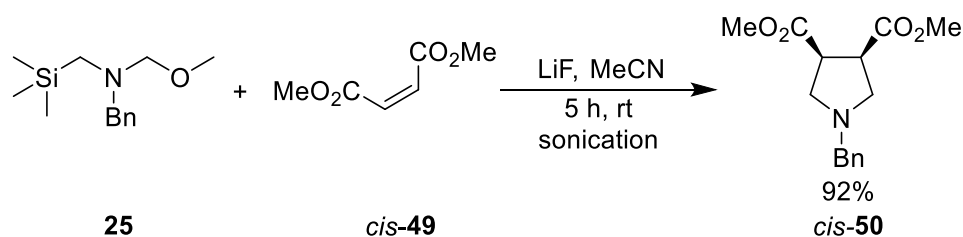
Scheme 2.3

More recently, Lupton *et al.*[61] used benzoyl fluoride as a sacrificial source of fluoride and catalytic DMAP to affect a wide variety of 1,3-dipolar cycloadditions, including reaction with methyl cinnamate *trans*-**55** to give pyrrolidine *trans*-**56** (Scheme 2.4). The reaction proceeds *via* attack of DMAP into benzoyl fluoride to generate fluoride which can then aid the decomposition of ylid precursor **25**.
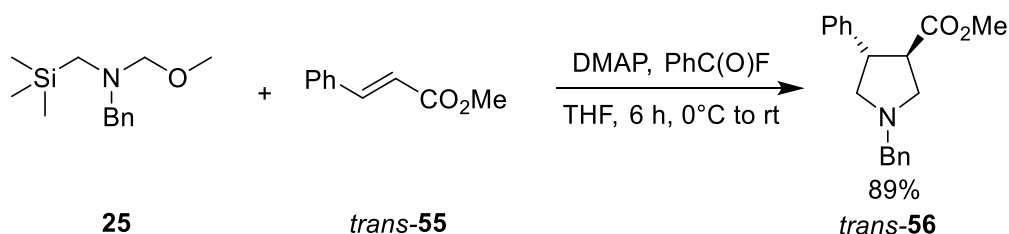
Scheme 2.4

Lupton's work also provided a first example of performing a 1,3-dipolar cycloaddition using precursor **25** with some form of enantioselectivity.[61] Ylid precursor **25** was reacted with alkene *trans*-**57** and a chiral isothiourea catalyst to give enantioenriched pyrrolidine *trans*-**56** in 35% yield and 14% ee (Scheme 2.5). The chiral catalyst adds into the acyl fluoride, generating the fluoride necessary to activate the ylid precursor. The ylid then has two options: either to react with the starting alkene *trans*-**57** or to react with the generated acyl thiourea *trans*-**58**. The acyl thiourea *trans*-**58** showed similar reactivity to the acyl fluoride *trans*-**57**, allowing for some enantioselectivity, but the two pathways were too similar in rate to generate higher levels of enantioselectivity.
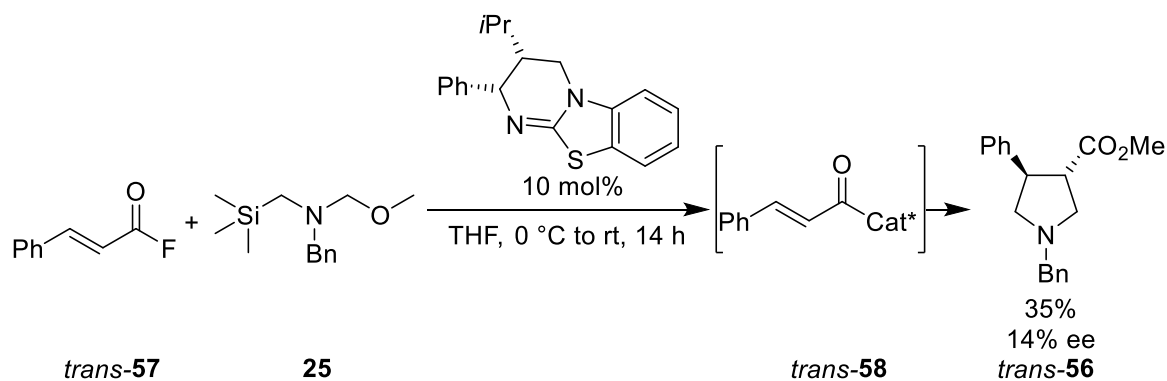
Scheme 2.5

Other ylids can also be generated for use in 1,3-dipolar cycloadditions towards pyrrolidines. *N*-Benzyl hydroxylamine has been reacted with formaldehyde and, under basic conditions, deprotonated to create an ylid. The resulting ylid then performed a 1,3-dipolar cycloaddition with dihydropyrrole **59** to synthesise bicycle **60** (Scheme 2.6).[62] Hydrogenation of bicyclic compound **60** both cleaved the benzyl group and hydrogenated the N-O bond to give 3,4-*cis*-pyrrolidine *cis*-**61**.
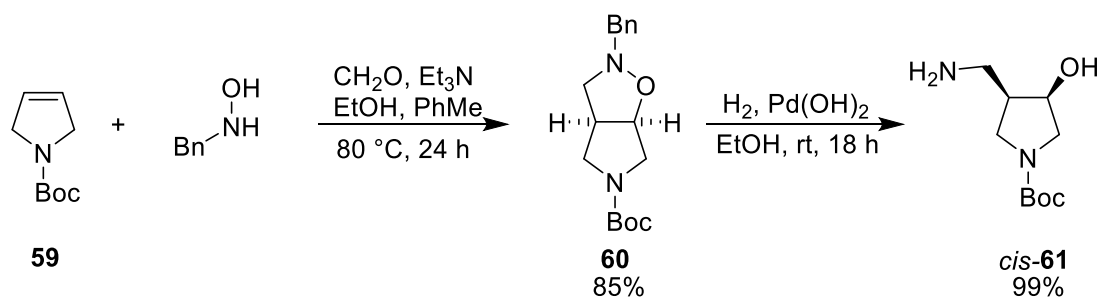
Scheme 2.6

Apart from the 1,3-dipolar cycloaddition strategy, there are few other routes towards monocyclic 3,4-*cis*-disubstituted pyrrolidines. One of those is a route designed by Smith *et al.*[63] where simple 3,4-*cis*-disubstituted pyrrolidines were synthesised as single enantiomers. The strategy involved the synthesis of building block **63** from acids **62** *via* ozonolysis and Wittig olefination or Grubbs metathesis. Intermediates **63** then underwent cyclisation to an intermediate bicycle by enolate conjugate addition and subsequent tetramisole-assisted lactone formation. The bicycle readily ring-opens to give pyrrolidines *cis*-**64** (Scheme 2.7). While this process can be telescoped using the Grubbs route and the enantioselectivity is good, the key limitation of this route is that pyrrolidines *cis*-**64** represent the simplest pyrrolidine that can be synthesised using this methodology.
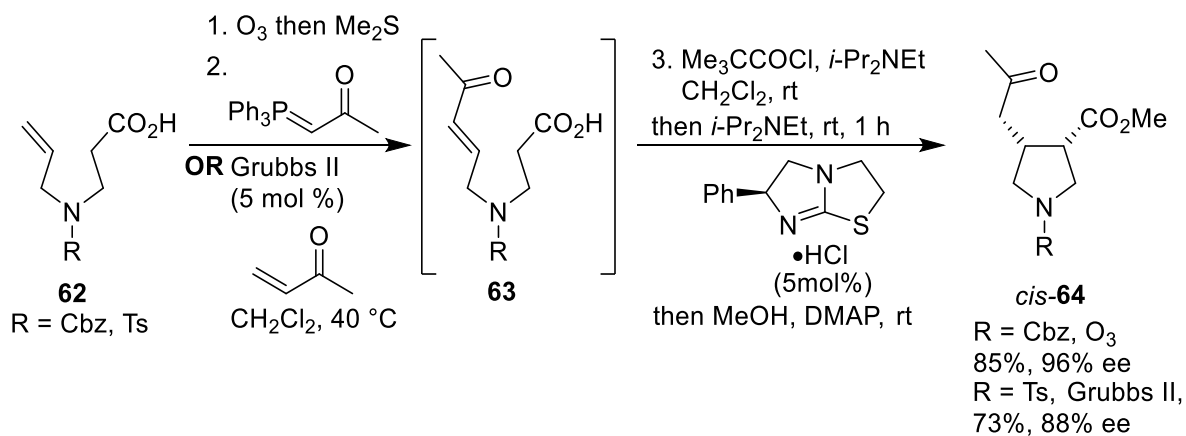
Scheme 2.7

Alternative routes to synthesise 3,4-disubstituted pyrrolidines with similar substituents include the zinc–based strategy of Chemla *et al.*[64] The zinc-mediated cyclisation of amines such as amine **65** can be used to generate a variety of *trans*-3,4-pyrrolidines in moderate yields. Treatment of amine **65** with LDA and ZnBr$_2$ gave pyrrolidine *trans*-**66** in 40% yield (Scheme 2.8). Zinc coordinates to the alkene, allowing for enolate addition into the alkene and generation of the pyrrolidine. The coordination of the zinc locks the conformation to give high diastereoselectivity in the cyclisation.
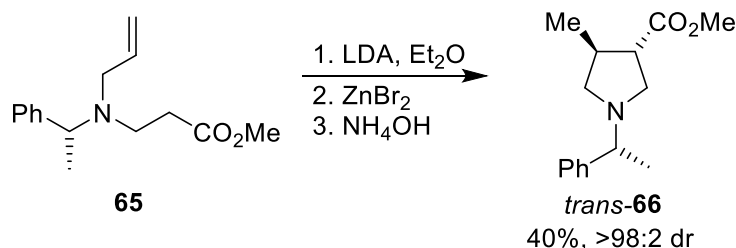
Scheme 2.8

Rinaldi *et al.* used enolate alkylation of 4-substituted pyrrolidine-2-ones to generate a 3,4-substitution pattern and then reduced out the lactam carbonyl to generate *trans*-3,4-pyrrolidines.[65] For example, pyrrolidinone **67** was deprotonated and then trapped with *i*-butyl iodide to synthesise pyrrolidinone **68**, which was then reduced with LiAlH$_4$ to give the desired pyrrolidine *trans*-**69** (Scheme 2.9). This approach is attractive due to the high level of diastereoselectivity.
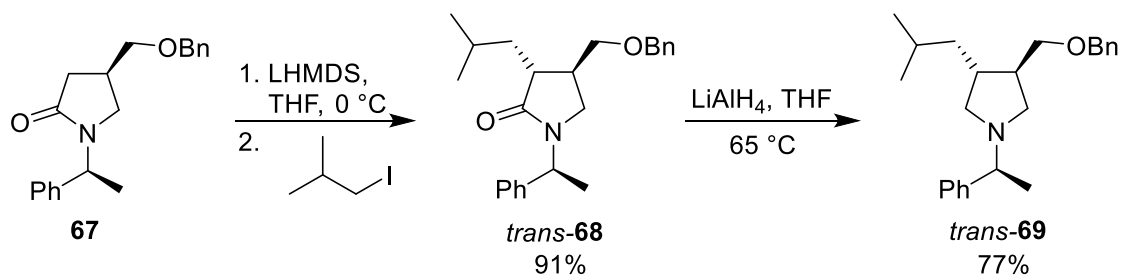
Scheme 2.9

Epoxidation followed by ring opening and Mitsunobu reaction is a popular alternative strategy to synthesise both *cis*- and *trans*-3,4-disubstituted pyrrolidines.[66,67] An example of this methodology is shown in Scheme 2.10.[68,69] Epoxide **70** was ring-opened with a vinyl cuprate to give pyrrolidine *trans*-**71**. The versatility of hydroxypyrrolidines such as *trans*-**71** was then demonstrated as the alcohol was converted directly into a fluoro-pyrrolidine by treatment with perfluorobutanesulfonyl fluoride to give pyrrolidine *cis*-**72**.[69]
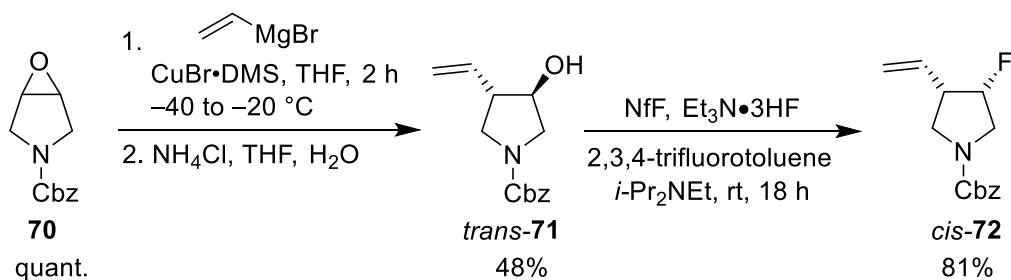
Scheme 2.10

Another strategy to 3,4-*trans*-pyrrolidines proceeded *via* dihydropyrrole **74** (Scheme 2.11).[70] Reduction of oxopyrrolidine **73** with NaBH$_3$CN gave the hydroxypyrrolidine, which was then eliminated using Mitsunobu conditions to give dihydropyrrole **74** in 90% yield over two steps. Dihydropyrrole **74** then acted as a Michael acceptor to synthesise pyrrolidine *trans*-**75** albeit in only 13% yield after chromatography.
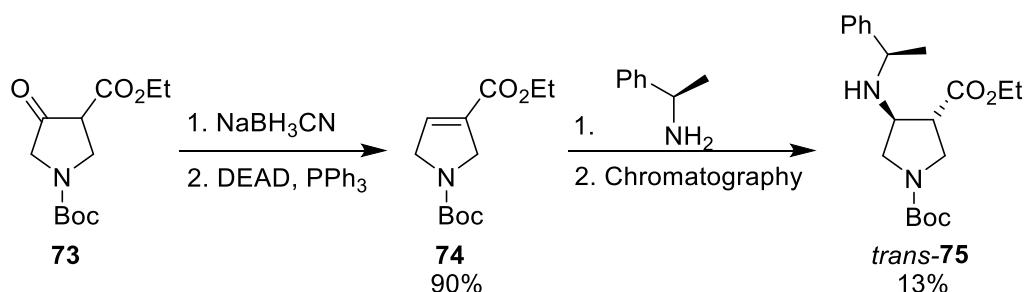
Scheme 2.11

Other methods for the synthesis of simple 3,4-*cis*-pyrrolidines include the use an Upjohn dihydroxylation, which gave diol *cis*-**77** from dihydropyrrole **76** (Scheme 2.12).[71] These alcohol groups can then be further manipulated to give a variety of *cis*-3,4-disubstituted pyrrolidines.
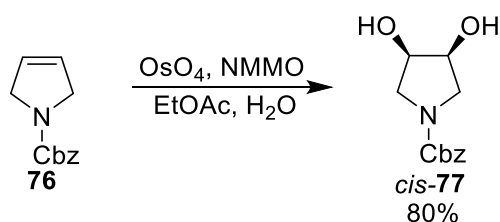
Scheme 2.12

During the course of this thesis, Bull *et al*. released work detailing a novel approach to the synthesis of 3,4-disubstituted pyrrolidines using C-H activation *via* palladium catalysis and a directing group.[72] The aminoquinoline amide in pyrrolidine **78** directed the palladium to perform a C-H insertion both regio and diastereoselectively. This then coupled with the aryl iodide to give pyrrolidine *cis*-**79** (Scheme 2.13). It was shown that a wide variety of aryl groups could be used, including heteroaryl groups. In addition, the directing group could be

removed to give a variety of medicinally-relevant functional groups including alcohols, esters, acids and amides.
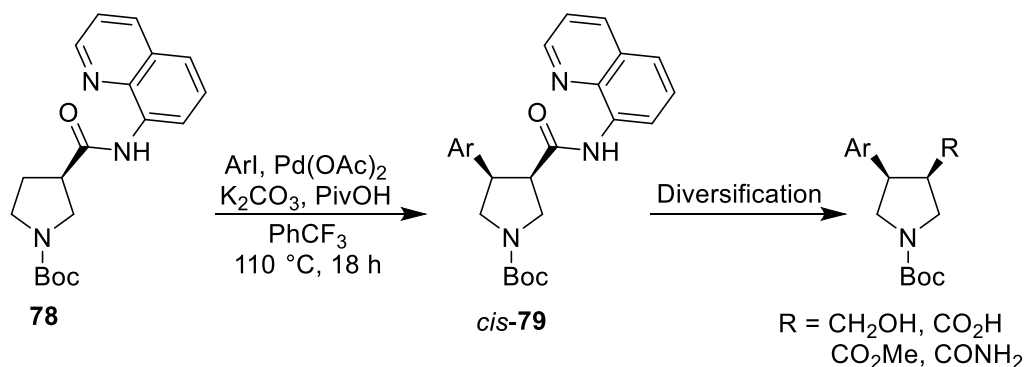
Scheme 2.13

Perhaps surprisingly, pyrrole reduction or hydrogenation is not used in the synthesis of simple 3,4-disubstituted pyrrolidines. However, reduction has been used in the synthesis of pyrrolidines with different or more complex substitution patterns such as pyrrolidine *cis*-**81**. In this case, Birch reduction of pyrrole **80** with lithium in ammonia followed by trapping of the resultant enolate intermediates with alkyl iodides gave access to 3,3,4,4-tetrasubstituted pyrrolidines in good yield (Scheme 2.14).
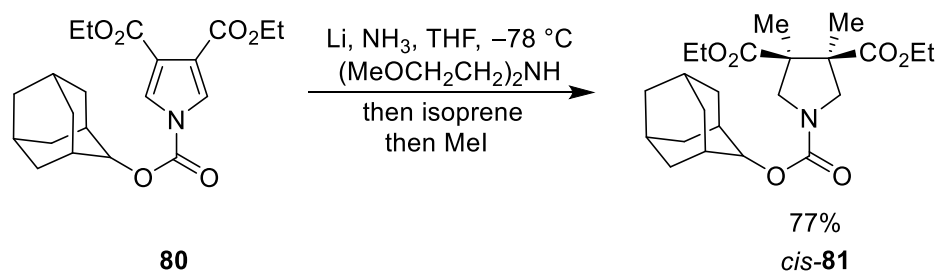
Scheme 2.14

2.1.2 1,3-Dipolar Cycloaddition Route

After considering a number of potential synthetic routes towards the 3,4-*cis*-disubstituted fragments, it was decided to first explore a 1,3-dipolar cycloaddition route. Initially, it was proposed to synthesise fragments *cis*-**42** and *cis*-**43** from benzylated pyrrolidine *cis*-**82**. Pyrrolidine *cis*-**82** would be synthesised *via* a cycloaddition involving silyl methoxyamine **25** and *cis*-methyl crotonate. This route would yield fragment *cis*-**42** in just two steps from **25**. However, some initial work on this route performed by another group member revealed that the required alkene was volatile and difficult to work with, as well as not being commercially available.[73] They were able to synthesise only a small amount of fragment *cis*-**42** *via* this diastereospecific route, although this could be used to confirm the stereochemistry of later syntheses. An alternative route was therefore proposed, using the corresponding

alkyne instead of the alkene. Use of an alkyne in the cycloaddition would give dihydropyrrole **83** and would add no extra steps to the synthesis, as it was anticipated that both the hydrogenation of the alkene and the hydrogenolysis of the benzyl group could be performed in one step (Scheme 2.15).
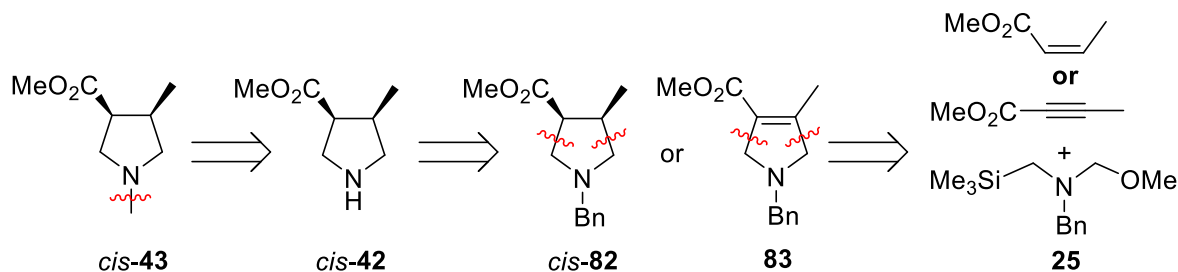
Scheme 2.15

To start, silyl methoxyamine **25** was synthesised *via* a simple two-step process. The first step was the reaction of benzylamine with chloromethyl trimethylsilane to give intermediate **85**. Using a procedure from Yarovskaya *et al*.,[74] benzylamine was reacted with (chloromethyl)trimethylsilane **84** in MeCN to give silyl amine **85** in 42% yield after chromatography (Scheme 2.16). Although the reaction was successful, an alternative route was sought due to the low yield. Sieburth *et al.* had reported the use of DMSO as solvent.[58] Performing the reaction by heating silane **84** and benzylamine at 80 ºC for 18 h in DMSO, followed by purification *via* chromatography gave silyl amine **85** in 73% yield (Scheme 2.16). Silyl amine **85** was then reacted with stoichiometric formaldehyde and methanol at rt for 4 h to yield methoxyamine **25** as a sufficiently pure crude product in 79% yield (Scheme 2.16). Both reactions proved amenable to scaling up, allowing for the synthesis of more than 5 g of silyl methoxyamine **25** in one run.
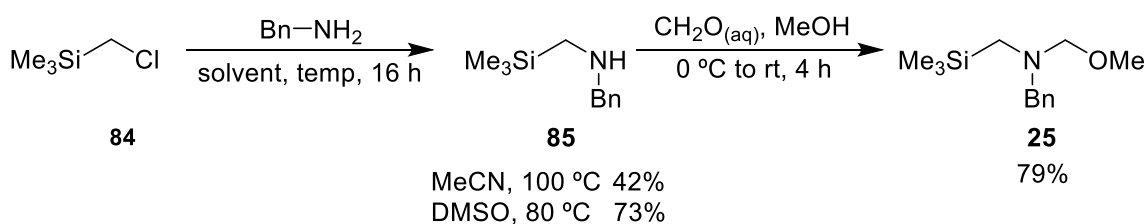
Scheme 2.16

With intermediate **25** in hand, it was now possible to investigate the key 1,3-dipolar cycloaddition step. Initial attempts used conditions reported by Yarovskaya *et al*.[74] Alkyne **86** was added dropwise to methoxyamine **25** and TFA at 0 ºC then stirred at rt for 16 h. Work-up and purification yielded the desired dihydropyrrole **83** in 32% yield (Scheme 2.17).
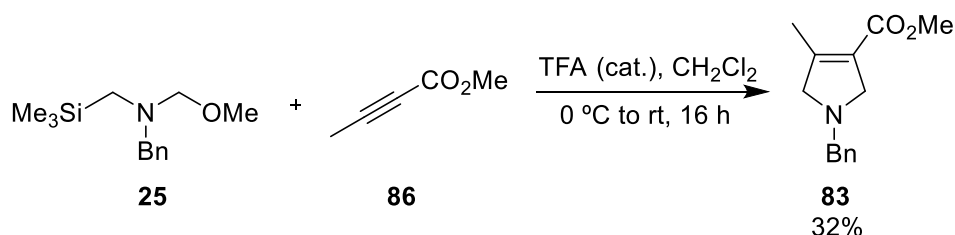
Scheme 2.17

Hydrogenation of dihydropyrrole **83** was expected to result in saturation of the double bond and removal of the *N*-benzyl protecting group. Hydrogenation of dihydropyrrole **83** was undertaken with 10% Pd/C under an H_2 atmosphere at rt for 16 h. After filtering through Celite and solvent removal, ^{1}H NMR spectroscopy showed evidence of the desired fragment *cis*-**42**. However, mass recovery was poor and attempts to remove the last traces of solvent resulted in no product *cis*-**42** being recovered (Scheme 2.18).
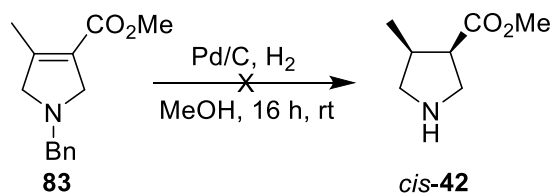
Scheme 2.18

Now knowing that the hydrogenation would require optimisation, alternative reaction conditions for the cycloaddition were sought to increase the yield and bring through larger quantities of material. There was a report of carrying out the reaction in THF[75] instead of CH_2Cl_2, with otherwise identical conditions and on similar scale (<200 mg). Pleasingly, this improved the yield from 32% to 48% (Scheme 2.19). Further optimisation to improve the yield of the cycloaddition and hydrogenation was desired, so it was decided to use alkyne **87** with an ethyl ester, which was substantially less expensive. Performing the same dipolar cycloaddition using the ethyl ester gave dihydropyrrole **88** in a 56% yield (Scheme 2.19).
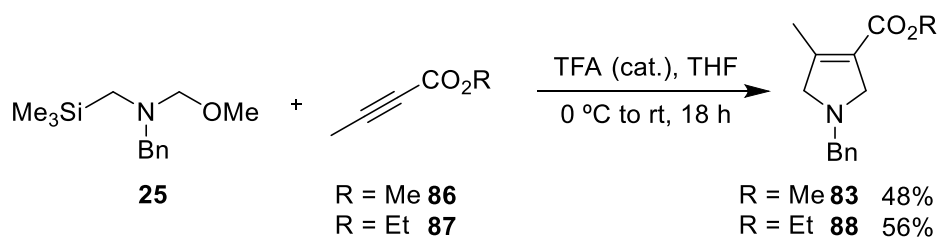
Scheme 2.19

With the reaction in THF appearing promising the reaction was scaled up. However, it quickly became apparent that on larger scale ($\geq$ 0.5 g), the yields of the cycloaddition dropped significantly to 20-25% for both ethyl ester dihydropyrrole **88** and methyl ester dihydropyrrole **83**. The reactions were repeated a number of times with similar results. During purification by chromatography, a significant amount of a by-product was isolated. ^{1}H NMR spectroscopy showed a mixture of three compounds that displayed trimethylsilyl, aromatic and methoxy peaks but we were unable to assign the structures of any of these compounds. The signals in the ^{1}H NMR spectrum indicated that these by-products were formed from side-reactions of the methoxyamine **25**.

With this reaction not working as well as expected on scale, alternative conditions were explored. Lupton *et al.* had reported the use of DMAP and a sacrificial source of fluoride to give high yields in these types of dipolar cycloadditions (see Scheme 2.4).[61] It was decided to repeat the literature example with alkyne **89**, which was reported to give a 90% yield of dihydropyrrole **90**. In our hands, reaction of alkyne **89** with methoxyamine **25** using benzoyl fluoride and catalytic DMAP in THF gave an 86% yield of dihydropyrrole **90** (Scheme 2.20). Now confident with these conditions, they were then used with methyl-substituted alkyne **86**. However, purification by chromatography proved difficult as TLC showed that at least eight different compounds were present in the reaction mixture and ^{1}H NMR spectroscopy of the crude product showed no evidence of the desired product **83** (Scheme 2.20).
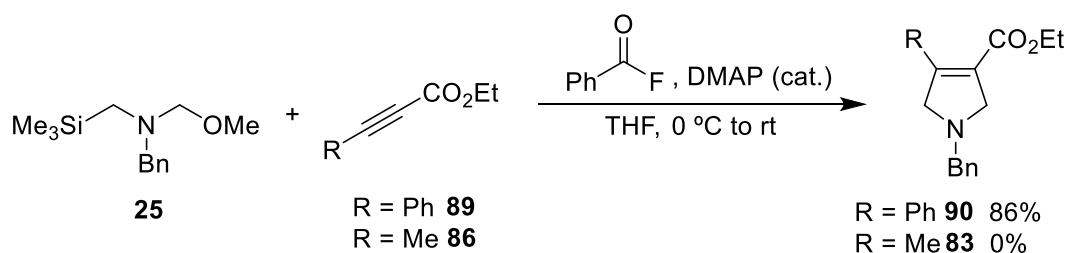
Scheme 2.20

It was hypothesised that the reason the cycloaddition step was proving so difficult was the electron density of the alkyne compared to other examples in the literature. There are no known examples of alkynes used in these 1,3-dipolar cycloadditions that contain at least one simple alkyl substituent. Aryl, ester, CF_3 and SF_5 substituents have been used previously, all of which help reduce the electron density on the alkyne. The most similar example of this reaction to ours was performed by both Achiwa *et al.*[46] and at UCB.[76] In the hands of Achiwa *et al.*, alkyne **91** reacted with methoxyamine **25** to give dihydropyrrole **92** in 58% yield

(Scheme 2.21). At UCB, the reaction was performed on larger scale (40 mmol of alkyne **91**) for a slightly shorter time and a significantly lower yield of 29% was obtained (Scheme 2.21). These examples also give further evidence of the reduced yields in dipolar cycloadditions when the scale is increased.

3 h, 6 mmol	58%
2.5 h, 40 mmol	29%
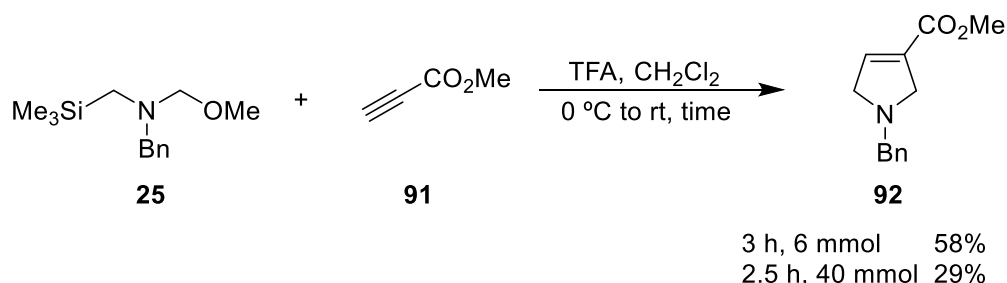
Scheme 2.21

It was therefore decided to stop further optimisation of the cycloaddition step and move on to the hydrogenation. Transfer hydrogenation with ammonium formate has been used by our group with success in the past, so it was decided to attempt the hydrogenation of dihydropyrrole **83** using the group conditions.[77] Ammonium formate and $Pd(OH)_2$ were added to dihydropyrrole **83** and the mixture refluxed in methanol for 4 h (Scheme 2.22). However, after the reaction only ammonium formate was recovered.
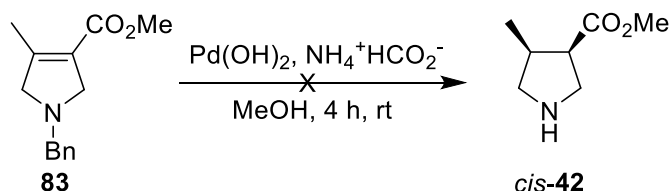
Scheme 2.22

Through the evaporation of solvent and drying on the high vacuum line in both this reaction and the hydrogenation shown in Scheme 2.22, it was realised that the desired pyrrolidines *cis*-**42** and *cis*-**43** were volatile. Now knowing this, and with the intermediate dihydropyrroles **83** and **88** being valuable compounds, it was decided to optimise the hydrogenation conditions on a model system.

Proline derivative (*S*)-**94** was chosen as the model system due to its availability and similarity to dihydropyrrole **83** both in molecular weight and functionality. Using a literature procedure,[78] synthesis of (*S*)-**94** proceeded *via* esterification of proline (*S*)-**93** with acetyl chloride and methanol followed by protection of the nitrogen with benzyl bromide (Scheme 2.23).
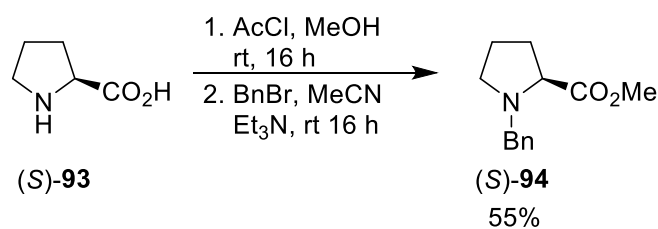
Scheme 2.23

With pyrrolidine (*S*)-**94** now in hand, conditions were considered that would allow for handling of the volatile product. Two strategies were identified: immediate hydrochloride salt formation to yield salt (*S*)-**95**•HCl or immediate Boc protection to give a non-volatile, isolable compound followed by deprotection to form the same salt (*S*)-**95**•HCl. In both routes, pyrrolidine (*S*)-**94** would be subjected to transfer hydrogenolysis by Pd(OH)$_2$ in methanol and then filtered through Celite to remove the catalyst. The solution would then either be subjected to HCl in Et$_2$O or Boc protection conditions (Scheme 2.24).
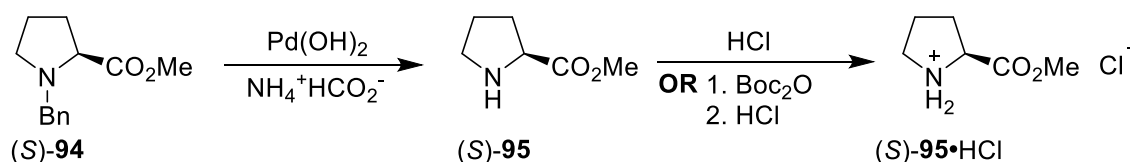
Scheme 2.24

The Boc protection route was attempted first. Pyrrolidine (*S*)-**94** was stirred with ammonium formate and 5% Pd(OH)$_2$ at reflux for 3 h in methanol and then filtered through Celite. Reaction with Boc$_2$O and Et$_3$N (1.3 eq) at rt for 16 h gave very poor mass recovery and there was no evidence of *N*-Boc pyrrolidine (*S*)-**96** by ^{1}H NMR spectroscopy. Surprised at the lack of mass recovery, the reaction was re-attempted while increasing the number of equivalents of Et$_3$N in the Boc protection step from 1.3 to 6 eq and adding catalytic DMAP. Under the new conditions, the reaction proceeded to give pyrrolidine (*S*)-**95** in 99% yield (Scheme 2.25).
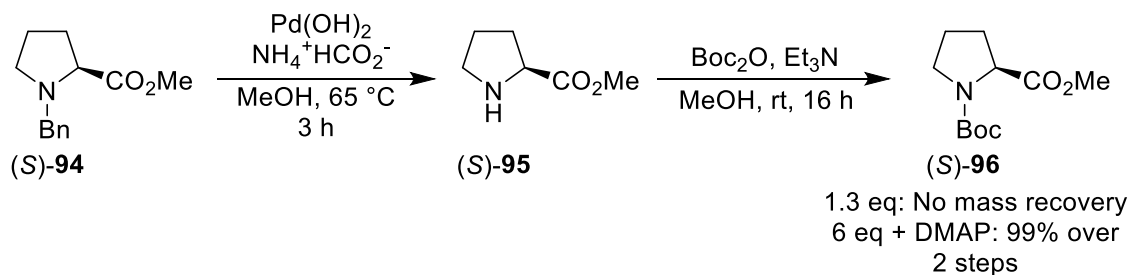
Scheme 2.25

Transfer hydrogenation of pyrrolidine (*S*)-**94** and hydrochloride salt formation using HCl in Et$_2$O was attempted next. However, this resulted in a mixture of a small amount of product (*S*)-**95** and ammonium formate, as shown by ^{1}H NMR spectroscopy (Scheme 2.26). It was therefore decided to proceed *via* formation of the *N*-Boc pyrrolidine (*S*)-**96** as the reaction was working in excellent yield and forming the *N*-Boc as opposed to the NH system meant that chromatography could be performed easily to purify the product after the hydrogenation step.
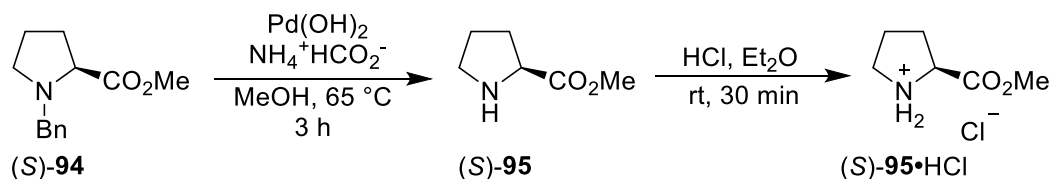
Scheme 2.26

The new protocol was then applied to the real system. Scaling the cycloaddition up to 0.5 g of methoxyamine **25** resulted in the reaction giving a 24% yield of dihydropyrrole **83**. Hydrogenation of dihydropyrrole **83** followed by Boc protection gave a 90:10 mixture (by ^{1}H NMR spectroscopy) of desired pyrrolidine *cis*-**97** and dihydropyrrole **98** after chromatography. Interestingly, this indicated that under these conditions the alkene hydrogenation was occurring slower than the *N*-debenzylation. The 90:10 mixture was then subjected to Pd/C and H$_2$ in MeOH for 16 h to complete the hydrogenation and gave *N*-Boc pyrrolidine *cis*-**97** in 77% yield from dihydropyrrole **83** (Scheme 2.27).
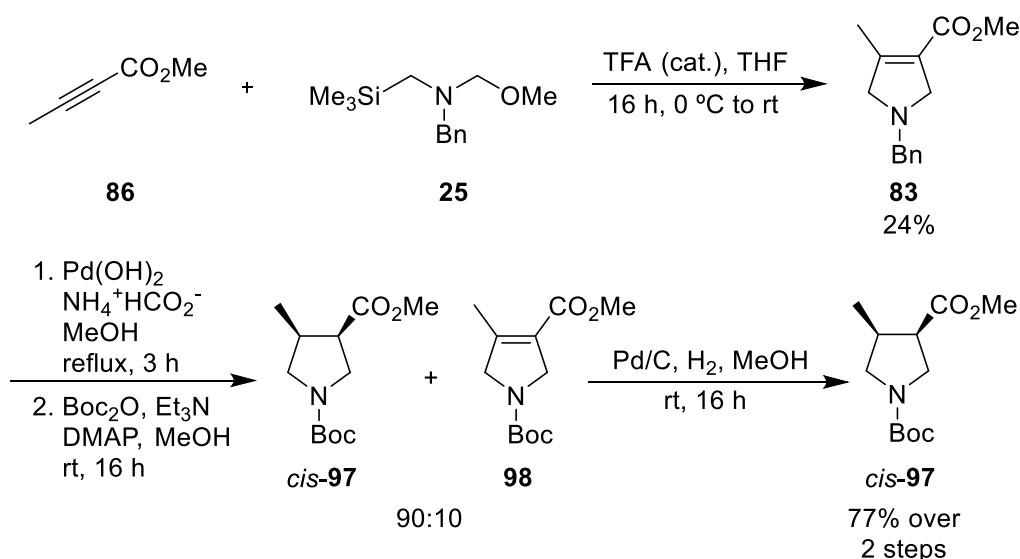
Scheme 2.27

With the *N*-Boc pyrrolidine *cis*-**97** now in hand, it was possible to deprotect and form one of the desired fragments, *cis*-**42**. Adding HCl in Et$_2$O to *cis*-**97** in CH$_2$Cl$_2$ and stirring at rt for 16 h allowed for deprotection to form fragment *cis*-**42**•HCl in 97% yield (Scheme 2.28). The ^{1}H NMR spectrum of *cis*-**42**•HCl displayed broad signals, but there was only one doublet corresponding to the methyl group, suggesting that no epimerisation had occurred.
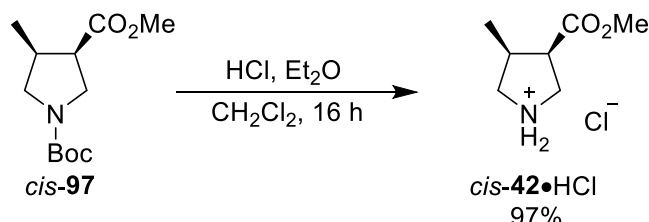
Scheme 2.28

Unfortunately, compound *cis*-**42** proved to be unstable as the hydrochloride salt. This issue occurred with several other fragments synthesised early on in the project. The fragments were shown to be degrading when stored as the HCl salt. It was therefore decided to store fragments as the more stable acetic acid salts in the future. ^{1}H NMR spectra were taken at different time intervals of all fragments to check that no epimerisation or degradation was occurring.

In order to synthesise fragment *cis*-**42** as the acetic acid salt, it was proposed to synthesise dihydropyrrole **83** on a large scale and then hydrogenate using Pd/C and H$_2$ to give fragment *cis*-**42** directly, which could then be converted into the acetic acid salt. Performing the reactions on large scale would help minimise the volatility issues, although the dipolar cycloaddition yield would likely suffer when performed on large scale.

Free base fragment *cis*-**42** was prepared by another member of the group on a large scale (~20 g of methoxyamine **25**) using the optimised route . Despite starting with 20 g of methoxyamine **25**, after purification, only 550 mg (3% yield over 3 steps) of fragment *cis*-**42**•AcOH was isolated. However, this was sufficient to both add the fragment to the library and to give enough material to perform *N*-methylation in order to prepare fragment *cis*-**42**.

Conditions had been optimised in the group for the effective methylation of pyrrolidine fragments using aqueous formaldehyde, sodium triacetoxyborohydride and MgSO$_4$ in 3:1 CH$_2$Cl$_2$–AcOH. Using these reductive amination conditions followed by aqueous work-up and stirring of the resulting organic layer with acetic acid, a 75:25 ratio of acetic acid and fragment *cis*-**43**•AcOH was isolated. Importantly, the acetic acid was added to the organic

layer before removing the solvent, ensuring that minimal loss occurred due to volatility. Despite repeated drying on the high vacuum line, the remaining acetic acid could not be completely removed, so a yield of 41% for the step was calculated, taking into account the remaining acetic acid (Scheme 2.29).

1. CH$_2$O(aq), MgSO$_4$
   NaB(OAc)$_3$, CH$_2$Cl$_2$
   AcOH, rt, 1 h
2. AcOH, CH$_2$Cl$_2$
   rt, 30 min

cis-**42**•AcOH

cis-**43**•AcOH

41%
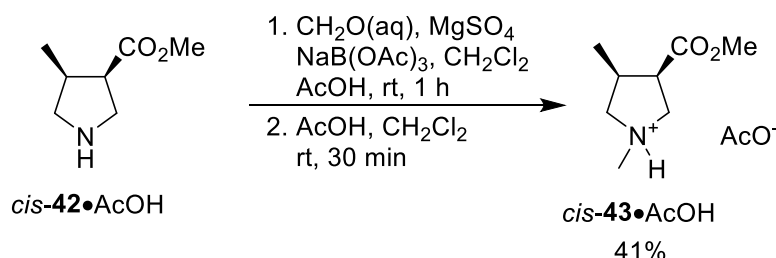
Scheme 2.29

2.1.3 Enol Triflate/Michael Addition Route

An alternative route to fragments *cis*-**42** and *cis*-**43** was also investigated. In particular, we focussed on a route that had the potential to be more readily scaled up. As outlined in Scheme 2.30, it was envisioned that fragments *cis*-**42** and *cis*-**43** could be synthesised from dihydropyrrole **98**. Dihydropyrrole **98** would be generated from triflate **99**, the product of trapping *β*-ketoester **100** as the enol triflate. *β*-Ketoester **100** can in turn be synthesised in one step from *N*-Boc glycine using a literature procedure.[79]

cis-**42**   *cis*-**97**   **98**

99   **100**   **101**
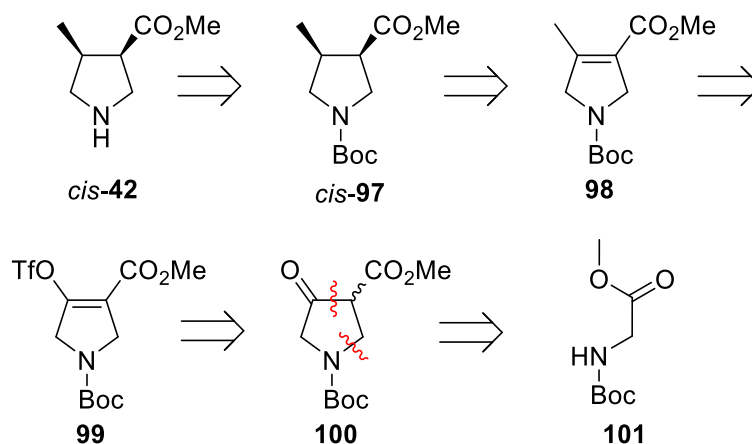
Scheme 2.30

The synthesis of oxopyrrolidines such as **100** *via* a tandem Michael addition/Dieckmann cyclisation of an *N*-carbamyl amino acid ester and an acrylate ester is well described in the literature.[79,80] It was first performed by Rigo *et al.*[80] using an *N*-ethylcarbamate system **102** and later by Schmidt *et al.*[79] using *N*-Boc glycine methyl ester **101** (Scheme 2.31). In each case, the *N*-protected glycine was first deprotonated on the nitrogen. The reaction then proceeded *via* aza-Michael addition to give a diester such as **103** which underwent a

Dieckmann cyclisation. The synthesis of pyrrolidinones **104** and **100** proceeded in ≥ 85% yield with the Dieckmann cyclisation occurring completely regioselectively.
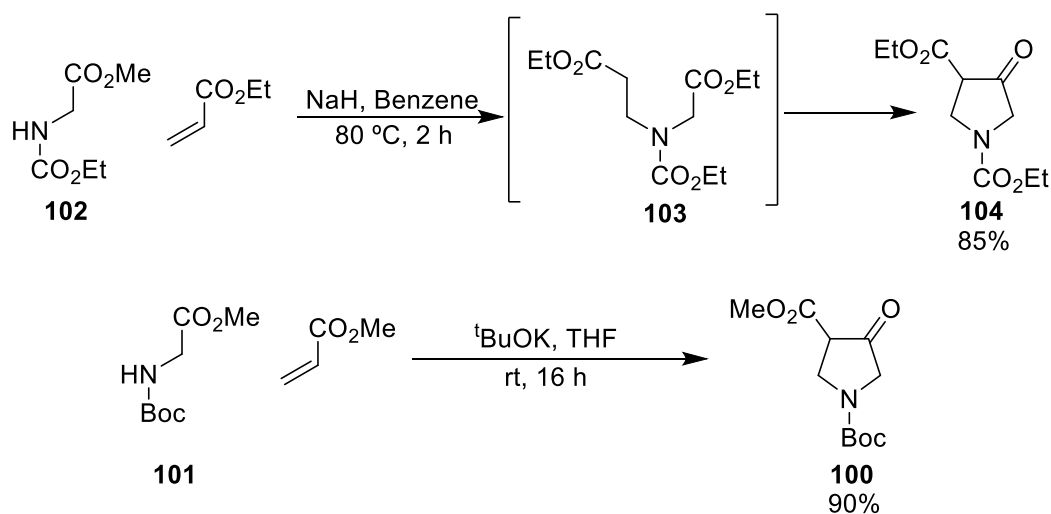
Scheme 2.31

To start our synthetic efforts, glycine methyl ester hydrochloride was Boc protected in near-quantitative yield to give **101**, which was subjected to the same conditions reported by Schmidt *et al.*[79] Work-up and purification by flash column chromatography gave the desired oxopyrrolidine **100** in 90% yield (Scheme 2.32). The ^{1}H NMR spectrum of oxopyrrolidine **100** was complicated and difficult to interpret. The complexity arises from the fact that oxopyrrolidine **100** actually exists as a mixture of keto tautomer **100** and enol tautomer **100a**, and the spectrum is further complicated by *N*-Boc rotamers. Interpretation was made possible by comparison with the literature data[79] and it was concluded that a 50:50 mixture of tautomers **100** and **100a** were formed.
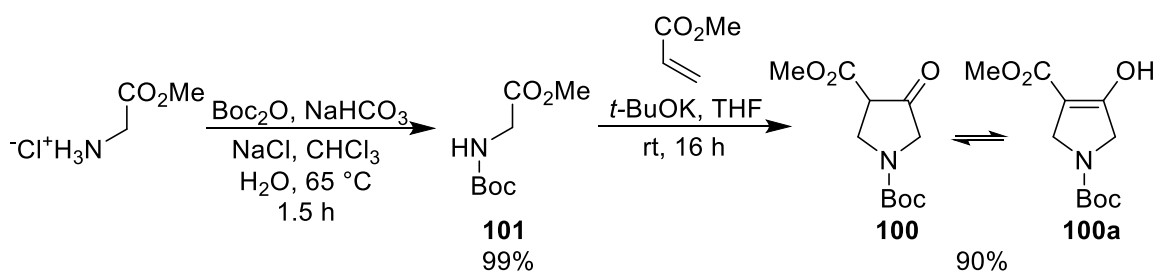
Scheme 2.32

The next step involved conversion of oxopyrrolidine **100** into enol triflate **99**. Burton *et al.* had reported using triflic anhydride and Hünig's base to successfully triflate cyclopentane *β*-keto ester in 92% yield.[81] Using these conditions, reaction of oxopyrrolidine **100** with Hünig's base and triflic anhydride at −78 °C and then at rt gave enol triflate **99** in 71% yield after chromatography (Scheme 2.33).
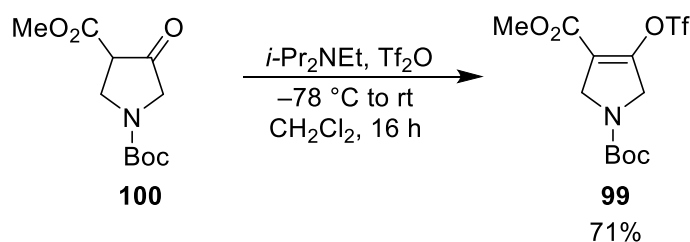
Scheme 2.33

The key step in the proposed fragment synthesis was the triflate substitution reaction. There is precedent for performing cuprate additions on similar triflates. For instance, Tius *et al.*[82] showed that reaction of enol triflate **105** with CuCN and MeLi gave ester **106** in 48% yield (Scheme 2.34). There was no cuprate addition to the product **106**, which could potentially also function as a Michael acceptor. A similar reaction was also performed by Fallis *et al.* on triflate **107**. The cuprate was preformed from MeLi and CuI at 0 °C before reacting with the triflate at –78 °C then at rt. The desired cyclohexene **108** was isolated in 99% yield (Scheme 2.34).
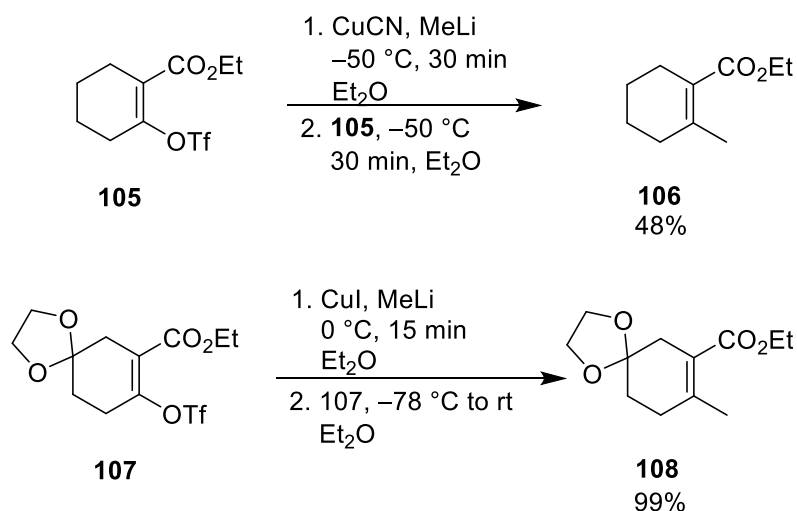
Scheme 2.34

Using the conditions reported by Tius *et al.*, an alkyl cuprate was generated by premixing of 1.4 equivalents of methyl lithium and copper(I) cyanide. Reaction with enol triflate **99** was carried out at –50 °C. ^{1}H NMR spectroscopy of the crude product was very promising, appearing to show an 80:20 mixture of the desired product **98** and detriflated product **109** (Scheme 2.35).
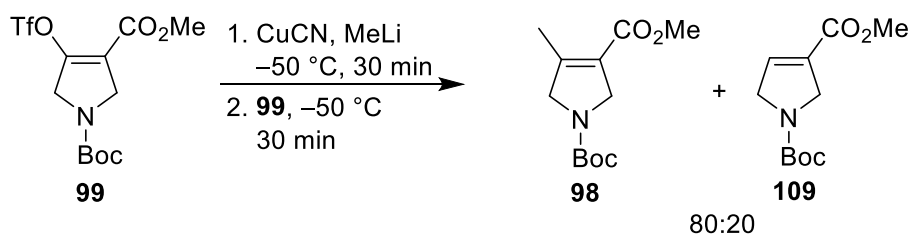
Scheme 2.35

Determination of the ratio of the products was performed by comparison of the diagnostic signals in the ^{1}H NMR spectrum: dihydropyrrole **98** showed a methyl singlet at 2.1 ppm, whereas dihydropyrrole **109** had an alkene signal at 6.7 ppm. Disappointingly, chromatography of the crude mixture did not yield either compounds **98** or **109**. Despite flushing the column, there was little trace of either compound and only half of the crude mass could be recovered which was a mixture of complex products.

With compound **98** proving either unstable on silica or when stored, it was decided to repeat the cuprate addition and attempt to hydrogenate the crude product directly. The cuprate addition gave an 80:20 crude mixture (by ^{1}H NMR spectroscopy) of compounds **98** and **109** after filtration through Celite. This mixture was then treated with 10% Pd/C and H_2 in MeOH at rt for 16 h. However, ^{1}H NMR spectroscopy of the crude product showed the presence of only dihydropyrroles **98** and **109**. The mixture was therefore treated with 10% Pd(OH)$_2$/C and H_2 in MeOH. ^{1}H NMR spectroscopy of the crude product showed a mixture of products including starting dihydropyrrole **98** and desired pyrrolidine *cis*-**97** in an 85:15 ratio as well as other minor products (Scheme 2.36).
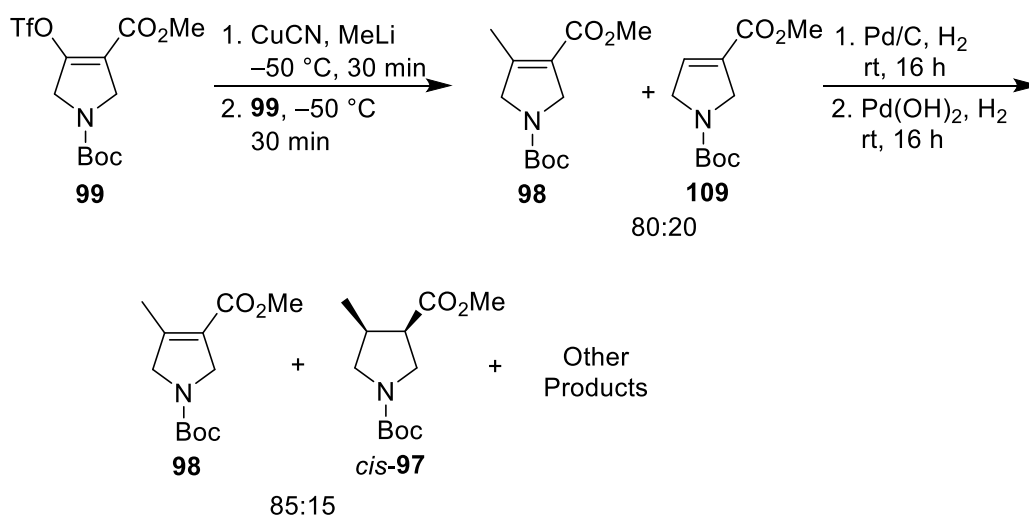
Scheme 2.36

Another member of the group attempted a Negishi coupling on dihydropyrrole triflate **99** using Me$_2$Zn and Pd(PPh$_3$)$_4$ based on a reaction on a tetrahydropyran enol triflate from a

patent by Novartis.[83,84] Treatment of enol triflate **99** with Me$_2$Zn and Pd(PPh$_3$)$_4$ successfully gave the desired dihydropyrrole **98** in 81% yield. However, the hydrogenation step proved more challenging. Reaction with 10% Pd/C and H$_2$ in MeOH for 16 h showed no conversion of dihydropyrrole **98** into the desired pyrrolidine *cis*-**97** (Scheme 2.37).
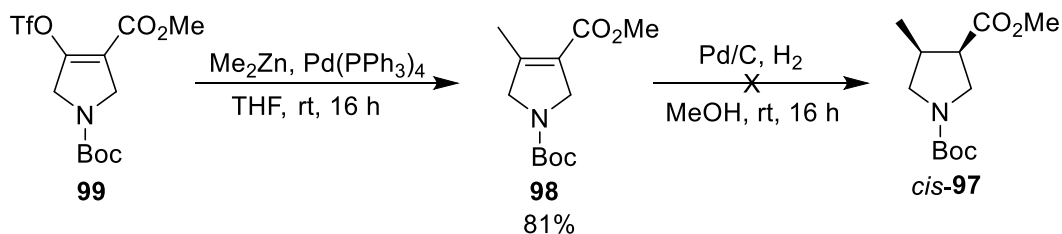
Scheme 2.37

At this point, due to our lack of success, this approach to fragments *cis*-**42** and *cis*-**43** was abandoned. Further work could have been focussed on the hydrogenation step. However, since the 1,3-dipolar cycloaddition route described in Section 2.1.2 had been successful, no further work was carried out on the synthesis of fragments *cis*-**42** and *cis*-**43**.

2.2 Synthesis of 2,4-Disubstituted Pyrrolidine Fragments

The structures of two 2,4-disubstituted pyrrolidines to be synthesised (*trans*-**37** and *cis*-**37**) are shown in Figure 2.4.
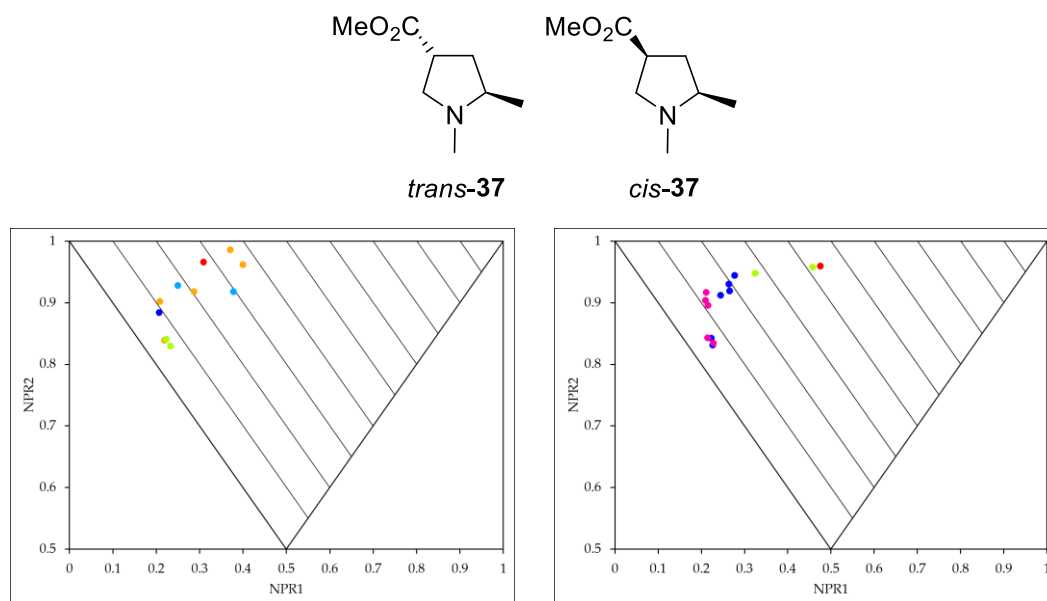
Figure 2.4: The two 2-4 disubstituted pyrrolidines to be synthesised and their PMI plots

Despite the fact that fragments *trans*-**37** and *cis*-**37** both appear relatively simple, they were both novel compounds and would therefore require carefully chosen synthetic routes. Initially, it was uncertain whether the best approach would be to synthesise a mixture of the two diastereomers, which would then be separated by chromatography, or to attempt to synthesise each fragment selectively by a separate route. A third potential strategy would be to synthesise one of the two diastereomers and then explore epimerisation to access the other. A detailed literature review was therefore undertaken to assess which strategy would be most attractive.

2.2.1 Overview of Previous Synthetic Routes to 2,4-Disubstituted Pyrrolidines

2,4-Disubstituted pyrrolidines are a relatively uncommon substitution pattern, despite such compounds having been shown to be useful proline-type chiral catalysts.[85] The synthesis of 2,4-disubstituted pyrrolidines with an ester at the 2-position often starts from derivatives of pyroglutamic acid such as **110**, which is commercially available as either enantiomer. Enolate chemistry can then be used to attach substituents at the 4-position. For instance, deprotonation of pyroglutamate **110** using LHMDS followed by trapping with methyl iodide gave a separable mixture of pyrrolidinone *trans*-**111**, pyrrolidinone *cis*-**111** and pyrrolidinone **112** (Scheme 2.38).[86] The slight *trans*-selectivity potentially arises from the alkylation occurring on the less sterically hindered face, opposite to the ester.
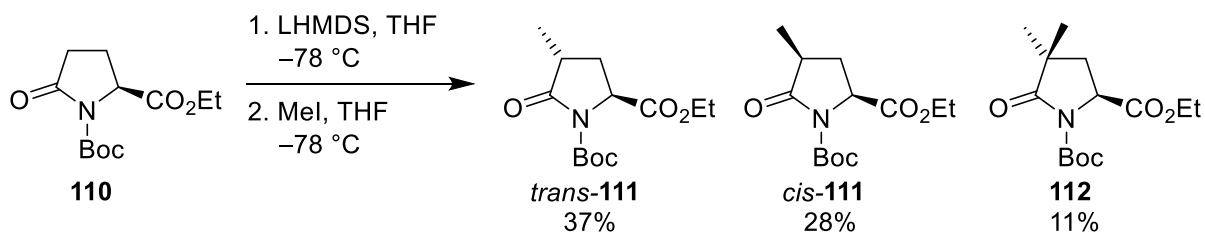
Scheme 2.38

A different approach was used to synthesise pyrrolidinone *cis*-**115**.[87] Reaction of pyroglutamate **113** with Bredereck's reagent gave intermediate enamine **114**. Mechanistically, Bredereck's reagent works by generating tBuO⁻ which can then deprotonate the pyrrolidinone. The enolate then adds into the generated amidinium cation and the resulting aminal then breaks down to give enamine **114**. Hydrogenation of enamine **114** gave pyrrolidinone *cis*-**115** (Scheme 2.38). Presumably, enamine hydrogenation, E1cB-type elimination of the NMe_2 group, and then hydrogenation of the so-generated alkene on the face opposite to the ester group accounts for the formation of *cis*-**115**.
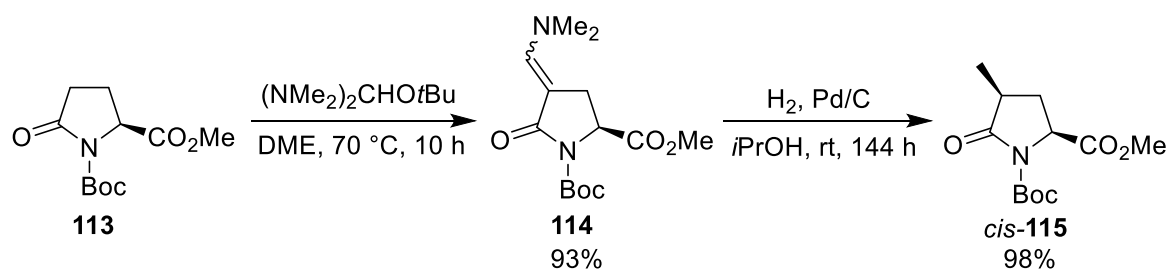
Scheme 2.38

Another popular starting material for the synthesis of 2,4-disubstituted pyrrolidines is 4-hydroxyproline or derivatives thereof. The hydroxy group has been used in Mitsunobu reactions to introduce a variety of groups stereospecifically. For example, diphenylphosphoryl azide is a source of azide which, under Mitsunobu conditions, reacted with pyrrolidine *cis*-**116** to give pyrrolidine *trans*-**117** (Scheme 2.39, yield not given).[88] Pyrrolidine *trans*-**116** is also available and can be subjected to similar reactions. For example, electrophilic fluorination of pyrrolidine *trans*-**116** with DAST generated 4-fluoropyrrolidine *cis*-**118** in quantitative yield (Scheme 2.39).[89]
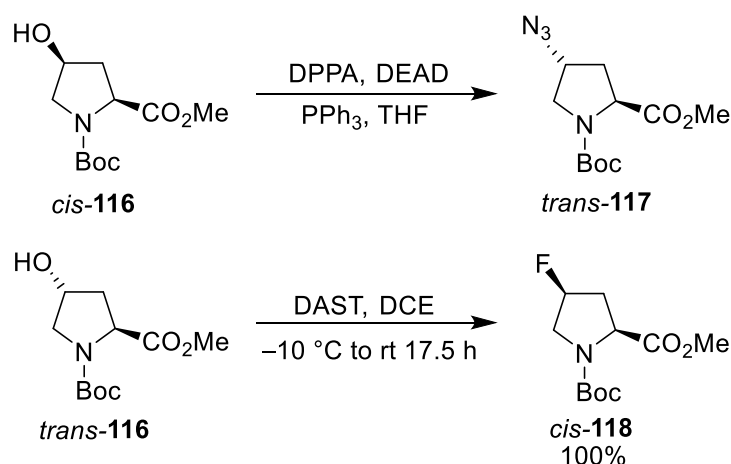
Scheme 2.39

4-Hydroxyproline *trans*-**119** has been used in the synthesis of pyrrolidine *trans*-**124** *via* a long synthetic route. The synthesis from Barbas *et al.* is shown in Scheme 2.40 and shows a variety of intermediate 2,4-disubstituted pyrrolidines *en route* to pyrrolidine *trans*-**124**.[85] Key steps included the inversion of pyrrolidine *trans*-**120** to pyrrolidine *cis*-**121** using TsCl and NH$_4$OAc followed by a second inversion which used mesyl chloride and sodium cyanide to form pyrrolidine *trans*-**123** from pyrrolidine *cis*-**122**. The synthesis of *trans*-**124** occured in an overall yield of 23% over 13 steps, a very lengthy synthesis for such a seemingly simple molecule.
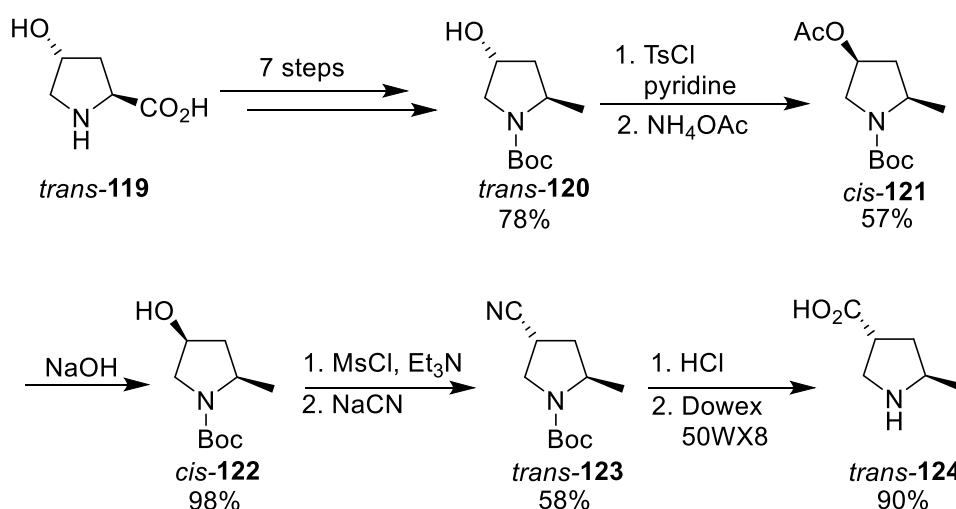
Scheme 2.40

Structurally-related pyrrolidines, such as *trans*-**127** and *cis*-**127**, can be synthesised using a Claisen condensation approach. Trapping of the enolate derived from *N*-benzyl pyrrolidinone **125** using ethyl chloroformate generated intermediate pyrrolidinones **126**, which were then globally reduced using LiAlH$_4$ to give pyrrolidines *cis*-**127** and *trans*-**127**

(Scheme 2.41).[90] The lack of diastereoselectivity could be due to enolisation of the acidic 'malonate-type' proton of pyrrolidinone **126** leading to facile epimerisation.
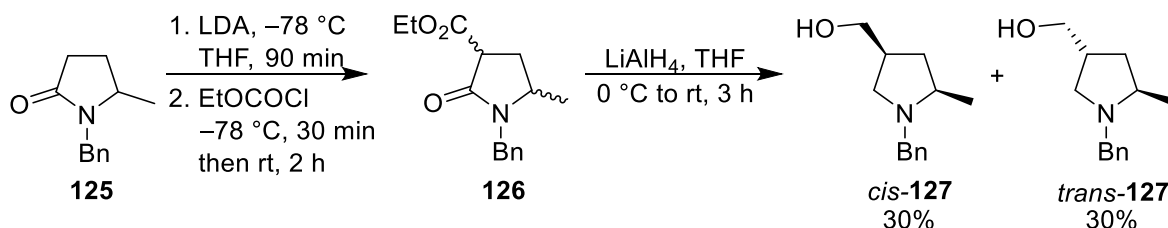
Scheme 2.41

Similarly, Claisen condensation of *N*-Boc pyrrolidinone **128** using ethyl chloroformate was used in the synthesis of pyrrolidines **130**.[91] Pyrrolidinone **128** was subjected to LHMDS followed by ethyl chloroformate trapping to give pyrrolidinones **129**. Selective reduction of pyrrolidinones such as **129** can be difficult due to the presence of carbamate, amide and ester carbonyl groups. In this case, the Boc group was removed and the amide *O*-alkylated using Meerwein's salt before reduction. This process gave a 50:50 mixture of diastereomeric pyrrolidines **130** in 74% yield over 3 steps (Scheme 2.42).
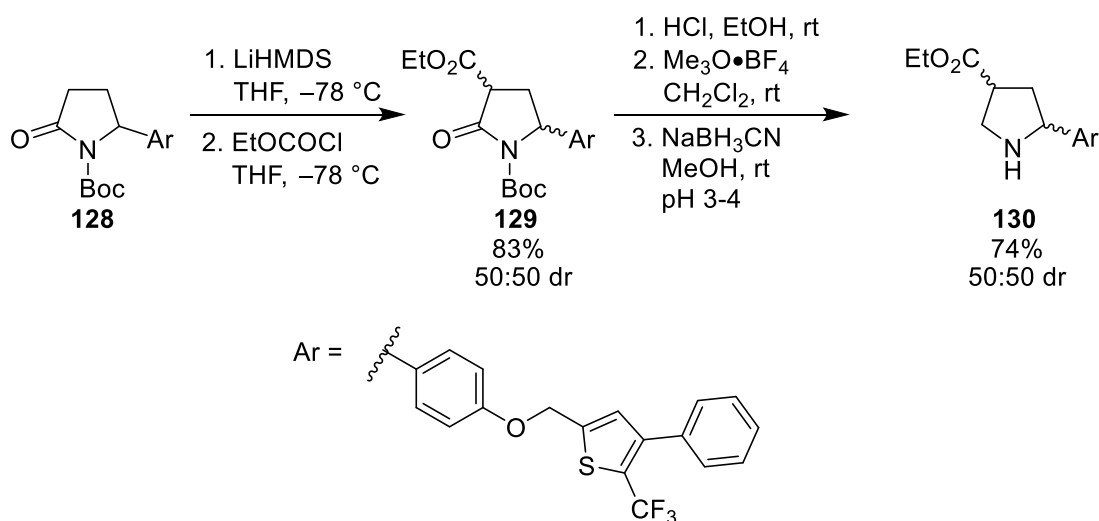
Scheme 2.42

In 2017, some time after we had begun our attempts at the synthesis of the target 3-D fragments *trans*-**37** and *cis*-**37**, Tanaka *et al.* showed that 2-alkyl-4-carboxypyrrolidines such as *cis*-**124** could be synthesised in a simple two-step process.[92] Stereocontrolled nitro-aldol addition of nitromethane to Michael acceptor **131** using a chiral thiourea catalyst generated intermediate **132** in 75% yield and an impressive 97% ee. Hydrogenation of intermediate **132** with Pd/C and H_2 then gave pyrrolidine *cis*-**124** in 90% yield (Scheme 2.43). The hydrogenation first reduces the nitro group to an amine, which then cyclised onto the pendant ketone. This gives a cyclic imine that can also be hydrogenated, allowing for the rapid

generation of 2,4-disubstituted pyrrolidines. The reason for such high diastereoselectivity was not commented on in the paper.
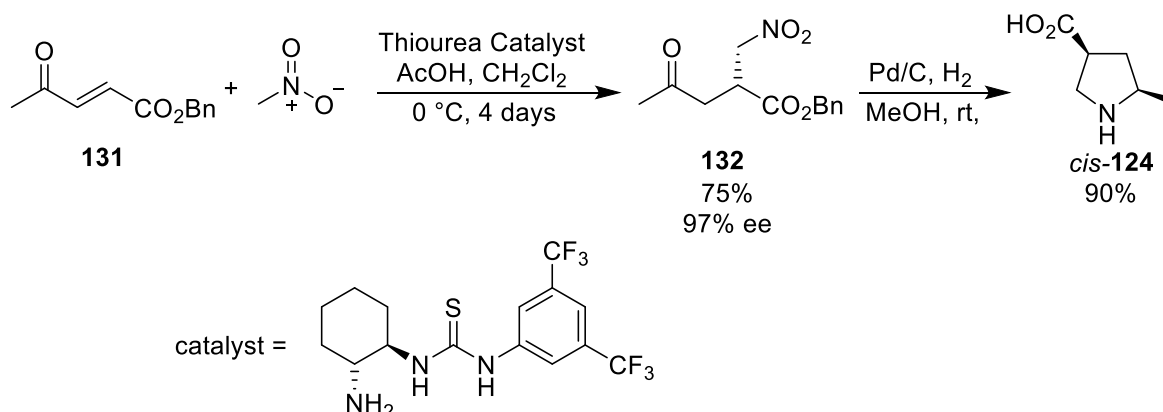
Scheme 2.43

Other concise methods for the synthesis of 2,4-disubstituted pyrrolidines include the use of zirconium to transform *N*-tosyl carbamates such as **133a** and **133b** into pyrrolidines.[93] Treatment of carbamate **133a** with ZrCp$_2$ and iodine gave intermediate iodide **134a**. Iodide **134a** could not be purified and was directly cyclised in the presence of K$_2$CO$_3$ to give a 2:1 mixture of pyrrolidines *cis*-**135a** and *trans*-**135a** in 48% yield (Scheme 2.44). However, when a propyl group was used in place of a methyl group, the intermediate iodide **134b** could be purified and cyclisation gave the corresponding pyrrolidine **135b** in 80% yield with much higher diastereoselectivity. A proposed mechanism for some of the key steps in the ZrCp$_2$/I$_2$ reaction is shown in Scheme 2.45. The zirconium co-ordinates to the alkene in carbamate **133** and then adds into the carbonyl group. The resulting bicycle can rearrange to form an intermediate 7-membered ring, which then breaks down in the presence of an electrophile to give the product, iodide **134**.
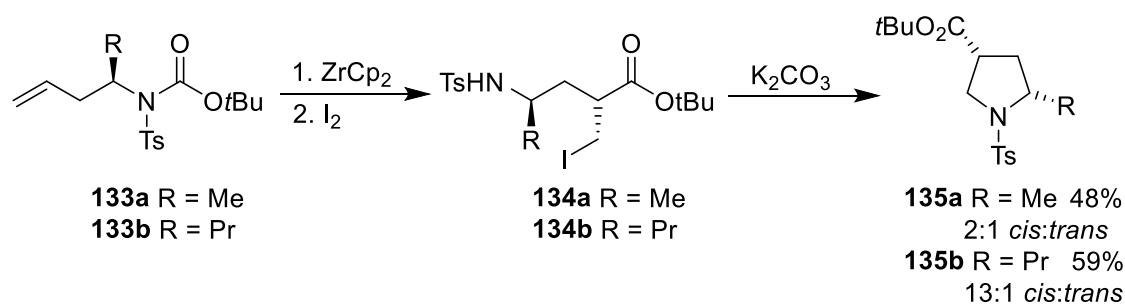
Scheme 2.44
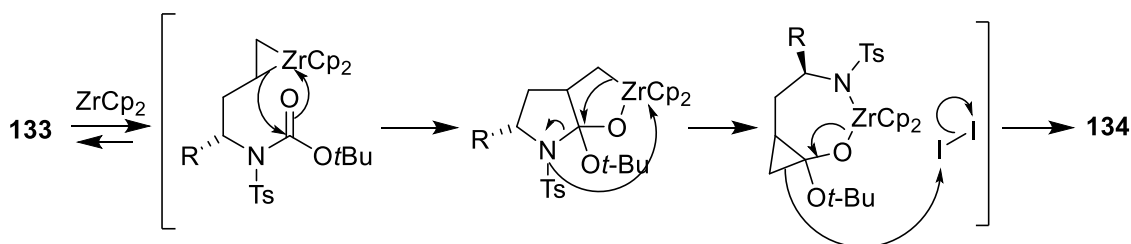
Scheme 2.45

Another noteworthy route for the synthesis of 2,4-disubstituted pyrrolidines is the use of pyrrole hydrogenation. Although uncommon, there are some limited examples of pyrrolidines such as *cis*-**138** and *trans*-**138** being synthesised by hydrogenation. For example, hydrogenation of a mixture of pyrrole **136** and 2-chloropyrrole **137** gave a 75:25 mixture of diastereomeric pyrrolidines *cis*-**138** and *trans*-**138** (Scheme 2.46, yield not given).[94] However, high pressures and long reaction times are typically required for these types of hydrogenations.
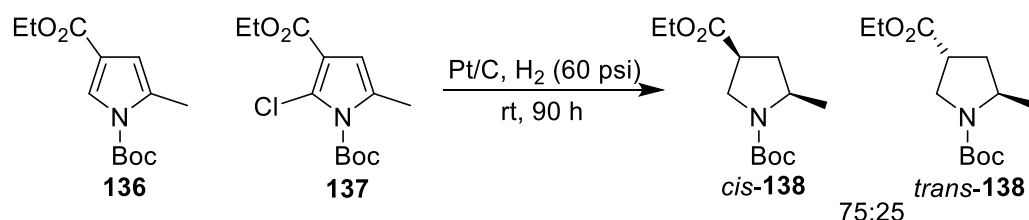
Scheme 2.46

2.2.2 Claisen Condensation Route

The first route considered for the synthesis of fragments *trans*-**37** and *cis*-**37** was based on installing the ester using a Claisen condensation, similar to the examples shown in Scheme 2.41 and Scheme 2.42.[90,91] It was proposed that target fragments **37** could be synthesised by chemoselective reduction of the corresponding pyrrolidinone **139**. Pyrrolidinone **139** would be derived from a Claisen condensation of *N*-methyl pyrrolidinone **140** (Scheme 2.47).
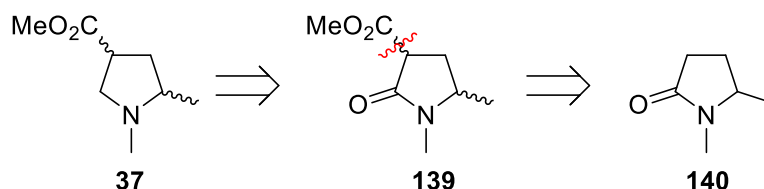
Scheme 2.47

The Claisen condensation of *N*-alkyl pyrrolidin-2-ones is a well-known reaction.[95,96,97] For example, Takeda and Toyota showed that *N*-methyl pyrrolidinone **141** could be deprotonated with LDA at –78 °C and then trapped with methyl chloroformate to give pyrrolidinones **142** in 86% yield (Scheme 2.48). Tanaka *et al.* performed a similar reaction on a 2-substituted

pyrrolidinone **143**. Deprotonation this time was performed at rt to give the enolate which was reacted with diethyl carbonate to give 2,4-disubstituted pyrrolidinones **144** in 85% yield (Scheme 2.48).
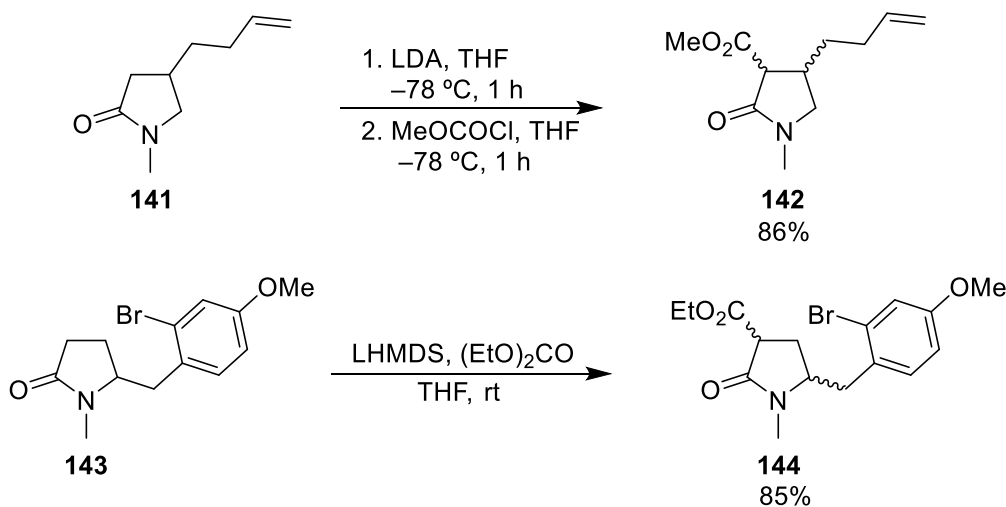
Scheme 2.48

To start our synthetic work, the Claisen condensation of pyrrolidinone **140** with methyl chloroformate was attempted. Deprotonation of pyrrolidinone **140** with KHMDS (1.1 eq) in THF at −78 °C was followed by reaction with methyl chloroformate. This gave a 77:23 mixture (by ^{1}H NMR spectroscopy) of starting pyrrolidinone **140** and double addition product **145** after work-up and chromatography. From the mass of the mixture, a 9% yield of pyrrolidinone **145** was calculated (Scheme 2.49). There was no evidence of the desired pyrrolidinones **139**. Any that had formed underwent a second Claisen condensation.
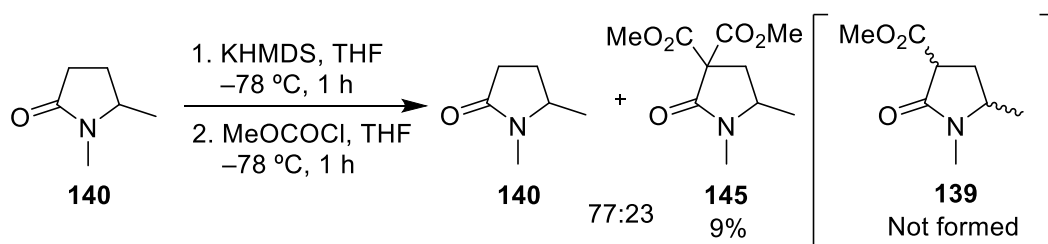
Scheme 2.49

Due to this discouraging result, we turned our attention to *N*-Boc pyrrolidinones which also have good literature precedent for Claisen condensations and have different electronics.[98–100] Bogle *et al*. had reported the successful condensation of *N*-Boc pyrrolidinone **146** with methyl chloroformate to give pyrrolidinone **147** in 96% yield (Scheme 2.50).[98]
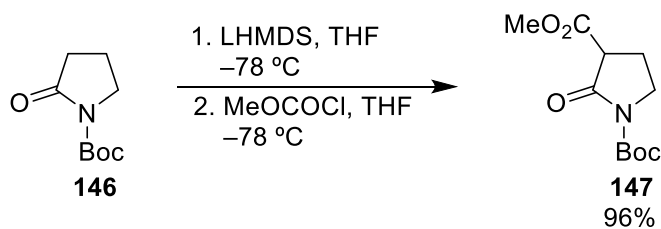
Scheme 2.50

It was therefore decided to attempt the same conditions as in Scheme 2.49 using *N*-Boc methyl pyrrolidinone **148**. First, *N*-Boc methyl pyrrolidinone **149** was synthesised by reaction of methyl pyrrolidinone **148** with Boc$_2$O for 16 h at rt in 85% yield. The Claisen condensation was then attempted using KHMDS. Changing from *N*-methyl pyrrolidinone **140** to *N*-Boc pyrrolidinone **149** proved successful with the reaction proceeding in 33% yield (Scheme 2.51). Pyrrolidinones **150** were obtained as a 67:33 mixture of diastereomers with diagnostic methyl signals at 1.42-1.36 and 1.33-1.27 ppm in the ^{1}H NMR spectrum. The two diastereomers proved inseparable by chromatography and we were unable to assign which diastereomer of pyrrolidine **150** was the major product.
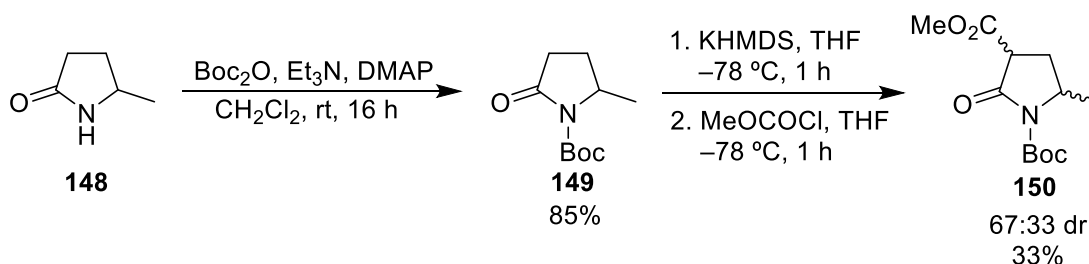
Scheme 2.51

The reaction was next attempted using the conditions described by Dixon *et al.*, which involved LHMDS as base, a 5-minute reaction time and addition of the pyrrolidinone to the base as opposed to the base being added to the pyrrolidinone. This resulted in a substantial increase in yield of pyrrolidinones **150** (90%) (Scheme 2.52). The diastereomeric ratio (67:33) was the same as when using KHMDS.
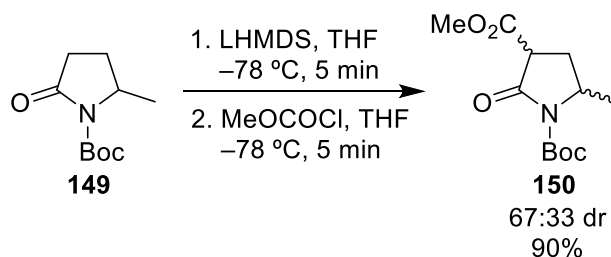
Scheme 2.52

With pyrrolidinones **150** in hand, the next step was to attempt the chemoselective reduction of the lactam carbonyl. BH$_3$•DMS had recently been used in the group to prepare one of the other fragments on this project. In that case, pyrrolidinone **115**, with the methyl and methyl ester groups transposed compared to our system, had been reacted with BH$_3$•DMS to give pyrrolidine **151** in 66% yield (Scheme 2.53).
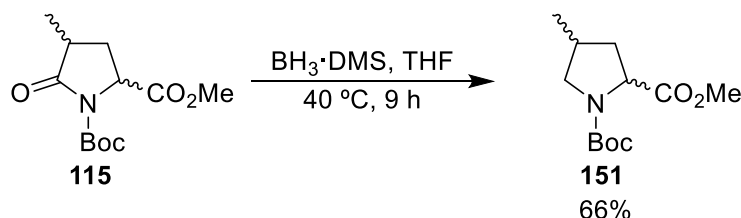
Scheme 2.53

These conditions were then attempted with pyrrolidinones **150**, with BH$_3$•DMS being added to pyrrolidinone **150** and heated at 70 °C in THF. The reaction was performed over 20 h, with TLCs being carried out to check the reaction progress. However, after 20 h, only the starting pyrrolidinones **150** were recovered (Scheme 2.54).
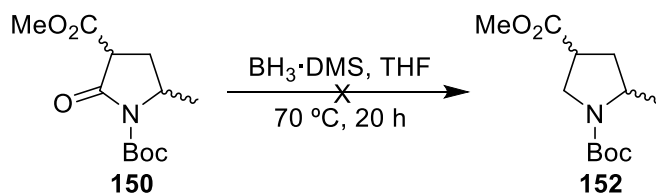
Scheme 2.54

Alternative conditions were then explored for the reduction. A two-step process involving reduction of pyrrolidinone **153** to an aminal intermediate with LiBHEt$_3$ and then further reduction with Et$_3$SiH and BF$_3$•Et$_2$O was used successfully by Schneider *et al.*[101] to give pyrrolidine **154** in 84% yield (Scheme 2.55).
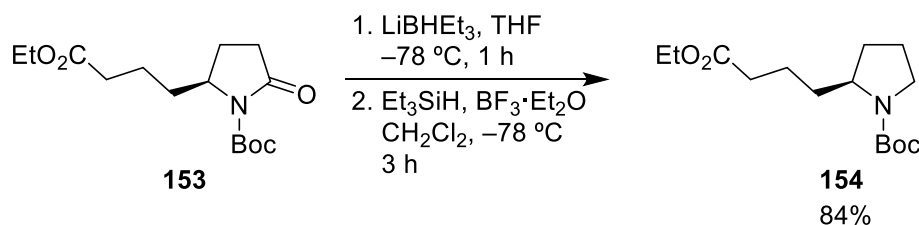
Scheme 2.55

Therefore, LiBHEt$_3$ was reacted with pyrrolidinones **150** in THF at –78 °C for 30 min. After quenching with NaHCO$_{3(aq)}$ and work-up with H$_2$O$_2$, the presumed intermediate aminal was

further reduced with Et_3SiH and $BF_3 \cdot Et_2O$ at -78 °C. However, only starting pyrrolidinones **150** were recovered. This reaction was also tried using similar conditions with sodium borohydride in the initial step. The reaction yielded a complex mixture of products, with ^1H NMR spectroscopy showing many doublets corresponding to the methyl group at δ 0.92-0.82 ppm (Scheme 2.56).
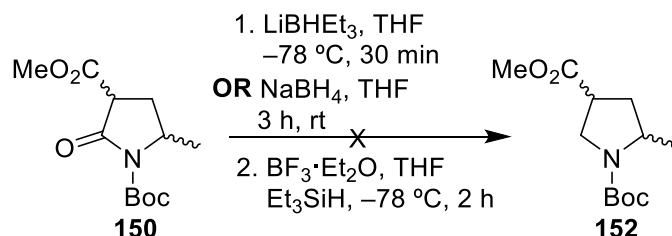
Scheme 2.56

The final reduction conditions considered used Meerwein's salt followed by sodium cyanoborohydride to reduce the pyrrolidinone. An example of this chemistry is shown in Scheme 2.42.[91] These conditions were therefore attempted on pyrrolidinones **150**. Treatment of pyrrolidinones **150** with TFA (to remove the Boc group) then trimethyloxonium tetrafluoroborate appeared by ^1H NMR spectroscopy to have alkylated **150** to give intermediate **155**, evidenced by pairs of singlets that integrated to a total of 3H each at 3.764 and 3.758 ppm and 3.69 and 3.68 ppm. It was not possible to tell whether this was due to *O*- or *N*-alkylation. Subsequent treatment with sodium cyanoborohydride at acidic pH gave a complex mixture of products by ^1H NMR spectroscopy (Scheme 2.57).
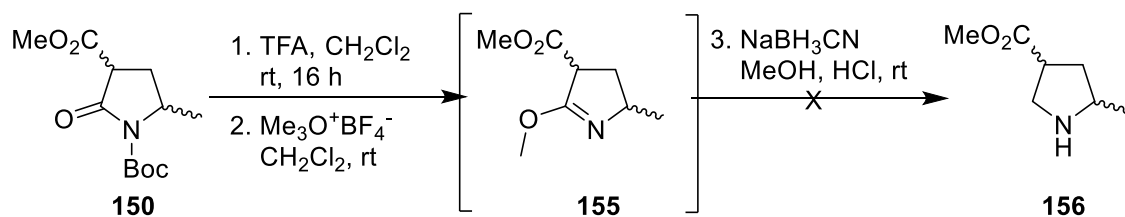
Scheme 2.57

With this reduction proving so difficult and the route giving a mixture of diastereomers that had so far proved impossible to separate, it was decided to investigate an alternative route to fragments *cis*-**37** and *trans*-**37**.

2.2.3 Tandem Michael Addition/Dieckmann Cyclisation Route

With the lack of success with the Claisen condensation route, an alternative route to fragments *trans*-**37** and *cis*-**37** was considered. The new route proposed for the synthesis of fragments *trans*-**37** and *cis*-**37** involved the hydrogenation of dihydropyrrole **157** to give pyrrolidines **152**. Dihydropyrrole **157** would be formed from the reduction and elimination of β-ketoester **158**, which would in turn be formed from a tandem Michael addition/Dieckmann cycisation of *N*-Boc alanine methyl ester **159** and methyl acrylate (Scheme 2.58). A similar cyclisation was used to prepare β-ketoester **100** (see Section 2.1.3)
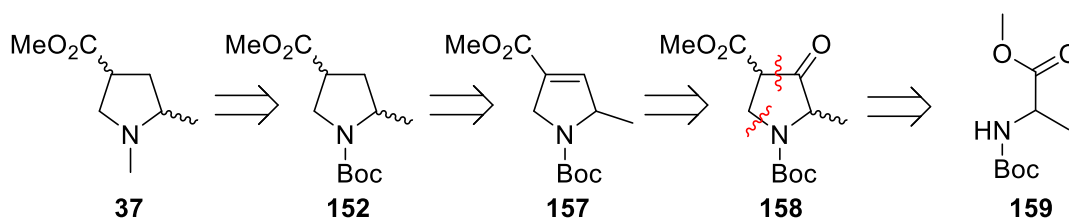
Scheme 2.58

Although this route was quite a few steps, there was good precedent for each step. For example, the synthesis of a dihydropyrrole from an oxopyrrolidine very similar to **158** had been performed by Wang *et al.*[70] Reaction of oxopyrrolidine **73** with NaBH$_3$CN in MeOH gave alcohol **160**. The alcohol was then eliminated using Mitsunobu-type conditions to give dihydropyrrole **74** in 90% yield over two steps (Scheme 2.59).
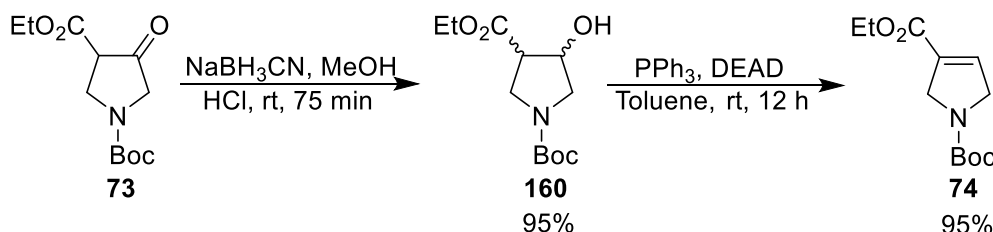
Scheme 2.59

The tandem Michael/Dieckmann step in the proposed synthesis of fragments *trans*-**37** and *cis*-**37** had only been carried previously on glycine derivatives. Boc protection of alanine methyl ester proceeded smoothly using NaHCO$_3$, Boc$_2$O and NaCl in CHCl$_3$–H$_2$O.[102] Work-up yielded *N*-Boc alanine **159** in quantitative yield which required no purification (Scheme 2.60). Using the same *t*BuOK conditions as for *N*-Boc glycine **101** (see Scheme 2.32), the desired 2-methyl oxopyrrolidine **158** was isolated in 50% yield after purification by chromatography (Scheme 2.60). Characterisation of oxopyrrolidine **158** by ^{1}H and ^{13}C NMR spectroscopy was problematic due to the mixture of tautomers, rotamers and diastereomers

present. Mass spectrometry and IR spectroscopy indicated that the reaction was successful and subsequent reactions of **158** showed that oxopyrrolidine **158** had indeed been formed.
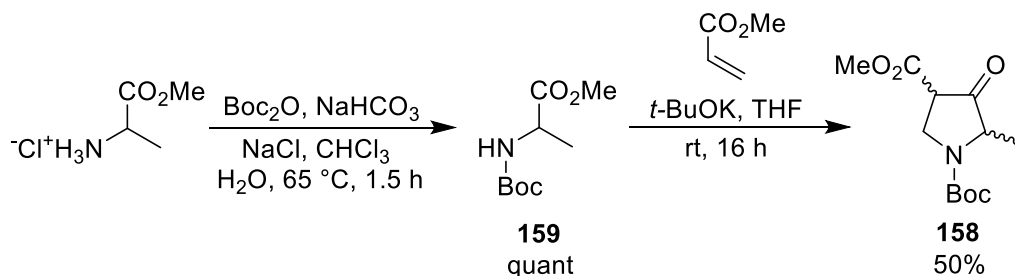
Scheme 2.60

The next steps in the synthesis to be attempted were ketone reduction and alcohol elimination. For this study, we used the simpler oxopyrrolidine **100**. The procedure from Wang *et al.*[70] (see Scheme 2.59) was followed, starting with reaction of oxopyrrolidine **100** with NaBH$_3$CN in MeOH at rt at pH ~4. After work-up, the crude product was reacted with PPh$_3$ and DIAD in toluene. Unfortunately, the reaction resulted in a complex mixture of products that were inseparable by chromatography (Scheme 2.61). Alternative conditions were explored for the reduction step. The reaction was attempted using NaBH(OAc)$_3$. However, only starting oxopyrrolidine **100** was recovered. Luche reduction of the ketone using group conditions was also attempted, adding NaBH$_4$ to a stirred solution of oxopyrrolidine **100** and CeCl$_3$•H$_2$O in MeOH at –60 ℃.[103] However, after quenching and work-up the reaction yielded only the starting oxopyrrolidine **100** (Scheme 2.61).
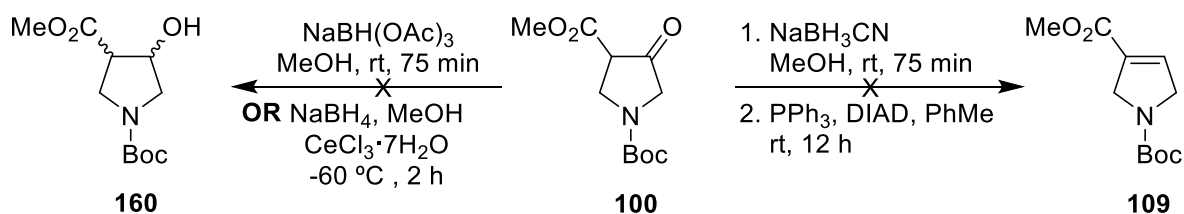
Scheme 2.61

With the reduction seemingly not working, a different strategy was devised. It was proposed that pyrrolidines **152** could come from hydrogenation of enol triflate **161**. Palladium catalysts would oxidatively insert into the vinyl triflate bond and then undergo reductive elimination to give dihydropyrrole **157**, which would undergo alkene hydrogenation (Scheme 2.62). If this did not proceed in one step then stepwise reduction of the triflate followed by hydrogenation of dihydropyrrole **157** could be performed. Triflate **161** would be derived from oxopyrrolidine **158**.
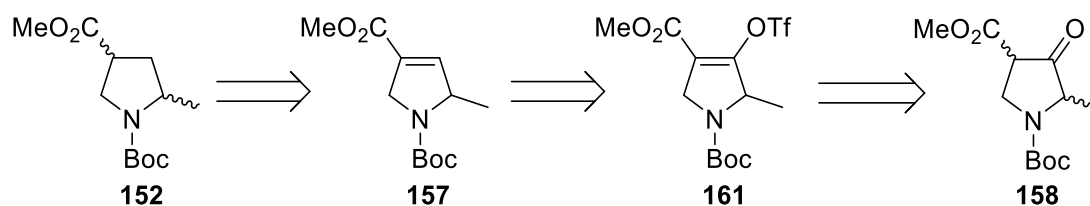
Scheme 2.62

The first step in this route involved conversion of oxopyrrolidines **158** into enol triflate **161**. Reaction of oxopyrrolidines **158** with Hünig's base and triflic anhydride at –78 °C and then at rt gave enol triflate **161** in 82% yield (Scheme 2.63). Characterisation by ^{1}H NMR spectroscopy showed triflate **161** to be pure, confirming that the previous step to synthesise oxopyrrolidine **158** had indeed proceeded cleanly.
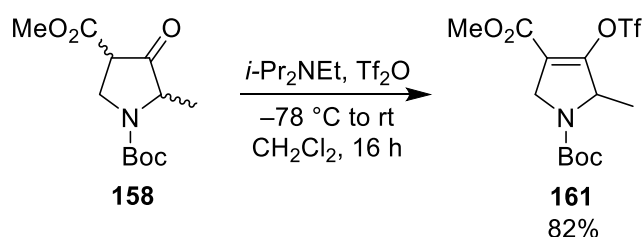
Scheme 2.63

The detriflation-hydrogenation of enol triflate **161** could now be explored. Standard hydrogenation conditions of H_2 and Pd/C in MeOH at rt were explored first and the expected *N*-Boc pyrrolidines **152** were not formed. In fact, the ^{1}H NMR spectrum of the crude product obtained after catalyst removal (by filtration over Celite) and solvent evaporation displayed two broad signals at 7.7 and 8.2 ppm and no diagnostic signal for the Boc group at ~1.5 ppm. This led to the realisation that the Boc group had been removed. The ^{1}H NMR spectrum also showed signals for six ring protons, indicating that triflate removal and alkene hydrogenation had both occurred. It was thus realised that reaction of enol triflate **161** with Pd/C and H_2 had yielded a 65:35 mixture of diastereomeric pyrrolidine salts *trans*-**156**•TfOH and *cis*-**156**•TfOH in 67% yield (Scheme 2.64). The assignment of pyrrolidine *trans*-**156**•TfOH as the major diastereomer is based on work that is described later in this Section. The ratio of diastereomers was determined by integration of the multiplets at 2.45 and 2.50 ppm in the ^{1}H NMR spectrum. Unfortunately, for reasons still unknown, the conversion of enol triflate **161** into triflate salts *trans*-**156**•TfOH and *cis*-**156**•TfOH was irreproducable despite several attempts.
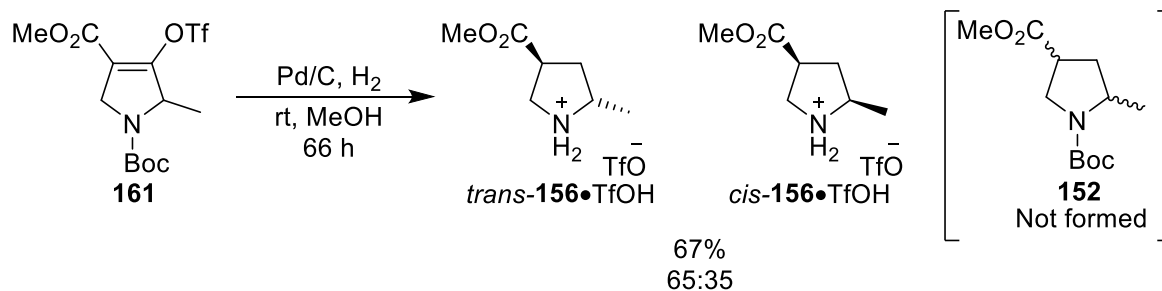
Scheme 2.64

Nevertheless, with triflate salts **156•TfOH** in hand, a way of separating the *cis-* and *trans-*diastereomers was explored. Thus, Boc and Cbz groups were attached to the nitrogen to see if the products would be separable. Reaction of the 65:35 mixture of *trans-***156•TfOH** and *cis-***156•TfOH** with Boc₂O and CbzCl gave protected compounds **152** and **162** in 52% and 70% yield respectively (Scheme 2.65). However, the diastereomers of each compound were inseparable by flash column chromatography.
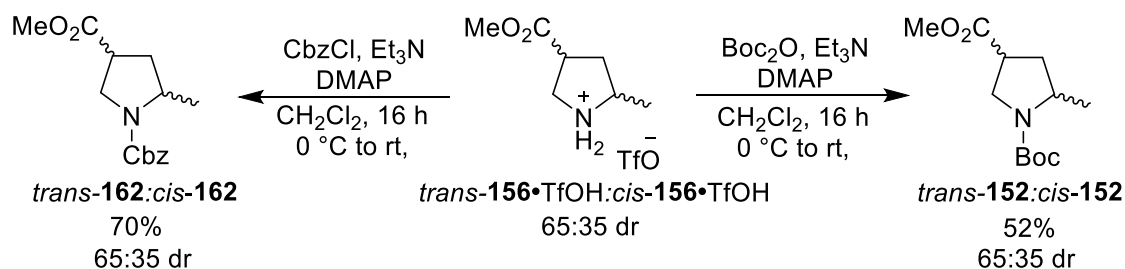
Scheme 2.65

The 65:35 mixture of triflate salts *cis-***156•TfOH** and *trans-***156•TfOH** was also subjected to the group's standard *N*-methylation conditions in order to access the desired 3-D fragments *cis-***37** and *trans-***37**. Thus, reductive amination with formaldehyde and sodium triacetoxyborohydride gave a 65:35 mixture of pyrrolidine fragments *cis-***37•AcOH** and *trans-***37•AcOH** in 23% yield (Scheme 2.66). These products were isolated as acetic acid salts due to volatility issues encountered with similar amines of such low molecular weight. As a result, we had successfully synthesised both target fragments *cis-***37** and *trans-***37**, albeit as a mixture.

Scheme 2.66

As the direct triflate hydrogenation with Pd/C shown in Scheme 2.64 could not be repeated, alternative hydrogenation conditions were considered. It was decided to attempt the hydrogenation in the presence of base, which would neutralise any triflic acid that was generated in the detriflation step. Treatment of enol triflate **161** with Pd/C, H$_2$ and Et$_3$N generated a complex mixture of products by ^{1}H NMR spectroscopy. However, after column chromatography, dihydropyrrole **157** was isolated in 17% yield (Scheme 2.67). Despite the low yield, the isolation of dihydropyrrole **157** was at least encouraging evidence that the stepwise process of removing the triflate group followed by hydrogenation could be successful. Isolating dihydropyrrole **157** was surprising given that such a compound would be expected to hydrogenate quickly under these conditions. It is possible that Et$_3$N was poisoning the catalyst and reducing the rate of the hydrogenation reaction. The reaction was therefore attempted using K$_2$CO$_3$ and this also gave a complex mixture of products by ^{1}H NMR spectroscopy. However, a single diastereomeric pyrrolidine, *cis*-**152**, was isolated in 8% yield (Scheme 2.67). Interestingly, the reaction gave the opposite major diastereomer to hydrogenation of enol triflate **161** in the absence of base (see Scheme 2.64).

Scheme 2.67

With the direct hydrogenation of enol triflate **161** proving difficult, the stepwise approach was considered to the desired pyrrolidines **152**. Sieburth *et al*. had shown that a triflate group could be removed from an α,β-unsaturated-*β*-triflate ester using Pd(PPh$_3$)$_4$ and Et$_3$SiH on a pyrone substrate.[104] In this reaction, the Et$_3$SiH acts as a hydride donor to the palladium, while the palladium oxidatively inserts into the vinyl triflate bond and then undergo es reductive elimination to give the desired product. Using these conditions, the triflate group of enol triflate **161** was selectively removed using Pd(PPh$_3$)$_4$ and Et$_3$SiH to give dihydropyrrole **157** in 56% yield (Scheme 2.68).[104] Frustratingly, the product was isolated as an 85:15 mixture of **157** and Et$_3$SiH, which despite work-up with sources of fluoride and chromatography could not be removed. However, ^{1}H NMR spectroscopy after all subsequent hydrogenations showed no remaining Et$_3$SiH and its presence caused no issues during these reactions.

Scheme 2.68

The next step was the hydrogenation of dihydropyrrole **157** and the results are summarised in Table 2.1. Hydrogenation of dihydropyrrole **157** using Pd/C and H_2 in MeOH at rt for 42 h gave, after filtration through Celite, a 29% yield of an 85:15 mixture of pyrrolidines *cis-***152** and *trans-***152** (entry 1). A similar result was obtained with an 18 h reaction time (entry 2). In contrast, use of Pd(OH)$_2$/C gave an 81% yield of a 55:45 mixture of *cis-***152** and *trans-***152** (entry 3). Although Pd(OH)$_2$ gave a poor diastereoselectivity, the yield was much higher than that for Pd/C (entry 1). It was postulated that the low diastereoselectivity of the reaction with Pd(OH)$_2$ might due to the long reaction time, allowing for epimerisation of the product. The reaction was therefore repeated with a reduced reaction time of 1 h. The diastereoselectivity did not change, but the shorter reaction time did improve the yield to 97% (entry 4). Finally, hydrogenation using PtO$_2$ as the catalyst was explored but this returned only starting material (entry 5).
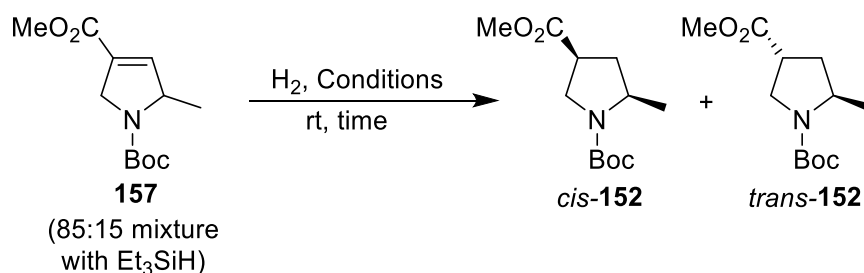
Entry	Conditions	Time (h)	Yield (%)[a]	*cis:trans*[b]
1	Pd/C, MeOH	42	29	85:15
2	Pd/C, MeOH	18	27	75:25
3	Pd(OH)₂/C, MeOH	18	81	55:45
4	Pd(OH)₂/C, MeOH	1	97	55:45
5	PtO₂, AcOH	18	0	N/A

[a] % Yield of crude product
[b] Ratio of *cis*-**152** and *trans*-**152** determined by ¹H NMR spectroscopy of the crude product

Table 2.1: Investigation of the hydrogenation of dihydropyrrole **157**

The *cis* stereochemistry of the major product, *cis*-**152**, was ascertained later in the project (see Section 2.2.4). The difference in diastereoselectivity caused by changing catalyst from Pd/C to Pd(OH)₂ was substantial, and surprising given that both catalysts involve the hydrogenation step occurring on a heterogeneous palladium surface. However, the low yield of the Pd/C catalysed hydrogenations (entries 1 and 2) indicates that other processes may be occurring in the reaction. Our attempt to explain the *cis*-diastereoselectivity is shown in Figure 2.5. It is postulated that the planar *N*-Boc group forces the *α*-methyl group into a *pseudo*-axial position. This causes steric clashing between the methyl group and the palladium, which results in hydrogenation of the opposite face being favoured and the ester group being pushed into a *cis* position relative to the methyl group. The difference in the levels of *cis*-selectivity between the Pd/C and Pd(OH)₂/C catalysts is difficult to explain without further studies into the surface of the catalysts.
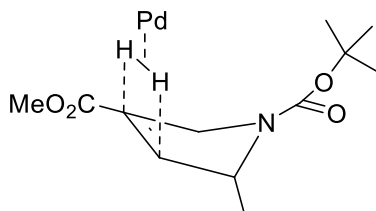
Figure 2.5: Postulated transition state during the hydrogenation of **157**.

Next, we wanted to find an *N*-substituent that would allow for the separation of the diastereomers. Boc and Cbz groups had already been shown not to work, so other common

nitrogen-protecting groups were considered. A 55:45 mixture of *N*-Boc pyrrolidines *cis*-**152** and *trans*-**152** was deprotected using TFA. Then, reaction with PhCHO and NaBH(OAc)$_3$ gave *N*-benzyl derivatives **163** in 41% yield (over two steps). Reaction with 2-NsCl gave *N*-nosyl derivatives **164** in 20% yield. The diastereomeric ratio was retained in each case (Scheme 2.69).
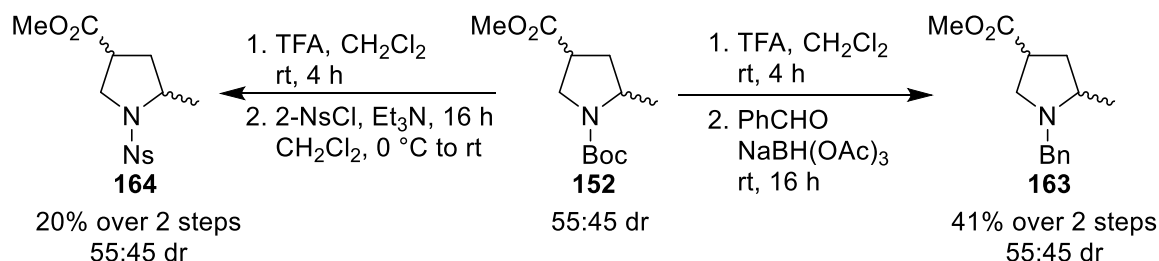
Scheme 2.69

Chromatography of the nosyl derivatives **164** showed some separation of the diastereomers but not enough to fully separate them. Chromatography of the benzyl derivatives **163** proved more successful, and a 10% yield of pure *cis*-**163** was isolated. However, the diastereomers were indistinguishable by TLC and the only way to determine that a single diastereomer was present in the fraction was to perform ^{1}H NMR spectroscopy on each one. This was possible but very time consuming. At this point, the route had substantially increased in steps and still lacked diastereoselectivity in the hydrogenation step or an easy way to separate the diastereomers. Therefore, this route was abandoned and it was decided to move on to a new route.

2.2.4 Nitrile Hydrogenation Route

A route that would number no more than six steps and had the potential to be diastereoselective was sought to synthesise the target fragments. A hydrogenation route was proposed that would involve pyrrolidine **156** being obtained from hydrogenation of keto nitrile **165**. The required keto nitrile **165** could be formed using an enolate alkylation approach with methyl cyanoacetate **166** and chloroacetone **167** (Scheme 2.71).
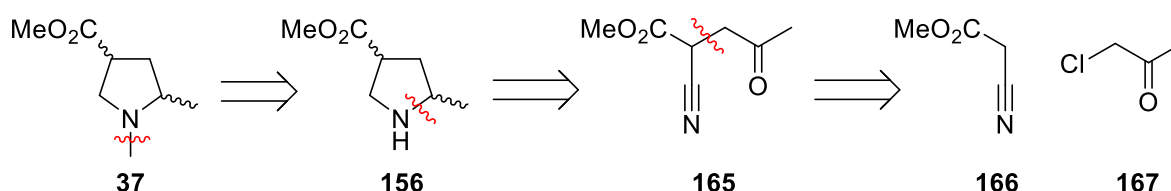
Scheme 2.71

The mechanism of the key ring-forming step is shown in Scheme 2.72. Amine **168** required for the cyclisation step would have to be masked in some fashion, and for this we considered a nitrile group. It was therefore proposed that pyrrolidine **156** could come from keto nitrile **165**, where hydrogenation would reduce keto nitrile **165** to amino ketone **168** which could then cyclise onto the pendant ketone. This would generate imine **169** which would also be hydrogenated to set the relative stereochemistry and build the ring in one step.
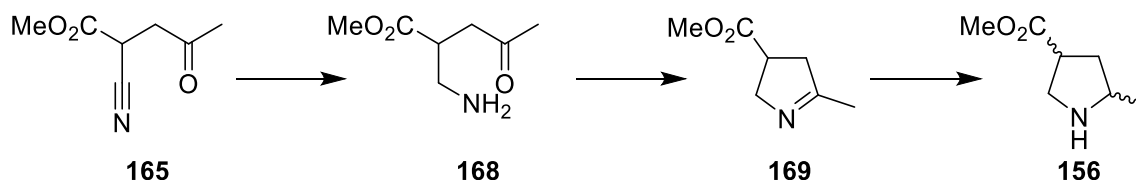
Scheme 2.72

This nitrile hydrogenation approach to a pyrrolidine had been first reported by Korte and Trautner in 1961,[105] where keto nitrile **170** was subjected to hydrogen gas at high pressure apparently in the absence of a transition metal catalyst. Reaction at rt and 100 atm exclusively gave pyrrole **171** (Table 2.2, entry 1). In contrast, at 250 atm, the reaction gave an 80:20 mixture of pyrrole **171** and pyrrolidines **172** (diastereomeric ratio and yields not given) (entry 2).

Table 2.2: Keto nitrile hydrogenation results
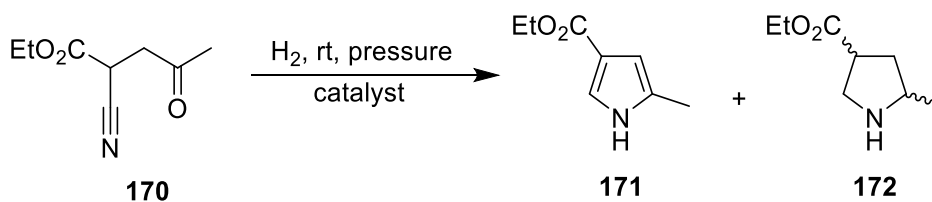
Entry	Pressure	Catalyst	171:172
1	100	none	100:0
2	250	none	80:20

A suggested mechanism for the formation of pyrrole **171** is shown in Scheme 2.73. Hydrogenation of the nitrile group will give the imine, which can tautomerize to form enamine **173**. Enamine **173** can then cyclise onto the ketone to give iminium **174**. Tautomerization of iminium **174** then gives pyrrole **171**. The relative rates of the hydrogenation of enamine **173** and the corresponding imine, the tautomerization between the imine and enamine forms of **174**, and the cyclisation of enamine **173** will all affect the ratio of pyrrole **171** and desired pyrrolidine **172** being formed.
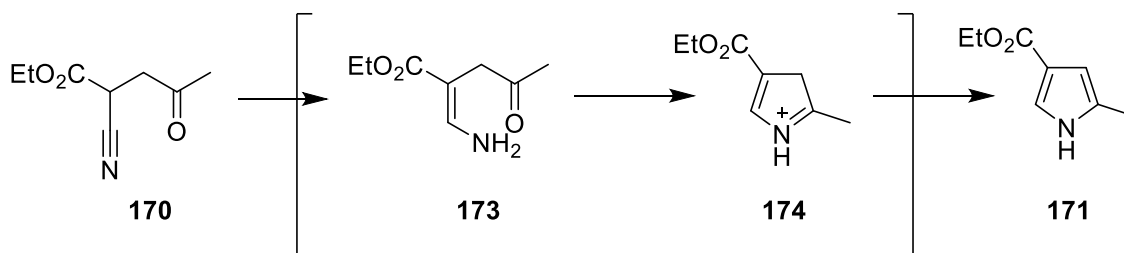
Scheme 2.73

The first step in this proposed route was the alkylation of methyl cyanoacetate with chloroacetone. Using conditions from Lee *et al.*,[106] methyl cyanoacetate was deprotonated with sodium methoxide and then trapped with chloroacetone to give nitrile **165** in 62% yield after chromatography (Scheme 2.74). This reaction was readily scaled up to give ~3 g of keto nitrile **165**. The hydrogenation of keto nitrile **165** was then attempted using conditions from an AstraZeneca patent where a similar nitrile-containing compound was hydrogenated. Reaction in AcOH using a balloon of H$_2$ and 5 mol% PtO$_2$ as catalyst at rt for 16 h and then filtering through Celite to remove the catalyst led to the formation of an 80:20 mixture of the desired pyrrolidines **156**•AcOH (as an 85:15 mixture of *cis* and *trans* diastereomers) and pyrrole **175** (Scheme 2.74). The product was isolated as the acetic acid salt due to the volatility of pyrrolidines **156**. It was difficult to determine an accurate yield for this reaction due to issues with completely removing the acetic acid. An acid-base work-up was attempted

to remove the pyrrole **175** from the crude mixture of pyrrolidines **156**•AcOH. However, pyrrolidines **156** proved to be highly soluble in water and difficult to extract even when basified. It was, however, possible to isolate pyrrole **175** in 13% yield from this work-up procedure.
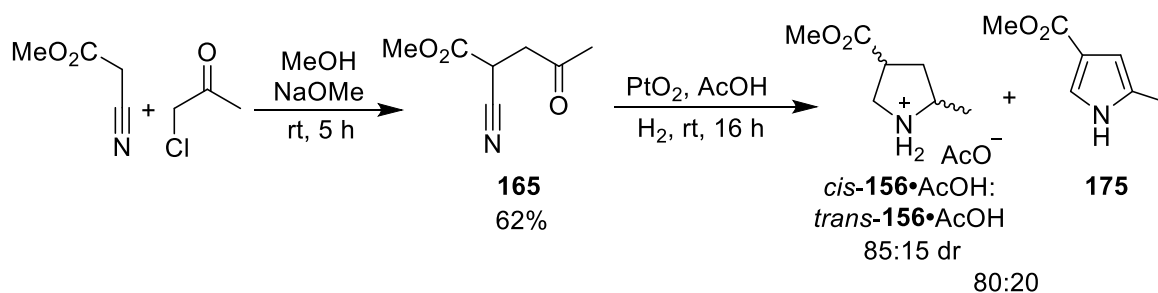
Scheme 2.74

Pyrrole **175** was identified from the ^{1}H NMR spectrum of the crude product: the spectrum showed two signals that integrated to 1 H each at 6.26 ppm and 7.26 ppm, corresponding to the two aromatic protons, and two singlet signals that integrated to 3 H each at 3.76 ppm and 2.23 ppm, corresponding to the methyl groups in the ester and attached to the ring respectively. These signals matched the literature signals for pyrrole **175**.[107]

At this point, we decided to Cbz protect the crude mixture as we realised that this could be used to assign the stereochemistry of pyrrolidines **156**. This was possible because *N*-Cbz ethyl ester pyrrolidine *trans-* was recently reported by Tanaka *et al.*, with its stereochemistry being established by NOE spectroscopy.[92] However, during the course of this PhD, a correction to the paper was issued stating that the stereochemistry had been misassigned and X-ray crystallography was used to prove that it was in fact *cis*-**176**. This resulted in us misassigning the major diastereomer of our hydrogenations as *trans*-**156** until late in the project. The stereochemistry of the 2,4-disubstituted pyrrolidines in this thesis is now reported correctly, with verification both through the method detailed below and *via* our own X-ray crystal structure as described in Section 2.3.

Cbz protection of pyrrolidines **156** gave protected pyrrolidines **164**, still as an 85:15 mixture of diastereomers, in 18% yield over the 2 steps of hydrogenation and Cbz protection. The static ratio of diastereomers led us to believe that no epimerisation had occurred. Pyrrolidines **164** were easily isolable by chromatography. Pyrrolidines **164** were then hydrolysed and esterified to give an 85:15 mixture of ethyl ester pyrrolidines *cis*-**176** and *trans*-**176** in 46% yield (Scheme 2.75).
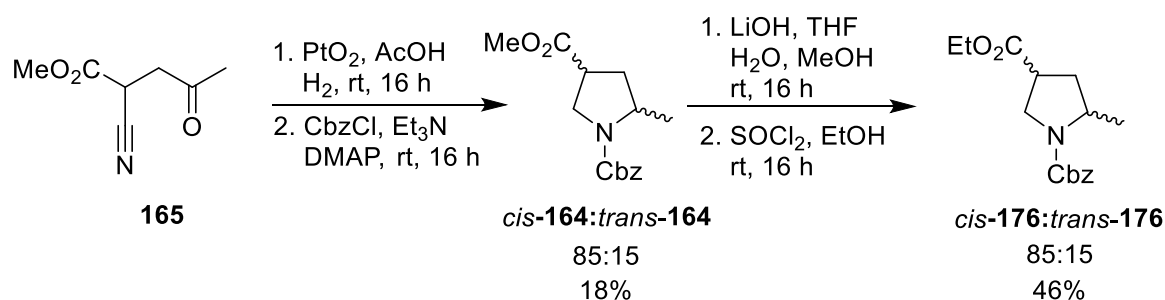
Scheme 2.75

Key signals in the ^{1}H NMR spectrum of pyrrolidines **176** (Figure 2.6) were the dd at 3.56 ppm corresponding to an NCH proton, the dddd at 2.94 ppm corresponding to the C*H*CO$_2$Et proton and the ddd at 2.38 ppm corresponding to a CH$_2$ proton, all of which integrated to 0.85H and matched the literature data for pure *cis*-**176**. Importantly, the corresponding signals for the NC*H*CO$_2$Et and CH$_2$ protons in *trans*-**176**, which were noticeably broader, appearing at 3.14 and 2.26 ppm, both integrated to 0.15H and were absent from the ^{1}H NMR spectrum of *cis*-**176** reported in the literature.[92] This gave us the proof that pyrrolidine *cis*-**156** was the major product of the hydrogenation and, by comparison of ^{1}H NMR spectra, allowed us to assign all of the stereochemistry in Sections 2.2 and 2.3.
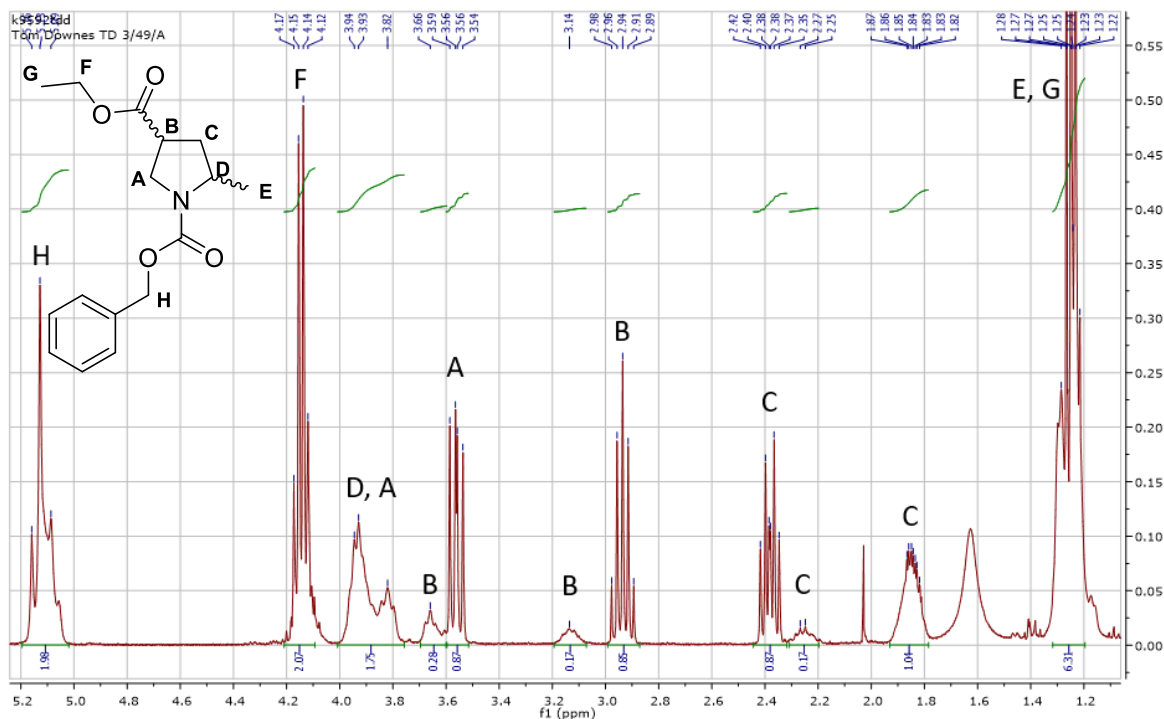
Figure 2.6

The formation of pyrrolidine *cis*-**156**•AcOH as the major product from the hydrogenation of keto nitrile **165** was consistent with results from Tanaka *et al.*[92] They showed that a similar synthetic route involving hydrogenation of nitro compounds **177** to synthesise a variety of

2,4-disubstituted pyrrolidines **179** gave the *cis*-diastereomer as the sole product (see Scheme 2.43), although they did not comment on the origin of the diastereoselectivity. Their hydrogenation used Pd/C in MeOH, meaning that hydrogenation of nitro compound **179** proceeded *via* intermediate imine **180**. Our route uses nitrile hydrogenation under acidic conditions and therefore proceeds *via* iminium intermediate **169** (Scheme 2.76). It is possible that the small difference in diastereoselectivity between these two routes may be caused by both the larger ester group and the difference between the hydrogenation of iminium **169** as opposed to an imine. Later work showed that the difference is not only due to sterics, as hydrogenation of the corresponding *t*-butyl ester using our conditions gave a 96:4 dr (see Section 2.3).
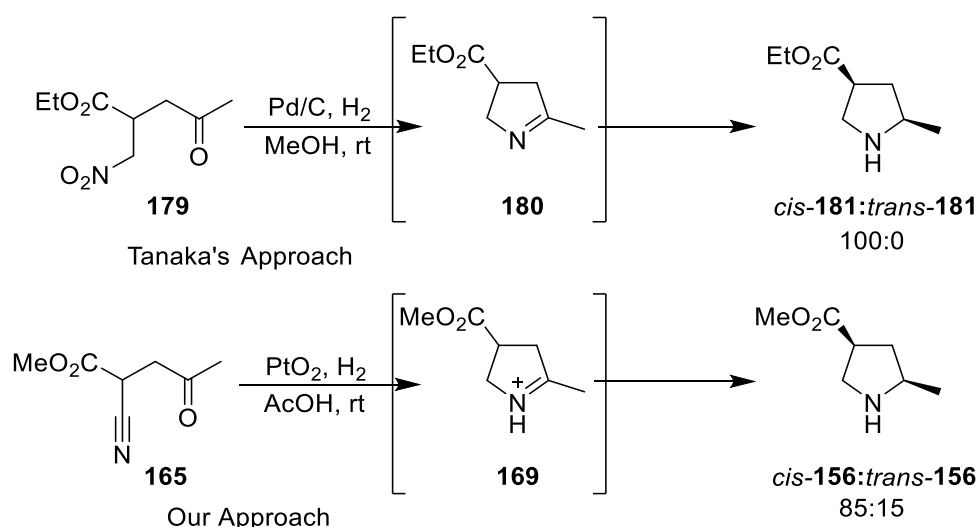
Scheme 2.76

The diastereoselectivity likely arises from hydrogenation on the opposite face to the sterically bulky ester group. This gives the *cis*-diastereomer as the major diastereomer (Figure 2.7). The increased steric bulk of the ethyl ester over the methyl ester helps make the reaction more selective while the difference between hydrogenation of an imine and an iminium could be due to several factors, including small changes in shape and the availability of the lone pair for co-ordination.
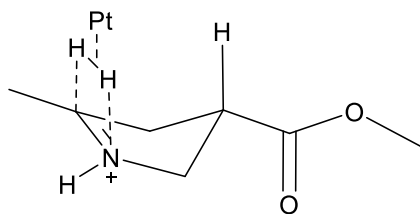
Figure 2.7: Transition state to explain the diastereoselectivity for *cis*-**156**

Then next challenge was to access pyrrolidine *cis*-**156** as a single diastereomer. In order to separate the diastereomers, an *N*-benzyl group was attached to pyrrolidines **156**•AcOH. After standard hydrogenation of keto nitrile **165**, subjection of pyrrolidines **156** to reductive amination conditions with benzaldehyde followed by chromatography gave pyrrolidine *cis*-**163** as a single diastereomer in 21% yield over 2 steps. An 80:20 mixture of pyrrolidines *cis*-**163** and *trans*-**163** was isolated in 37% yield (Scheme 2.77). Unfortunately, as discussed earlier, ^{1}H NMR spectra of individual fractions had to be carried out in order to isolate just 21% of pure *cis*-**163**, as the diastereomers did not appear separately by TLC.
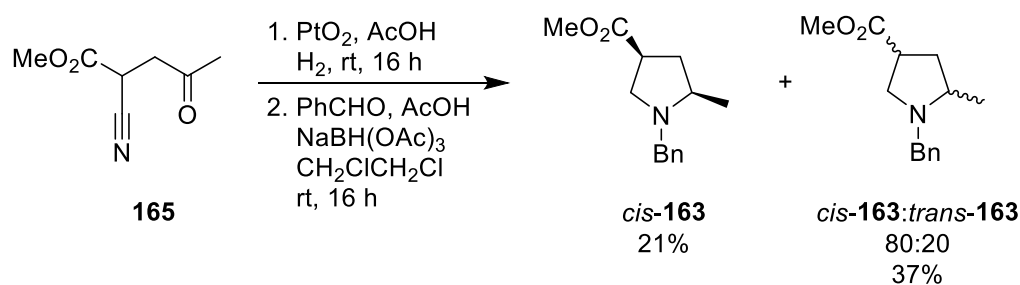
Scheme 2.77

Although we were pleased to finally have access to pyrrolidine *cis*-**163** as a single diastereomer, the route still required a difficult chromatography purification to obtain small amounts of pure *cis*-**163**. We therefore wondered if it would be possible to epimerise pyrrolidines **163** to give a higher percentage of the *cis*-diastereomer and thus make the route higher yielding. Epimerisation of pyrrolidines **163** might also give access to the *trans* diastereomer.

The first series of epimerisation reactions attempted were performed using NaOMe or K$_2$CO$_3$ as base in MeOH (Table 2.3). Reactions performed at rt (entries 1 and 3) appeared to give very slow or no epimerisation. However, epimerisation at 60 °C showed a signification change in the diastereomeric ratios. Use of NaOMe gave a 55:45 mixture of *cis*-**163** and *trans*-**163** in 94% yield (entry 2), and use of K$_2$CO$_3$ gave a 50:50 mixture of *cis*-**163** and *trans*-**163** in 22% yield (entry 4). It is possible that the low yield from the K$_2$CO$_3$ reaction at 60 °C may be due to hydrolysis of the ester occurring, an issue which had been shown to cause significantly reduced yields in the epimerisation reactions of analogous piperidine compounds by another member of our group.[103]

Table 2.3: Epimerisation of pyrrolidines **163**
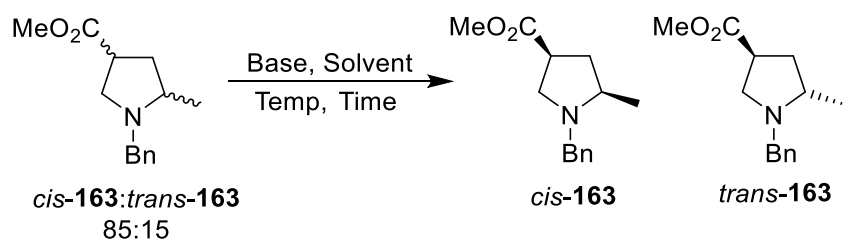
Entry	Base	Solvent	Temp. (°C)	Time (h)	Yield (%)[a]	*cis*:*trans*[b]
1	NaOMe	MeOH	rt	16	98	85:15
2	NaOMe	MeOH	60	16	94	55:45
3	K₂CO₃	MeOH	rt	16	100	85:15
4	K₂CO₃	MeOH	60	16	22	50:50

[a] % Yield of crude product
[b] Ratio of *cis*-**163** and *trans*-**163** determined by ^{1}H NMR spectroscopy of the crude product

Table 2.3: Epimerisation of pyrrolidines **163**

Thus far, no epimerisation conditions had given pyrrolidine *trans*-**163** as the major product or *cis*-**163** in better diastereoselectivity. Alternative epimerisation conditions were therefore explored. Previous work in the group on the epimerisation of piperidines had found that *t*-BuOK at –78 °C in THF gave significant diastereoselectivity.[108] Treatment of pyrrolidines **163** with *t*-BuOK at –78 °C for 2 h in THF, followed by quenching with saturated NH₄Cl(aq), gave a 40:50:10 mixture of pyrrolidine *cis*-**163**, pyrrolidine *trans*-**163** and transesterified pyrrolidine *cis*-**182** in quantitative yield (Scheme 2.78).
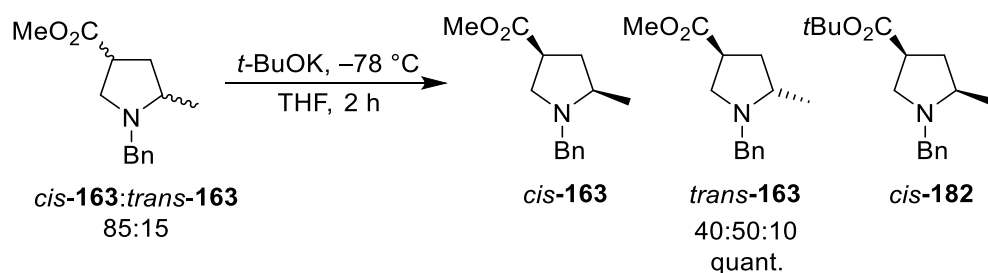
Scheme 2.78

With epimerisations of *N*-benzyl pyrrolidines proving unselective, it was decided to attempt the epimerisation of *N*-Boc pyrrolidines **152**. First, pyrrolidines **152** were synthesised in 48% yield (over 2 steps) from keto nitrile **165**. Pyrrolidines **152** were then subjected to the NaOMe and K₂CO₃ conditions (Table 2.4). Pleasingly, reactions at rt gave a 50:50 mixture of diastereomers in very high yields (entries 1 and 3) while heating gave pyrrolidine *trans*-**152** as the major product (entries 2 and 4). However, diastereomers *cis*-**152** and *trans*-**152**

were inseparable and as the results were not substantially better than the *N*-benzyl system, these results were not used moving forward.
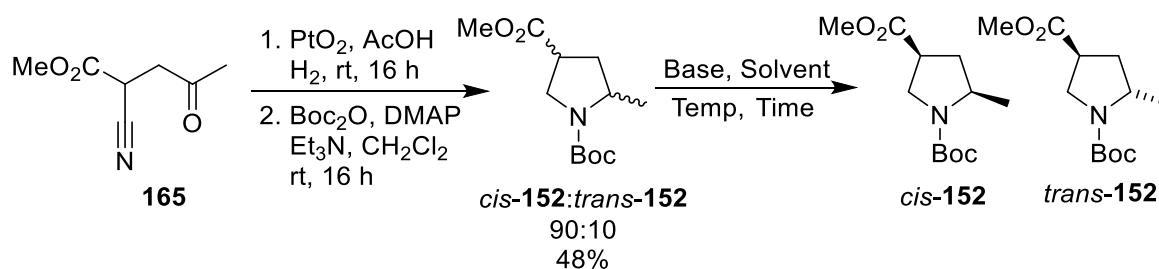
Entry	Base	Solvent	Temp. (°C)	Time (h)	Yield (%)[a]	*cis*:*trans*[b]
1	NaOMe	MeOH	rt	16	100	50:50
2	NaOMe	MeOH	60	16	88	40:60
3	K₂CO₃	MeOH	rt	16	98	50:50
4	K₂CO₃	MeOH	60	16	64	35:65

[a] % Yield of crude product
[b] Ratio of *cis*-**152** and *trans*-**152** determined by ^{1}H NMR spectroscopy of the crude product

Table 2.4: Epimerisation of *N*-Boc pyrrolidines **152**

The synthesis of the targeted 3-D fragment *N*-Me pyrrolidine *cis*-**37** could now be carried out. We planned to use the sample of pure *cis*-**156**•AcOH obtained from the *N*-benzylation route to synthesise *N*-Me fragment *cis*-**37**. However, as this material was precious, the reaction was first attempted on an 85:15 mixture of diastereomers. Hydrogenation of keto nitrile **165** gave pyrrolidines **156**, which were reacted under standard *N*-methylation conditions (Scheme 2.79). This appeared to give some product, but placing it on the high vacuum line to remove the remaining AcOH led to disappearance of all of the product. This is in contrast with the reaction shown in Scheme 2.66, although this *N*-methylation was done on smaller scale to replicate the amount of pure *cis*-**156** available which may account for the difficulty in isolating any product. As a result, the reaction with pure *cis*-**156** was not attempted.
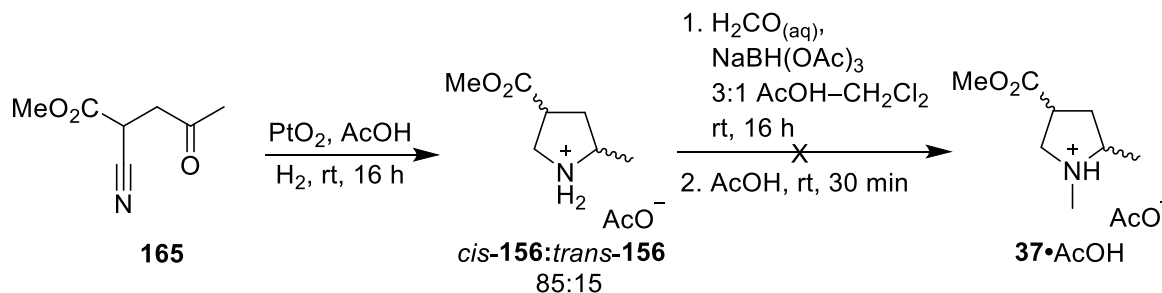
Scheme 2.79

Despite exploring multiple routes to fragments *cis*-**37** and *trans*-**37**, we were still unable to obtain either as a single diastereomer. A 65:35 mixture of fragments *trans*-**37** and *cis*-**37** had been obtained *via* the triflate hydrogenation route and, using the keto nitrile route, we had the potential to synthesise an 85:15 mixture of *cis*-**37** and *trans*-**37**. However, we had been unable to either increase the diastereoselectivity or effectively separate the diastereomers in either route. We therefore sought to synthesise some closely related 2,4-diubstituted pyrrolidine fragments that could replace *cis*-37 and *trans*-**37** in the library and be obtained as single diastereomers.

2.3 Design and Synthesis of *t*-Butyl Ester Fragments

Although it had not yielded either fragment as a single diastereomer, the nitrile hydrogenation route described in Section 2.2.4 was still very attractive to us as a way of synthesising fragments. It contained only four straightforward steps to reach a potential *N*-H fragment, which could then be further diversified. A way of increasing the diastereoselectivity in the key hydrogenation step to allow us to synthesise fragments from this route as single diastereomers was therefore sought. It was proposed that using a more sterically bulky *t*-butyl ester group would increase the *cis*-selectivity of the reaction and allow access to *cis*-**45** as a single diastereomer (Scheme 2.80).
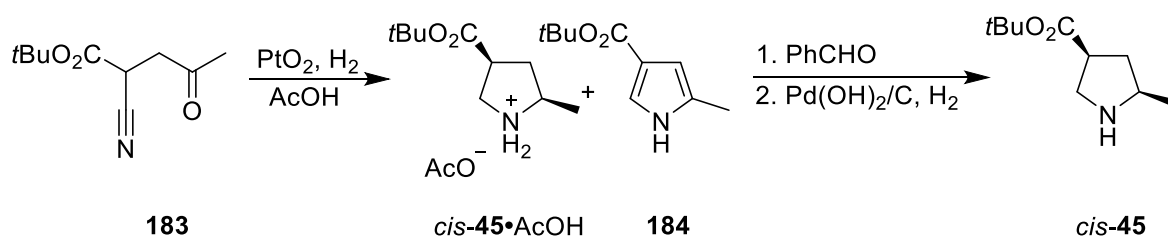
Scheme 2.80

The larger *t*-butyl ester group would have the added benefit of reducing any potential volatility issues. Thus, it was decided to target *N*-H *t*-butyl ester fragment *cis*-**45**, and to attach the other three standard groups to the nitrogen to give fragments *cis*-**46**, *cis*-**47** and *cis*-**48** (Figure 2.8).
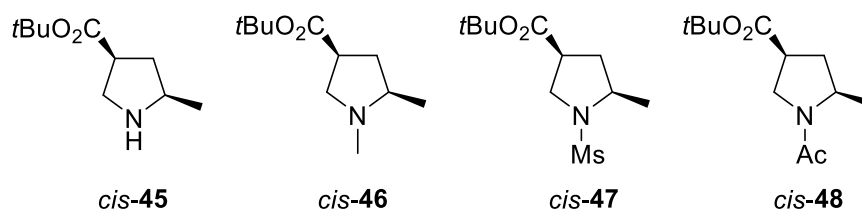
Figure 2.8: Structures of the target *t*-butyl ester fragments

PMI analysis was then performed on these target fragments to check their 3-D shape before synthesis. Pleasingly all four fragments had good 3-D shape, particularly the *N*-H, *N*-Me and *N*-Ac fragments which had conformations with $\sum$NPR > 1.3 while the *N*-Ms fragment showed conformers with $\sum$NPR > 1.15 (Figure 2.9). All four were therefore selected for synthesis.
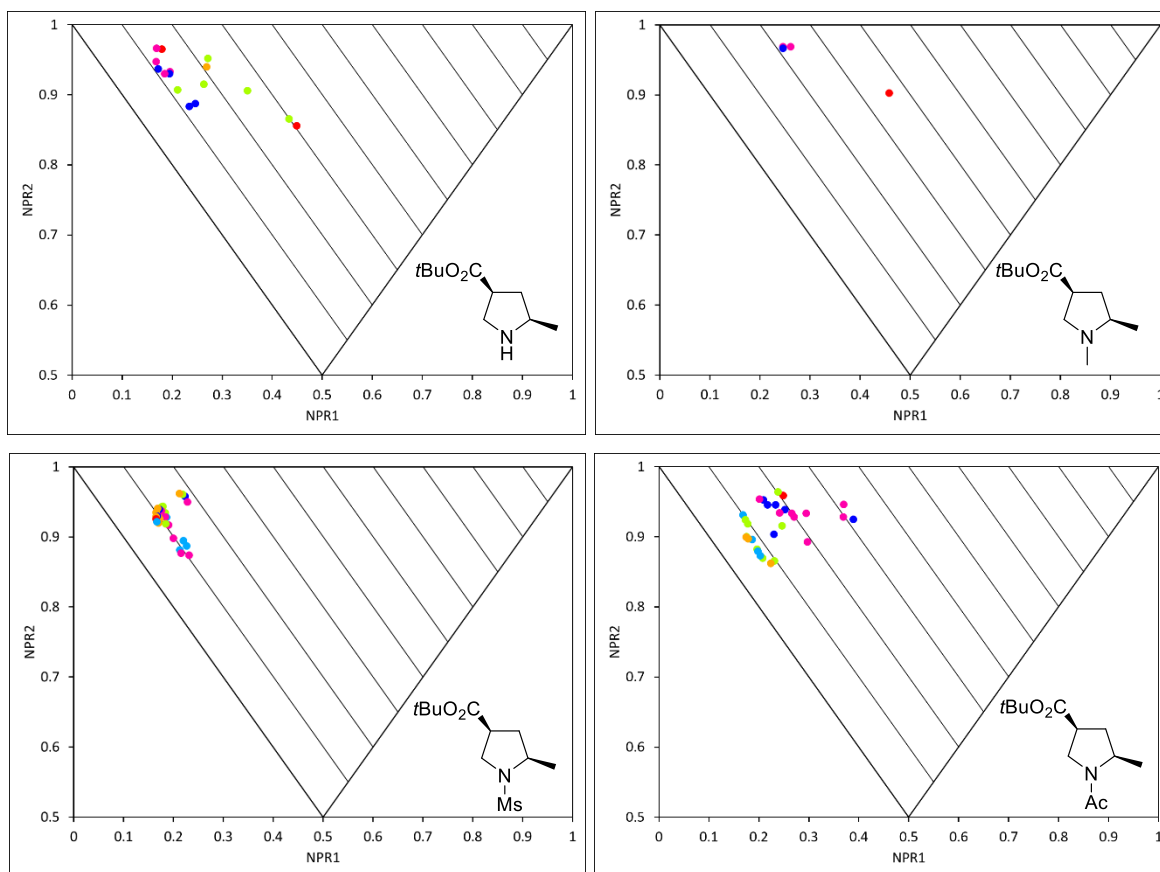
Figure 2.9: PMI plots of the potential *t*-butyl ester fragments

The first step in the synthesis was to synthesise starting keto nitrile **183**. Nitrile **185** was reacted with *t*-BuOK and chloroacetone either in THF at rt or in *t*-BuOH at 40 °C. Reaction in THF at rt gave nitrile **183** in 63% yield, whereas the same reaction performed in *t*-BuOH at 40 °C gave nitrile **183** in 76% yield (Scheme 2.81).

185

183

THF, rt, 5 h: 63%
t-BuOH, 40 °C, 5 h: 76%
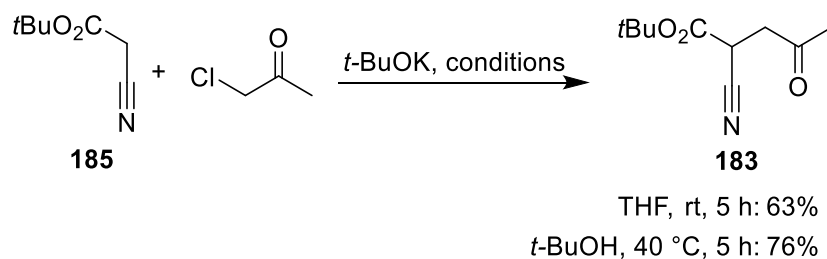
Scheme 2.81

The next step wa the hydrogenation of keto nitrile **183**. Pleasingly, hydrogenation of **183** under the standard conditions (PtO$_2$, AcOH, H$_2$) gave an 85:15 mixture of desired pyrrolidine *cis*-**45** (in >95:5 dr) and pyrrole **184**. The amine was then benzyl protected to give a single diastereomeric pyrrolidine, *cis*-**182** in 30% yield over the two steps (Scheme 2.82). This increased level of diastereoselectivity in the hydrogenation meant that

chromatography proceeded without the need to use ^{1}H NMR spectroscopy on each fraction to obtain a pure diastereomer, thus making obtaining pure *cis*-**182** quick and easily scalable.
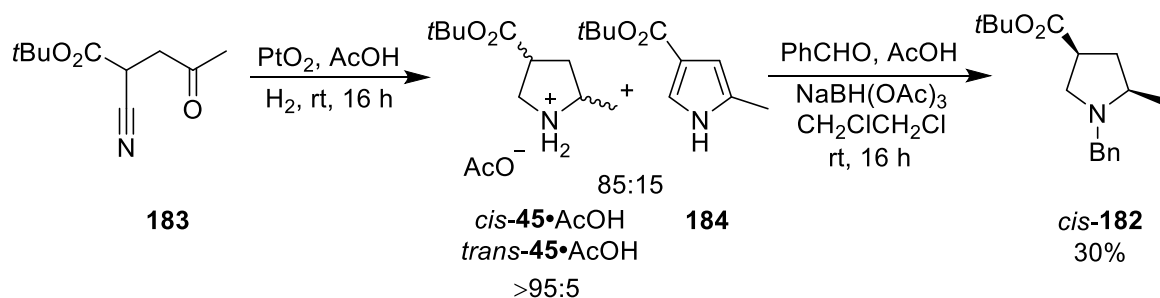
Scheme 2.82

Hydrogenation of *N*-benzyl pyrrolidine *cis*-**182** gave pyrrolidine *cis*-**45**•AcOH in 79% yield after filtration through Celite. Pyrrolidine *cis*-**45**•AcOH was then subjected to the standard *N*-methylation conditions to give pyrrolidine *cis*-**46**•AcOH in 16% yield (Scheme 2.83). It is not clear why this reaction is so low yielding.
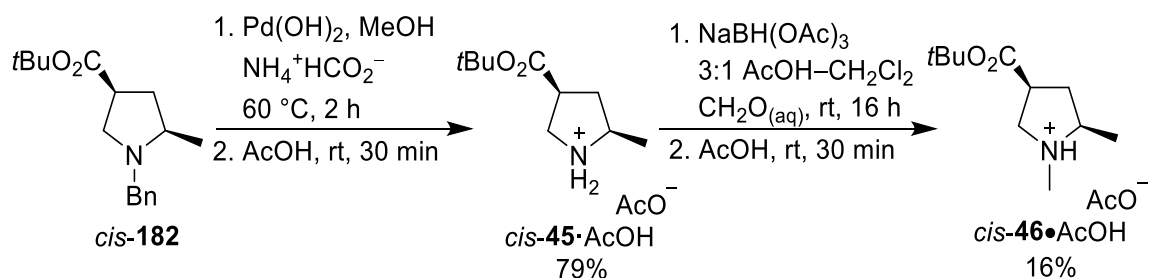
Scheme 2.83

With two fragments already in hand, attention turned to the N-Ms fragment. Pyrrolidine *cis*-**45**•AcOH was reacted with mesyl chloride and Et$_3$N (4.0 eq) in CH$_2$Cl$_2$ to give the crude product. Inspection of the ^{1}H NMR spectrum showed a 3H singlet at 2.05 ppm, which is more upfield than would be expected for an NSO$_2$Me signal. Furthermore, the ^{13}C NMR also showed additional signals at 172.5 and 172.2 ppm, leading to the realisation that the product formed was in fact the *N*-acetyl pyrrolidine *cis*-**48** rather than the *N*-mesyl pyrrolidine *cis*-**47**. The structure was confirmed by mass spectrometry and the presence of rotamers as opposed to diastereomers was confirmed by variable temperature ^{1}H NMR spectroscopy. This reaction gave pyrrolidine *cis*-**48** in 52% yield with no *N*-mesyl pyrrolidine *cis*-**47** observed (Scheme 2.84). Happily, this meant that we did not need to carry out a separate synthesis of *N*-Ac fragment *cis*-**48**!
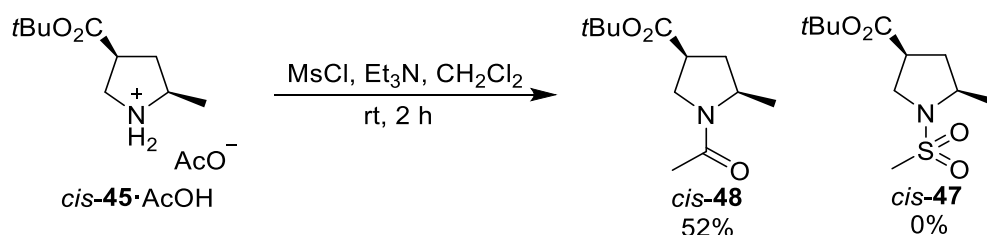
Scheme 2.84

It was proposed that pyrrolidine *cis*-**48** was being formed due to the acetate attacking the generated sulfonyl intermediate **185**. This would lead to the formation of mixed anhydride **186**, which would then be highly susceptible to nucleophilic attack from pyrrolidine *cis*-**45** (Scheme 2.85).
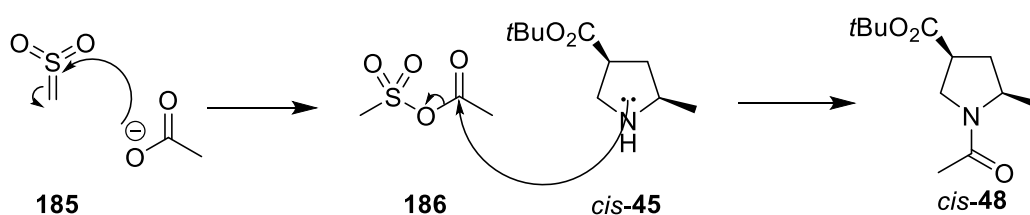
Scheme 2.85

The mesylation reaction was then repeated using pyridine as both the solvent and base. The mechanism for mesylation reactions works differently with a weaker base such as pyridine, as the mesyl chloride no longer undergoes elimination but the pyridine instead acts as a nucleophilic catalyst. Subjection of pyrrolidine *cis*-**45**•AcOH to mesyl chloride in neat pyridine at rt gave pyrrolidine *cis*-**47** in 83% yield (Scheme 2.86).
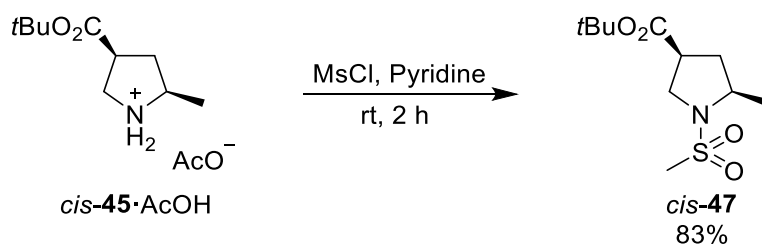
Scheme 2.86

Crystals of fragment *cis*-**47** suitable for X-ray crystallography were then successfully grown. The X-ray crystal structure of *cis*-**47** is shown in Figure 2.10 and clearly shows that the methyl and *t*-butyl ester groups are *cis* to each other. The identification of the stereochemistry of *cis*-**47** by X-ray crystallography was important as it fully supported the assignment of stereochemistry of the 2,4-disubstituted compounds in Section 2.2. We felt it reasonable to assume that the major products of the methyl ester keto nitrile hydrogenation (85:15 dr) and the *t*-butyl ester keto nitrile hydrogenation (95:5 dr) had the same relative

stereochemistry and this fitted with the stereochemical assignment by comparison with literature ^{1}H NMR spectroscopy data detailed in Section 2.2.3. As such, we felt confident to add these fragments to our library as the *cis*-diastereomers.
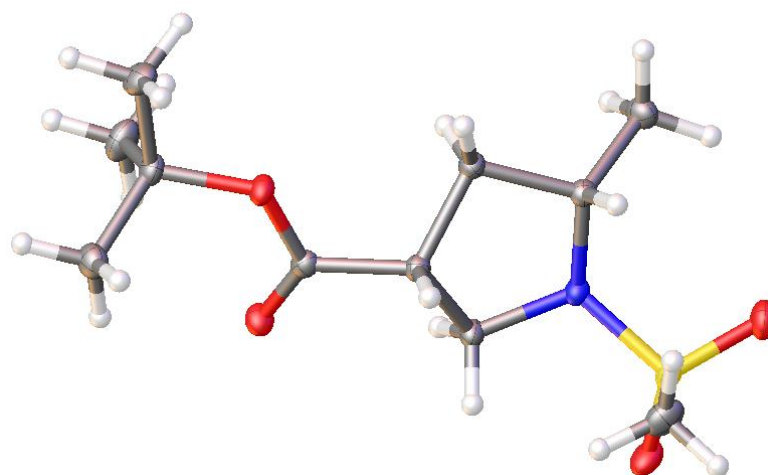
Figure 2.10: X-ray crystal structure of fragment *cis*-**47**

2.4 Conclusions

Although we had not been successful in synthesising all of the four fragments initially targeted at the beginning of this Chapter, we did successfully synthesise six new 3-D fragments to add to the library (Figure 2.11). These included initial targets *cis*-**42** and *cis*-**43**, synthesised *via* a 1,3-dipolar cycloaddition route, as well as four 2,4-disubstituted fragments: *cis*-**45**, *cis*-**46**, *cis*-**47** and *cis*-**48** which were synthesised via a nitrile hydrogenation route.
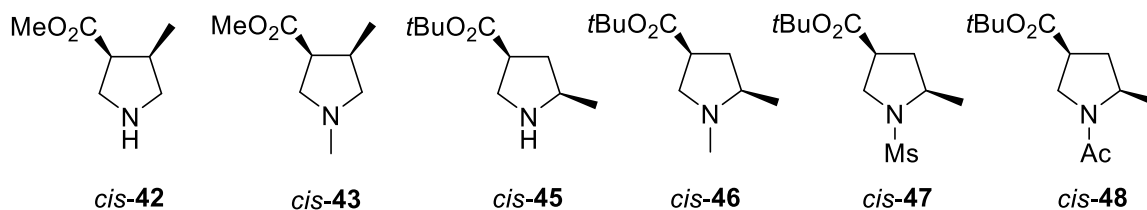
Figure 2.11: 3-D Fragments synthesised in this Chapter

Work towards fragments *cis*-**42** and *cis*-**43** included both a 1,3-dipolar cycloaddition route and the enol triflate Michael addition route. Although the Michael addition route proved unsuccessful, the triflate intermediate provided the inspiration for the design of our 2nd generation fragments, and the work done on the synthesis of triflate **99** ensured that 2nd generation fragments could be accessed quickly without optimisation of the synthesis of the key intermediate being needed (Scheme 2.87).
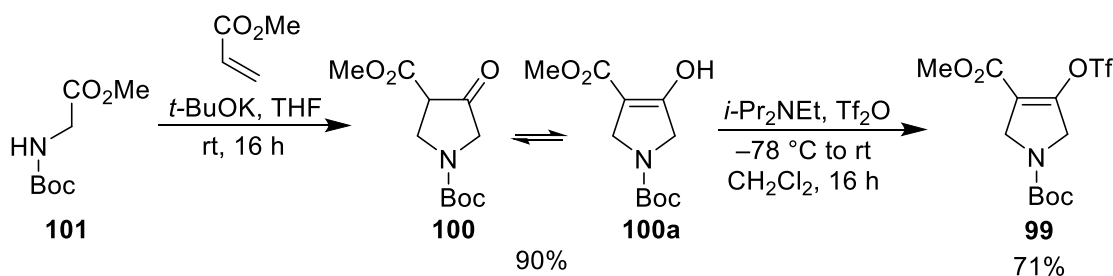
Scheme 2.87

Routes to access target fragments *trans*-**37** and *cis*-**37** were even more varied, with work done on a Claisen condensation route (Section 2.2.2), a triflate hydrogenation route (Section 2.2.3) and a nitrile hydrogenation route (Section 2.2.4). All three routes came very close to synthesising the target fragments, but none were able to synthesise either as a single diastereomer. However, the triflate hydrogenation route did give access to a 65:35 mixture of fragments *trans*-**37** and *cis*-**37**, while the short, diastereoselective nitrile hydrogenation route ultimately resulted in the synthesis of the four *t*-butyl ester fragments (Scheme 2.88).
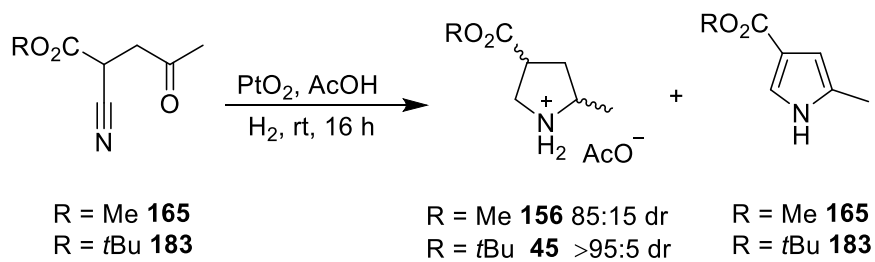
Scheme 2.88

With the 1st generation of fragments now complete, we sought to apply our learnings from the selection and synthesis

of this initial fragment library to guide the creation of a 2nd generation of 3-D fragments that would expand our collection. This work is detailed in Chapter 3.

CHAPTER 3: DESIGN AND SYNTHESIS OF 2nd GENERATION 3-D FRAGMENTS

After the completion of the synthetic work detailed in Chapter 2, it was decided that an alternative approach to the synthesis of 3-D fragments should be explored. Although the 1st generation fragments possessed both the requisite 3-D shape and properties, each substitution pattern required its own synthetic route, meaning that it took a long time to synthesise a significant number of 3-D fragments. A new strategy was therefore explored which would allow for rapid access to a large number of fragments whilst mantaining good physicochemical properties and interesting 3-D shape. The new strategy, presented in detail in Section 3.1, involved trapping a selection of β-ketoesters **187** as enol triflates **188** followed by Suzuki-Miyaura coupling with aryl boronic acids to give substituted alkenes **189** and then hydrogenation and derivatisation to give 3-D fragments *cis*-**44** (Scheme 3.1).
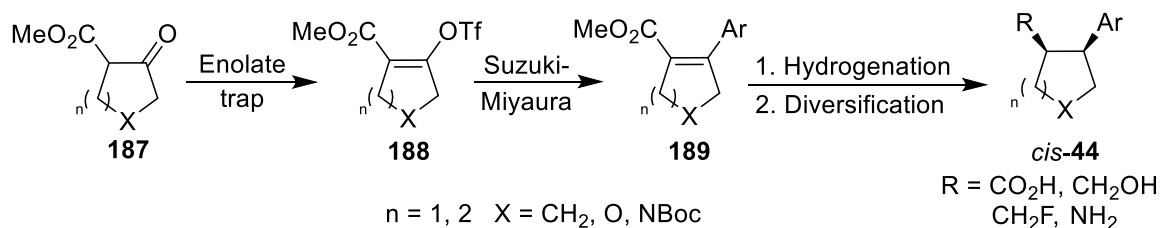
Scheme 3.1

After reviewing the relevant literature (Section 3.2), the synthesis of enol triflates **188** and the scope of the Suzuki-Miyaura coupling is described (Section 3.3). Then, optimisation of the hydrogenation is presented (Section 3.4). In Section 3.5, initial ester diversification work on a pyrrolidine system and synthesis of two 3-D fragments are presented. The learnings from this were then used to divide the diversification into two discrete routes, a reduction route (Section 3.6) and a hydrolysis route (Section 3.7) which were used to synthesise a further 22 fragments.

3.1 Issues with the 1st Generation Fragments and Introduction of the the New Strategy for 2nd Generation Fragment Synthesis

Those fragment libraries whose synthesis are detailed in the literature (see Section 1.3) show one feature in common: they are directed by a synthetic strategy as opposed to being designed exclusively based on criteria such as 3-D shape or physicochemical properties. While our group's strategy of selecting fragments primarily on 3-D shape had resulted in a shape-diverse set of attractive 3-D fragments, it had taken significant time and effort to synthesise the 35 fragments. We therefore sought to access the benefits of using a single synthetic strategy while continuing to prioritise diverse functionality and 3-D shape. It was decided to target 25 new 3-D fragments by using a single synthetic route, which is the focus of this chapter.

When designing the 2nd generation fragments, several new design features were included whilst continuing to work on disubstituted saturated heterocycles. To aid with both screening and protein binding, an aromatic group was included in each fragment. This would increase both the molecular weight and lipophilicity as well as providing potential new binding modes and making protein screening by ^{1}H NMR spectroscopy easier. We also wanted to introduce greater variation of pharmacophore. Previously, only esters and primary alcohols had been used in combination with the differentially functionalised amino group. In the new approach, the pendant pharmacophore as well as the core saturated heterocycle would be diversified to add greater diversity in the synthesised fragments.

During work on the synthesis of fragments *cis*-**42**, *cis*-**43** and *cis*-**37**, vinyl triflates **99** and **161** had been synthesised as intermediates (Figure 3.1). Although the routes to the 3-D fragments involving vinyl triflates **99** and **161** were ultimately unsuccessful, the compounds themselves appeared to have potential as building blocks towards other fragments.

Figure 3.1: Previously synthesised vinyl triflates

Enol triflates **99** and **161** contain three points of diversification: the vinyl triflate, the amino substituent and the ester group. The vinyl triflate group in **99** could be used in Suzuki-Miyaura cross-coupling to introduce an aryl group to give alkenes **190**. Hydrogenation of alkenes **190** would give the *cis* stereochemistry in 3-D fragments *cis*-**191.** Diversification of

the amino group had already been established in the synthesis of the 1st generation fragments and esters are versatile and could be diversified to groups such as alcohols, alkyl fluorides, amines or acids to give fragments *cis*-**192**. (Scheme 3.2).

Scheme 3.2

The core heterocycle also had the potential to be varied. If different β-ketoesters (Figure 3.2), the precursors to the vinyl triflates, could be obtained, then it should be possible to synthesise a diverse set of 3-D fragments. The availability of β-keto esters **100** and **193-196** (Figure 3.2) was therefore investigated. Cyclopentane ester **193** and the NH precursor to piperidine ester **196** are commercially available. The synthesis of esters **194** and **195** has been reported[109–111] and the synthesis of pyrrolidine ester **100** was carried out in Chapter 2 (see Scheme 2.32). With ready access to these β-keto esters, the route shown in Scheme 3.3 looked to be a viable strategy for the synthesis of 2nd generation 3-D fragments.
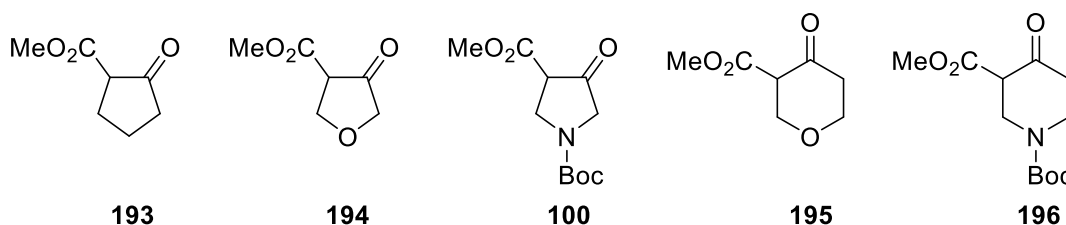
Figure 3.2: The proposed β-ketoester starting materials
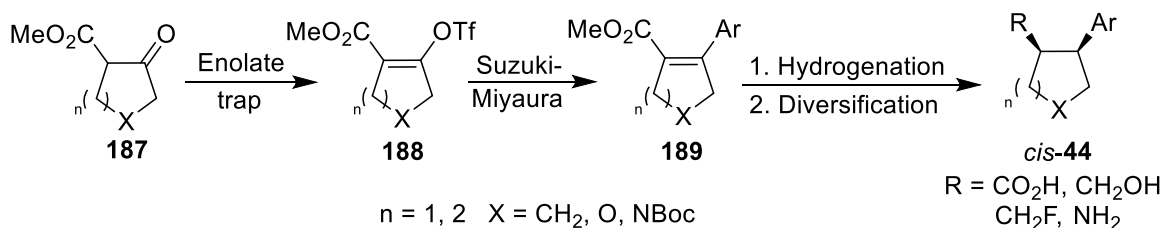
Scheme 3.3

Before their synthesis, potential fragments were subjected to PMI analysis to assess their 3-D shape. Only fragments with at least one conformation less than 1.5 kcalmol^{-1} above the ground state energy with $\sum$NPR $\geq$ 1.15 were selected for synthesis. Detailed 3-D shape analysis of the synthesised fragments is presented in Section 4.3.

3.2 Overview of Previous Syntheses of 3,4-Disubstituted Saturated Cyclic Compounds using the Triflate Coupling Route

There are a handful of reported examples of the synthesis of *cis*-3,4-disubstituted cyclic compounds using the proposed triflate coupling route. For example, Zhang *et al.*[112] showed that enol triflate **197** could be easily prepared from cyclopentyl β-ketoester **193**. Subsequent Suzuki-Miyaura coupling with phenylboronic acid gave disubstituted cyclopentene **198** in 85% yield. Hydrogenation then gave cyclopentane ester *cis*-**199** in 95% yield (Scheme 3.4).
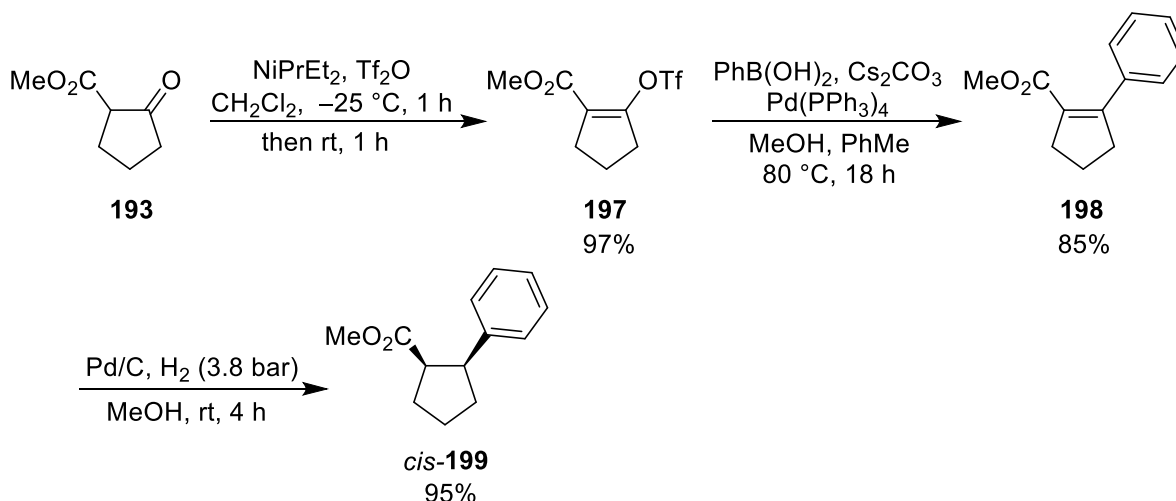
Scheme 3.4

Much work in this general area has focussed on the synthesis of 3,4-disubstituted piperidines. This is due to the development of Paroxetine, a successful antidepressant discovered in 1973 and launched by SmithKline Beecham in 1992.[113] Although Paroxetine is a *trans*-3,4-disubstituted piperidine, attempts to create analogues have involved the synthesis of *cis*-3,4-disubstituted piperidines. A patent from 2016 reported the deprotonation of *β*-ketoester **196** with NaH and trapping with PhNTf₂ to give enol triflate **200** in 75% yield. Suzuki-Miyaura coupling with phenylboronic acid and Pd(PPh₃)₄ worked well to give piperidine **201**.[114] Hydrolysis of the ester in piperidine **202** with NaOH at 70 °C and hydrogenation at high pressure with Pd/C as the catalyst gave acid *cis*-**203** in 78% yield over 2 steps (Scheme 3.5).
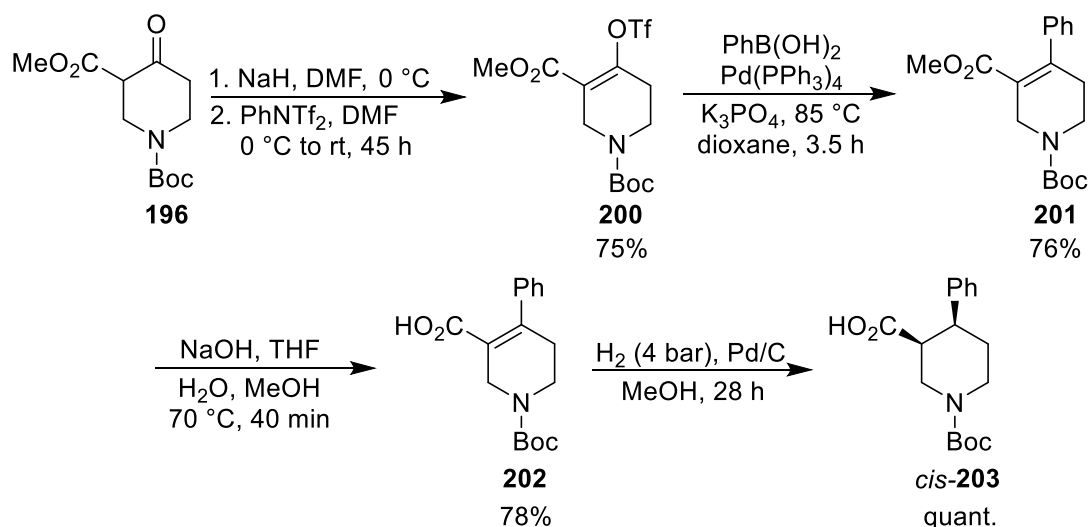
Scheme 3.5

Work has also been reported on the synthesis of *cis-* and *trans-*3,4-disubstituted THFs. Chen *et al.* have synthesised a number of 3,4-disubstituted THFs and tetrahydrothiophenes as potential melanocortin-4 receptor ligands.[115] In one example, THF *β*-ketoester **194** was triflated using NaH and Tf_2O to give enol triflate **204** in 23% yield. Then, Suzuki-Miyaura coupling with 4-chlorophenyl boronic acid gave dihydrofuran **205** in 40% yield. Dihydrofuran **205** was reduced using $NaBH_4$ and $NiCl_2$ to give an 85:15 mixture of THFs *trans-***206** and *cis-***206** in 76% yield (Scheme 3.6).
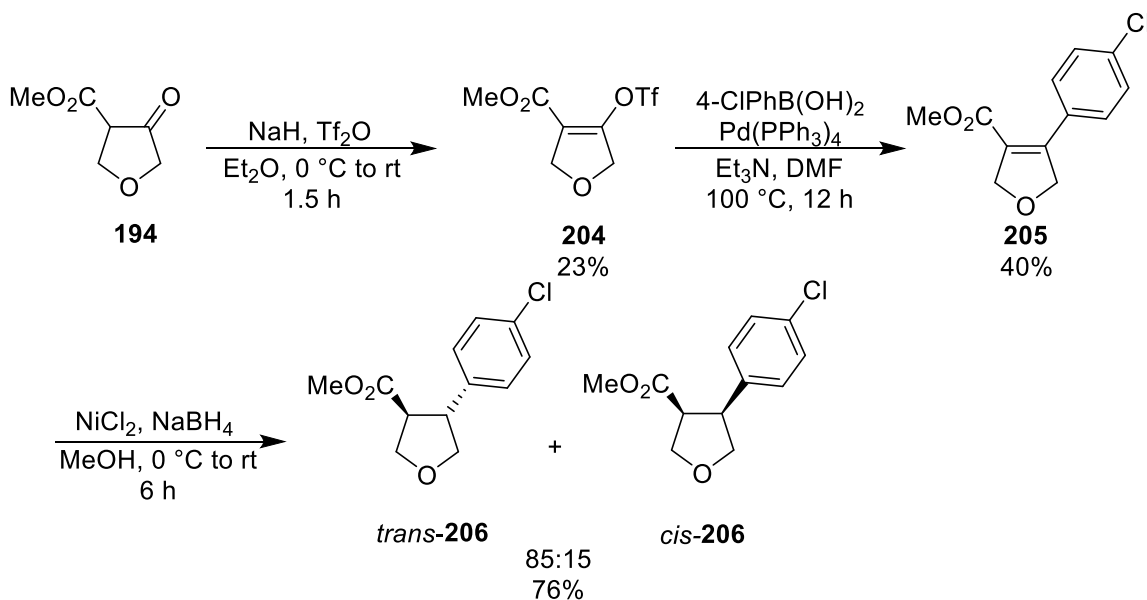
Scheme 3.6

Together, $NiCl_2$ and $NaBH_4$ typically form $Ni(BH_4)_2$ *in situ*, which could perform a 1,4-conjugate addition of hydride into the alkene to give an enolate. The high *trans-*selectivity of this reduction is interesting as the kinetic product could be expected to be *cis-***206**, with protonation of the enolate occurring on the opposite face to the aromatic ring. Therefore, it

is possible that epimerisation to *trans*-**206** occurred after the reduction under these conditions. Unfortunately, the stereoselectivity of this reaction is not commented on in the paper.

The examples shown in Schemes 3.5 and 3.6 indicated that the proposed new route to 3-D fragments was appropriate. We planned to use the literature knowledge to act as a starting point for identifying a single set of conditions for each step in the route that could be applied to all substrates and easily performed. Once conditions had been established, around 25 3-D fragments would be synthesised using the synthetic route set out in Scheme 3.3.

3.3 Synthesis of Enol Triflates and Investigation of Suzuki-Miyaura Cross-Couplings

To start with, the required enol triflates were prepared. In some cases, it was also necessary to prepare the β-ketoesters. Using literature conditions,[81] cyclopentene enol triflate **197** was synthesised in 92% yield from β-ketoester **193** (Scheme 3.7). Piperidine enol triflate **200** was synthesised in a similar manner. Boc protection of the commercially available salt **207**•HCl proceeded in 95% yield to give the enol tautomer of β-ketoester **196a**.[116] Then, triflation of *N*-Boc piperidine enol ester **196a** using *i*-PrNEt$_2$ and Tf$_2$O gave triflate **200** in 90% yield (Scheme 3.7).

Scheme 3.7
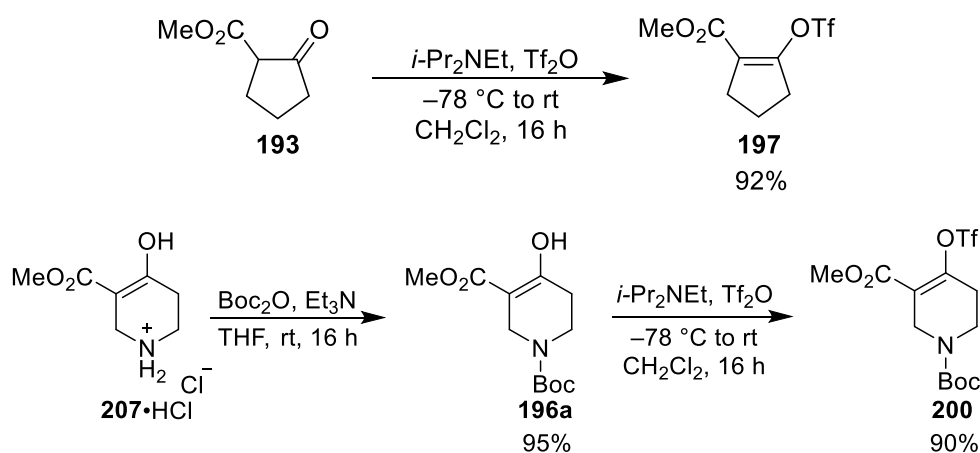
The final two enol triflates to be synthesised were the THF and THP enol triflates. Neither THF β-ketoester **194** nor THP β-ketoester **195** are commercially available. They were each synthesised by another group member.[83] Following a literature procedure, THF β-ketoester **194** was prepared in 53% yield from hydroxyester **208** and methyl acrylate. A different route was used for THP β-ketoester **195**. Reaction of ketone **209** with LHMDS and trapping with an imidazole-containing electrophile gave β-ketoester **195** in 45% yield (Scheme 3.8).

Scheme 3.8
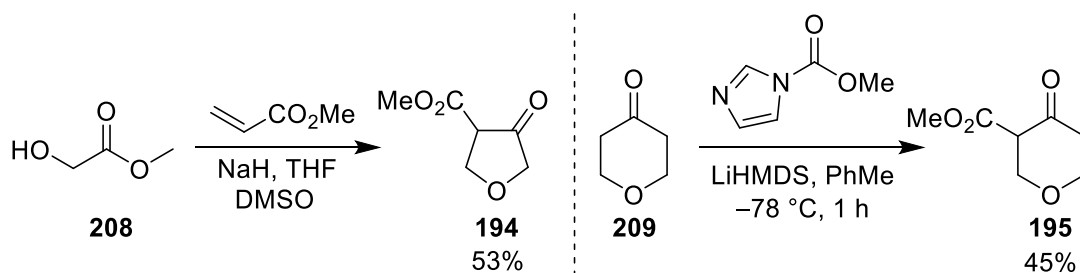
With each of β-ketoesters **194** and **195** in hand, their triflation was explored. The synthesis of THF triflate **204** was attempted using our standard conditions of *i*-PrNEt$_2$ and Tf$_2$O. The triflation appeared to be successful by ^{1}H NMR spectroscopy of the product obtained after

chromatography (Scheme 3.9). However, THF enol triflate **204** proved to be unstable, with the sample physically degrading after 1-2 days.
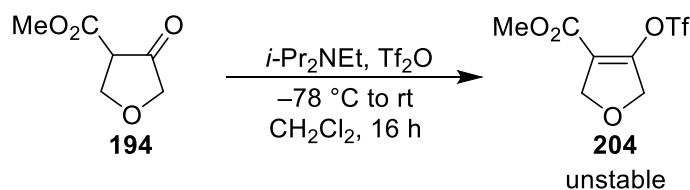
Scheme 3.9

The decision was therefore made to prepare fresh enol triflate **204** and then carry out the Suzuki-Miyaura reaction immediately after purification by chromatography. It was decided to use the same process with THP β-ketoester **195**, even though we had no information on the stability of THP enol triflate. This was because the electrophile required in the synthesis of THP β-ketoester **195** had to be synthesised separately and purification of THP β-ketoester **195** proved difficult, meaning that synthesis of THP β-ketoester **195** was very time-consuming.

With the starting enol triflates now available, the next step to explore was the Suzuki-Miyaura couplings. Coupling of pyrrolidine enol triflate **99** with phenylboronic acid was attempted first. Using similar conditions to those used by Zhang *et al.*,[112] reaction using Pd(PPh$_3$)$_4$ as catalyst and THF as solvent and heating to 65 °C for 18 h gave the desired dihydropyrrole **210** in only 33% yield (Scheme 3.10). To attempt to improve the yield, the solvent was changed since much of the material appeared not to dissolve. Use of 4:1 THF–H$_2$O resulted in complete dissolution of all reagents and a substantial increase in yield of **210** to 83% (Scheme 3.10). The increase in yield may also be due in part to water increasing the amount of the intermediate oxo-palladium species available, which is the active species in the transmetallation step.[117]
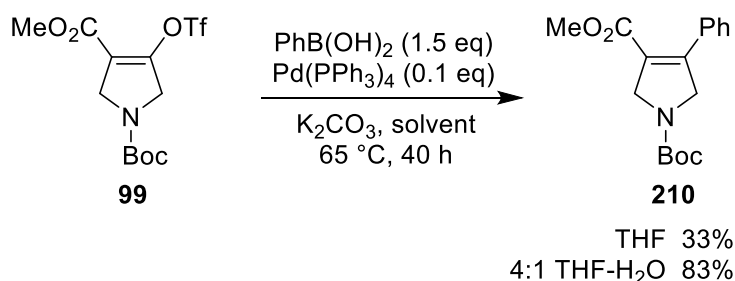
Scheme 3.10

With suitable cross-coupling conditions identified, each enol triflate was cross-coupled with a selection of boronic acids. A variety of arylboronic acids, including some heteroarylboronic acids, were chosen to ensure that the 3-D fragments would have a range

of protein binding modes and physicochemical properties. Couplings of pyrrolidine enol triflate **99** were performed first (Table 3.1), with 2-furanboronic acid giving **211** in 72% yield (entry 2) and 2-fluorophenylboronic acid giving **212** in 57% yield (entry 3).
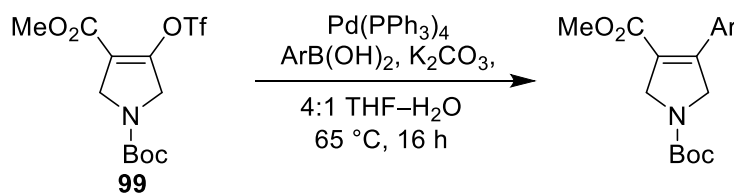
Entry	Boronic Acid	Compound	Yield/%[a]
1	B(OH)$_2$	**210**	83
2	O B(OH)$_2$	**211**	72
3	B(OH)$_2$ F	**212**	57

[a]Yield after chromatography

Table 3.1: Pyrrolidine Suzuki-Miyaura cross-couplings

Cross-couplings were then attempted with cyclopentyl enol triflate **197**. Heteroarylboronic acids were chosen for the cross-couplings to compensate for the lack of heteroatoms in the core scaffold. The results with four different boronic acids are shown in Table 3.2. Medicinally relevant heteroaromatic boronic acids were chosen to add a second binding mode, as the cyclopentane core was unlikely to form key interactions The reactions all proceeded successfully although 3-pyridineboronic acid gave **213** in only 35% yield (entry 1). In contrast, pyrimidine, pyrazole and thiophene boronic acids all reacted in yields of over 80% to give **214**, **215** and **216** respectively (entries 2-4).
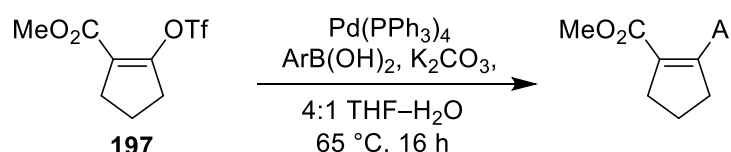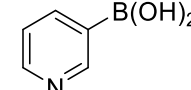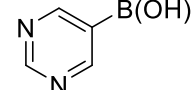
Entry	Boronic Acid	Compound	Yield/%[a]
1		**213**	35
2		**214**	81
3		**215**	88
4		**216**	81
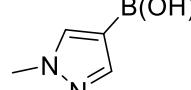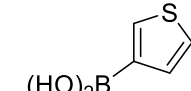
[a] Yield after chromatography

Table 3.2: Cyclopentane Suzuki-Miyaura cross-couplings

Next, cross-couplings with piperidine enol triflate **200** were carried out (Table 3.3). Cross-coupling with phenylboronic acid (using Pd(PPh$_3$)$_4$, conditions A) proceeded smoothly to give **201** in 86% yield (entry 1). However, when the reaction was attempted with pyrimidine boronic acid, ^{1}H NMR spectroscopy of the crude product showed only starting material (entry 2). Use of Pd(dppf)Cl$_2$ as catalyst (conditions B) resulted in product **217** being visible in the ^{1}H NMR spectrum of the crude product, but none was isolated after column chromatography (entry 3). It was reasoned that either the product was degrading or the presence of two basic amines in the molecule was causing the product to bind to the silica. The reaction was therefore repeated, but the column was basified with Et$_3$N before elution of the crude product. This resulted in the isolation of the desired product **217** in 57% yield (entry 4).
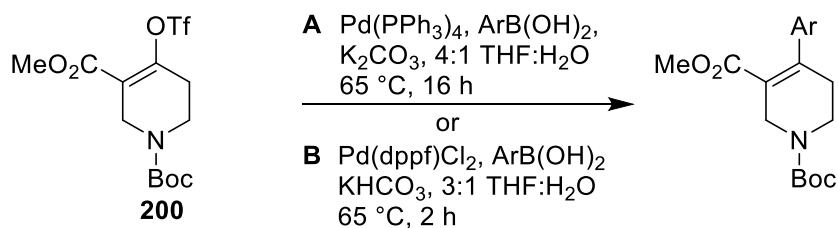
Entry	Boronic Acid	Conditions	Compound	Yield/%[a]
1	B(OH)$_2$ (phenyl)	A	**201**	86
2	B(OH)$_2$ (pyrimidinyl)	A	**217**	0
3	B(OH)$_2$ (pyrimidinyl)	B	**217**	0
4	B(OH)$_2$ (pyrimidinyl)	B[b]	**217**	57

[a] Yield after chromatography
[b] Column basified with Et$_3$N before purification

Table 3.3: Piperidine Suzuki-Miyaura cross-couplings

The final enol triflates to be coupled were THF **204** and THP **218** (Table 3.4). Starting THF β-ketoester **194** was reacted overnight with *i*-PrNEt$_2$ and Tf$_2$O to give crude THF enol triflate **204**. Triflate **204** was then purified by chromatography and subjected to the Suzuki-Miyaura cross-coupling on the same day to minimise degradation of the enol triflate. Cross-coupling with 4-fluorophenylboronic acid gave the desired product **219** in 53% yield over two steps (entry 1). However, coupling with 2-fluorophenylboronic acid (entry 2) and *o*-tolylboronic acid (entry 3) gave mixtures of product and boronic acid that proved very difficult to separate. Further reactions of these mixtures did allow access to 3-D fragments as described in Section 3.5. Coupling with 3-pyridylboronic acid was successful but gave **222** in only 23% yield (entry 4). The only attempted coupling with THP β-ketoester **195** was with 3-methoxyboronic acid and this gave **223** in 52% yield (entry 5).

Entry	β-Ketoester	Coupling Partner	Compound	Yield/%[a]
1			**219**	53
2			**220**	28[b]
3			**221**	44[c]
4			**222**	23
5			**223**	52

[a] Yield over two steps after chromatography
[b] Isolated as an inseparable 60:40 mixture of product **220** and boronic acid
[c] 16% of pure **221**, 28% obtained as a 60:40 mixture of **221** and the arylboronic acid

Table 3.4: THF and THP Suzuki-Miyaura cross-couplings

In total, 14 Suzuki-Miyaura cross-coupled products were synthesised using a range of cores and arylboronic acids. With the exception of the pyrimidine-coupled piperidine **217**, all the cross-couplings used the same reaction conditions.

Now that the Suzuki-Miyaura cross-couplings had been successfully performed, the next step was the hydrogenation of the alkenes to introduce the *cis*-stereochemistry in the 3-D fragments. Reaction of dihydropyrrole **210** with Pd/C under H_2 in MeOH gave the desired product, *cis*-**224**, as a single diastereomer in 97% yield (Scheme 3.11). The stereochemistry of *cis*-**224** was proven by changing the *N*-Boc group into an *N*-Ac group and comparison of the NMR spectroscopic data with *N*-Ac *trans*-**227**, which was independently synthesised by another member of the group. This proof of stereochemistry is discussed later (see Scheme 3.19).
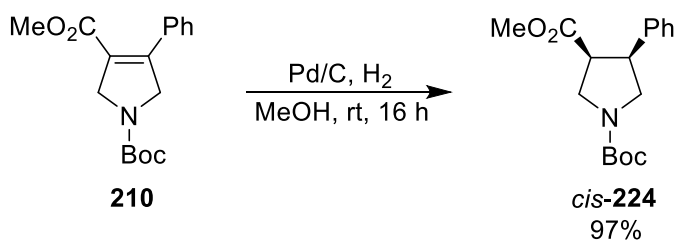
Scheme 3.11

The next hydrogenation attempted was phenyl-coupled piperidine **201** (Table 3.5). Reaction with Pd/C under H_2 in MeOH for 16 h gave almost complete conversion to piperidine *cis-***225** (entry 1). Changing the catalyst to PtO_2 reduced conversion to only 25% (entry 2), but use of $Pd(OH)_2$/C resulted in complete conversion (entry 3). Transfer hydrogenation using $Pd(OH)_2$/C and $NH_4^+HCO_2^-$ also gave complete conversion to *cis-***225** (entry 4). The crude mass recovery in all four reactions was greater than 85%
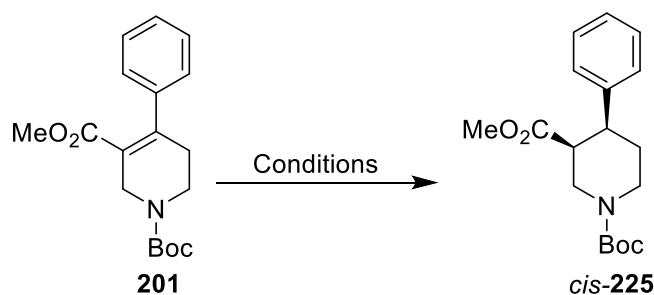
Entry	Conditions	*cis-***225**:**201**[a]
1	Pd/C, H_2, MeOH, rt, 16 h	95:5
2	PtO_2, H_2, MeOH, rt, 16 h	25:75
3	$Pd(OH)_2$/C, H_2, MeOH, rt, 16 h	100:0
4	$Pd(OH)_2$/C, $NH_4^+HCO_2^-$, MeOH, 60 °C, 3 h	100:0

[a] Ratio determined by ^1H NMR spectroscopy of the crude product

Table 3.5 Screening of conditions for the hydrogenation of **201**

The *cis* stereochemistry of piperidine **225** was confirmed using X-ray crystallography (Figure 3.2).
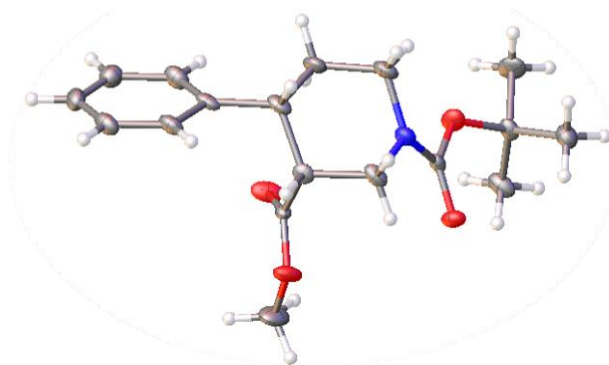
Figure 3.2: X-ray crystallography of piperidine *cis-***225**

The hydrogenation of compounds containing heteroaryl groups was then attempted. Cyclopentyl alkenes **213**, **214** and **215** were chosen for hydrogenation as the resulting products would all be 3-D fragments. However, hydrogenation of these compounds using the transfer hydrogenation conditions gave complex mixtures of products in all cases (Scheme 3.12). Frustrated by this result, it was postulated that the reaction was not working due to the basic heteroaromatic nitrogens forming formate salts. It was decided to perform a second hydrogenation optimisation based on what was anticipated to be the most difficult Suzuki-Mitaura product to hydrogenate, pyrimidine-coupled piperidine **217**.
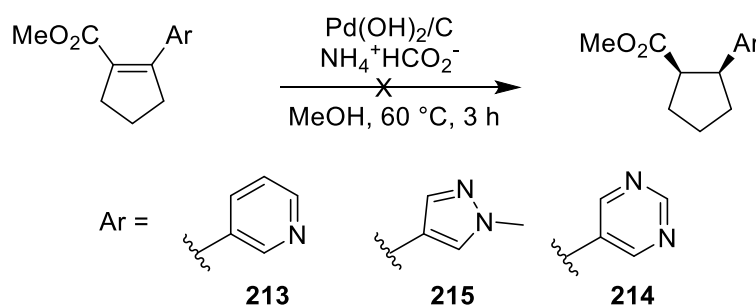
Scheme 3.12

The results of the hydrogenation of piperidine alkene **217** are summarised in Table 3.6. Both Pd/C and Pd(OH)$_2$/C (entries 1 and 2) showed 90% conversion and, although not attempted, it was postulated that leaving either of these reactions for longer would likely result in complete conversion to the final product. Mass recovery in both of these systems was good with 80% recovery for Pd/C and 90% recovery for Pd(OH)$_2$/C. Pd(OH)$_2$/C hydrogenation with 3 equivalents of acetic acid added to prevent potential poisoning of the catalyst by the basic nitrogens proved unsuccessful (entry 3). In this case, the ^{1}H NMR spectrum of the crude product lacked peaks in the aromatic region, indicating that the pyrimidine ring had likely been hydrogenated. Interestingly, the transfer hydrogenation conditions (entry 4) were more successful than they had been with cyclopentenes **213-215** (see Scheme 3.12), with a 65:35 ratio of starting material **217** and product *cis*-**226** identifiable by ^{1}H NMR spectroscopy of the crude. However, the crude mass recovery was only 70% and the conversion was still much worse than it had been with phenyl substituted piperidine **201** (see entry 4, Table 3.6).
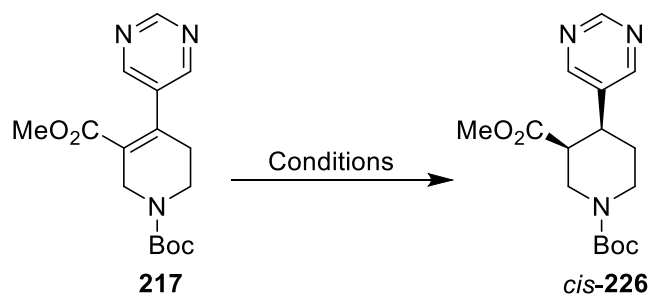
Entry	Conditions	cis-**226:217**[a]
1	Pd/C, H$_2$, MeOH, rt, 16 h	90:10
2	Pd(OH)$_2$/C, H$_2$, MeOH, rt, 16 h	90:10
3	Pd(OH)$_2$/C, H$_2$, AcOH (3 eq) MeOH, rt, 16 h	–[b]
4	Pd(OH)$_2$/C, NH$_4$$^+HCO_2$$^-$, MeOH, 60 °C, 3 h	35:65

[a] Ratio determined by ^{1}H NMR spectroscopy of the crude product
[b] No aromatic peaks visible by ^{1}H NMR spectroscopy

Table 3.6: Screening of conditions for the hydrogenation of **217**

From the two hydrogenation optimisations, we concluded that use of Pd/C or Pd(OH)$_2$/C as catalyst with H$_2$ in MeOH (Table 3.6, entries 1 and 3) were the best conditions to proceed with. Reactions would be monitored by TLC and allowed to continue to completion.

3.4 Initial Ester Diversification Work

With two suitable conditions for the hydrogenation step identified, a strategy for the diversification of the ester group was proposed. Pyrrolidine *cis*-**224** was selected as a representative example to test the toolkit of reactions and our initial plans are shown in Scheme 3.13. First, the Boc group would be replaced with an acetyl group to give the first fragment, *cis*-**227**. The strategy then involved three reactions on ester *cis*-**227**: ester reduction to give alcohol *cis*-**228**, ester hydrolysis to give acid *cis*-**229** or direct amidation to give amide *cis*-**230**. It was anticipated that acid *cis*-**229** and alcohol *cis*-**228** could be further diversified to give other functional groups. However, this would be dependent on our ability to synthesise the alcohol and acid fragments.
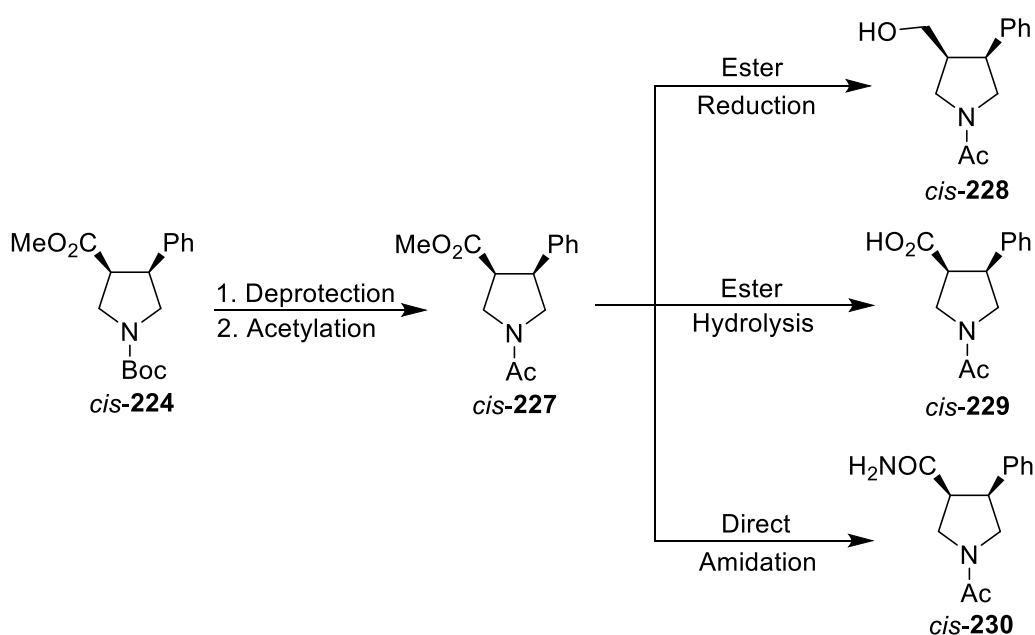
Scheme 3.13

Synthesis began with the deprotection and acetylation of pyrrolidine *cis*-**224**. Deprotection was performed using TFA. Subsequent acylation using AcCl and Et$_3$N at rt followed by chromatography gave the desired pyrrolidine *cis*-**227** in 49% yield (Scheme 3.14).
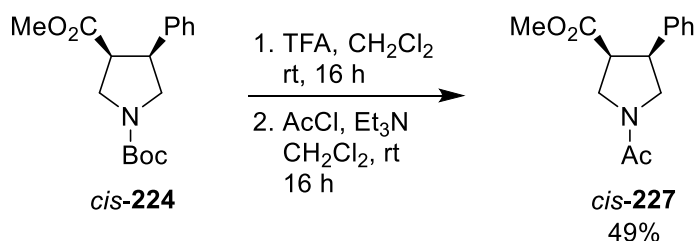
Scheme 3.14

3.4.1 Investigation of the Pyrrolidine Ester Reduction

Diversification started with the reduction of ester *cis*-**227** to give alcohol *cis*-**228**. Ester *cis*-**227** was reacted with LiAlH$_4$ at 0 °C for 2 h. ^{1}H NMR spectroscopy of the crude product showed that the reaction was unsuccessful, with a mixture of products formed that contained pyrrolidine *cis*-**231** as the major product. Pyrrolidine *cis*-**231** had been formed due to both the ester and the amide groups bring reduced, giving an *N*-ethyl group (Scheme 3.15). Unfortunately, pyrrolidine *cis*-**231** proved difficult to purify by column chromatography, which prevented its addition to the fragment library.
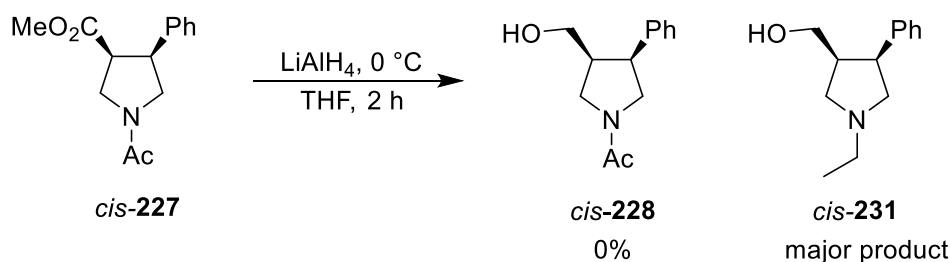
Scheme 3.15

The use of LiBH$_4$ was then explored as it would be less likely to reduce the *N*-Ac group. Reaction of ester *cis*-**227** with LiBH$_4$ at 0 °C for 2 h gave no reaction (Table 3.7, entry 1). However, increasing the reaction temperature to rt and time to 16 h gave a 50:50 mixture of desired alcohol *cis*-**228** and starting ester *cis*-**227**. A selection of times, temperatures and equivalents were then tested to attempt to improve the conversion of ester *cis*-**227** into alcohol *cis*-**228**, with the ratio of products being determined by ^{1}H NMR spectroscopy of the crude product. Heating the reaction to 65 °C gave a complex mixture of products, with small amounts of *cis*-**227** and *cis*-**228** present (entry 3). Increasing the reaction time to 64 h at rt showed no improvement in conversion (entry 4), but use of 4 eq. of LiBH$_4$ gave an improvement to a 75:25 ratio (entry 5), with the reaction being monitored by TLC. Importantly, none of these conditions showed any indication of epimerisation.

Table 3.7: Optimisation of the reduction of pyrrolidine *cis*-**227**
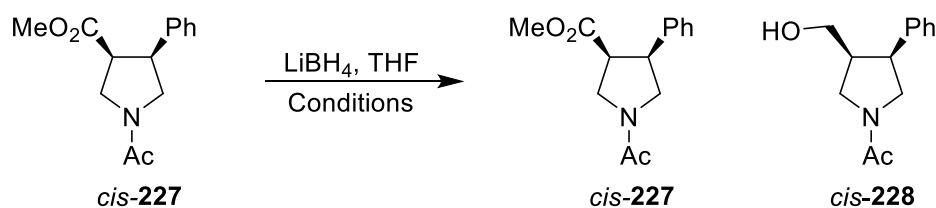
Entry	Time/h	Eq. of LiBH₄	Temp./ °C	*cis*-**227**:*cis*-**228**[a]
1	2	2	0	100:0
2	16	2	rt	50:50
3	5	2	65	–[b]
4	64	2	rt	50:50
5	64	4	rt	25:75

[a] Ratio of *cis*-**227** and *cis*-**228** determined from the ¹H NMR spectrum of the crude product
[b] Some evidence of *cis*-**227** and *cis*-**228** by ¹H NMR spectroscopy amidst other products

The reduction of ester *cis*-**227** to alcohol *cis*-**228** was then performed on larger scale using 4 eq. of LiBH₄. The reduction gave alcohol *cis*-**228** in 37% yield after chromatography to separate it from the starting ester *cis*-**227** (Scheme 3.16).
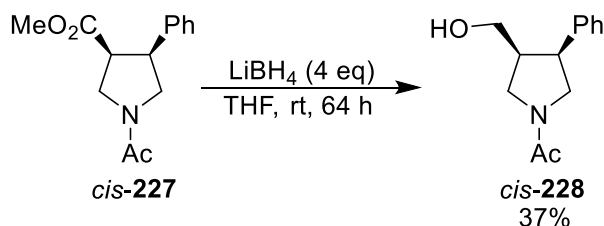
Scheme 3.16

Ideally, the next steps would have been to attempt the further diversification of alcohol *cis*-**228** by hydroxyl substitution. However, insufficient amounts of alcohol *cis*-**228** were synthesised to both continue the diversification and add alcohol *cis*-**228** to the library. It was therefore decided to add alcohol *cis*-**228** to the 3-D fragment library and investigate the synthesis of alcohol *cis*-**228** *via* a different route.

We proposed that performing the reduction on dihydropyrrole **210** could prevent the over-reduction issues. The reduction was therefore performed on dihydropyrrole **210** using LiAlH₄ at 0 °C (Scheme 3.17). However, the ¹H NMR of the crude reaction mixture showed a complex mixture of products, with neither starting material **210** nor product **232** being evident.
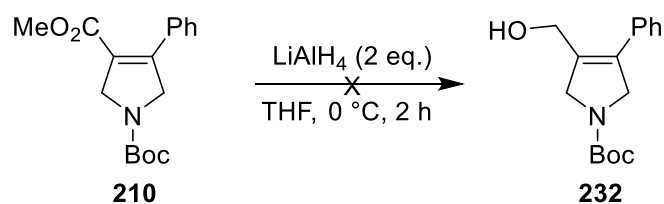
Scheme 3.17

This was surprising as the reduction of the corresponding tetrahydropyridine system **201** to alcohol **233** under very similar conditions was reported by Kanai *et al.* (Scheme 3.18).[114] We therefore decided to stop work on the synthesis of alcohol *cis*-**228** here but to apply the learnings from this route to other 3-D fragment syntheses. First, we would perform reductions after the hydrogenation as these were shown to work quickly and effectively (see Scheme 3.19). For pyrrolidine and piperidine fragments, ester reduction would be performed on the *N*-Boc compound which would then be deprotected to give NH fragments. Acetyl groups would not be used as they caused issues with chemoselectivity of the reduction if attached beforehand, or chemoselectivity issues with the acetylation potentially occurring on both the oxygen and nitrogen if attached after the reduction.
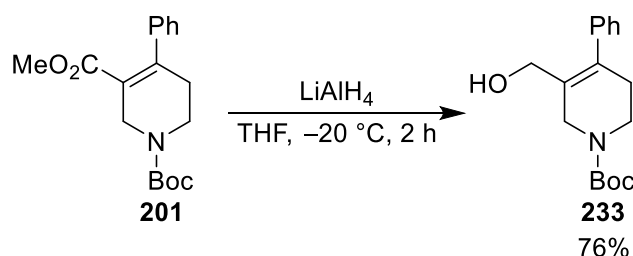
Scheme 3.18

3.4.2 Investigation of the Pyrrolidine Ester Hydrolysis

The next diversification route to be attempted was the synthesis of acid *cis*-**229** *via* hydrolysis of ester *cis*-**227** (Table 3.8). Basic hydrolysis using LiOH at rt for 16 h gave a mixture of products containing an 85:15 mixture of diastereomeric pyrrolidines **229** as determined by the ^{1}H NMR spectrum of the crude product (entry 1). Shortening the reaction time to 2 h also resulted in epimerisation to a 75:25 mixture of pyrrolidines **229** (entry 2). Interestingly shortening the reaction time gave lower diastereoselectivity, indicating that epimerisation may be occurring to give *trans*-**229** as the major product. This also substantially increased the mass recovery, with only small amounts of other products visible in the ^{1}H NMR spectrum. Acidic hydrolysis with sulfuric acid at rt had no effect (entry 3), while heating resulted in decomposition (entry 4).
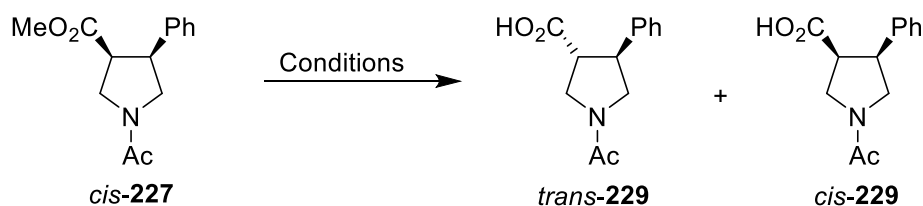
Entry	Reagent	Solvent	Temp/° C	Time/h	*trans*-**229**:*cis*-**229**[a]
1	LiOH	4:1:1 THF-H$_2$O-MeOH	rt	16 h	85:15
2	LiOH	4:1:1 THF-H$_2$O-MeOH	rt	2 h	75:25
3	H$_2$SO$_4$	1:1 THF-H$_2$O	rt	16 h	−[b]
4	H$_2$SO$_4$	1:1 THF-H$_2$O	65 °C	16 h	−[c]

[a] Ratio of *trans*-**229** and *cis*-**229** determined by ^{1}H NMR spectroscopy
[b] Full recovery of *cis*-**227**
[c] Complex mixture of products obtained

Table 3.8: Hydrolysis of ester *cis*-**227**

The identity of *cis*-**229** and *trans*-**229** were proven by the synthesis of acid *trans*-**229** by another group member using the cycloaddition strategy shown in Scheme 3.19.[83]
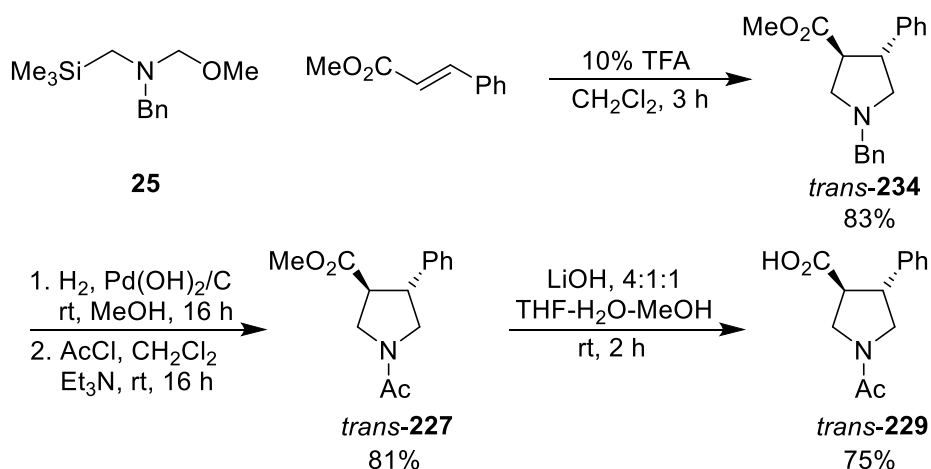
Scheme 3.19

The cycloaddition is stereospecific (see Scheme 2.1)[46] and therefore comparison of the ^{1}H NMR spectra allowed us to confirm which diastereomer of acid **229** was the major product. Figure 3.3 shows the areas of the ^{1}H NMR spectrum corresponding to the ring proton adjacent to the acid group (left) and the *N*-Ac protons (right). The ^{1}H NMR spectrum of the 85:15 mixture from Table 3.8 entry 1 is shown above, and comparison with the ^{1}H NMR spectrum of pure *trans*-**229** below for each signal shows *trans*-**229** to be the major product from the basic hydrolyses.
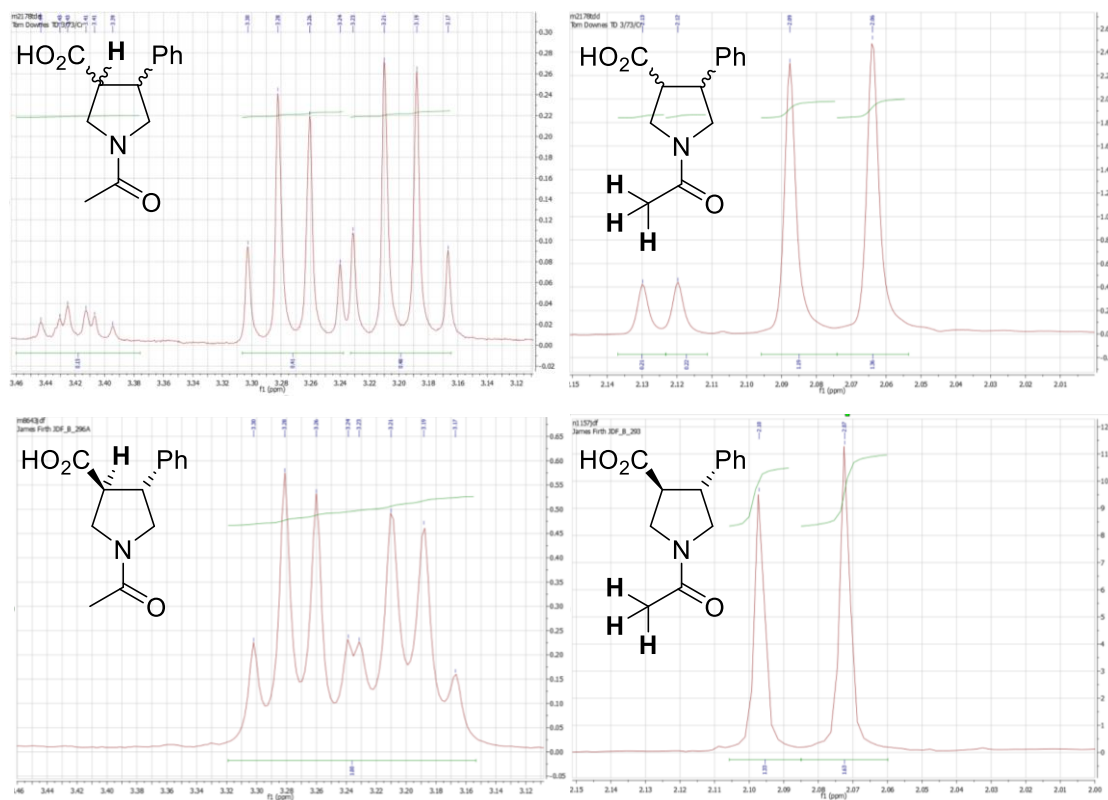
Figure 3.3: Key signals in the ^{1}H NMR spectra of the 85:15 mixture of *trans*-**229** and *cis*-**229** (above) and pure *trans*-**229** (below)

The synthesis of ester *trans*-**227** was also useful for proving the stereochemistry since ester *cis*-**227** had been synthesised previously (see Scheme 3.14). Comparison of the ring and ester proton region (3.15-4.10 ppm) of the ^{1}H NMR spectra of *cis*-**227** (Figure 3.4, left) and *trans*-**227** (Figure 3.4, right) showed the two compounds to be different diastereomers, confirming that the hydrogenation of the dihydropyrrole proceeded with complete *cis*-diastereoselectivity (see Scheme 3.11). In particular, the rotameric methyl groups of the methyl esters were clearly visible at significantly different ppm values.
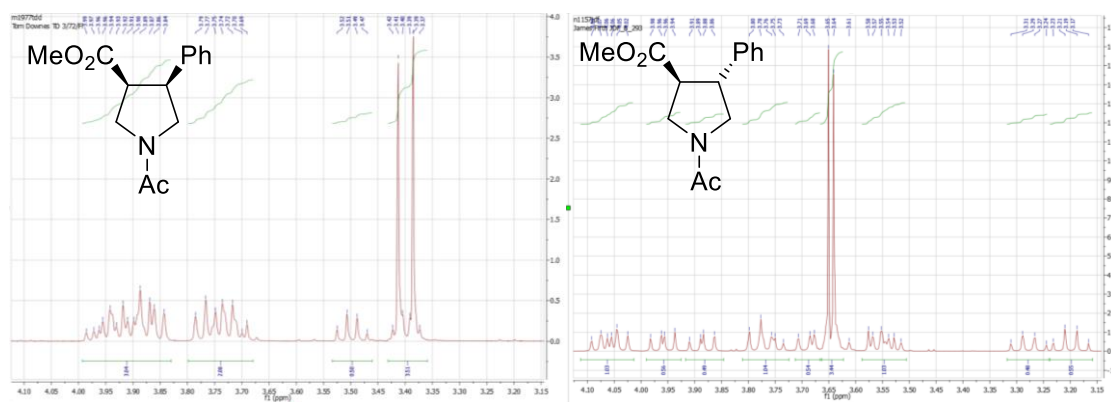
Figure 3.4: Comparison of the ^{1}H NMR spectra of esters *cis*-**227** and *trans*-**227**

As ester *cis*-**227** and/or acid *cis*-**229** was prone to epimerisation, we attempted the hydrolysis of dihydropyrrole **210**. Performing the hydrolysis earlier in the route on dihydropyrrole **210** could potentially avoid any potential epimerisation issues. Using LiOH, hydrolysis gave a complex mixture of products with neither starting material **210** nor desired acid **235** being detected by ^{1}H NMR spectroscopy (Scheme 3.20).
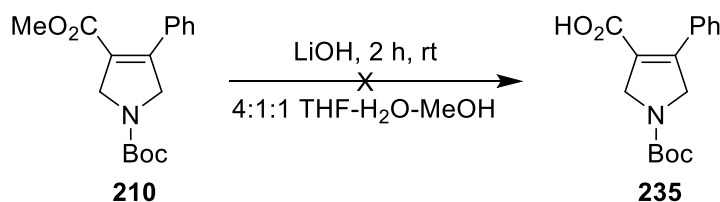
Scheme 3.20

This was particularly surprising as harsher hydrolysis conditions have been shown to work on the corresponding tetrahydropyridine **201**. Metcalf and Li reported the hydrolysis of tetrahydropyridine **201** with NaOH at 70 °C to give acid **236** (Scheme 3.21).[118]
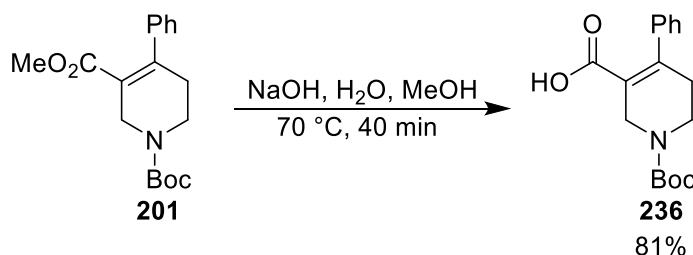
Scheme 3.21

With dihydropyrrole **210** proving unstable to both hydrolysis and reduction, it was concluded that the difficulties with the reductions and hydrolyses detailed in this section were due to the pyrrolidine system that had been chosen as opposed to a flaw in the overall strategy. It was therefore decided to perform hydrolysis at the alkene stage on other systems and to only synthesise pyrrolidine fragments *via* the alcohol route. This would ensure that no epimerisation could occur during ester hydrolysis.

3.4.3 Investigation of the Direct Amidation of Pyrrolidine *cis*-227

The final strategy involved bypassing acid *cis*-**229** and the potential epimerisation issues by attempting to synthesise an amide *via* direct amidation of an ester. Woodward *et al*. have reported that by using a DABCO•AlMe$_3$ adduct **237** known as 'DABAL', amides can be formed directly from the ester and amine with no requirement to form the carboxylic acid.[119] Scheme 3.22 shows an example of this chemistry from Woodward *et al*. where *n*-butylamine was first reacted with the DABAL at 40 °C for 1 h before the ester was added and the reaction

stirred at reflux for 18 h. Quenching with 2 M HCl$_{(aq)}$ gave the desired amide **238** in 99% yield. In our hands, the same reaction proceeded in high yield, confirming that the process and reagents would not be an issue in future reactions.
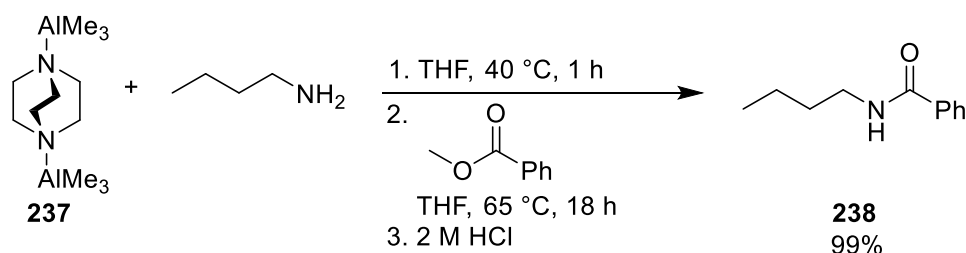
Scheme 3.22

The reaction was therefore attempted on ester *cis*-**224**. Butylamine, one of the examples from the original paper,[119] was chosen as the amine partner to test the reaction. Treatment of DABAL with butylamine at 40 °C for 1 h followed by addition of ester *cis*-**224** and heating at 65 °C for 18 h frustratingly returned only starting material *cis*-**237** (Scheme 3.23).
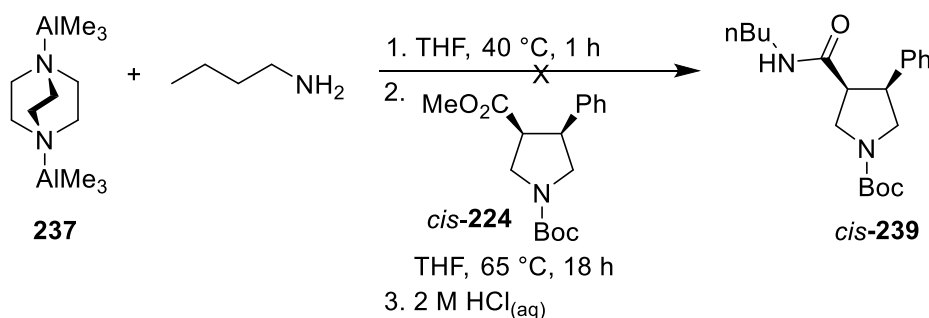
Scheme 3.23

The reaction was also attempted on the dihydropyrrole as the dihydropyrrole does not have an acidic enol proton. Although the literature shows that the reaction does tolerate enolisable centres, the yields did tend to be lower.[119] However, repeating the reaction shown in Scheme 3.24 on dihydropyrrole **210** also gave only starting material (Scheme 3.24). With the reaction not working, we decided to move on to other systems to synthesise the desired 3-D fragments.

Scheme 3.24

3.5 Diversification *via* the Ester Reduction Route

Now that the potential issues with the diversification steps were better understood, we proposed to break down the diversification into two discrete routes from the Suzuki-Miyaura coupling products **189**. The first route (Scheme 3.25) would initially involve hydrogenation to form esters *cis*-**44**, which would be 3-D fragments. Fragments *cis*-**44** would then be reduced using LiAlH₄ to give alcohol fragments *cis*-**241**. Unlike pyrrolidine *cis*-**227**, we would ensure that the ester group was the only group present that could be reduced. Alcohols *cis*-**227** could then be further developed in one of two ways: use of a fluorination reagent such as PyFluor or DAST would substitute the alcohol group for a fluorine to give *cis*-**242**, or the alcohol would be treated with mesyl chloride, substituted with sodium azide and then reduced in a Staudinger reaction to give primary amines *cis*-**243** (Scheme 3.25).

Scheme 3.25

In total, 16 3-D fragments were proposed to be synthesised using this ester reduction approach and their structures are shown in Figure 3.5. These fragments would be synthesised from the Suzuki-Miyaura products detailed in Tables 3.1-3.4.

Figure 3.5: Proposed fragments to be synthesised using the ester reduction route

The 3-D shape of the proposed fragments was analysed using PMI plots to ensure that all fragments had at least one conformation with $\sum NPR \geq 1.15$. The PMI plot of these fragments is shown in Figure 3.6 and demonstrates an excellent spread of points with no conformers near the rod-disc axis and all compounds qualifying for synthesis.
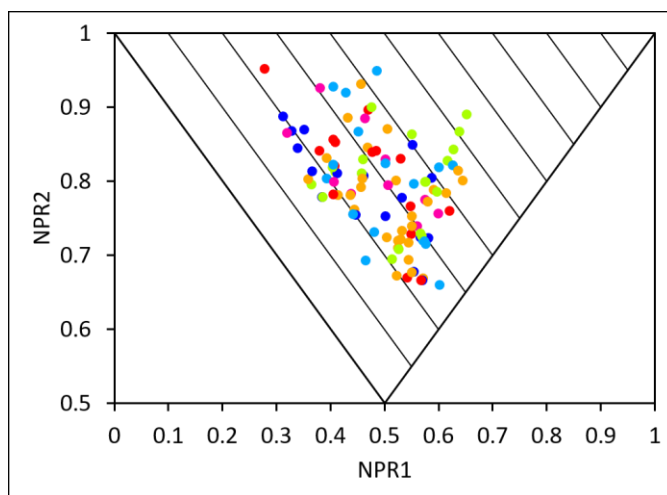
Figure 3.6: PMI plot of the 16 proposed ester reduction fragments

Fragments *cis*-**252**, *cis*-**253** and *cis*-**254** were selected for synthesis first to test this route. Hydrogenation of cyclopentene **215** had been unsuccessfully attempted previously (see Scheme 3.12). However, using Pd/C as the catalyst, hydrogenation this time proceeded to give fragment *cis*-**254** in 92% yield, albeit with a very long reaction time (Scheme 3.26).
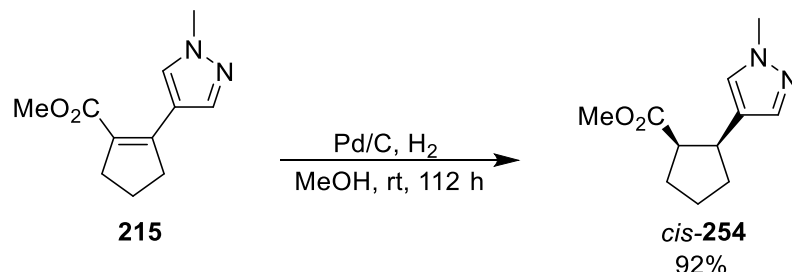
Scheme 3.26

With the first fragment now in hand, the diversification to give alcohol *cis*-**252** and fluoro-cyclopentane *cis*-**253** could now be attempted. Reduction using LiAlH$_4$ at 0 °C for 2 h proceeded uneventfully and gave the desired alcohol *cis*-**252** in 98% yield (Scheme 3.27).
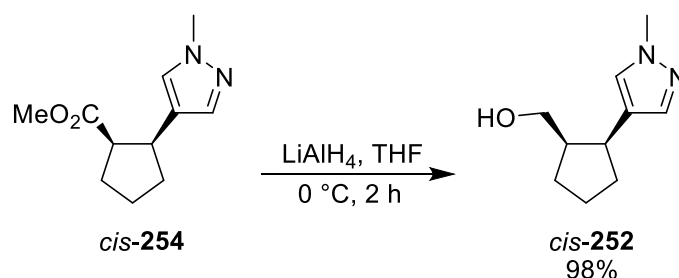
Scheme 3.27

The conversion of alcohol *cis*-**252** into fluoro-cyclopentane *cis*-**253** was also studied. A variety of fluorinating reagents are commercially available[120–122] and, of these, we chose PyFluor due to its availability, ease of handling and the literature precedent for using it on similar systems to ours.[122] Scheme 3.28 shows examples where a hydroxyproline ester, *trans*-**116** was converted into *cis*-**118** in 73% yield and heteroaromatic-containing compound **260** was converted into **261** in 64% yield. The conditions for the two reactions are slightly different, with the proline alcohol *trans*-**116** requiring heating to improve the reaction rate and the heteroaromatic compound **260** used a different base to reduce elimination. However, the latter reaction still proceeded in 41% yield when DBU was used as the base and it was reasoned that a functioning set of conditions could be found to work on our desired system.
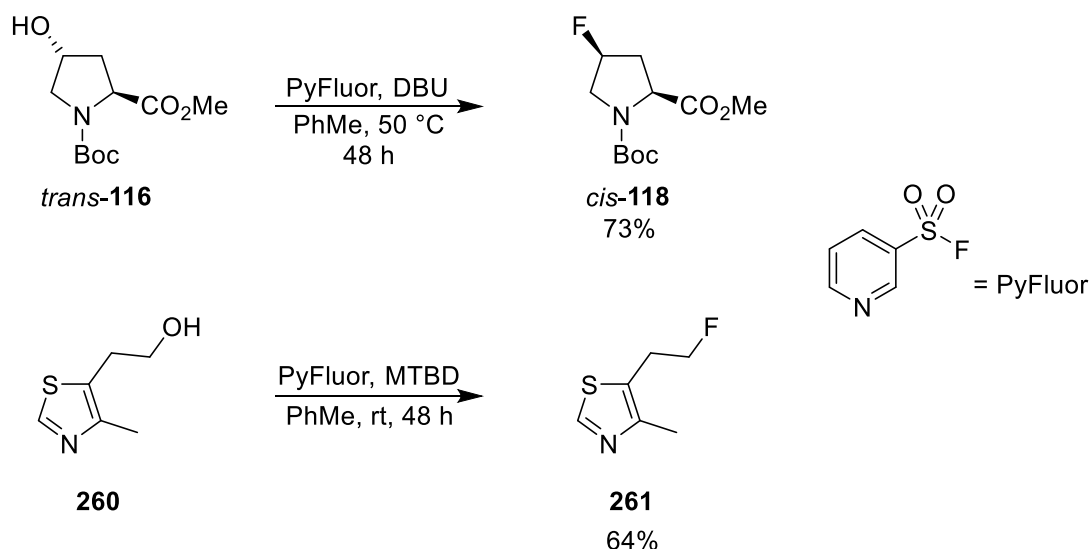
Scheme 3.28

The first fluorination was attempted using DBU as the base at rt, due to the potential for elimination to form the alkene at higher temperatures. The reaction was allowed to run until TLC showed that there was no more starting material remaining. As per the literature procedure, the reaction mixture was loaded directly on to a column following completion. However, purification by flash column chromatography yielded only 12% of the desired product *cis*-**253** (Scheme 3.29).
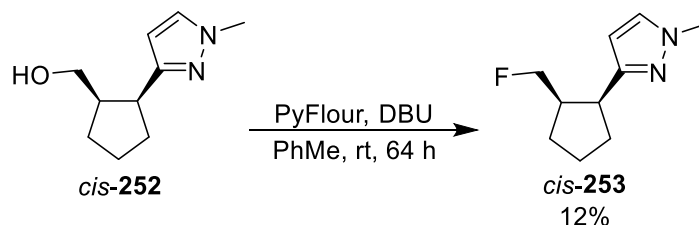
Scheme 3.29

The reaction was then repeated with an aqueous work-up inserted before chromatographic purification. The crude mixture was analysed using ^{1}H NMR spectroscopy and it showed that starting alcohol *cis*-**252** was completely consumed. However, after purification by column chromatography no products were recovered (Scheme 3.30). Another member of the group who was carrying out the same type of reaction on a similar compound, isolated a sulfonate intermediate, the analogue of *cis*-**262**, when performing the reaction at rt.[103] We therefore proposed that sulfonate *cis*-**262** was forming in our reaction but was too polar to elute from the column.
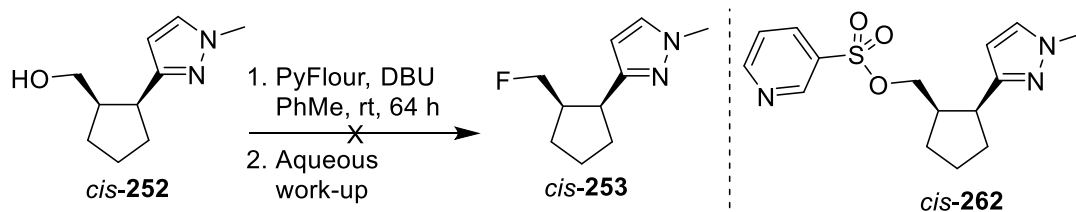
Scheme 3.30

The ^{1}H NMR spectrum of the crude product showed evidence for the formation of sulfonate intermediate *cis*-**262**. Intermediate *cis*-**262** is derived from successful attack of alcohol *cis*-**252** into the sulfonyl fluoride. However, the second step, substitution of the sulfonate group by fluoride, was not occurring at rt. Raising the reaction temperature was therefore considered. Initial attempts from the group member working on a similar system had shown that the sulfonate intermediate remained when the reaction was performed at 50 °C for 2 days, but none remained from a reaction at 70 °C.[103] The reaction was therefore attempted at 70 °C. Monitoring by TLC showed that sulfonate *cis*-**262** was still present after 2 days, but after 3 days it had been consumed. The reaction was then stopped and analysed by ^{1}H NMR spectroscopy. The ^{1}H NMR spectrum of the crude product showed an 80:20 mixture of desired fluoro-cyclopentane *cis*-**253** and the alkene **263**, the product of an elimination reaction (Scheme 3.31). Alkene **263** could be identified by diagnostic broad singlets in the ^{1}H NMR spectrum at 4.91 and 4.70 ppm, corresponding to the exocyclic alkene protons, and a broad dd signal at 3.46 ppm corresponding to the proton next to the aromatic ring. Column chromatography to separate the two was challenging, but a 22% yield of fragment *cis*-**253** was obtained. This gave 56 mg of fragment *cis*-**253**, which was enough to add the fragment to the library.
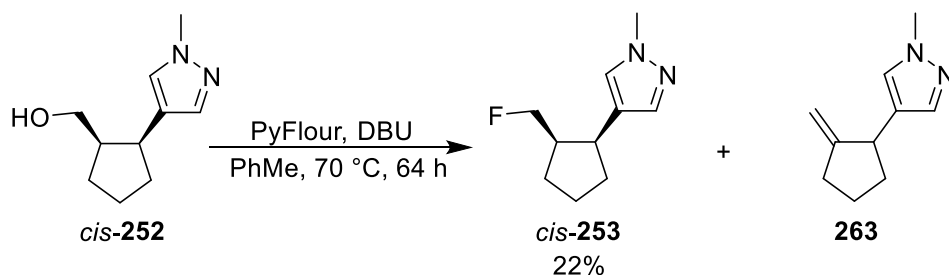
Scheme 3.31

The other cyclopentane fragments to be synthesised using this route were pyridine-containing ester *cis*-**250**, alcohol *cis*-**249** and fluoro-cyclopentane *cis*-**248**. Hydrogenation of cyclopentene **213** using Pd/C was successfully performed in 63% yield to give the first of these fragments, *cis*-**250**. Ester *cis*-**250** was then reduced using LiAlH₄ in 83% yield to give fragment *cis*-**249** (Scheme 3.32).
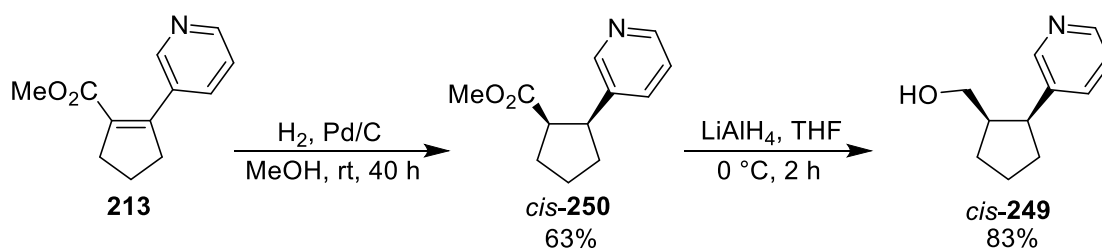
Scheme 3.32

The final step explored was the fluorination of alcohol *cis*-**249**. Due to our experience with the fluorination of alcohol *cis*-**252** which had led to competing elimination, it was decided to perform the reaction at a temperature lower than 70 °C. However, the reaction still needed to be performed at elevated temperature to ensure that the fluoride displacement step occurred. Reaction at 50 °C for 40 h gave fluorinated fragment *cis*-**248** in 36% yield (Scheme 3.33).
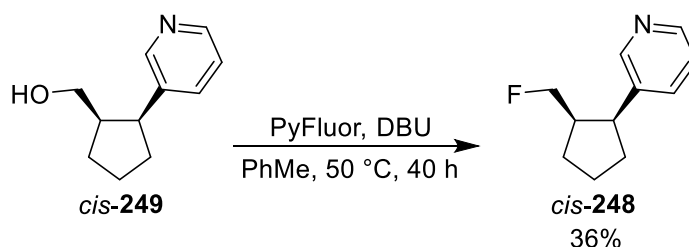
Scheme 3.33

Small amounts of pure dihydrofurans **222** and **221** were available and therefore it was decided to hydrogenate these to give 3-D ester fragments directly. Both reactions worked well to give single diastereomers. Hydrogenation of dihydrofuran **222** gave fragment *cis*-**259** in 96% yield and hydrogenation of dihydrofuran **221** gave fragment *cis*-**258** in 64% yield (Scheme 3.34).
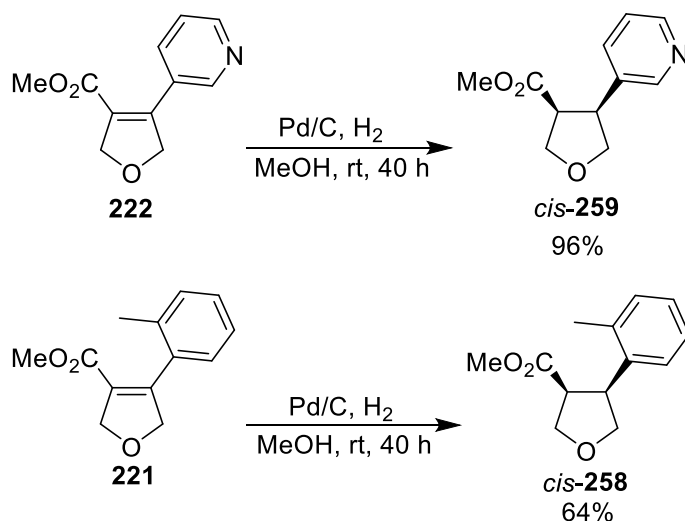
Scheme 3.34

The other two THF fragments to be synthesised were alcohol *cis*-**257** and primary amine *cis*-**256**. As described previously (see Table 2.4 entry 2), the Suzuki-Miyaura cross-coupling gave an inseparable 60:40 mixture of the desired product **220** and the boronic acid after chromatography (28% yield of alkene **220**). This mixture was hydrogenated in the hope that ester *cis*-**264** would be separable from the boronic acid. However, ester *cis*-**264** also proved to be inseparable from the boronic acid by column chromatography (66% yield of *cis*-**264**). The 60:40 mixture of ester *cis*-**264** and boronic acid was therefore reduced with LiAlH$_4$ to give alcohol *cis*-**257** in 79% yield, which was separated from the boronic acid by column chromatography. This sequence gave fragment *cis*-**257** in an overall 15% yield from β-ketoester **194** over four steps (Scheme 3.35).
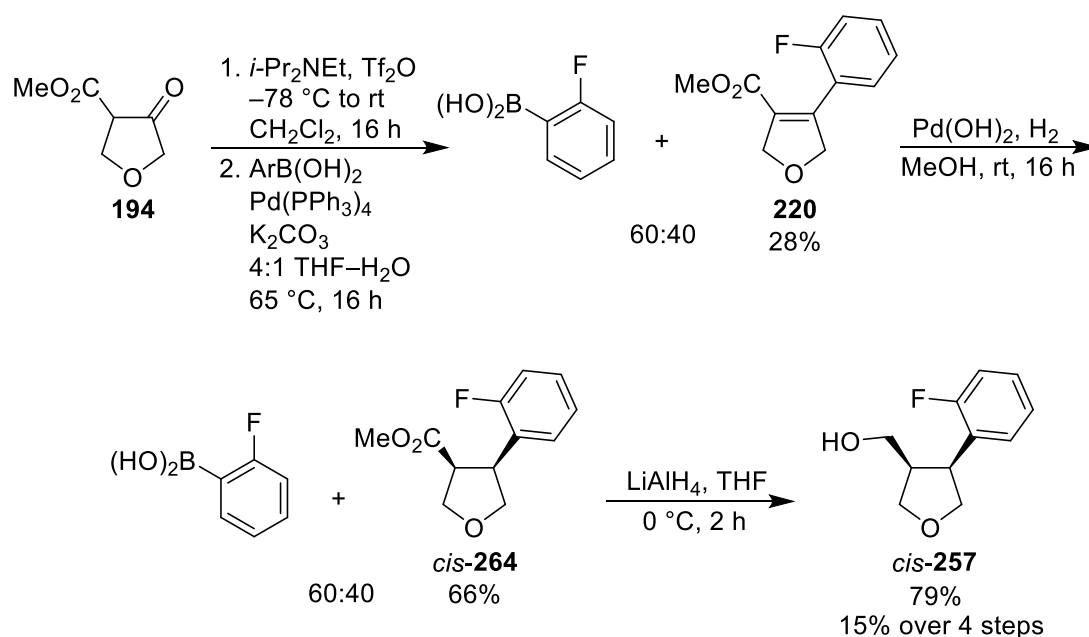
Scheme 3.35

Amine 3-D fragment *cis*-**256** was then synthesised from alcohol *cis*-**257** in a three-step process. First, alcohol *cis*-**257** was treated with mesyl chloride to give mesylate *cis*-**265** in 63% yield. Then, mesylate *cis*-**265** was heated with sodium azide in DMF at 120 °C, resulting in the successful substitution of the mesyl group to give azide *cis*-**266** in 89% yield. The final step was the Staudinger reduction of the azide group to the amine. Treatment of azide *cis*-**266** with PPh$_3$ at 65 °C in a mixture of water and THF gave the desired 3-D fragment, amine *cis*-**256** in 87% yield (Scheme 3.36).

Scheme 3.36

The next fragments whose synthesis was attempted were piperidines *cis*-**244** and *cis*-**245** and pyrrolidines *cis*-**246** and *cis*-**247**. Hydrogenation of piperidine **217** had already been optimised (see Table 3.6, entries 1 and 2) and using Pd/C for 16 h, the reaction proceeded in 99% yield. Some of compound *cis*-**226** was subjected to Boc group removal using HCl in Et_2O. This gave the desired ester fragment *cis*-**244•**HCl in 92% yield (Scheme 3.37).

Scheme 3.37

The synthesis of alcohol *cis*-**245** was also explored. The plan was to reduce ester *cis*-**226** using $LiAlH_4$ and then remove the Boc group to give fragment *cis*-**245•**HCl. However, treatment of ester *cis*-**226** with $LiAlH_4$ at 0 °C resulted in a complex mixture of products (Scheme 3.38) and other reducing agents were not investigated.

Scheme 3.38

The pyrrolidine fragments selected for synthesis were analogous to piperidines *cis*-**244** and *cis*-**245**. Both the hydrogenation using Pd/C and the Boc group removal with HCl proceeded in quantitative yield to give the desired pyrrolidine ester fragment *cis*-**246** (Scheme 3.39).
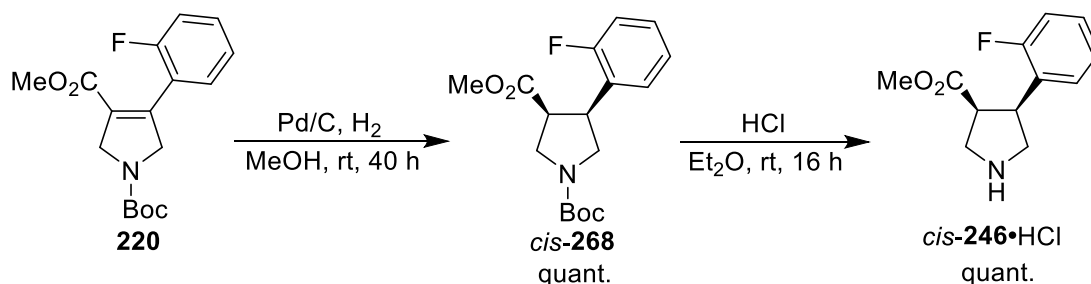
Scheme 3.39

The final fragment to be synthesised using this route was alcohol *cis*-**247**. In contrast to the issues encountered with the reduction of *N*-acetyl pyrrolidine *cis*-**227**, reduction of *N*-Boc protected ester *cis*-**268** with LiAlH$_4$ proceeded relatively smoothly. The reaction gave alcohol *cis*-**269** in 56% yield. Final deprotection with HCl in Et$_2$O gave desired fragment *cis*-**247**•HCl in 97% yield (Scheme 3.40).
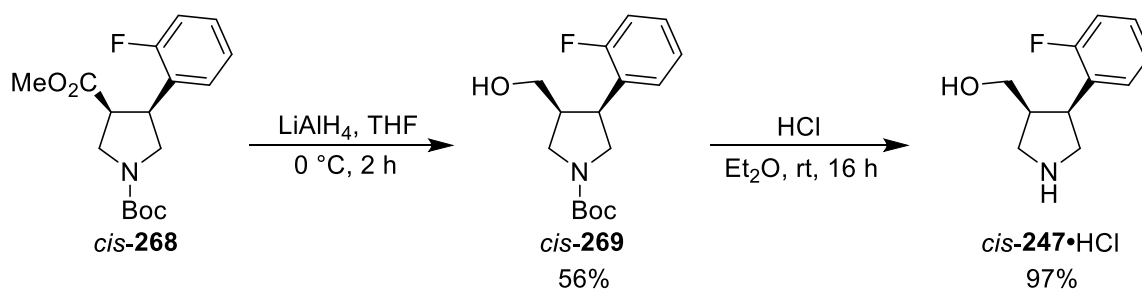
Scheme 3.40

The other Suzuki-Miyaura coupling products to be hydrogenated were THP **223** and cyclopentene **216**. Each was successfully hydrogenated using Pd/C to give THP *cis*-**255** in 82% yield and cyclopentane *cis*-**251** in 69% yield (Scheme 3.41).

127
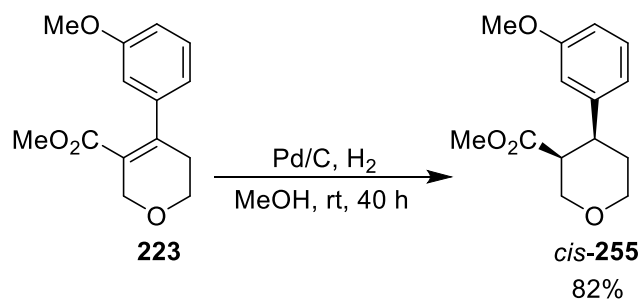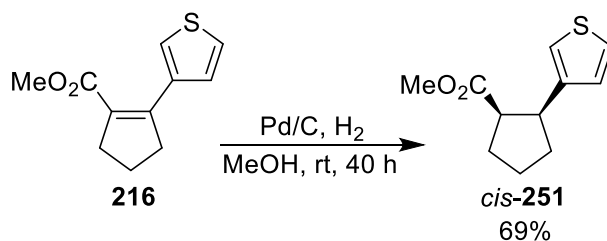
Scheme 3.41

The synthesis of tetrahydropyran *cis*-**255** was important as it was the first 6-membered ring product that had distinct signals in the ^{1}H NMR spectrum and thus allowed full analysis of coupling constants. This enabled us to provide proof that *cis*-**255** had been generated in the hydrogenation step. We expected the stereochemistry of the hydrogenation to be *cis* and THP **255** could adopt one of two possible *cis*-conformations, with one group axial and one group equatorial (Figure 3.7). Therefore, we initially set out to see if the ^{1}H NMR spectrum matched with either conformation *cis*-**255**A or *cis*-**255**B. The key area of the ^{1}H NMR spectrum (Figure 3.8) was analysed to see if it was possible to determine which of these conformations **255** had adopted.
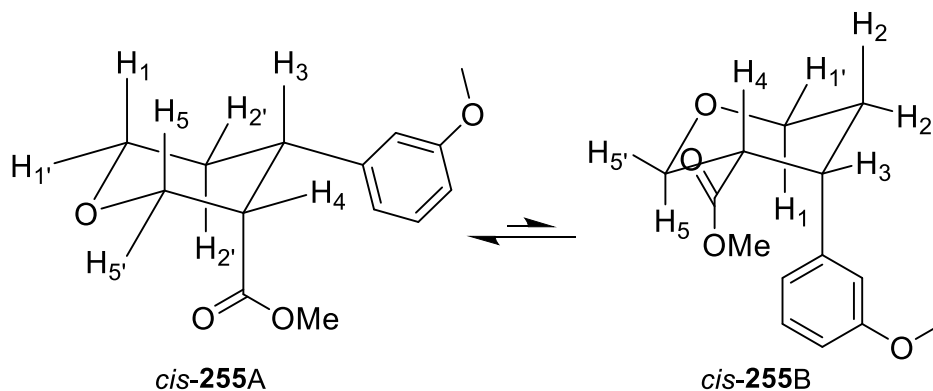
Figure 3.7: Possible conformations of fragment *cis*-**255**
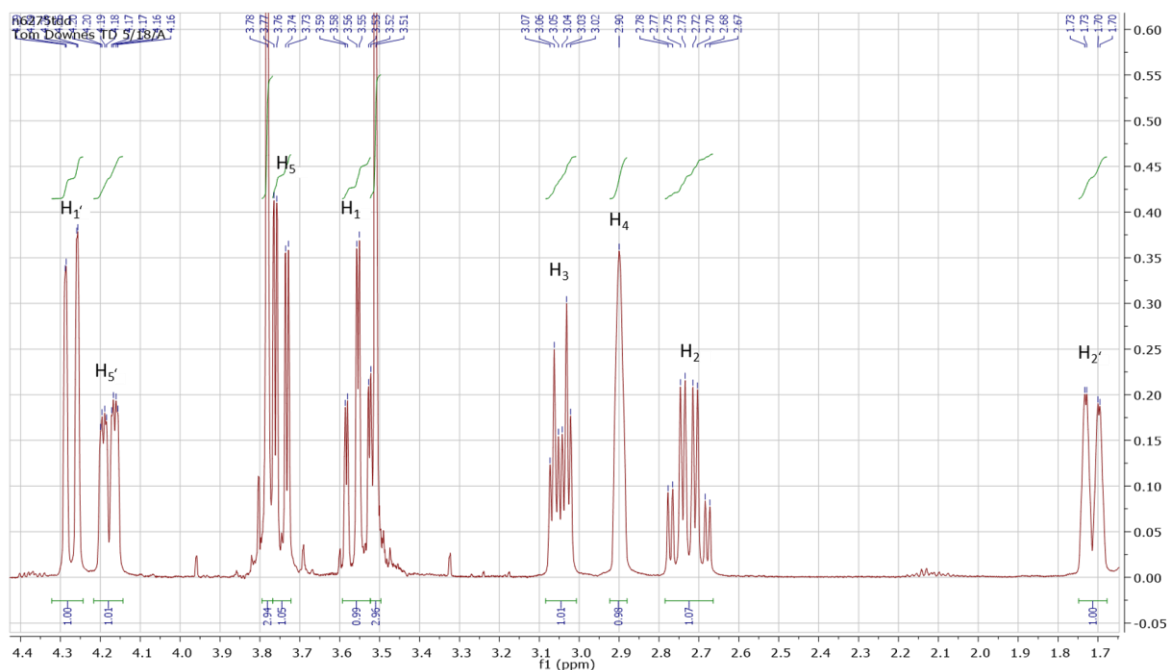
Figure 3.8: ^{1}H NMR spectrum of THP *cis*-**255**

Starting with the most downfield signals, the signals at 4.27 and 4.18 ppm were assigned as H$_{1'}$ and H$_{5'}$ with the determination of which of these signals was which being performed using 2D NMR spectra. Both were next to an oxygen and would be expected to show a single large ^2J value coupling to H$_1$ or H$_5$ and either one (H$_{5'}$) or two (H$_{1'}$) small couplings to protons on the adjacent carbon. The next two signals, at 3.75 ppm and 3.55 ppm were expected to belong to H$_1$ and H$_5$, and the HMQC NMR spectrum confirmed this. H$_1$ was expected to show two large J values: a geminal coupling with H$_{1'}$ and an axial-axial ^3J coupling with H$_2$. As only one of these signals contained two large couplings, it was assigned to the signal at 3.55 ppm. The signal at 3.75 ppm, H$_5$, had only one large coupling. This provided evidence that the conformation was *cis*-**255**A, as in *cis*-**255**B, proton H$_4$ is equatorial and would therefore not cause a second large coupling.

The next signals at 3.05 and 2.90 ppm further confirmed this hypothesis. Using the HMBC NMR spectrum, the signal at 3.05 ppm was assigned as H$_3$. This signal showed as a ddd with one large and two small coupling constants. Conformation *cis*-**255**A would show one large axial-axial coupling and two small axial-equatorial couplings. Conformation *cis*-**255**B would show three small couplings, adding to the evidence that *cis*-**255**A was the preferred conformation. This signal also allowed us to confirm that the hydrogenation had proceeded with *cis*-diastereoselectivity and had not given either conformation of ester *trans*-**255** (Figure 3.9).
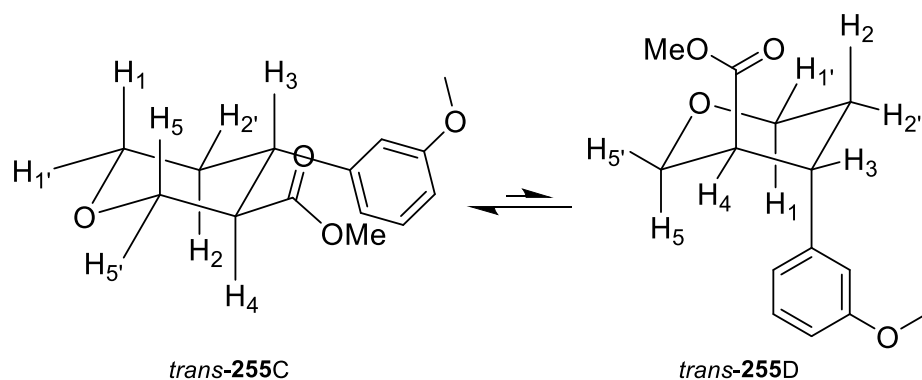
Figure 3.9: Possible conformations of fragment *trans*-**255**

For the signal at 3.05 ppm, conformation *trans*-**255**C would show two large couplings and one small and conformation *trans*-**255**D would show no large couplings. Neither of these fit with the one large and two small couplings shown in Figure 3.8. Finally, the signal at 2.90 ppm, belonging to H$_4$, showed no large coupling values. In both *cis*-**255**B and *trans*-**255**C that proton is axial and would show at least one large *J* value, whereas in *cis*-**255**A the proton is equatorial and shows no large couplings. We were therefore confident in confirming that the hydrogenation had proceeded with complete *cis*-diastereoselectivity, based on the ^{1}H NMR spectroscopic assignments that showed *cis*-**255**A to be the conformation adopted by *cis*-**255**.

We had now proved that the hydrogenation proceeded with complete *cis*-diastereoselectivity in both the THP and pyrrolidine systems. Furthermore, the C*H*Ar proton signal in the ^{1}H NMR spectrum of piperidine ester *cis*-**244** showed very similar coupling constants to the C*H*Ar proton in THP *cis*-**255**, providing some evidence that it too had *cis*-stereochemistry. With the stereochemistry proved in both a 5-and 6-membered ring system, we felt comfortable to assign the stereochemistry of the other hydrogenation products by analogy.

3.6 Diversification *via* the Ester Hydrolysis Route

The second route, which would be used to create acid-, amide- and secondary amine-containing 3-D fragments (Scheme 3.42), would begin with the hydrolysis of esters **189** to give acids **270**. Hydrolysis at the unsaturated stage would hopefully avoid any epimerisation issues. Acids **270** would then be hydrogenated using either Pd/C or Pd(OH)$_2$/C to acid fragments *cis*-**271**. Acids *cis*-**271** could then undergo either amide coupling with aqueous ammonia to give amides *cis*-**272** or Curtius rearrangement to give secondary amines *cis*-**273**.

Scheme 3.42
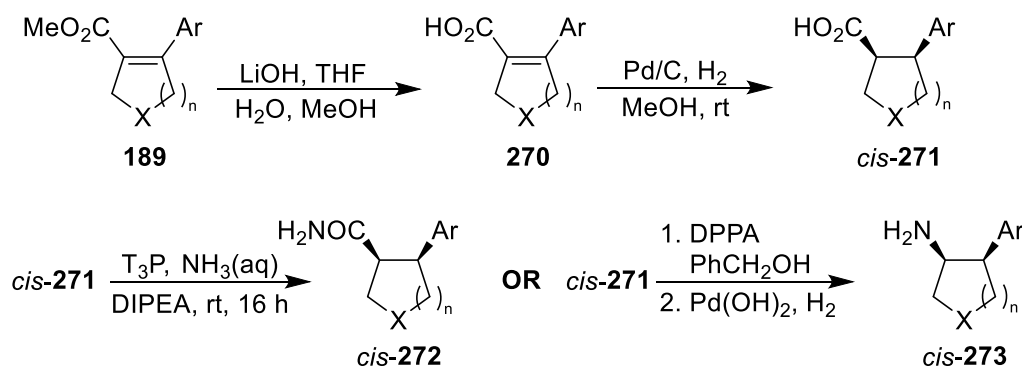
The eight selected 3-D fragments to be synthesised *via* this route are shown in Figure 3.10. These included THP, THF and cyclopentane fragments. No pyrrolidine or piperidine fragments were chosen due to the previously encountered stability issues of the dihydropyrrole ester during hydrolysis (see Scheme 3.20) and the potential for zwitterion formation during Boc removal. Potential zwitterion formation was also the reason that no fragments with heteroaryl groups containing basic nitrogens were selected.
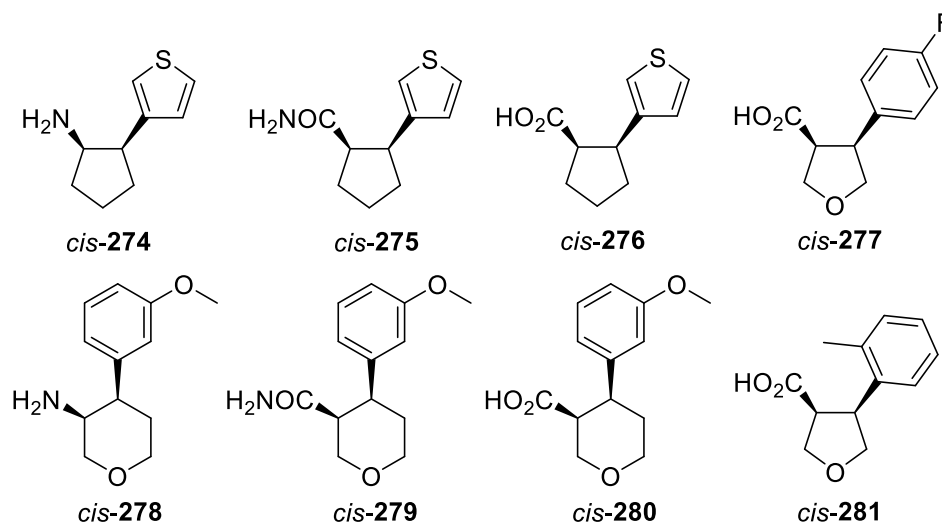
Figure 3.10: Structures of the eight acid route fragments

Shape analysis of the eight proposed fragments was then carried out before their synthesis. As the PMI plot shows (Figure 3.11), the proposed 3-D fragments have a good spread across the plot from $\sum$NPR = 1.13 to $\sum$NPR = 1.52. Interestingly, these fragments appeared higher up on the PMI plot than the 16 ester reduction fragments (see Figure 3.11), meaning that the combination of these two sets of fragments would give excellent coverage across the plot. All eight proposed fragments passed the selection criteria for synthesis (at least one conformation with $\sum$NPR $\geq$ 1.15).
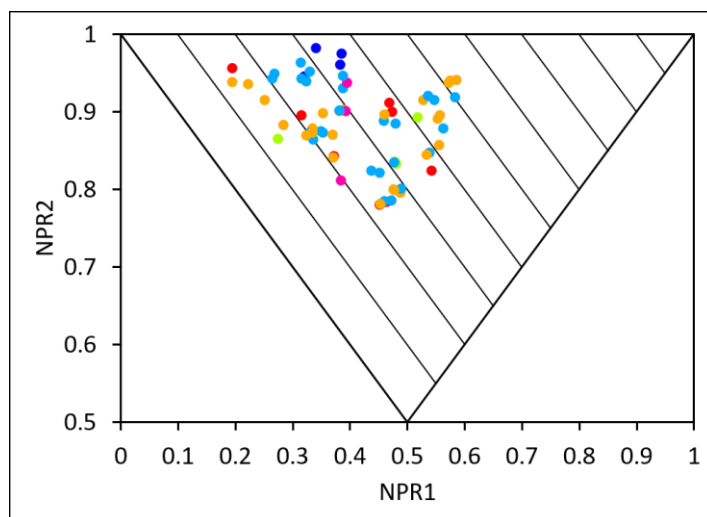
Figure 3.11: PMI plot of the eight proposed ester hydrolysis 3-D fragments

Cyclopentene ester **216** was selected as the first compound to be derivatised using this approach. Treatment of ester **216** with NaOH at 70 °C for 1 h hydrolysed the ester to give acid **282** in 84% yield. The conditions were those that Metcalf and Li used to hydrolyse tetrahydropyridine **201** (see Scheme 3.21).[118] Acid **282** was then hydrogenated with Pd/C and H$_2$ to give the desired fragment *cis*-**276** in 93% yield as a single diastereomer (Scheme 3.43).
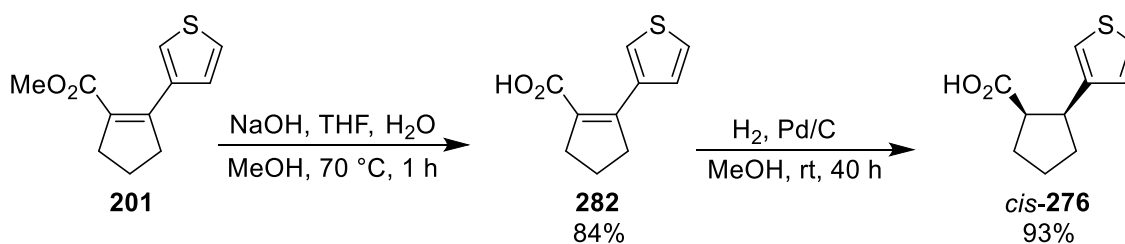
Scheme 3.43

An X-ray crystal structure of acid *cis*-**276** was obtained to prove the stereochemistry of the hydrogenation on a cyclopentane system (Figure 3.12)
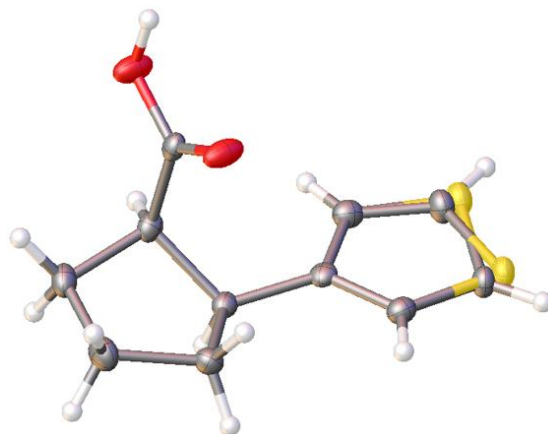
Figure 3.12: X-ray crystallography of cyclopentane acid *cis*-**276**

Curtius rearrangement of acid *cis*-**276** to give amine *cis*-**274** and amide coupling of acid *cis*-**276** to give amide *cis*-**275** were then explored. The amide coupling was attempted first, with NH$_{3(aq)}$ and T3P as the coupling agent. However, an initial attempt gave no reaction. It was speculated that the ammonia in the reaction may be evaporating and being absorbed into the suba seal. Therefore, the reaction was reattempted using a glass stopper. This resulted in the reaction proceeding successfully in 48% yield to give amide *cis*-**275** (Scheme 3.44).
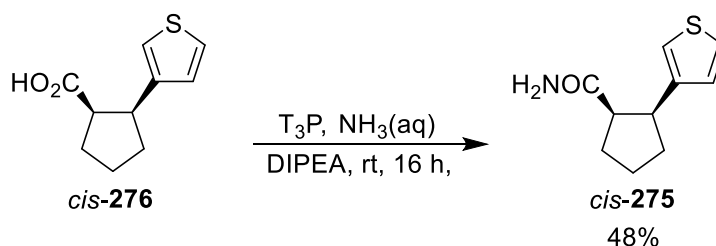
Scheme 3.44

Next, acid *cis*-**276** was treated with DPPA and benzyl alcohol at 85 °C in an attempt to form the Cbz protected amine *cis*-**283**. However, after column chromatography only a very small amount of what appeared from the ^{1}H NMR spectrum to be product mixed with some impurities was isolated (Scheme 3.45). Due to the lack of material, it was decided not to further explore the synthesis of fragment *cis*-**274**.
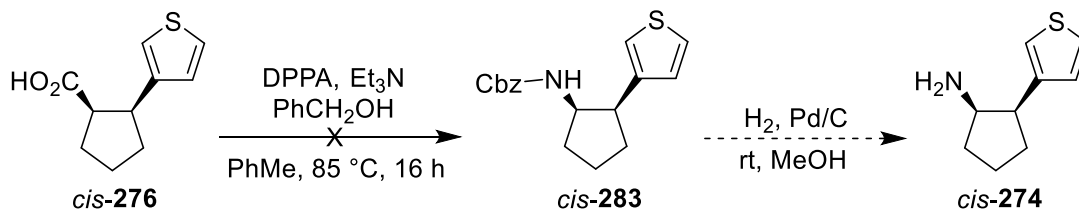
Scheme 3.45

Dihydropyran **223** was then selected for derivatisation. Hydrolysis using NaOH at 70 °C gave acid **284** in 86% yield. Hydrogenation of acid **284** using Pd/C gave the desired acid fragment *cis*-**280** as a single diastereomer in 98% yield (Scheme 3.46). Analysis of the ^{1}H NMR spectrum in the same manner as the corresponding ester *cis*-**255** (see Figure 3.8) showed that the reaction proceeded with complete *cis*-diastereoselectivity.
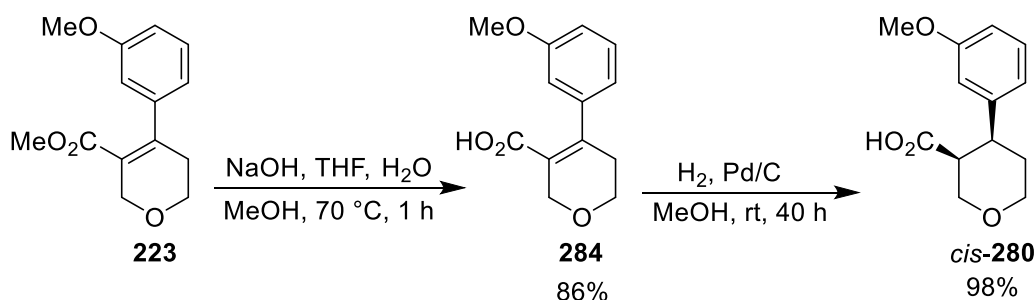
Scheme 3.46

Acid *cis*-**280** was then split three ways. A sample was added to the 3-D fragment library, some was taken on for amide coupling and the rest was used in a Curtius rearrangement. The amide coupling was performed with T3P and ammonia in a flask with a glass stopper and proceeded smoothly to give *cis*-**279** as a single diastereomer in 41% yield (Scheme 3.47). We were pleased that ^{1}H NMR spectroscopic analysis of fragments *cis*-**280** and *cis*-**279** confirmed the *cis*-diastereoselectivity of both reactions as this allowed us to assign the other acid hydrogenations as *cis* and that epimerisation of the acid had not occurred under the amide coupling conditions.
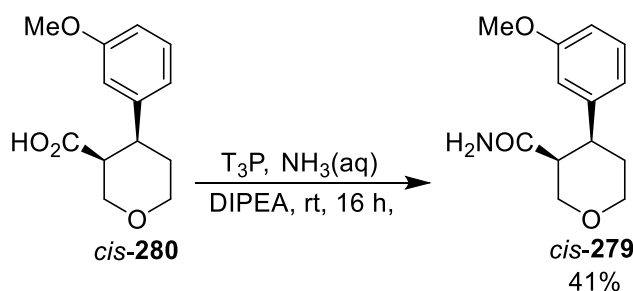
Scheme 3.47

The last THP fragment to be synthesised was the Curtius rearrangement product *cis*-**278**. The previous attempt at a Curtius rearrangement on acid *cis*-**276** (see Scheme 3.45) had been largely unsuccessful, although a small amount of product had been detected. It was decided to perform this reaction in neat benzyl alcohol, as opposed to using 5 eq. of benzyl alcohol in toluene as solvent. Reaction of THP acid *cis*-**280** with DPPA in benzyl alcohol at 85 °C pleasingly gave Cbz-protected amine *cis*-**285** in 62% yield after chromatography. The Cbz group was then removed by hydrogenation with Pd(OH)$_2$ as catalyst to give 3-D fragment *cis*-**278** in quantitative yield (Scheme 3.48).
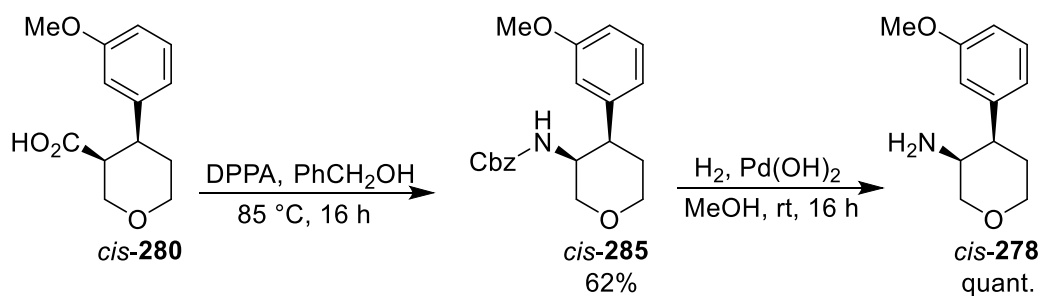
Scheme 3.48

The final two fragments to be synthesised were THF acids *cis*-**277** and *cis*-**281**. Using the hydrolysis conditions from Scheme 3.20, the hydrolysis of THF **219** was successfully performed to give acid **286** in 78% yield (Scheme 3.49).
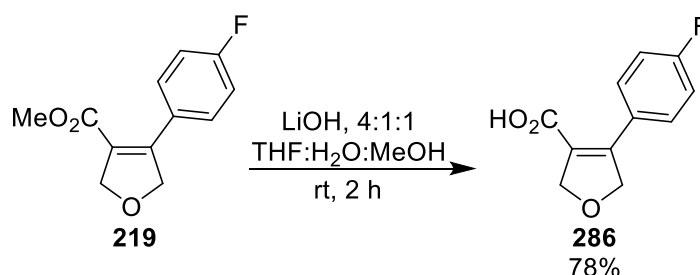
Scheme 3.49

The next step in the synthesis of fragment *cis*-**277** was the hydrogenation, using Pd/C as the catalyst. The ^{1}H NMR spectrum of the crude product appeared to show no starting material remaining, but a mixture of three products. Purification by column chromatography allowed fragment *cis*-**277** to be isolated in 58% yield (Scheme 3.50). In addition, a mixture of two other compounds was isolated, which appeared from their ^{1}H NMR spectrum to be an 85:15 mixture of isomerised starting material **287** and oxidised furan **288**.
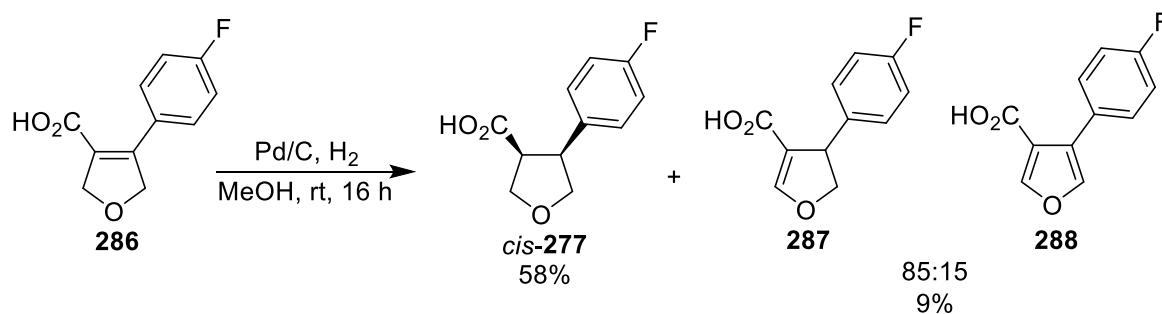
Scheme 3.50

An X-ray crystal structure of THF *cis*-**277** was obtained to prove the *cis* stereochemistry (Figure 3.13). With this X-ray crystal structure, the stereochemistry of the hydrogenation step had been proven on an example of each of the five fragment cores.
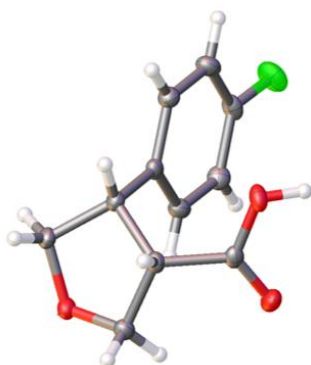
Figure 3.13: X-ray crystal structure of THF acid *cis*-**277**

The product of the Suzuki-Miyaura coupling to give dihydrofuran **221** had been a mixture of the desired product and the tolyl boronic acid. Hydrolysis was performed on the mixture using the NaOH conditions from Metcalf and Li.[118] The crude reaction mixture still showed traces of tolyl boronic acid, but purification by flash column chromatography allowed for the isolation of dihydrofuran acid **289** in 78% yield. Subsequent hydrogenation using Pd(OH)$_2$ as catalyst for 64 h and purification by flash column chromatography gave desired fragment *cis*-**281** in 64% yield (Scheme 3.51).
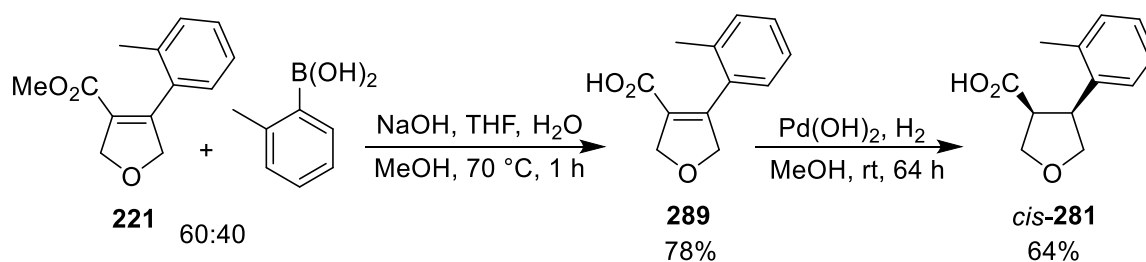
Scheme 3.51

3.7 Conclusions

The addition of the seven fragments synthesised *via* the ester hydrolysis route gave 24 3-D fragments in total (Figure 3.12). It was pleasing that these 2nd generation, diverse 3-D fragments had taken just under a year to synthesise. This compared very favourably with the time taken to synthesise the 1st generation fragments, validating our new approach. Furthermore, the fragments synthesised using the new approach showed much more functional group diversity than the 1st generation fragments, as demonstrated structures shown in Figure 3.12. The 24 synthesised fragments were combined with a set of 26 fragments synthesised using a different route by another group member (see Section 4.5), to form a larger library of 50 2nd generation fragments.
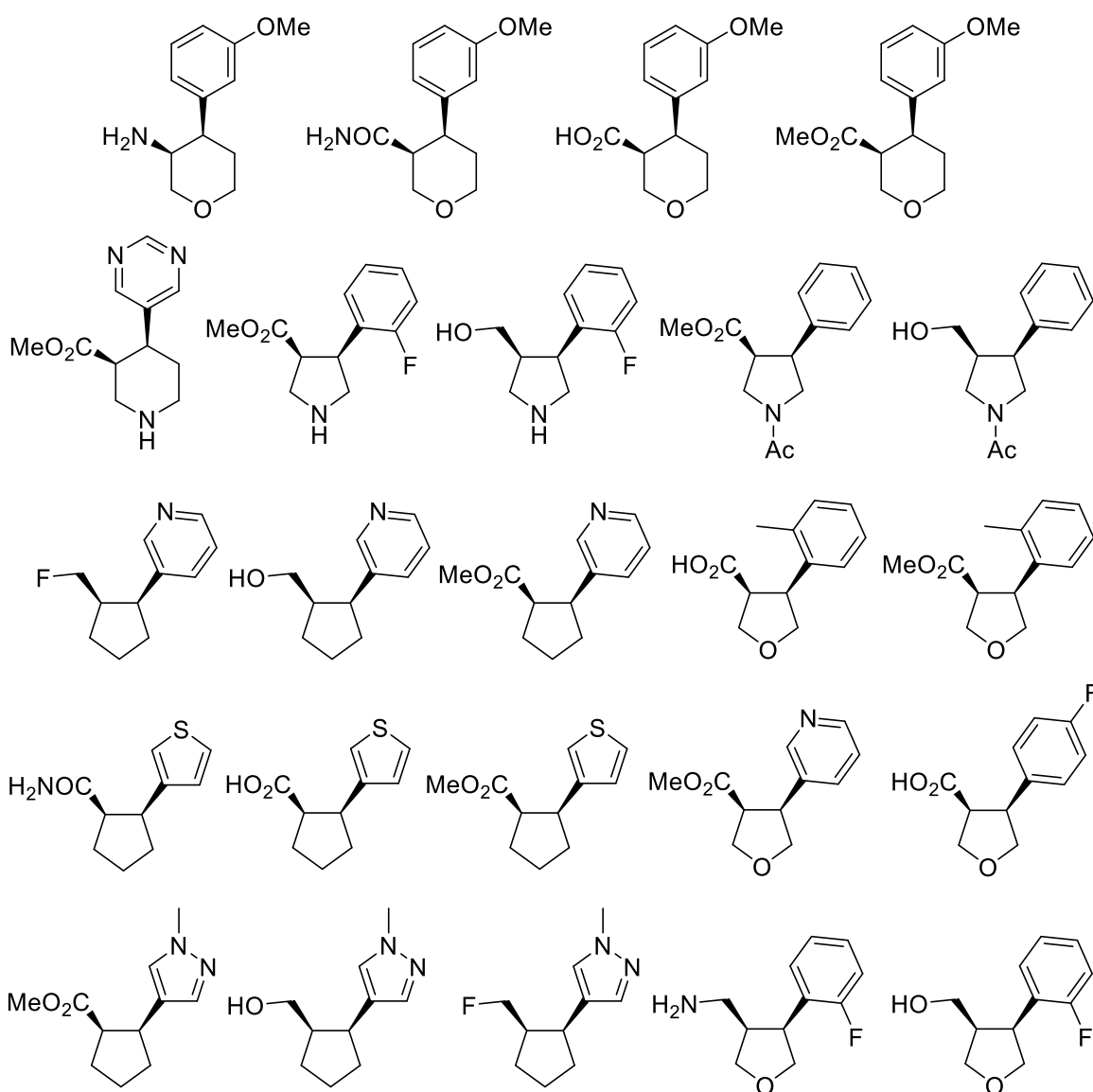
Figure 3.12: The 24 fragments synthesised using the new approach

It was anticipated that the methodology and toolkit of reactions we had optimised could easily be applied to other *β*-ketoesters (cyclohexane and 5- and 6-membered cyclic sulfones, for example) and other boronic acids to further increase the number of potential products from this approach if desired. The approach did have some limitations, particularly the inability to attach acid, amine and amide groups to pyrrolidines and piperidines and the stability issues with the pyrrolidines and dihydropyrroles, but most fragment syntheses proved to be straightforward and achieved in 3-5 steps from the *β*-ketoesters.

CHAPTER 4: PROPERTY ANALYSIS OF THE SYNTHESISED FRAGMENT LIBRARIES, CONCLUSIONS AND FUTURE WORK

With the synthetic work now completed, an analysis of the properties of all of the 3-D fragments that have been synthesised in the group was carried out. Section 4.1 sets out the properties that will be analysed. These include 3-D shape analysis by principal moments of inertia (PMI) and plane of best fit (PBF) as well as molecular weight (MW), heavy atom count (HAC), cLogP, rotatable bonds, H-bond acceptors and H-bond donors. The 3-D fragments were split up into four subsets for analysis. Analysis of the initial 32 pyrrolidine and piperidine fragments whose selection is described in Section 1.4 and the larger group of 1st generation fragments which these compounds formed part of is described in Section 4.2. The properties of the fragments whose synthesis is described in Chapter 2 are highlighted in these sections. Then, the properties of the 24 fragments whose synthesis is detailed in Chapter 3 and the larger group which these fragments formed part of (2nd generation fragments) are presented (Section 4.3). Some representative examples of 1st and 2nd generation fragments are shown in Figure 4.1, including fragments synthesised in the results presented in Chapters 2 and 3 (*cis*-**37**, *cis*-**45**, *cis*-**278**, *cis*-**253** and *cis*-**247**).
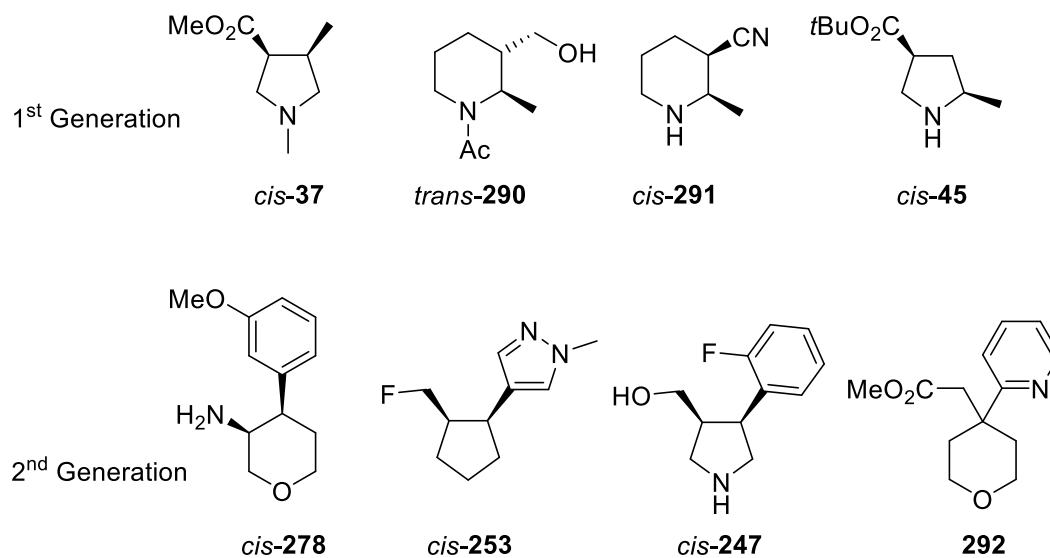
Figure 4.1: Examples of 1st and 2nd generation fragments

Throughout this chapter, the 3-D shape of our subset libraries is compared to a selection of commercially available fragment libraries. Furthermore, the physicochemical properties of our fragments are compared to industry-recommended guidelines to assess their suitability for screening. Conclusions drawn from the project and potential future work are detailed in Section 4.4

4.1 Identification of Properties for Analysis

Guidelines on fragment properties in the literature are relatively varied, with many pharmaceutical companies having their own definition of what constitutes a fragment. The broadest definition of a fragment, and the most accepted one, is a molecule with a MW of ≤300. This definition comes from the fragment 'rule of three',[12] an adapted version of Lipinski's 'rule of five' for drug-like compounds.[13] The 'rule of three' also gives guidelines for the lipophilicity, number of hydrogen bond donors and acceptors and rotatable bonds for fragment molecules. These guidelines are, however, very broad, and pharmaceutical companies will typically target a narrower range of properties. Astex published an updated list of guidelines for fragment properties in 2016 based on their own library and what had succeeded and failed in drug discovery programmes.[123] They suggested a narrower band of molecular weight that was significantly lower than the 300 suggested in the 'rule of three', as well as giving a tighter restriction on lipophilicity that contained a lower limit of cLogP ≥ 0. However, it is worth noting the following quotation in the paper: 'These are the properties we currently aspire to and are based on over a decade of FBDD research. Note that there are many examples of fragments outside of these guidelines that have been progressed into useful leads'.

Analysis of the properties of our libraries will therefore use both the 'rule of three' and the updated guidelines (Table 4.1) as points of comparison. The properties analysed will be MW, HAC, cLogP and number of rotatable bonds, H-bond acceptors and H-bond donors. Ideally, fragments will fit both the updated guidelines and the 'rule of three', but fragments will only be omitted from the 3-D fragment library if they significantly flout the 'rule of three'.

Property	'Rule of Five'	'Rule of Three'	Updated Guidelines
Molecular Weight (Da.)	≤ 500	≤ 300	140-230
Heavy Atom Count (HAC)	N/A	N/A	10-16
cLogP	≤ 5	≤ 3	0-2
Rotatable Bonds	N/A	≤ 3	N/A
H-Bond Donors	≤ 5	≤ 3	N/A
H-Bond Acceptors	≤ 10	≤ 3	N/A

Table 4.1: Summary of the suggested properties for drug molecules and fragments

The 3-D shape of the fragments will also be analysed. As explained in Section 1.4, PMI plots have been used in this project to quantify 3-D shape and to select fragments for synthesis. The 3-D fragments have therefore been analysed using two types of plots: normal PMI plots

and cumulative PMI plots. Normal PMI plots (Figure 4.2, left) give an indication of both the shape and shape-diversity of the fragments in the library. Clustering indicates that molecules have similar shapes, which would ideally be avoided, while the spread towards the top right corner ($\sum$NPR = 2.0) indicates the most spherical molecules.
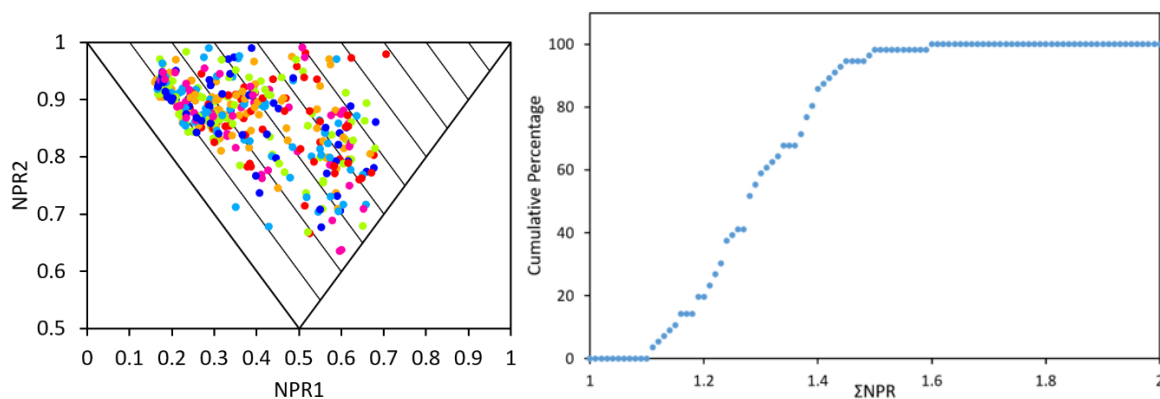
Figure 4.2: Example PMI plot (left) and cumulative PMI plot (right)

Cumulative PMI plots (Figure 4.2, right), show the percentage of conformations of the library that have a $\sum$NPR below a certain value. The advantage of cumulative PMI plots is that they allow for easier comparison of different libraries. Six fragment libraries from both commercial and academic sources have been selected and analysed for their 3-D shape.[83] These include Maybridge, Chembridge and Enamine 'rule of three' libraries, which are not specifically designed for their 3-D shape, and Life Chemicals, ChemDiv and Enamine libraries which were specifically designed to have interesting 3-D shape.

One of the difficulties of using cumulative PMI plots is that not all compounds have the same number of conformations. For example, a compound with 10 conformations will affect the cumulative PMI plot 10 times as much as a compound with a single low energy conformer. Therefore, when plotting cumulative plots an average $\sum$NPR value, taken from the equally weighted average of the $\sum$NPR values of all low energy conformations of a compound, was used instead of adding each conformation individually. Figure 4.3 shows the difference between plotting the average $\sum$NPR values and all the $\sum$NPR values of each molecule in a dataset. These two plots show significant difference in shape, accounted for by the fact that some compounds in the selection display as many as 29 low energy conformations while others display as few as two.
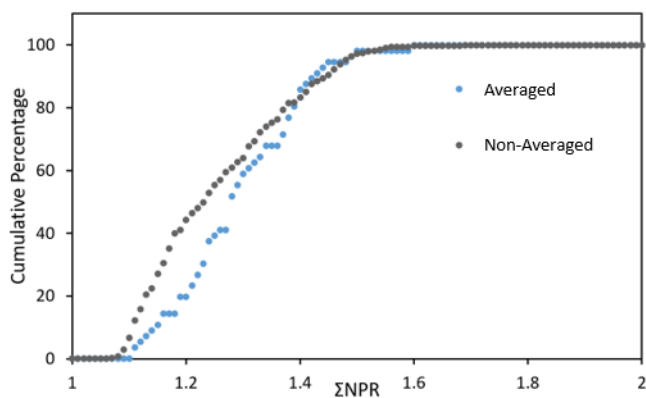
Figure 4.3: Averaged and non-averaged cumulative PMI plots

Each library or subset of compounds will therefore be analysed using the physicochemical properties detailed in Table 4.1 and PMI and cumulative PMI plots to assess 3-D shape. Where available, PBF data will also be analysed.

4.2 Property Analysis of the 56 1st Generation York 3-D Fragments

At the outset of the project, 33 pyrrolidine and piperidine 3-D fragments were selected for synthesis (see Section 1.4). Of these, 31 were successfully synthesised since we were unable to synthesise the 2,4-disubstituted pyrrolidines (see Chapter 2). However, the *t*-butyl ester analogue, fragment *cis*-**46**, was synthesised, taking the total up to 32 3-D fragments (Figure 4.4). Physicochemical and 3-D shape analysis was carried out on all of these compounds and, in addition, a PBF analysis was recorded for the initial 33 target fragments.
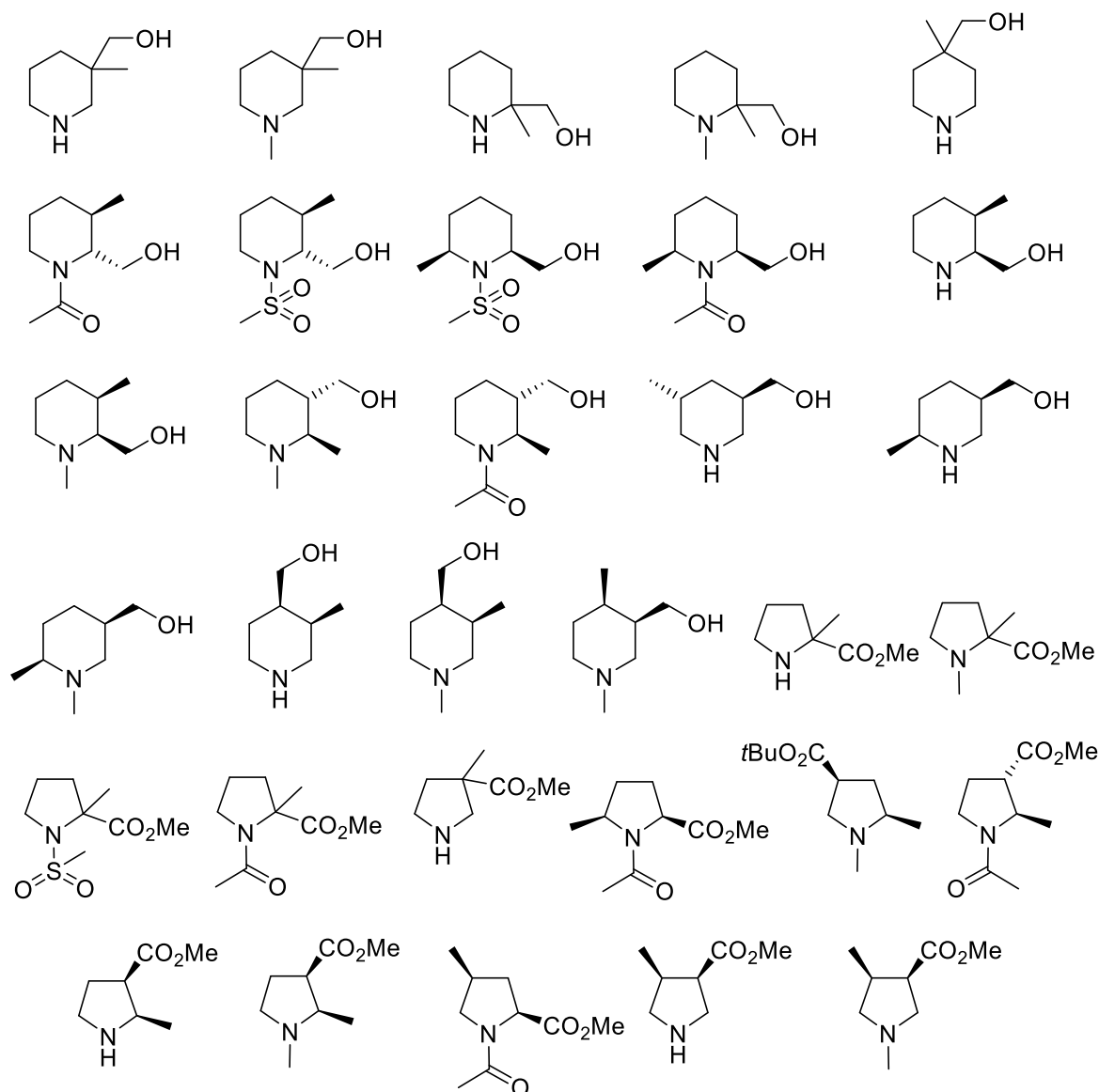
Figure 4.4: Structures of the 32 synthesised initial fragments

The properties of the 32 3-D fragments shown in Figure 4.4 are shown in Table 4.2. Since the properties of all the potential fragments had previously been calculated during the design and selection process (see Section 1.4), the values were expected to be in line with the fragment guidelines. These 32 compounds fit the 'rule of three' completely, with only ten

fragments not completely meeting the stricter updated guidelines. Nine of these were either too small (MW of 129, HAC of 9), too polar (cLogP between –0.18 and 0) or both and one fragment failed due to having four H-bond acceptors. A potential criticism of these fragments is that they are relatively small and polar, which could make hit detection difficult.

Property	'Rule of Three'	Updated Guidelines	32 3-D Fragments
Molecular Weight (Da.)	≤ 300	140-230	158 ± 26
Heavy Atom Count (HAC)	N/A	10-16	10.8 ± 1.6
cLogP	≤ 3	0-2	0.54 ± 0.46
Rotatable Bonds	≤ 3	N/A	1.53 ± 0.61
H-Bond Donors	≤ 3	N/A	1.28 ± 0.71
H-Bond Acceptors	≤ 3	N/A	1.81 ± 0.85

Table 4.2: Analysis of the physicochemical properties of 32 3-D fragments

The 3-D shape properties of these fragments were then analysed using PMI plots. The PMI plot of all conformations up to 1.5 kcalmol^{-1} in energy above the ground state is shown in Figure 4.5. The plot showed an even spread of conformations all the way up to $\sum$NPR = 1.7.
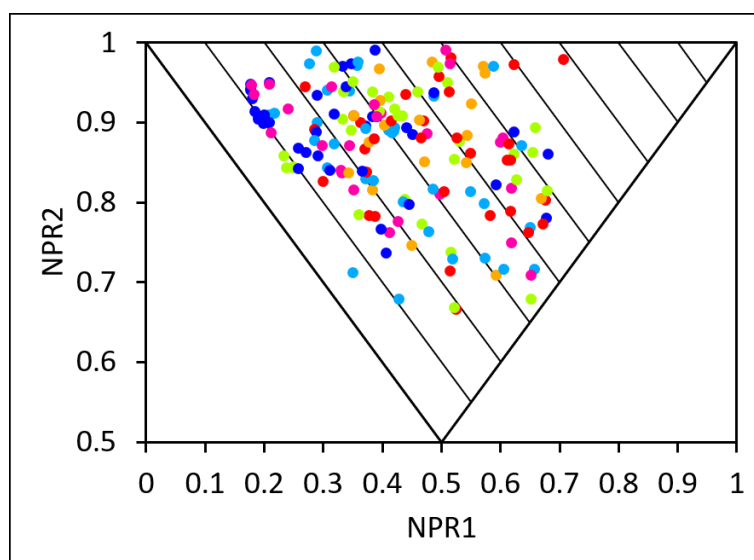
Figure 4.5: PMI plot of the 32 3-D fragments

The individual PMI plots of the three fragments that form part of this set and whose synthesis was decribed in Chapter 2 are shown in Figure 4.6. Notably, the *t*-butyl ester analogue fragment still fits the shape selection criteria by having a low energy conformation with $\sum$NPR $\geq$ 1.36.
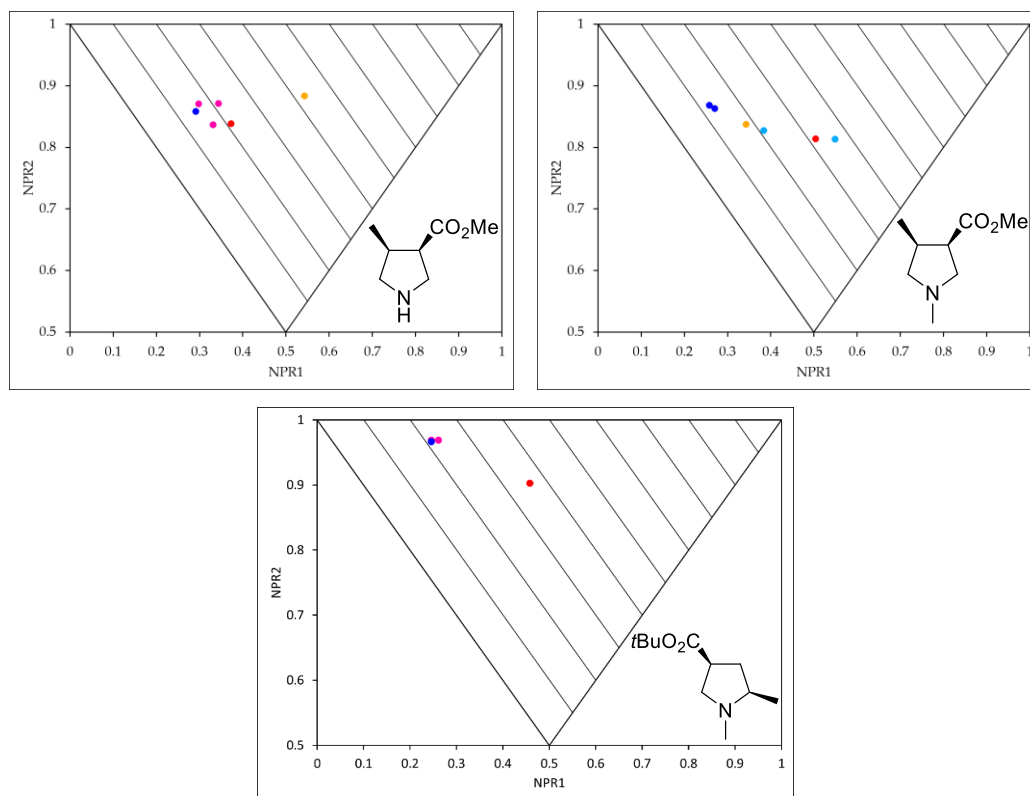
Figure 4.6: PMI plots of the target fragments whose synthesis is described in this thesis

A plane of best fit (PBF) analysis was conducted on the 33 initially selected 3-D fragments. This was done to confirm that PMI was a valid way of analysing the 3-D shapes of these molecules. As described in Section 1.2, the PBF score measures the deviation of a molecule from its plane of best fit. Like PMI plots, there are many definitions of whether a molecule is 3-D as measured by PBF. For example, Astex define molecules with PBF $\geq$ 0.05 as 3-D,[124] whereas AstraZeneca use PBF $\geq$ 0.25 as their criterium.[50] The 31 fragments of those initial 33 that were synthesised would all be classified as 3-D, with each fragment having a PBF value > 0.67.

The library of the first 32 York 3-D fragments was then compared to the other libraries identified in Section 4.1. Using average $\sum$NPR values, Figure 4.7 shows the cumulative PMI plot of both the 32 York 3-D fragments and the six chosen other libraries. The York 3-D fragments are shifted substantially to the right of the other libraries, indicating much greater 3-D character. To use one point as an example, 50% of the 32 York 3-D fragments have an average $\sum$NPR > 1.3. This contrasts with less than 10% for the Enamine 3-D library, and less than 5% for the other five libraries, clearly demonstrating that our compounds are more effective at exploring the under-represented areas of 3-D space.
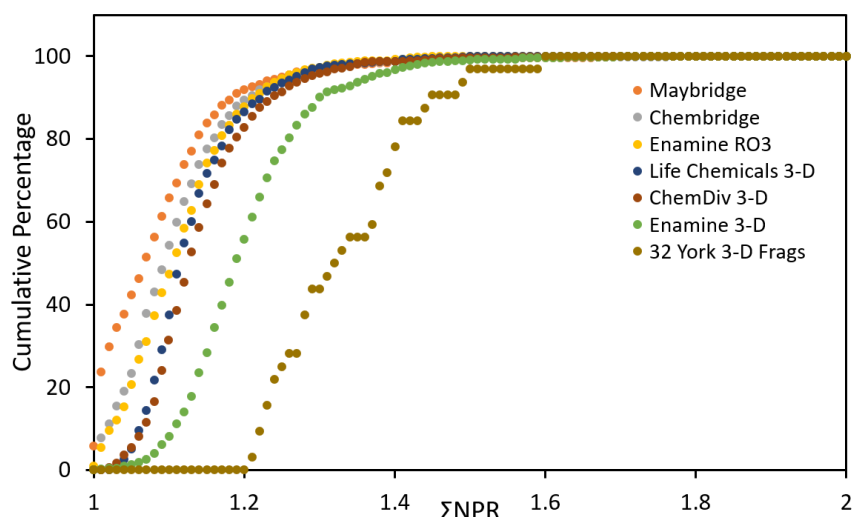
Figure 4.7: Cumulative PMI plot of the Original 32 fragments and other libraries

As the synthesis of the first 32 York 3-D fragments was nearing completion, it was decided to use some of the chemistry developed during that process to synthesise derivatives with different functional groups. The aim was to produce a library of at least 50 fragments while increasing the functional group variation. Fragments which showed good 3-D shape (based on PMI analysis) and had simple synthetic routes were derivatised resulting in the 24 3-D fragments shown in Figure 4.8. Together with the 32 compounds synthesised previously, this created a library of 56 1st generation 3-D fragments.
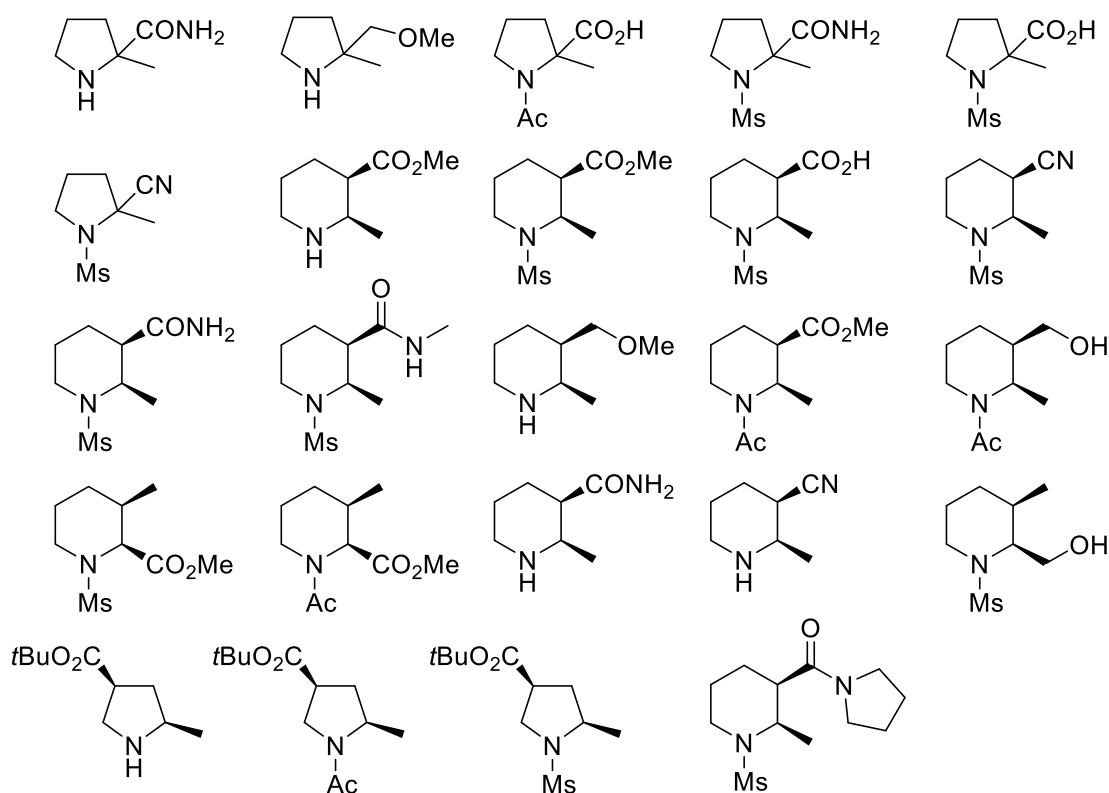
Figure 4.8: Structures of 24 additional 1st generation 3-D fragments

The additional fragments were notable for being on average of higher MW than the original 32 fragments, bringing the overall average MW up from 158 to 173, and for having more H-bond acceptors (Table 4.3). The increase in both of these properties is due in part to the increased prevalence of mesyl groups in the new fragments. A mesyl group adds a molecular weight of 79 and two H-bond acceptors and half of the 24 fragments contain mesyl groups. Overall however, the fragments still broadly fit the criteria, with the only non-'rule of three' compliant fragments being those with four H-bond acceptors.

Property	'Rule of Three'	Updated Guidelines	1st Generation
Molecular Weight (Da.)	≤ 300	140-230	173 ± 38
Heavy Atom Count (HAC)	N/A	10-16	11.8 ± 2.3
cLogP	≤ 3	0-2	0.54 ± 0.55
Rotatable Bonds	≤ 3	N/A	1.64 ± 0.77
H-Bond Donors	≤ 3	N/A	0.89 ± 0.70
H-Bond Acceptors	≤ 3	N/A	2.68 ± 0.73

Table 4.3: Properties of the 56 1st generation fragments

Each of the 24 3-D fragments had been analysed for its 3-D shape using PMI plots before synthesis to ensure that shape diversity was maintained. The PMI plot of the 56 1st generation fragments (Figure 4.9) shows more clustering than the PMI plot of the original 32 (Figure 4.5), although this is to be expected given the additional compounds. Importantly, there are still very few conformations with $\sum NPR \leq 1.1$, showing that the library is still highly 3-D in character, and there are no conformations with $\sum NPR \leq 1.06$.
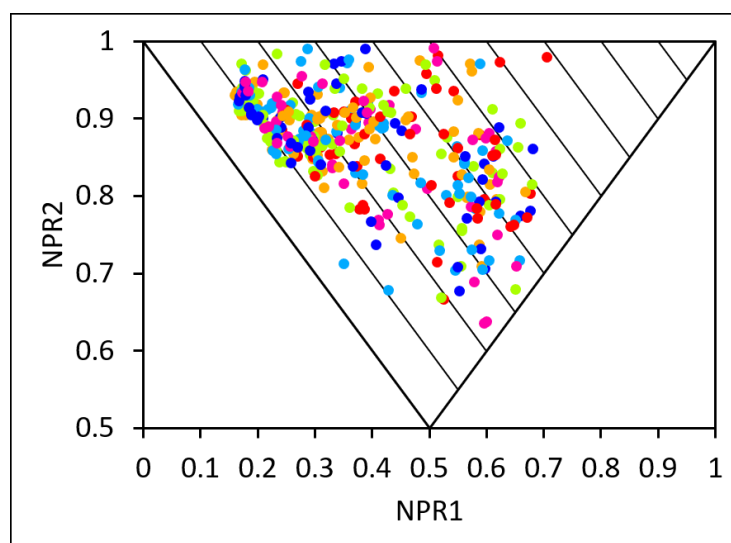
Figure 4.9: PMI plot of the 56 1st generation fragments

Thee synthesis of three of these 24 fragments is described in this thesis (Section 2.3). Their PMI plots are shown in Figure 4.10. Both the N-H and N-Ac fragments had low energy conformations with $\sum$NPR $\geq$ 1.3, although the N-Ms fragment had no conformations with $\sum$NPR $\geq$ 1.2.
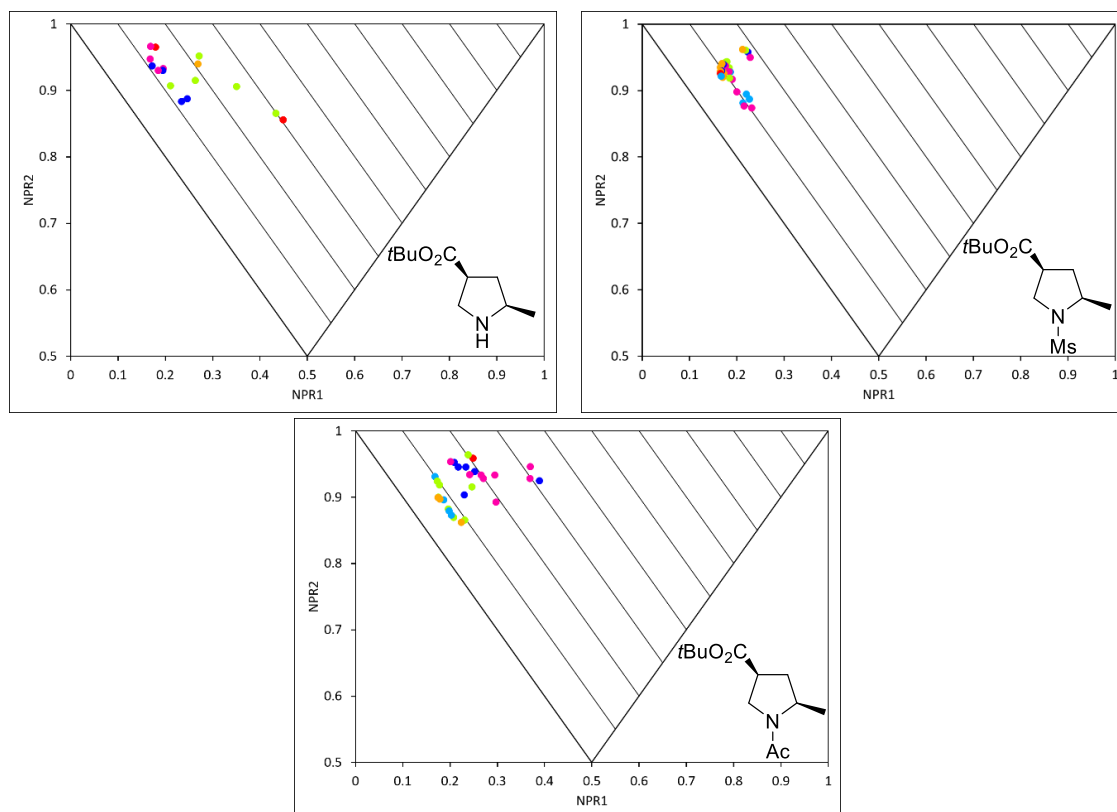
Figure 4.10: PMI plots of the three additional *t*-butyl ester fragments

The 56 1st generation 3-D fragments were then plotted on a cumulative PMI plot to compare the 3-D shape of the library with other fragment libraries. As shown in Figure 4.11, the 1st generation library has less 3-D character than the original 32 but still substantially more 3-D character than the other fragment libraries that were analysed.
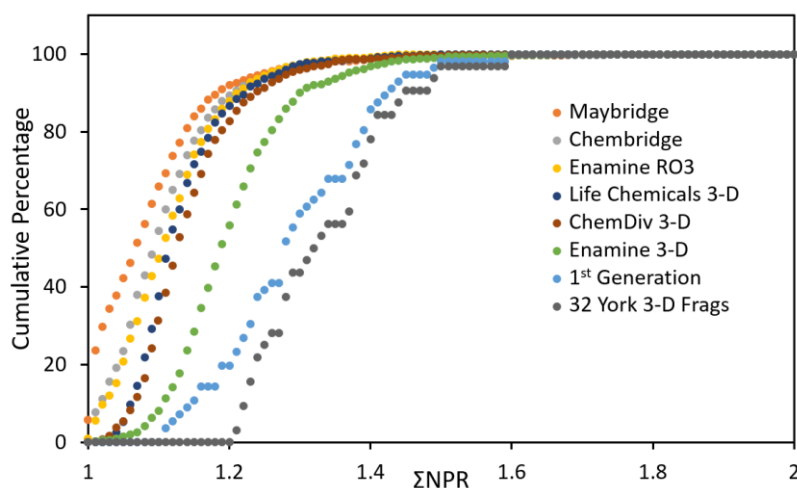
Figure 4.11: Cumulative PMI plot of the 56 1st generation fragments and other libraries

4.3 Property Analysis of the 50 2ⁿᵈ Generation York 3-D Fragments

As described in Section 3.1, once the 1ˢᵗ generation fragments had been synthesised a new approach was desired that put more emphasis on ease of synthesis while not compromising on 3-D shape. The structures of the 24 fragments synthesised by the Suzuki-hydrogenation route in Chapter 3 are shown in Figure 4.12. In contrast to the 1ˢᵗ generation fragments, these compounds show a wide variety of cores, functional groups and aromatics to ensure that the fragments covered a wide range of properties and potential binding modes.
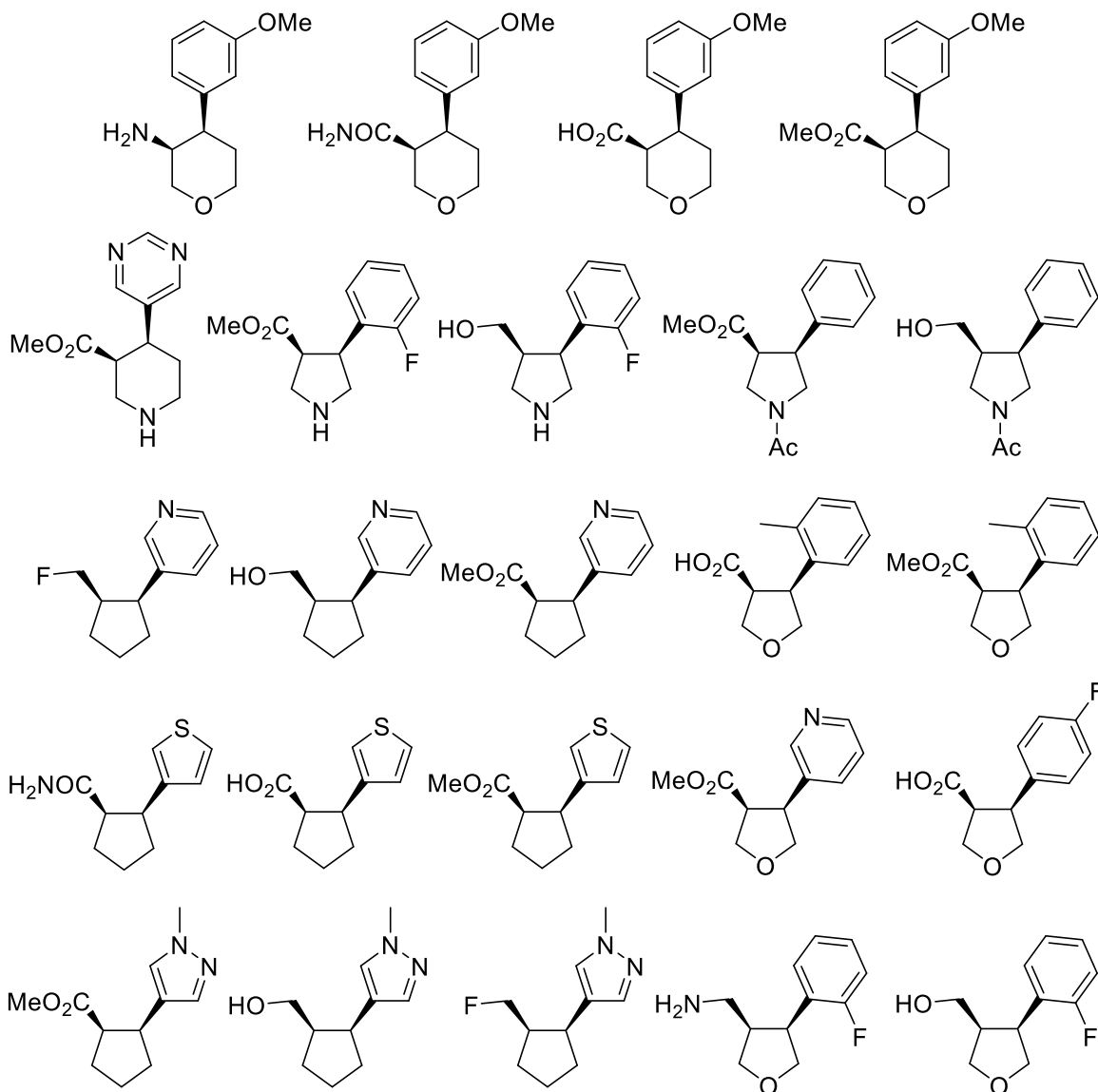
Figure 4.12: Structures of the 24 fragments synthesised by the Suzuki-hydrogenation route

The properties of these 24 3-D fragments are shown in Table 4.4. The fragments are heavier than the 1ˢᵗ generation fragments, as expected due to the presence of the aromatic rings. These 24 fragments are also significantly more lipophilic, with an average cLogP value of 1.32. However, this is still well within both sets of guidelines. The only property in which

some of the fragments break the 'rule of three' is H-bond acceptors, although no compounds have more than four. Overall, the 24 2nd generation York 3-D fragments were mostly compliant with both the updated guidelines and the 'rule of three' while also occupying a different area of chemical space to the 1st generation fragments.

Property	'Rule of Three'	Updated Guidelines	24 York 3-D Fragments
Molecular Weight (Da.)	≤ 300	140-230	209 ± 20
Heavy Atom Count (HAC)	N/A	10-16	14.9 ± 1.6
cLogP	≤ 3	0-2	1.32 ± 0.77
Rotatable Bonds	≤ 3	N/A	2.13 ± 0.33
H-Bond Donors	≤ 3	N/A	0.50 ± 0.58
H-Bond Acceptors	≤ 3	N/A	2.67 ± 0.94

Table 4.4: Physicochemical properties of the 24 2nd generation York 3-D fragments

Although 3-D shape was not a primary selection criterion, all potential 2nd generation fragments were run through Pipeline Pilot and plotted on PMI plots to assess their 3-D shape before synthesis. Those that did not display conformers with $\sum NPR \geq 1.15$ were not synthesised. The wide variety of possible functional group, core and aromatic group combinations meant that avoiding compounds with poor 3-D shape was relatively straightforward and this was further compounded by the fact that the substitution patterns of 2nd generation fragments were chosen based partly on the fact that the substitution pattern gave high 3-D character. The PMI plot of the 24 2nd generation York 3-D fragments is shown in Figure 4.13. The fragments gave an excellent spread on the PMI plot from $\sum NPR = 1.13$ to $\sum NPR = 1.55$ with minimal clustering and no conformations close to the rod-disc axis.
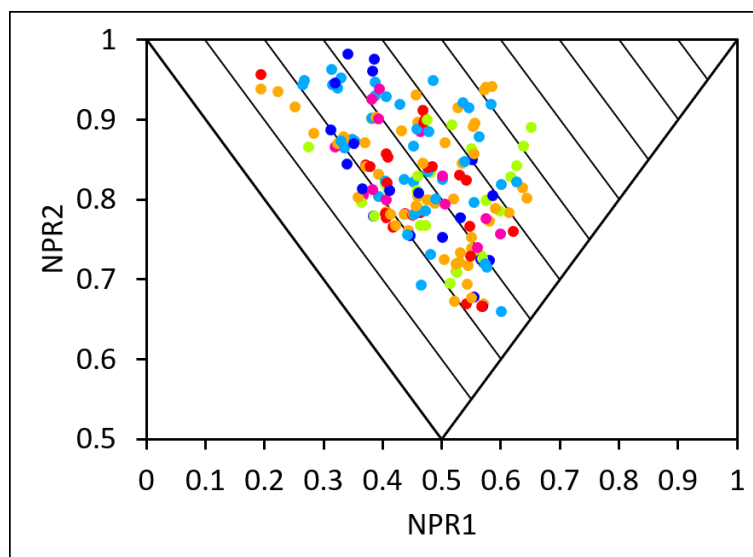
Figure 4.13: PMI plot of the 24 York 3-D fragments

The cumulative PMI plot showed significantly more 3-D character than any of the commercial libraries (Figure 4.14). Only two of the synthesised compounds showed an average $\sum$NPR value below 1.2 with the half of the conformers having $\sum$NPR $\geq$ 1.24.
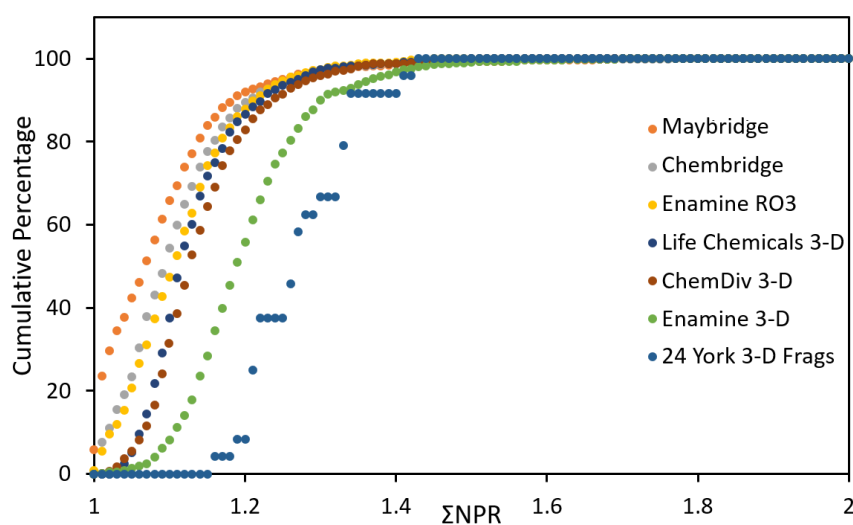
Figure 4.14: Cumulative PMI plot of the 24 York 3-D fragments

During work on the 24 York 3-D fragments whose synthesis was detailed in Chapter 3, another group member synthesised 26 fragments using a similar approach to give an overall library of 50 2nd generation 3-D fragments. Like the fragments detailed in Chapter 3, these 3-D fragments were all synthesised using a single piece of methodology to give fragments with a range of cores, aromatic groups and functional groups. The structures of the 26 fragments, all synthesised using α-arylation methodology, are shown in Figure 4.15.
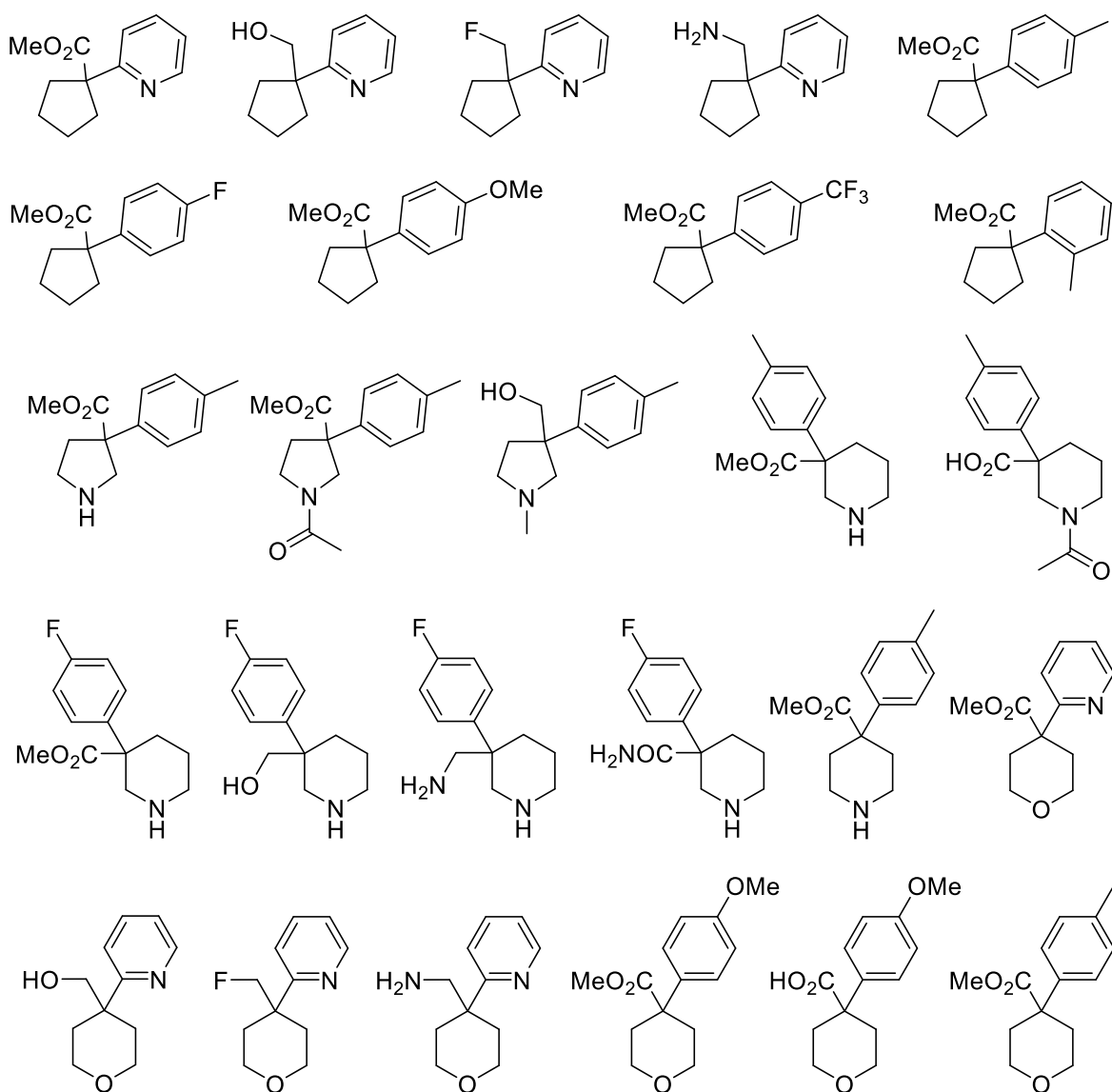
Figure 4.15: Structures of the 26 additional 2nd generation fragments

The properties of these additional 26 3-D fragments (Table 4.5) synthesised by another group member are very similar to those from the route described in Chapter 3, with the exception that on average these fragments tended to be more lipophilic. Five of the additional 26 fragments did not fit within the 'rule of three' with cLogP > 3 and brought the average cLogP value for the 2nd generation fragments up to 1.57. However, none were excluded. Given the polar nature of the 1st generation fragments, the increased lipophilicity of the 2nd generation fragments gives good variation across the range of desirable cLogP values. Properties of the whole library, including all 1st and 2nd generation fragments will be discussed in Section 4.4.

Property	'Rule of Three'	Updated Guidelines	2nd Generation
Molecular Weight (Da.)	≤ 300	140-230	215 ± 23
Heavy Atom Count (HAC)	N/A	10-16	15.4 ± 1.7
cLogP	≤ 3	0-2	1.57 ± 1.03
Rotatable Bonds	≤ 3	N/A	2.12 ± 0.32
H-Bond Donors	≤ 3	N/A	0.56 ± 0.67
H-Bond Acceptors	≤ 3	N/A	2.54 ± 0.90

Table 4.5: Physicochemical properties of the 50 2nd generation fragments

The PMI plot of the 50 2nd generation fragments (Figure 4.16) showed very little clustering. This was particularly pleasing given the similar structures of many of the compounds and demonstrates how difficult it is to predict 3-D shape based on the structural drawing. The 26 α-arylation fragments did not have as many highly 3-D conformers as the first 24 3-D fragments – the area of the plot with $\sum$NPR ≥ 1.4 looks almost identical to that in Figure 4.12 but importantly there are still no conformations with $\sum$NPR ≤ 1.1.
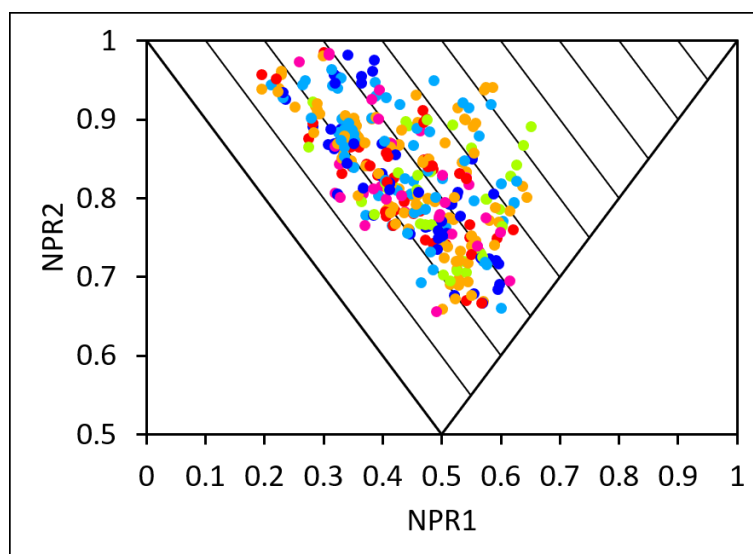
Figure 4.16: PMI plot of the 50 2nd generation fragments

As expected from the PMI plot, the cumulative PMI plot for the 50 2nd generation 3-D fragments (Figure 4.17) looks very similar to that of the 24 York 3-D fragments, particularly at lower $\sum$NPR values. While the profile of the 2nd generation curve is moving closer towards the other libraries, particularly the Enamine 3D library, the key difference is that no York 3-D fragments have $\sum$NPR values close to 1.0. The lowest $\sum$NPR value conformer (1.12) of any 2nd generation fragment has a higher $\sum$NPR than 28% of the Enamine 3-D library

conformers, 64% of the ChemDiv 3-D library conformers and 72% of the Life Chemicals 3-D library conformers, showing just how stringent our criteria for selecting fragments are.
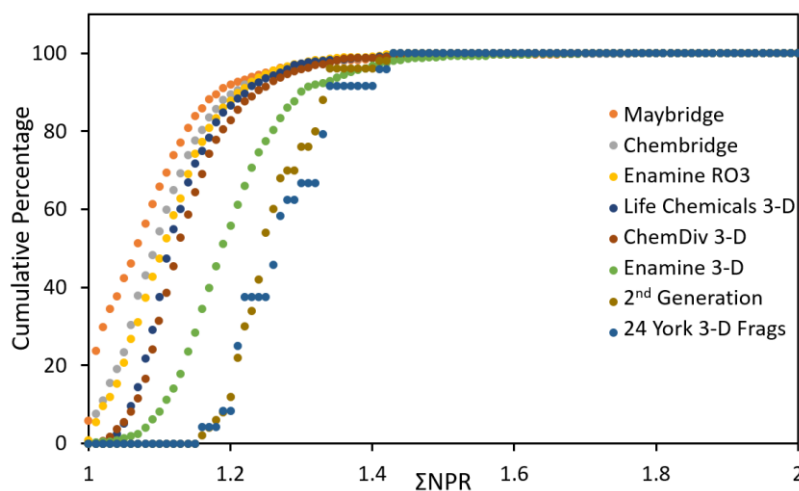
Figure 4.17: Cumulative PMI plot of the 50 2nd generation fragments

Importantly, preliminary fragment screens have already shown 2nd generation fragments to have a better hit rate than the 1st generation fragments. As mentioned in Section 4.3, these 50 fragments were designed to be more lipophilic than their 1st generation counterparts and to have additional potential binding modes. One of the 26 α-arylation fragments has already been confirmed as a hit against a key confidential protein target by NMR, SPR and X-ray crystallography. One of the 24 fragments synthesised in Chapter 3 has shown as a hit by SPR and is currently undergoing soaking to attempt to achieve an X-ray crystal structure of the bound compound. This is very encouraging and has started to validate this approach. We hope that, as these fragments are screened against more protein targets, we will be able to demonstrate the value of having fragments with varied 3-D shape to complement existing collections and ensure hits against a wider range of targets.

4.4 Comparison of Overall Library Properties and 1st and 2nd Generation Fragments

With the 2nd generation York 3-D fragments complete and the combined library of the 1st and 2nd generations being screened currently, the combined library was briefly analysed to ascertain how successful the project had been in its aim: to synthesise a library of fragments with diverse and interesting 3-D shapes. The distribution of properties is shown in Figure 4.18. Each graph shows the distribution of a key physicochemical property of the 106 fragments. The 'rule of three' limit for MW, HAC and number of H-bond donors and acceptors is shown on the graphs in red, while the updated guidelines are shown in green.
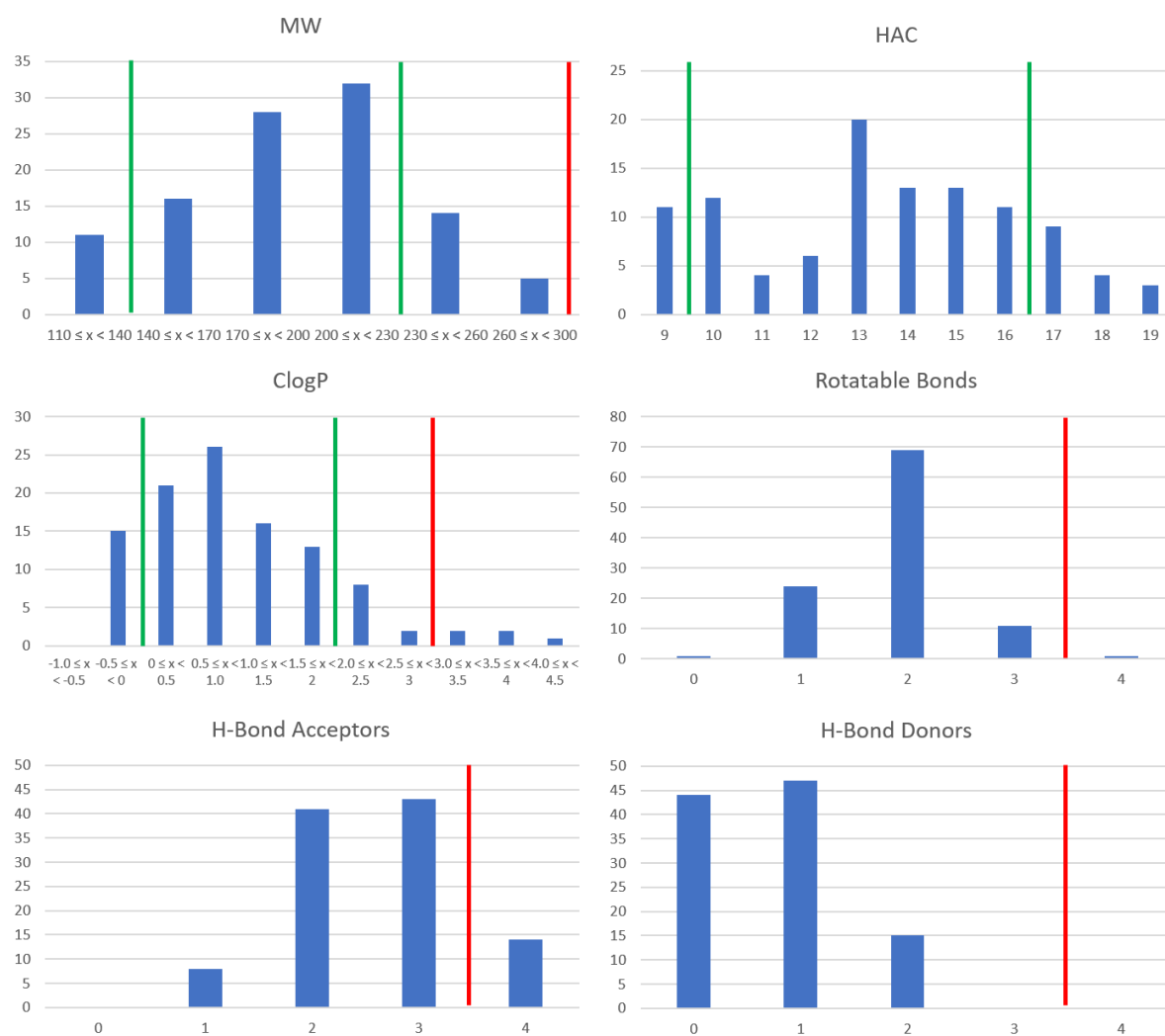
Figure 4.18: Distribution of the properties of the York 3-D fragment library, showing number of fragments against selected property

The graphs in Figure 4.18 show that the York 3-D fragment library has an excellent profile of physicochemical properties. Few fragments break the 'rule of three', with those that do having one too many H-bond acceptors or being too lipophilic. Most fragments were also shown to fit with the more stringent updated guidelines, with more than 70% of fragments

being compliant in each category. Importantly, the fragments display diverse properties whilst also ensuring that all desired criteria are represented.

A PMI analysis of these 106 1st and 2nd generation York 3-D fragments was performed to check the spread of conformers (Figure 4.19). The PMI plot shows minimal clustering and no compounds on or near the rod-disc axis ($\sum$NPR $\leq$ 1.05). The conformations are distributed relatively evenly between $\sum$NPR = 1.1 and $\sum$NPR = 1.5, clearly demonstrating that our aim of exploring underrepresented areas of pharmaceutical space has been successful.
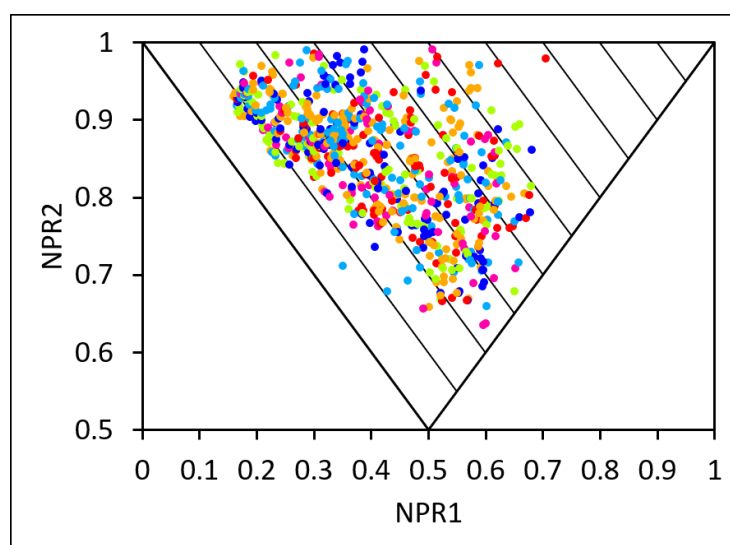
Figure 4.19: PMI plot of the 106 compound York 3-D fragment library

Finally, the cumulative PMI plot was compared to the commercial libraries. As shown in Figure 4.20, more than 50% of the 106 York 3-D fragments had an average $\sum$NPR > 1.26. This demonstrates the exceptional 3-D character of these fragments, particularly when compared to the commercial libraries.
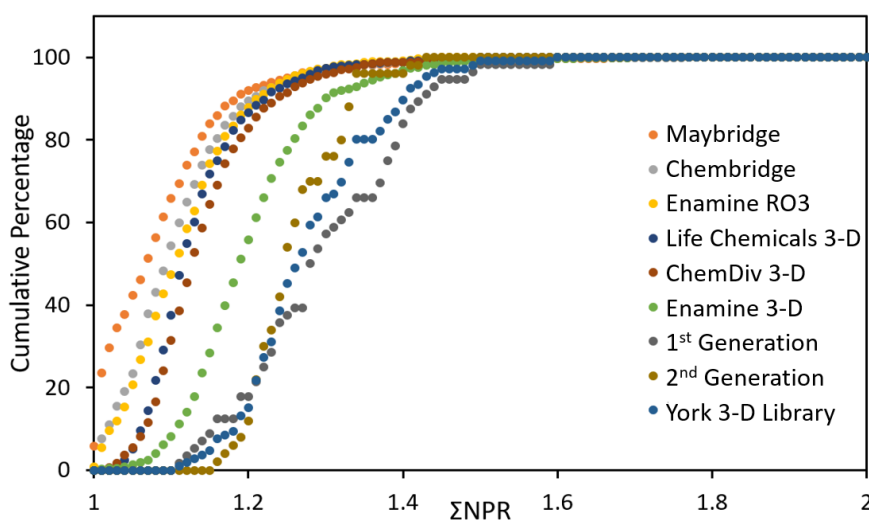
Figure 4.20: Cumulative PMI plot of the York 3-D fragment library

4.5 Overall Conclusions and Future Work

In total 30 fragments were synthesised in this work, which were then added to compounds synthesised by others to give a library of 106 3-D fragments. All 106 fragments have been shown to have both excellent physicochemical properties and 3-D shape. The process began with the design and selection of 33 pyrrolidine and piperidine fragments (Section 1.4). Of these, 31 fragments including *cis*-**42** and *cis*-**43** were synthesised (Section 2.1) and a *t*-butyl ester analogue of fragment *cis*-**37** was synthesised (Section 2.2). Then, an additional 24 related 3-D fragments, including *cis*-**45**, *cis*-**47** and *cis*-**48** (Section 2.3) were synthesised to bring the total up to 56 1st generation fragments.

As described in Chapter 2, synthesis of the initially selected 33 fragments proved difficult and time consuming, with unique synthetic routes having to be found for each substitution pattern. It was therefore decided to alter our approach to using just two synthetic routes to create a library of 50 2nd generation fragments. This thesis details the synthesis of 24 fragments by a single route (Chapter 3). Each route contained three points of diversification, allowing us to access interesting 3-D fragments quickly. This new approach allowed us to access 50 new 3-D fragments in less than 12 months. A detailed property analysis was then carried out to compare the properties of the 106 York 3-D fragments with other available libraries (Chapter 4). This showed our library to have good physicochemical properties and that our fragments effectively explored under-represented areas of 3-D space better than currently available libraries. These fragments are now undergoing screening, and preliminary screens have shown exciting potential for these new compounds. The York 3-D fragment library has also been deposited at the Diamond XChem facility to allow for future screening and collaborations.

In conclusion, a library of 106 highly 3-D fragments (as shown by PMI analysis) has been synthesised and is now undergoing screening. Lessons learned from the synthesis of the 56 1st generation fragments have allowed us to refine our approach and led to the synthesis of 50 2nd generation 3-D fragments in much less time.

Future work on this project would involve the design of new synthetic routes to access 3-D fragments, using a similar strategy to that detailed in Chapter 3. One potential strategy would be to use the same methodology described in Chapter 3 but to epimerise after the hydrogenation step in order to access the *trans*-diastereomer of each fragment. Bull *et al*. showed during their work on *cis*-3,4-disubstiuted pyrrolidines that these systems could be completely epimerised to the *trans*-diastereomer (Scheme 4.1).[72] Reaction of *cis*-**293**, with the aminoquinoline directing group attached, with Cs_2CO_3 at 100 °C gave pyrrolidine *trans*-

294. Alternatively, reaction of *cis*-**293** with NaOH and EtOH at 100 °C hydrolysed the carbamate and epimerisation occurred to give acid *trans*-**295**. Both these reactions proceeded in very high yield and would provide a good starting point for the potential epimerisation of our ester 3-D fragments.
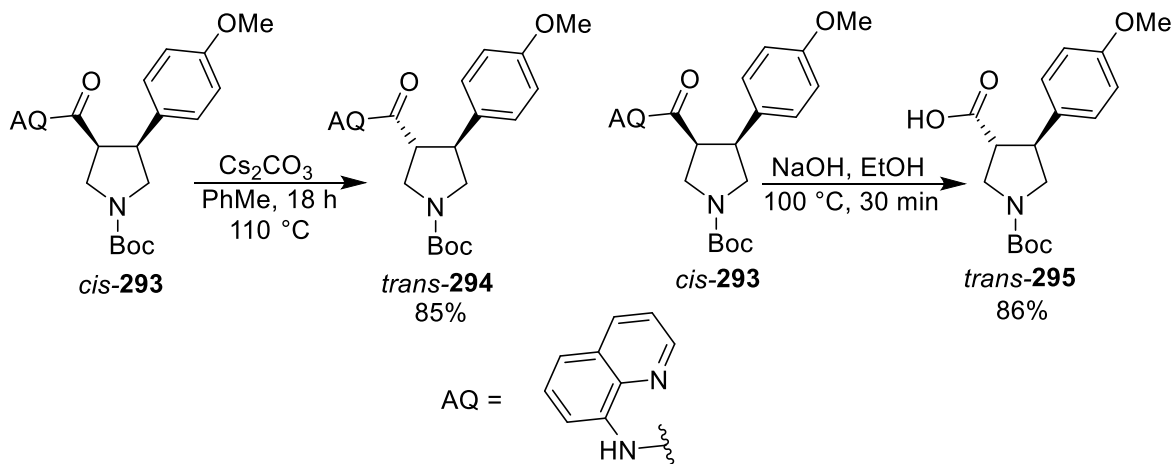
Scheme 4.1

Alternatively, a new synthetic approach could be considered. Bode *et al.* have developed SnAP reagents for the rapid synthesis of saturated heterocycles and partially saturated bicycles.[125,126] Scheme 4.2 shows two examples of the use of SnAP reagents to give products **297** and *trans*-**299**. Both of these compounds contain ester groups that could be diversified or subjected to the α-arylation methodology used to synthesise the fragments in Figure 4.13.
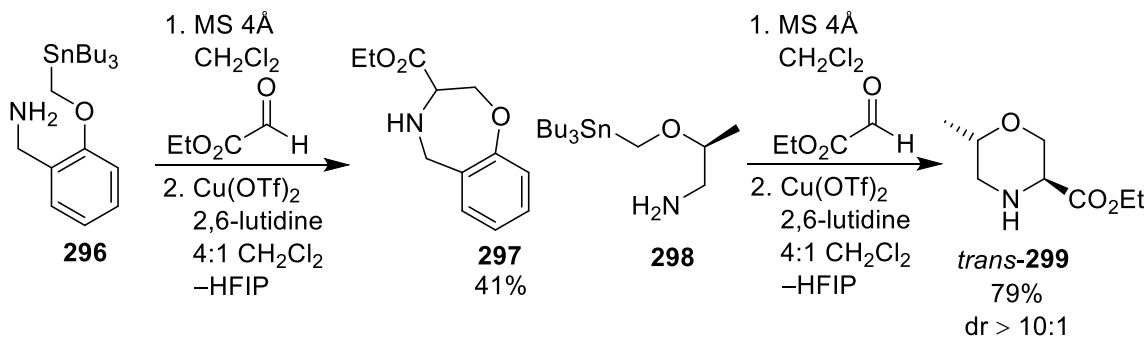
Scheme 4.2

CHAPTER 5: EXPERIMENTAL

5.1 General Methods

5.1.1 3-D Shape Analysis Protocol

A SMILES file containing the SMILES strings for all fragment compounds was generated using ChemDraw 18.0. 3-D structures were generated Pipeline Pilot 8.5.0.200, 2011, Accelrys Software Inc. Generated conformations were used to generate the three Principal Moments of Inertia (I1, I2 and I3) which were then normalised by dividing the two lower values by the largest (I1/I3 and I2/I3) using Pipeline Pilot built-in components. Prior to conformer generation a wash step was performed, which involved stripping salts and ionising the molecule at pH 7.4. Any stereocentre created here was left with undefined stereochemistry. SMILES strings were converted to their canonical representation. A list of allowed chirality at each centre is generated and a SMILES file with all possible stereoisomers was written. Conformers were generated using the BEST method in Catalyst using the rel option, run directly on the server and not through the built-in Conformation Generator component with a chosen maximum relative energy threshold of 20 kcal mol^{-1}, maximum of 255 conformers for each compound. Conformations were read, ones that cannot be represented by the canonical SMILES are discarded, with the remaining ones standardised to a single enantiomer. Duplicates were filtered with a RMSD threshold of 0.1. Minimisation with 200 steps of Conjugate Gradient minimisation with an RMS gradient tolerance of 0.1 was performed using the CHARMm forcefield with Momany-Rone partial charge estimation and a Generalised Born implicit solvent model. Duplicates were filtered again with a RMSD setting of 0.1.

5.1.2 cLogP Calculations

cLogP Values were calculated at AstraZeneca using Daylight/Biobyte software (version 4.3.0)

5.1.3 General Synthetic Methods

Non-aqueous reactions were purged and back filled with Ar three times in flame dried glassware. Diethyl ether and THF were distilled over sodium and benzophenone respectively. Alkyllithiums were titrated using N-benzylbenzamide prior to use. Flash column chromatography was carried out using Fluka Chemie GmbH silica (220-440 mesh). Thin layer chromatography was carried out using commercially available Merk F254

aluminium backed silica plates. Proton (400 MHz) and carbon (100.6 MHz) NMR spectra were recorded on a Jeol ECX-400 instrument using an internal deuterium lock. For samples recorded in CDCl$_3$, chemical shifts are quoted in parts per million relative to CHCl$_3$ (δ_H 7.26) and CDCl$_3$ (δ_C 77.1, central line of triplet). For samples recorded in d4-MeOH, chemical shifts are quoted on parts per million relative to d4-MeOH (δ_H 3.31, central line of quintet) and d4-MeOH (δ_C 49.15, central line of septet). Carbon NMR spectra were recorded with broad band decoupling and assigned using DEPT experiments. Coupling constants (J) are quoted in Hertz. Melting points were carried out on a Gallenkamp melting point apparatus. Infrared spectra were recorded on an ATI Mattson Genesis FT-IR spectrometer. Electrospray high and low resonance mass spectra were recorded at room temperature on a Bruker Daltronics micrOTOF spectrometer.

5.2 Synthetic Procedures

5.2.1 General Procedures

General Procedure A: Hydrogenation

10% Pd/C or 10% Pd(OH)$_2$/C (0.01-0.03 eq) was added to a stirred solution of the alkene (0.23-6.07 mmol, 1.0 eq) in MeOH (5-50 mL) at rt. The reaction flask was evacuated under reduced pressure and back-filled with Ar three times. Then, the reaction flask was evacuated under reduced pressure and back-filled with H$_2$ three times. After the final evacuation, H$_2$ was charged and the reaction mixture was stirred vigorously under a H$_2$ balloon at rt for 2-112 h. Then, the solids were removed by filtration through Celite and the solvent was evaporated under reduced pressure to give the crude product.

General Procedure B: Formation of enol triflates

*i*Pr$_2$NEt (5.0 eq) was added dropwise to a stirred solution of the *β*-ketoester (1.41-21.6 mmol, 1.0 eq) in CH$_2$Cl$_2$ (25-200 mL) at –78 °C under Ar. The resulting solution was stirred at –78 °C for 10 min and then trifluoromethanesulfonic anhydride (1.2 eq) was added dropwise over 15 min. The resulting solution was allowed to warm to rt and stirred at rt for 16 h. H$_2$O (25-100 mL) and then 5% citric acid$_{(aq)}$ (25-200 mL) were added and the aqueous layer was extracted with CH$_2$Cl$_2$ (3 x 25-100 mL). The combined organic extracts were dried (Na$_2$SO$_4$) and evaporated under reduced pressure to give the crude product.

General Procedure C: Suzuki-Miyaura Coupling

K$_2$CO$_3$ (2.5 eq) was added portionwise to a stirred mixture of the enol triflate (0.37-7.29 mmol, 1.0 eq) and aryl boronic acid (1.5 eq) in THF (4-40 mL) and H$_2$O (1-10 mL) at rt. The reaction flask was evacuated under reduced pressure and back-filled with Ar three times. Then, Pd(PPh$_3$)$_4$ (0.05-0.1 eq) was added and the resulting mixture was stirred and heated at 65 °C for 16 h. The mixture was allowed to cool to rt and H$_2$O (10-100 mL) was added. The aqueous layer was extracted with EtOAc (3 x 10-100 mL). The combined organic extracts were dried (Na$_2$SO$_4$) and evaporated under reduced pressure to give the crude product.

5.2.2 Synthetic Procedures for Chapter 2

N-Benzyl-1-(trimethylsilyl)methanamine 85

$$Me_3Si \diagdown \overset{\underset{\displaystyle H}{|}}{N} \diagup Ph$$

85
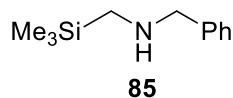
Benzylamine (3.74 mL, 34.2 mmol, 2.1 eq) was added dropwise to a stirred solution of (chloromethyl)trimethylsilane (2.28 mL, 16.3 mmol, 1 eq) in DMSO (50 mL) at rt. The resulting solution was stirred and heated at 80 °C for 16 h. After being allowed to cool to rt, water (100 mL) was added and the mixture was extracted with EtOAc (3 × 100 mL). The combined organic extracts were washed with 1% $Na_2CO_{3(aq)}$ (50 mL), dried ($MgSO_4$) and evaporated under reduced pressure to give the crude product.[58] Purification by flash column chromatography on silica with 400:100:1 hexane-EtOAc-Et_3N as eluent gave amine **85** (2.44 g, 77%) as a colourless oil, R_F (400:100:1 hexane-EtOAc-Et_3N) 0.21; ^{1}H NMR (400 MHz, $CDCl_3$) δ 7.39-7.20 (m, 5H, Ph), 3.79 (s, 2H, NCH_2Ph), 2.05 (s, 2H, NCH_2SiMe_3), 1.20 (br s, 1H, NH), 0.03 (s, 9H, $SiMe_3$); ^{13}C NMR (100.6 MHz, $CDCl_3$) 140.8 (*ipso*-Ph), 128.5 (Ph), 128.3 (Ph), 127.0 (Ph), 58.3 (NCH_2Ph), 39.7 (NCH_2SiMe_3), –2.4 ($SiMe_3$); MS (ESI) *m/z* 194 (M + H)[+]. Spectroscopic data are consistent with those reported in the literature.[58]

Lab Book Reference: TD 1/33

N-Benzyl-*N*-methoxymethyl-1-(trimethylsilyl)methanamine 25

$$Me_3Si \diagdown \overset{\underset{\displaystyle Bn}{|}}{N} \diagup OMe$$

25
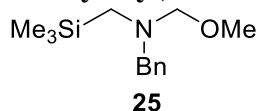
MeOH (0.26 mL, 6.33 mmol, 1.1 eq) was added dropwise to a stirred mixture of 37% aqueous formaldehyde (0.47 mL, 6.33 mmol, 1.1 eq) and amine **85** (1.11 g, 5.76 mmol, 1 eq) at 0 °C. The resulting mixture was stirred at 0 °C for 30 min and then allowed to warm to rt over 4 h. K_2CO_3 (500 mg) was added and the organic layer was decanted. K_2CO_3 (50 mg) was added and the organic layer was decanted. The inorganic residue was washed with Et_2O (2 x 10 mL) and the combined decanted layers and washings were evaporated under reduced pressure to give crude methoxyamine **25** (1.08 g, 79%) as a yellow oil, ^{1}H NMR (400 MHz, $CDCl_3$) δ 7.35-7.20 (m, 5H, Ph), 4.00 (s, 2H, NCH_2O), 3.76 (s, 2H, NCH_2Ph), 3.24 (s, 3H, OMe), 2.18 (s, 2H, NCH_2SiMe_3), 0.05 (s, 9H, $SiMe_3$); [13]C (100.6 MHz, $CDCl_3$) δ 139.7 (*ipso*-Ph), 128.9 (Ph), 128.2 (Ph), 126.7 (Ph), 88.4 (NCH_2O), 59.7 (NCH_2Ph), 55.4 (OMe), 42.9 (NCH_2SiMe_3), –1.5 ($SiMe_3$). Spectroscopic data are consistent with those

reported in the literature.[127] The crude methoxyamine **25** was sufficiently pure for use without further purification.

Lab Book: TD 1/7

Methyl 1-benzyl-4-methyl-2,5-dihydro-1H-pyrrole-3-carboxylate 83
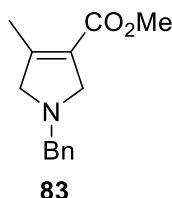
Methoxyamine **25** (500 mg, 2.1 mmol, 1 eq) was added dropwise to a stirred solution of methyl 2-butynoate (0.315 mL, 3.15 mmol, 1.5 eq) and TFA (0.015 mL, 0.21 mmol, 0.1 eq) in THF (25 mL) at 0 °C. The resulting solution was allowed to warm to rt and stirred at rt for 16 h. Then, the solvent was evaporated under reduced pressure and EtOAc (25 mL) was added. The solution was washed with saturated $NaHCO_{3(aq)}$ (2 x 20 mL) and brine (20 mL), dried (Na_2SO_4) and evaporated under reduced pressure to give the crude product. Purification by flash column chromatography on silica with 80:20 hexane-EtOAc as eluent gave dihydropyrrole **83** (117 mg, 24%) as a yellow oil, R_F (80:20 hexane-EtOAc) 0.17; IR (ATR) 2789, 1714 (C=O), 1452, 1246, 853, 696 cm^{-1}; ^{1}H NMR (400 MHz, CDCl$_3$) δ 7.32-7.20 (m, 5H, Ph), 3.75 (s, 2H, NCH$_2$Ph), 3.69 (s, 3H, OMe), 3.67 (tq, J = 4.0, 2.0 Hz, 2H, NCH$_2$), 3.54 (tq, J = 4.0, 1.0 Hz, 2H, NCH$_2$), 2.07 (tt, J = 2.0, 1.0 Hz, 3H, CMe); ^{13}C (100.6 MHz, CDCl$_3$) δ 165.0 (C=O), 152.4 (=CMe), 139.0 (*ipso*-Ph), 129.0 (=CCO$_2$Me), 128.7 (Ph), 128.5 (Ph), 127.2 (Ph), 65.9 (NCH$_2$Ph), 60.12 (NCH$_2$), 60.10 (NCH$_2$), 51.1 (OMe), 14.1 (CMe); MS (ESI) *m/z* 232 [(M + H)$^+$, 100]; HRMS (ESI) *m/z* calcd for C$_{14}$H$_{17}$NO$_2$ (M + H)$^+$ 232.1330, found 232.1332 (+0.7 ppm error).

Lab Book Reference: TD 1/43

Smaller Scale Procedure

Methoxyamine **25** (100 mg, 0.42 mmol, 1 eq) was added dropwise to a stirred solution of methyl 2-butynoate (0.063 mL, 0.63 mmol, 1.5 eq) and TFA (0.003 mL, 0.04 mmol, 0.1 eq) in THF (5 mL) at 0 °C. The resulting solution was allowed to warm to rt and stirred at rt for 16 h. Then, the solvent was evaporated under reduced pressure and EtOAc (10 mL) was added. The solution was washed with saturated $NaHCO_{3(aq)}$ (2 x 10 mL) and brine (10 mL), dried (Na_2SO_4) and evaporated under reduced pressure to give the crude product.

Purification by flash column chromatography on silica with 80:20 hexane-EtOAc as eluent gave dihydropyrrole **83** (47 mg, 48%) as a yellow oil

Lab Book Reference: TD 1/23

Ethyl 1-benzyl-4-methyl-2,5-dihydro-1H-pyrrole-3-carboxylate 88
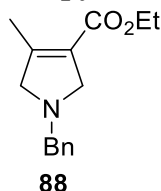
Procedure using TFA as Activating Agent

Methoxyamine **25** (200 mg, 0.84 mmol, 1 eq) was added dropwise to a stirred solution of ethyl 2-butynoate (0.15 mL, 1.26 mmol, 1.5 eq) and TFA (0.006 mL, 0.08 mmol, 0.1 eq) in THF (10 mL) at 0 °C. The resulting solution was allowed to warm to rt and stirred at rt for 16 h. Then, the solvent was evaporated under reduced pressure and EtOAc (25 mL) was added. The solution was washed with saturated $NaHCO_{3(aq)}$ (2 x 20 mL) and brine (20 mL), dried (Na_2SO_4) and evaporated under reduced pressure to give the crude product. Purification by flash column chromatography on silica with 80:20 hexane-EtOAc as eluent gave dihydropyrrole **88** (116 mg, 56%) as a yellow oil, R_F (80:20 hexane-EtOAc) 0.13; ^{1}H NMR (400 MHz, CDCl$_3$) δ 7.36-7.22 (m, 5H, Ph), 4.16 (q, J = 7.0 Hz, 2H, OCH$_2$), 3.76 (s, 2H, NCH$_2$Ph), 3.71-3.66 (m, 2H, NCH$_2$), 3.55-3.52 (m, 2H, NCH$_2$), 2.07-2.04 (m, 3H, Me), 1.25 (t, J = 7.0 Hz, 3H, CH$_2$*Me*); ^{13}C NMR (100.6 MHz, CDCl$_3$) δ 165.4 (C=O), 151.8 (=*C*Me), 137.0 (*ipso*-Ph), 128.9 (=*C*CO$_2$Et), 128.7 (Ph), 128.5 (Ph), 127.3 (Ph), 65.8 (NCH$_2$), 60.1 (NCH$_2$Ph), 59.9 (NCH$_2$), 59.3 (OCH$_2$), 14.6 (CH$_2$*Me*), 14.1 (=C*Me*). Spectroscopic data are consistent with those reported in the literature.[76]

Lab Book Reference: TD 1/13

Procedure using Fluoride as Activating Agent

A solution of DMAP (0.24 mg, 0.002 mmol, 0.01 eq) in THF (1 mL) was added dropwise to a stirred solution of benzoyl fluoride (25 mg, 0.2 mmol, 1 eq), methoxyamine **25** (52 mg, 0.22 mmol, 1.1 eq) and ethyl propiolate (22 mg, 0.2 mmol, 1 eq) in THF (3 mL) at 0 °C. The resulting solution was stirred at 0 °C for 30 min. After being allowed to warm to rt, the solution was stirred at rt for 6 h. The solvent was evaporated under reduced pressure to give the crude product which contained a complex mixture of compounds (by ^{1}H NMR spectroscopy) that were inseparable by attempted flash column chromatography.

Lab Book Reference: TD 1/10

Ethyl 1-benzyl-4-phenyl-2,5-dihydro-1H-pyrrole-3-carboxylate 90

90
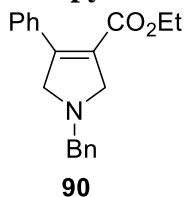
A solution of DMAP (0.3 mg, 0.002 mmol, 0.01 eq) in THF (1 mL) was added dropwise to a stirred solution of benzoyl fluoride (25 mg, 0.2 mmol, 1 eq), methoxyamine **25** (52 mg, 0.22 mmol, 1.1 eq) and ethyl phenylpropiolate (35 mg, 0.2 mmol, 1 eq) in THF (3 mL) at 0 °C. The resulting solution was stirred at 0 °C for 30 min. After being allowed to warm to rt, the solution was stirred at rt for 6 h. The solvent was evaporated under reduced pressure to give the crude product. Purification by flash column chromatography on silica with 75:25 hexane-EtOAc as eluent gave dihydropyrrole **90** (53 mg, 86%) as a colourless oil, R_F (75:25 hexane-EtOAc) 0.30; ^{1}H NMR (400 MHz, CDCl$_3$) δ 7.48-7.16 (m, 10H, Ph), 4.10 (q, J = 7.0 Hz, 2H, OCH$_2$), 3.91 (br s, 4H, NCH$_2$), 3.85 (s, 2H, NCH$_2$Ph), 1.14 (t, J = 7.0 Hz, 3H, Me); ^{13}C NMR (100.6 MHz, CDCl$_3$) δ 164.7 (C=O, CO$_2$Et), 150.5 (=CPh), 136.5 (*ipso*-Ph), 134.8 (*ipso*-Ph), 129.4 (Ph), 129.1 (Ph), 128.8 (=CCO$_2$Me or Ph), 128.6 (=CCO$_2$Me or Ph), 128.2 (Ph), 127.8 (Ph), 127.5 (Ph), 65.4 (NCH$_2$), 61.5 (NCH$_2$), 60.1 (NCH$_2$Ph), 59.6 (OCH$_2$), 14.4 (Me). Spectroscopic data are consistent with those reported in the literature.[128] Lab Book Reference: TD 1/8

Methyl 1-benzylpyrrolidine-2-carboxylate (*S*)-94

(*S*)-**94**
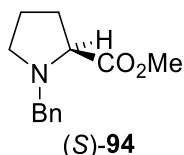
Acetyl chloride (1.90 mL, 26.07 mmol, 3 eq) was added dropwise to a stirred solution of (*S*)-proline (1.00 g, 8.69 mmol, 1 eq) in MeOH (20 mL) at rt under Ar. The resulting solution was stirred at rt for 16 h. The solvent was then evaporated under reduced pressure to give the intermediate crude product as a colourless oil. The intermediate crude product was dissolved in MeCN (20 mL) at rt and benzyl bromide (1.30 mL, 10.43 mmol, 1.2 eq) and Et$_3$N (2.90 mL, 26.07 mmol, 3 eq) were added sequentially. The resulting suspension was stirred at rt for 12 h. The solvent was evaporated under reduced pressure. Saturated NH$_4$Cl$_{(aq)}$ (50 mL) and Et$_2$O (50 mL) were added to the residue and the two layers were separated. The aqueous layer was extracted with Et$_2$O (3 x 50 mL) and the combined organic extracts were dried (MgSO$_4$) and evaporated under reduced pressure to give the crude product. Purification

by flash column chromatography on silica with 92:8 hexane-EtOAc as eluent gave *N*-benzyl pyrrolidine (*S*)-**94** (1.04 g, 55%) as a colourless oil, R_F (90:10 hexane-EtOAc) 0.15; $[\alpha]_D$ – 70.7 (*c* 1.00, MeOH) [lit.,[129] –61.4 (*c* 1.15, MeOH)]; ^{1}H NMR (400 MHz, CDCl$_3$) δ 7.35-7.20 (m, 5H, Ph), 3.87 (d, *J* = 13.0 Hz, 1H, NCHPh), 3.63 (s, 3H, OMe), 3.56 (d, *J* = 13.0 Hz, 1H, NCHPh), 3.23 (dd, *J* = 9.0, 6.5 Hz, 1H, NC*H*CO$_2$Me), 3.07-3.00 (m, 1H, NCH), 2.42-2.32 (m, 1H, NCH), 2.17-2.05 (m, 1H, CH), 2.00-1.81 (m, 2H, CH), 1.80-1.71 (m, 1H, CH); ^{13}C NMR (100.6 MHz, CDCl$_3$) δ 174.7 (C=O), 138.3 (*ipso*-Ph), 129.3 (Ph), 128.3 (Ph), 127.2 (Ph), 65.4 (N*C*HCO$_2$Me), 58.9 (NCH$_2$Ph), 53.4 (NCH$_2$), 51.8 (OMe), 29.5 (CH$_2$), 23.1 (CH$_2$). Spectroscopic data are consistent with those reported in the literature.[129]

Lab Book Ref: TD 1/55

1-*tert*-Butyl-2-methyl pyrrolidine-1,2-dicarboxylate (*S*)-96

(*S*)-**96**
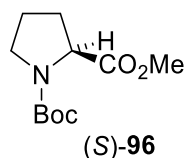
20% Pd(OH)$_2$/C (20 mg, 0.03 mmol) was added to a stirred solution of pyrrolidine (*S*)-**94** (237 mg, 1.06 mmol, 1 eq) and ammonium formate (336 mg, 5.31 mmol, 5 eq) in MeOH (25 mL) at rt. The resulting solution was stirred and heated at 60 ºC for 2 h. After being allowed to cool to rt, the solids were removed by filtration through Celite. Di-*tert*-butyl dicarbonate (231 mg, 1.06 mmol, 1 eq), Et$_3$N (0.888 mL, 6.38 mmol, 6 eq) and DMAP (13 mg, 0.11 mmol, 0.1 eq) were added to the filtrate at rt. The resulting solution was stirred at rt for 16 h. Then, the solvent was evaporated under reduced pressure to give the crude product. Purification by flash column chromatography with 80:20 hexane-EtOAc as solvent gave pyrrolidine (*S*)-**96** (242 mg, 99%) as a yellow oil, R_F (80:20 hexane-EtOAc) 0.27; $[\alpha]_D$ –47.3 (*c* 1.00, CH$_2$Cl$_2$) [lit. [130], –44.8 (*c* 1.05, CH$_2$Cl$_2$)]; ^{1}H NMR (400 MHz, CDCl$_3$) δ (60:40 mixture of rotamers) 4.29 (dd, *J* = 8.5, 3.5 Hz, 0.4H, C*H*CO$_2$Me), 4.19 (dd, *J* = 8.5, 4.0 Hz, 0.6H, C*H*CO$_2$Me), 3.70 (s, 1.2H, OMe), 3.69 (s, 1.8H, OMe) 3.59-3.29 (m, 2H, NCH), 2.27-2.09 (m, 1H, CH), 1.99-1.73 (m, 3H, CH), 1.43 (s, 3.6H, CMe$_3$), 1.38 (s, 5.4H, CMe$_3$); ^{13}C NMR (100.6 MHz, CDCl$_3$) δ 173.9 (C=O, CO$_2$Me), 173.6 (C=O, CO$_2$Me), 154.5 (C=O, Boc), 153.9 (C=O, Boc), 80.0 (*C*Me$_3$), 79.9 (*C*Me$_3$), 59.2 (*C*HCO$_2$Me), 58.8 (*C*HCO$_2$Me), 52.2 (OMe), 52.0 (OMe), 46.6 (NCH$_2$), 46.4 (NCH$_2$), 31.0 (CH$_2$), 30.0 (CH$_2$), 28.5 (C*Me*$_3$), 28.4 (C*Me*$_3$), 24.4 (CH$_2$), 23.8 (CH$_2$). Spectroscopic data are consistent with those reported in the literature.[32]

Lab Book Reference: TD 1/70

1-*tert*-Butyl-3-methyl 4-methylpyrrolidine-1,3-dicarboxylate *cis*-97

cis-**97**
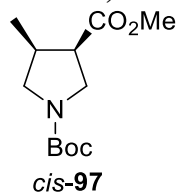
20% Pd(OH)$_2$/C (18 mg, 0.03 mmol) was added to a stirred solution of dihydropyrrole **83** (200 mg, 0.87 mmol, 1 eq) and ammonium formate (273 mg, 5.31 mmol, 5 eq) in MeOH (10 mL) at rt. The resulting solution was stirred and heated at 60 ºC for 2 h. After being allowed to cool to rt, the solids were removed by filtration through Celite. Di-*tert*-butyl dicarbonate (189 mg, 0.87 mmol, 1 eq), Et$_3$N (0.72 mL, 5.19 mmol, 6 eq) and DMAP (11 mg, 0.09 mmol, 0.1 eq) were added to the filtrate at rt. The resulting solution was stirred at rt for 16 h. Then, the solvent was evaporated under reduced pressure to give the crude product. Purification by flash column chromatography with 80:20 hexane-EtOAc as solvent gave pyrrolidine *cis*-**97** (153 mg) as a yellow oil, which contained some dihydropyrrole **83** by mass spectrometry. The mixture was then dissolved in MeOH (10 mL) and 5% Pd/C (15 mg, 0.01 mmol) was added to the stirred solution. The reaction flask was evacuated under reduced pressure and back-filled with Ar three times. After the final evacuation, H$_2$ was charged and the reaction mixture was stirred vigorously under an H$_2$ balloon at rt for 16 h. The solids were removed by filtration through Celite and the filtrate was evaporated under reduced pressure to give crude pyrrolidine *cis*-**97** (145 mg, 77% over 2 steps) as a yellow oil, R_F (80:20 hexane-EtOAc) 0.31; IR (ATR) 2974, 1731 (C=O, CO$_2$Me), 1693 (C=O, Boc), 1400, 1171 cm^{-1}; ^{1}H NMR (400 MHz, CDCl$_3$) (50:50 mixture of rotamers) δ 3.68 (s, 1.5H, OMe), 3.67 (s, 1.5H, OMe), 3.66-3.56 (m, 1H, C*H*CO$_2$Me), 3.52-3.42 (m, 2H, NCH), 3.20-3.13 (m, 0.5H, NCH), 3.11-2.97 (m, 1.5H, NCH), 2.58-2.46 (m, 1H, C*H*Me), 1.43 (s, 9H, C*Me*$_3$), 0.96 (d, J = 6.5 Hz, 1.5H, Me), 0.93 (d, J = 7.0 Hz, 1.5H, Me); ^{13}C NMR (100.6 MHz, CDCl$_3$) (rotamers) δ 172.8 (C=O, CO$_2$Me), 172.6 (C=O, CO$_2$Me), 154.6 (C=O, Boc), 79.5 (*C*Me$_3$), 79.4 (*C*Me$_3$), 52.3 (NCH$_2$), 52.1 (NCH$_2$), 51.73 (OMe), 51.68 (OMe), 47.5 (NCH$_2$), 46.9 (NCH$_2$), 46.7 (*C*HCO$_2$Me), 46.6 (*C*HCO$_2$Me), 35.8 (*C*HMe), 34.8 (*C*HMe), 28.59 (C*Me*$_3$), 28.57 (C*Me*$_3$), 14.5 (Me), 14.3 (Me); MS (ESI) *m/z* 266 [(M + Na)$^+$, 100]; HRMS (ESI) *m/z* calcd for C$_{12}$H$_{21}$NO$_4$ (M + Na)$^+$ 266.1363, found 266.1367 (–1.6 ppm error).

Lab Book Ref: TD 1/75

3-Methyl 4-methylpyrrolidine-3-carboxylate hydrochloride *cis*-42•HCl

cis-**42**·HCl
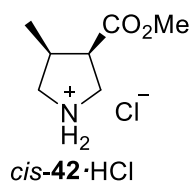
HCl (0.206 mL of a 2M solution in Et$_2$O, 0.411 mmol, eq) was added dropwise to a stirred solution of *N*-Boc pyrrolidine *cis*-**97** (20 mg, 0.08 mmol, 1 eq) in CH$_2$Cl$_2$ (2 mL) at rt under Ar. The resulting mixture was stirred at rt for 16 h. The solvent was evaporated under reduced pressure to give pyrrolidine *cis*-**42**•HCl (14 mg, 97%) as an orange oil, IR (ATR) 2964, 1730 (C=O), 1666, 1384, 733 cm^{-1}; ^{1}H NMR (400 MHz, d$_4$-MeOH) δ 3.69 (s, 3H, OMe), 3.59-3.51 (br s, 1H, NCH or C*H*CO$_2$Me), 3.47-3.37 (br s, 2H, NCH or C*H*CO$_2$Me), 2.99-2.89 (br s, 1H, NCH or C*H*CO$_2$Me), 2.76-2.62 (br s, 1H, NCH or C*H*CO$_2$Me), 2.13-1.96 (br s, 1H, C*H*Me), 1.00 (br s, 3H, CH*Me*); MS (ESI) *m/z* 144 [M$^+$, 100]; HRMS (ESI) *m/z* calcd for C$_7$H$_{14}$NO$_2$ (M + H)$^+$ 144.1019, found 144.1021 (–1.5 ppm error).

Lab Book Reference: TD 1/81

Methyl 1,4-dimethylpyrrolidine-3-carboxylate acetate *cis*-43•AcOH

cis-**43**·AcOH
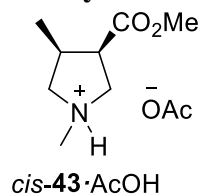
37% aqueous formaldehyde (1.534 mL, 20.6 mmol, 10 eq) was added dropwise to a stirred suspension of *cis*-**42** (295 mg, 2.06 mmol, 1 eq), NaBH(OAc)$_3$ (1.31 g, 6.18, mmol, 3 eq) and MgSO$_4$ (1.53 g) in 3:1 CH$_2$Cl$_2$–AcOH (20 mL) at rt under Ar. The resulting mixture was stirred at rt for 1 h. The solids were removed by filtration and NaHCO$_{3(aq)}$ was added to the filtrate until the mixture reached pH 9. The aqueous phase was extracted with CH$_2$Cl$_2$ (3 x 20 mL) and the combined organic extracts were washed with brine (20 mL) and dried (Na$_2$SO$_4$). AcOH (0.118 mL, 1 mmol, 1 eq) was added dropwise to the filtrate which was stirred at rt for 30 min. The solvent was evaporated under reduced pressure to give pyrrolidine *cis*-**43**•AcOH (165 mg, 76%) as a yellow oil, IR (ATR) 2958, 1720 (C=O), 1379, 1251, 1214 cm^{-1}; ^{1}H NMR (400 MHz, d$_4$-MeOH) δ 3.73 (s, 3H, OMe), 3.57-3.54 (m, 1H, C*H*CO$_2$Me), 3.51-3.44 (m, 1H, NCH), 3.29-3.27 (m, 3H, NCH, NCH, NCH), 2.89 (s, 3H, NMe), 2.83-2.77 (m, 1H, C*H*Me), 1.96-1.90 (m, 3H, MeCO$_2^-$) 1.02 (d, *J* = 7.0 Hz, 3H, CH*Me*); ^{13}C NMR (100.6 MHz, d$_4$-MeOH) δ 175.3 (C=O, MeCO$_2^-$), 172.5 (C=O, CO$_2$Me), 60.57 (NCH$_2$), 60.54 (NCH$_2$), 57.1 (*C*CO$_2$Me), 51.2 (OMe), 41.1 (NMe), 40.3 (*C*Me), 20.3

(Me, MeCO$_2^-$), 12.4 (C*Me*); MS (ESI) *m/z* 158 [M$^+$, 100]; HRMS (ESI) *m/z* calcd for C$_8$H$_{16}$NO$_2$ 158.1176 M$^+$, found 158.1179 (–1.8 ppm error).

Lab Book Reference: TD 2/30

N-*tert*-Butyloxycarbonyl glycine methyl ester 101

101
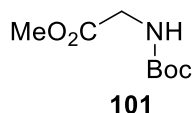
A solution of NaHCO$_3$ (334 mg, 3.98 mmol, 1 eq) in H$_2$O (5 mL) was added to a stirred suspension of glycine methyl ester hydrochloride (500 mg, 3.98 mmol, 1 eq) in CHCl$_3$ (5 mL) at rt. Then, a solution of di-*tert*-butyl dicarbonate (869 mg, 3.98 mmol, 1 eq) in CHCl$_3$ (2 mL) was added, followed by the addition of NaCl (814 mg, 13.9 mmol, 3.5 eq). The resulting mixture was stirred vigorously and heated at reflux for 1.5 h. After being allowed to cool to rt, the two layers were separated and the aqueous phase was extracted with CHCl$_3$ (2 x 10 mL). The combined organic extracts were dried (Na$_2$SO$_4$) and evaporated under reduced pressure to give crude *N*-Boc glycine **101** (745 mg, 99%) as a colourless oil, ^{1}H NMR (400 MHz, CDCl$_3$) δ 5.00 (br s, 1H, NH), 3.90 (d, *J* = 5.5 Hz, 2H, CH$_2$), 3.73 (s, 3H, OMe), 1.43 (s, 9H, CMe$_3$); ^{13}C NMR (100.6 MHz, CDCl$_3$) δ 170.9 (C=O, CO$_2$Me), 155.8 (C=O, Boc), 80.1 (*C*Me$_3$), 52.3 (OMe), 42.4 (NCH$_2$), 28.4 (C*Me$_3$*). Spectroscopic data are consistent with those reported in the literature.[131] The crude *N*-Boc glycine **101** was sufficiently pure for use without further purification.

Lab Book: TD 1/63

1-*tert*-Butyl-4-methyl 3-oxopyrrolidine-1,4-dicarboxylate 100

100   **100a**
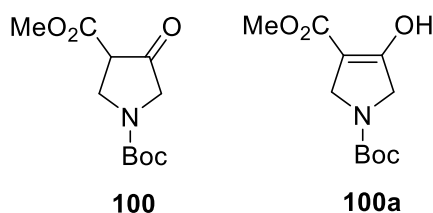
Methyl acrylate (0.44 mL, 4.89 mmol, 1 eq) was added dropwise to a stirred solution of dry *t*-BuOK (604 mg, 5.38 mmol, 1.1 eq) and *N*-Boc glycine **101** (926 mg, 4.89 mmol, 1 eq) in THF at 0 °C. The resulting solution was stirred at rt for 16 h and then the solvent was evaporated under reduced pressure. The residue was dissolved in CH$_2$Cl$_2$ (50 mL) and 1 M HCl$_{(aq)}$ (10 mL) was added. The two layers were separated and the aqueous layer was extracted with CH$_2$Cl$_2$ (3 x 20 mL). The combined organic layers were dried (Na$_2$SO$_4$) and

evaporated under reduced pressure to give the crude product. Purification by flash column chromatography on silica with 80:20 hexane-EtOAc as eluent gave oxopyrrolidine **100** (830 mg, 90%) as a red oil, R_F (80:20 hexane-EtOAc) 0.35; ^{1}H NMR (400 MHz, CDCl$_3$) (50:50 mixture of keto/enol tautomers) (rotamers) δ 10.01-9.99 (m, 0.5 H, enol OH), 4.25-4.13 (m, 1H), 4.13-4.01 (m, 1.5H), 3.99-3.82 (m, 1.5H), 3.77 (s, 3H, OMe), 3.69-3.56 (m, 0.5H), 1.47 (s, 4.5H, CMe$_3$), 1.46 (s, 4.5H, CMe$_3$) ; ^{13}C NMR (100.6 MHz, CDCl$_3$) δ 171.9 (C=O, CO$_2$Me), 167.2 (C=O, CO$_2$Me), 154.1 (C=O, Boc), 97.2 (=C), 81.0 (*C*Me$_3$), 80.2 (*C*Me$_3$), 53.1 (OMe), 51.60 (OMe or CH$_2$), 51.55 (OMe or CH$_2$), 51.4 (CH$_2$), 51.1 (CH$_2$), 48.8 (CH$_2$), 48.4 (CH$_2$), 28.5 (C*Me*$_3$), 28.4 (C*Me*$_3$). Spectroscopic data are consistent with those reported in the literature.[79]

Lab Book Reference: TD 1/94

1-*tert*-Butyl-4-methyl 3-trifluoromethylsulfonyl-2,5-dihydro-1H-pyrrole-1,4-dicarboxylate 99

99
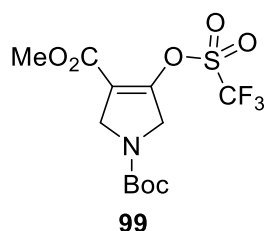
Using general procedure **B**, β-ketoester **100** (5.0 g, 19.4 mmol, 1.0 eq), *i*Pr$_2$NEt (16.9 mL, 97.2 mmol, 5.0 eq) and trifluoromethanesulfonic anhydride (3.92 mL, 23.3 mmol, 1.2 eq) in CH$_2$Cl$_2$ (200 mL) gave the crude product. Purification by flash column chromatography on silica with 80:20 hexane-EtOAc as eluent gave enol triflate **99** (5.18 g, 71%) as a brown solid, mp 59-62 °C; R_F (80:20 hexane-EtOAc) 0.30; IR (ATR) 1732 (C=O, CO$_2$Me), 1709 (C=O, Boc), 1682 (C=C), 1211, 1111 cm^{-1}; ^{1}H NMR (400 MHz, CDCl$_3$) δ 4.40-4.32 (m, 4H, NCH), 3.81 (s, 3H, OMe), 1.46 (s, 9H, CMe$_3$); ^{13}C NMR (100.6 MHz, CDCl$_3$) (rotamers) δ 160.5 (C=O, CO$_2$Me), 160.4 (C=O, CO$_2$Me), 153.5 (C=O, Boc or =CO), 153.3 (C=O, Boc or =CO), 147.5 (C=O, Boc or =CO), 147.0 (C=O, Boc or =CO), 119.4 (=C), 118.4 (q, *J* = 320 Hz, CF$_3$), 81.1 (*C*Me$_3$), 52.4 (OMe), 51.4 (NCH$_2$), 51.2 (NCH$_2$), 50.7 (NCH$_2$), 50.3 (NCH$_2$), 28.4 (C*Me*$_3$); MS (ESI) *m/z* 398 [(M + Na)$^+$, 100]; HRMS (ESI) *m/z* calcd for C$_{12}$H$_{16}$F$_3$NO$_7$S (M + Na)$^+$ 398.0492, found 398.0497 (–1.3 ppm error).

Lab Book Reference: TD 3/15

1-*tert*-Butyl-4-methyl 3-methyl-2,5-dihydro-1H-pyrrole-1,4-dicarboxylate 98 and 1-*tert*-Butyl-4-methyl 2,5-dihydro-1H-pyrrole-1,4-dicarboxylate 109
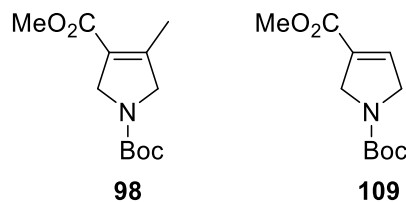
MeLi (0.309 mL of a 1.27 M solution in Et_2O, 0.39 mmol, 1.4 eq) was added dropwise to a stirred solution of CuCN (35 mg, 0.39 mmol, 1.4 eq) in Et_2O (1.5 mL) at –50 °C under Ar. The resulting solution was stirred at –50 °C for 30 min. Then, a solution of enol triflate **99** (100 mg, 0.28 mmol, 1.0 eq) in Et_2O (1.5 mL) pre-cooled to –50 °C was added dropwise. The resulting mixture was stirred at –50 °C for 30 min. Then, saturated $NH_4Cl_{(aq)}$ (5 mL) was added and the solids were removed by filtration through Celite. The resulting solution was extracted with EtOAc (3 x 10 mL) and the combined organic extracts were washed with H_2O (20 mL) and then brine (20 mL), dried (Na_2SO_4) and evaporated under reduced pressure to give an 80:20 mixture (by ^1H NMR spectroscopy) of dihydropyrrole **98** and dihydropyrrole **109**, ^1H NMR (400 MHz, $CDCl_3$) (rotamers) δ 6.77-6.70 (m, 0.2H, =CH), 4.35-4.16 (m, 4H, NCH), 3.79-3.74 (m, 3H, OMe), 2.14-2.12 (br m, 2.4H, CMe), 1.48 (br s, 9H, CMe_3). Purification by flash column chromatography on silica with 80:20 hexane-EtOAc as eluent gave no recoverable product.

Lab Book Reference: TD 3/33

1-*tert*-Butyl-4-methyl 3-methyl-2,5-dihydro-1H-pyrrole-1,4-dicarboxylate 98 and 1-*tert*-Butyl-4-methyl 3-methylpyrrolidine-1,4-dicarboxylate *cis*-97
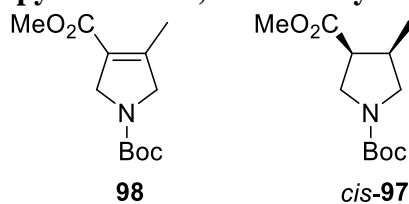
MeLi (0.309 mL of a 1.27 M solution in Et_2O, 1.17 mmol, 1.4 eq) was added dropwise to a stirred solution of CuCN (105 mg, 1.17 mmol, 1.4 eq) in Et_2O (5 mL) at –50 °C under Ar. The resulting solution was stirred at –50 °C for 30 min. Then, a solution of enol triflate **99** (300 mg, 0.84 mmol, 1.0 eq) in Et_2O (5 mL) pre-cooled to –50 °C was added dropwise. The resulting mixture was stirred at –50 °C for 30 min. Then, saturated $NH_4Cl_{(aq)}$ (20 mL) was added and the solids were removed by filtration through Celite. The resulting solution was extracted with EtOAc (3 x 20 mL) and the combined organic extracts were washed with H_2O (40 mL) and then brine (40 mL), dried (Na_2SO_4) and evaporated under reduced pressure to

give an 80:20 mixture (by ^{1}H NMR spectroscopy) of dihydropyrrole **98** and dihydropyrrole **109**. The mixture was dissolved in MeOH (10 mL) and 10% Pd/C (18 mg, 0.02 mmol, 0.02 eq) was added to the solution at rt. The reaction flask was evacuated under reduced pressure and back-filled with Ar three times. Then, the reaction flask was evacuated under reduced pressure and back-filled with H_2 three times. After the final evacuation, H_2 was charged and the reaction mixture was stirred vigorously under a H_2 balloon at rt for 16 h. Then, the solids were removed by filtration through Celite. The solvent was evaporated under reduced pressure to give the crude intermediate product, which showed no presence (by ^{1}H NMR spectroscopy) of desired dihydropyrrole *cis*-**97**. The mixture was dissolved in MeOH (10 mL) and 10% Pd(OH)$_2$/C (15 mg, 0.01 mmol, 0.01 eq) was added to the solution at rt. The reaction flask was evacuated under reduced pressure and back-filled with Ar three times. Then, the reaction flask was evacuated under reduced pressure and back-filled with H_2 three times. After the final evacuation, H_2 was charged and the reaction mixture was stirred vigorously under a H_2 balloon at rt for 16 h. Then, the solids were removed by filtration through Celite. The solvent was evaporated under reduced pressure to give a complex mixture of products including an 85:15 mixture (by ^{1}H NMR spectroscopy) of dihydropyrrole **98** and pyrrolidine *cis*-**97**

Lab Book Reference: TD 3/54

Dimethyl 1,2-dimethyl-5-oxopyrrolidine-4,4-dicarboxylate 145

$$\text{MeO}_2\text{C} \quad \text{CO}_2\text{Me}$$

145
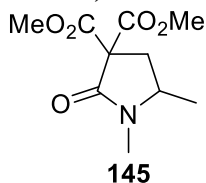
KHMDS (5.83 mL of a 0.5 M solution in THF, 2.92 mmol, 1.1 eq) was added dropwise to a stirred solution of 1,5-dimethylpyrrolidinone **140** (0.314 mL, 2.65 mmol, 1 eq) in THF (10 mL) at –78 ºC under Ar. The resulting solution was stirred at –78 ºC for 1 h. Then, methyl chloroformate (0.205 mL, 2.65 mmol, 1 eq) was added dropwise. The resulting solution was stirred at –78 ºC for 1 h. NaHCO$_{3(aq)}$ (10 mL) was added and the aqueous layer was extracted with EtOAc (5 x 10 mL). The combined organic extracts were washed with NaHCO$_{3(aq)}$ (20 mL) and brine (20 mL), dried (Na$_2$SO$_4$) and evaporated under reduced pressure to give the crude product. Purification by flash column chromatography with 50:50 EtOAc-hexane as eluent gave an inseparable 73:27 mixture of starting material **140** and double addition product **145** (122 mg, i.e. 55 mg (9%) of double addition product **145**), diagnostic ^{1}H NMR signals (400 MHz, CDCl$_3$) for **145**: δ 3.81 (s, 3H, OMe), 3.79 (s, 3H, OMe), 2.82 (s, 3H, NMe), 1.24 (d, J = 6.5 Hz, 3H, CH*Me*).

Lab Book Reference: TD 1/29

4-Methyl-2-methyl-5-oxopyrrolidine-1-carboxylate 149

149
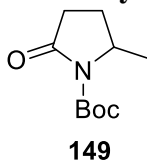
A solution of di-*tert*-butyl dicarbonate (4.84 g, 22.2 mmol, 1.1 eq) in CH$_2$Cl$_2$ (5 mL) was added dropwise to a stirred solution of 2-methyl-5-oxopyrrolidine **148** (2.00 g, 20.2 mmol, 1 eq), Et$_3$N (3.10 mL, 22.2 mmol, 1.1 eq) and DMAP (123 mg, 1.0 mmol, 0.05 eq) in CH$_2$Cl$_2$ (50 mL) at 0 ºC under Ar. The resulting solution was allowed to warm to rt and stirred at rt for 18 h. The solvent was evaporated under reduced pressure to give the crude product. Purification by flash column chromatography on silica with 50:50 EtOAc-hexane as eluent gave *N*-Boc pyrrolidinone **149** (3.44 g, 85%) as a yellow oil, R_F (80:20 hexane-EtOAc) 0.10; ^{1}H NMR (400 MHz, CDCl$_3$) δ 4.22 (dqd, J = 8.5, 6.5, 2.0 Hz, 1H, NC*H*Me), 2.58 (ddd, J = 17.5, 11.0, 9.0 Hz, 1H, CHCO), 2.40 (ddd, J = 17.5, 9.5, 3.0 Hz, 1H, CHCO), 2.21-2.09 (m, 1H, CH), 1.69-1.53 (m, 1H, CH), 1.50 (s, 9H, CMe$_3$), 1.30 (d, J = 6.5 Hz, 3H, CH*Me*); ^{13}C NMR (100.6 MHz, CDCl$_3$) δ 174.3 (C=O, NCO), 150.0 (C=O, Boc), 82.7 (*C*Me$_3$), 54.1

(NCH), 31.4 (*CH*$_2$CO), 28.1 (C*Me*$_3$), 25.2 (CH$_2$), 20.3 (Me). Spectroscopic data are consistent with those reported in the literature.[132]

Lab Book Ref: TD 1/41

1-*tert*-Butyl-4-methyl-2-methyl-5-oxopyrrolidine-1,4-dicarboxylate 150

150
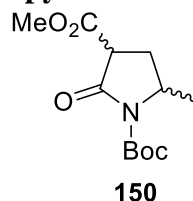
For Procedure using LHMDS

A solution of pyrrolidinone **149** (2.465 g, 12.4 mmol, 1 eq) in THF (20 mL) was added dropwise to a stirred solution of LHMDS (26 mL of a 1 M solution in THF, 26.0 mmol, 2.1 eq) at –78 °C under Ar. The resulting solution was stirred at –78 °C for 10 min. Then, methyl chloroformate (1.05 mL, 13.6 mmol, 1.1 eq) was added dropwise. The resulting solution was stirred at –78 °C for 10 min. Then, 1 M HCl$_{(aq)}$ was added dropwise until pH 1 was reached and the mixture was allowed to warm to rt. The two layers were separated and the aqueous phase was extracted with EtOAc (3 x 50 mL). The combined organic extracts were dried (Na$_2$SO$_4$) and evaporated under reduced pressure to give the crude product. Purification by flash column chromatography on silica with 75:25 hexane-EtOAc as eluent gave a 67:33 mixture (by ^{1}H NMR spectroscopy) of diastereomeric pyrrolidines **150** (2.865 g, 90%) as a yellow oil, R_F (75:25 hexane-EtOAc) 0.20; IR (ATR) 2980, 1785 (C=O), 1731 (C=O), 1718 (C=O), 1295, 1149 cm^{-1}; ^{1}H NMR (400 MHz, CDCl$_3$) δ 4.35-4.25 (m, 0.67H, NC*H*Me), 4.20-4.13 (m, 0.33H, NC*H*Me), 3.79-3.74 (m, 3H, OMe), 3.68-3.61 (m, 0.67H, C*H*CO$_2$Me), 3.54-3.48 (m, 0.33H, C*H*CO$_2$Me), 2.62-2.52 (m, 0.67H, CH), 2.47-2.36 (m, 0.33H, CH), 2.09-2.00 (m, 0.33H, CH), 1.92-1.85 (m, 0.67H, CH), 1.54-1.47 (m, 9H, CMe$_3$), 1.42-1.36 (m, 1H, CH*Me*), 1.33-1.27 (m, 2H, CH*Me*); ^{13}C NMR (100.6 MHz) δ 169.6 (C=O), 169.4 (C=O), 168.9 (C=O), 168.6 (C=O), 149.9 (C=O, Boc), 149.7 (C=O, Boc), 83.51 (*C*Me$_3$), 83.50 (*C*Me$_3$), 53.02 (OMe or C*H*CO$_2$Me), 52.97 (OMe or C*H*CO$_2$Me), 52.9 (OMe or C*H*CO$_2$Me), 52.3 (OMe or C*H*CO$_2$Me), 49.3 (*C*HMe), 48.7 (*C*HMe), 29.4 (CH$_2$), 28.5 (CH$_2$), 28.1 (C*Me*$_3$), 21.4 (Me), 20.4 (Me); MS (ESI) *m/z* 280 [(M + Na)$^+$, 100, (M + K)$^+$, 2]; HRMS (ESI) *m/z* calcd for C$_{12}$H$_{19}$NO$_5$ (M + Na)$^+$ 280.1155, found 280.1149 (+2.2 ppm error).

Lab Book Ref: TD 2/18/A

For Proceudre using KHMDS

KHMDS (2.10 mL of a 0.5 M solution in THF, 1.05 mmol, 1.1 eq) was added dropwise to a stirred solution of 4-methyl-2-methyl-5-oxopyrrolidine-1-carboxylate **149** (190 mg, 0.95 mmol, 1 eq) in THF (10 mL) at –78 ºC under Ar. The resulting solution was stirred at –78 ºC for 1 h. Then, methyl chloroformate (0.07 mL, 0.95 mmol, 1 eq) was added dropwise. The resulting solution was stirred at –78 ºC for 1 h. $NaHCO_{3(aq)}$ (10 mL) was added and the aqueous layer was extracted with EtOAc (5 x 10 mL). The combined organic extracts were washed with $NaHCO_{3(aq)}$ (20 mL) and brine (20 mL), dried (Na_2SO_4) and the solvent evaporated under reduced pressure to give the crude product. Purification by flash column chromatography with 75:25 hexane-EtOAc as eluent gave a 67:33 mixture (by ^{1}H NMR spectroscopy) of diastereomeric pyrrolidines **150** (77 mg, 33%) as a yellow oil.

Lab Book Reference: TD 1/39

N-*tert*-Butyloxycarbonyl alanine methyl ester 159

159
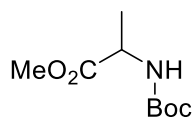
A solution of $NaHCO_3$ (301 mg, 3.58 mmol, 1 eq) in H_2O (5 mL) was added to a stirred suspension of glycine methyl ester hydrochloride (500 mg, 3.58 mmol, 1 eq) in $CHCl_3$ (5 mL) at rt. Then, a solution of di-*tert*-butyl dicarbonate (782 mg, 3.58 mmol, 1 eq) in $CHCl_3$ (2 mL) was added, followed by the addition of NaCl (732 mg, 12.53 mmol, 3.5 eq). The resulting mixture was stirred vigorously and heated at reflux for 1.5 h. After being allowed to cool to rt the organic phase was collected and the aqueous phase extracted with $CHCl_3$ (2 x 10 mL). The combined organic extracts were dried (Na_2SO_4) and evaporated under reduced pressure to give carbamate **159** (745 mg, quant.) as a colourless oil, ^{1}H NMR (400 MHz, $CDCl_3$) δ 5.03 (br s, 1H, NH), 4.37-4.23 (m, 1H, CH), 3.73 (s, 3H, CO_2Me), 1.43 (s, 9H, CMe_3), 1.36 (d, J = 7.0 Hz, 3H, CH*Me*); ^{13}C NMR (101.6 MHz, $CDCl_3$) δ 174.0 (C=O, CO_2Me), 146.8 (C=O, Boc), 85.3 (O*C*Me_3), 52.4 (OMe), 42.4 (NCH), 28.4 (C*Me_3*) 18.8 (CH*Me*). Spectroscopic data are consistent with those reported in the literature.[133] The crude carbamate **159** was sufficiently pure for use without further purification.

Lab Book Reference: TD 1/68

1-*tert*-Butyl-4-methyl-2-methyl-3-oxopyrrolidine-1,4-dicarboxylate 158

158
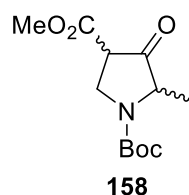
Methyl acrylate (0.876 mL, 9.74 mmol, 1 eq) was added dropwise to a stirred solution of dry *t*-BuOK (1.2 g, 10.72 mmol, 1.1 eq) and *N*-Boc alanine **159** (1.98 g, 9.74 mmol, 1 eq) in THF at 0 °C. The resulting solution was stirred at rt for 16 h and then the solvent was evaporated under reduced pressure. The residue was dissolved in CH_2Cl_2 (100 mL) and 1 M $HCl_{(aq)}$ (20 mL) was added. The two layers were separated and the aqueous layer was extracted with CH_2Cl_2 (3 x 20 mL). The combined organic extracts were dried (Na_2SO_4) and evaporated under reduced pressure to give the crude product. Purification by flash column chromatography on silica with 80:20 hexane-EtOAc as eluent gave pyrrolidine **158** (1.26 g, 50%) as a red oil, R_F (80:20 hexane-EtOAc) 0.27; IR (ATR) 2977, 1770 (C=O), 1736 (C=O), 1697 (C=O), 1639 (C=O), 1391, 1161 cm^{-1}; ^{1}H NMR (400 MHz, CDCl$_3$) (mixture of diastereomers, rotamers and tautomers) δ 10.10-9.80 (m, 0.3H), 6.17 (m, 0.03H), 5.58 (m, 0.03H), 5.10-4.95 (m, 0.17H), 4.57-4.49 (m, 0.17H), 4.48-4.39 (m, 0.17H), 4.35-3.96 (m, 1.8H), 3.90-3.79 (m, 0.37H), 3.76-3.72 (m, 3H), 3.72-3.58 (m, 0.57H), 3.58-3.52 (m, 0.17H), 3.48-3.42 (m, 0.08H), 3.33 (m, 0.03H, 3.30 (m, 0.03H), 1.50-1.30 (m, 9H), 1.40-1.30 (m, 3H); ^{13}C NMR (100.6 MHz, CDCl$_3$) δ 174.6, 172.53, 172.48, 172.2, 168.9, 168.7, 168.7, 168.0, 155.0, 154.7, 154.6, 149.8, 126.7, 96.24, 96.07, 81.38, 80.75, 80.58, 61.10, 58.70, 58.55, 58.50, 53.75, 53.65, 53.03, 52.19, 52.13, 49.83, 48.80, 48.30, 29.16, 29.08, 29.00, 19.37, 19.05, 18.29, 14.89; MS (ESI) *m/z* 256 [(M - H)$^-$, 100]; HRMS (ESI) *m/z* calcd for $C_{12}H_{19}NO_5$ (M – H)$^-$ 256.1190, found 256.1190 (0.0 ppm error).

Lab Book Ref: TD 2/24

1-*tert*-Butyl-4-methyl 3-trifluoromethylsulfonyl-2-methyl-2,5-dihydro-1H-pyrrole-1,4-dicarboxylate 161

161
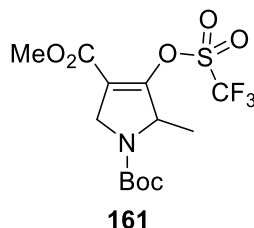
Using general procedure **B**, iPr$_2$NEt (1.46 mL, 8.36 mmol, 5.0 eq), β-ketoester **158** (1.46 mL, 8.36 mmol, 5.0 eq) and trifluoromethanesulfonic anhydride (0.34 mL, 2.0 mmol, 1.2 eq) in CH$_2$Cl$_2$ (30 mL) gave the crude product. Purification by flash column chromatography with 75:25 hexane-EtOAc as eluent gave enol triflate **161** (490 mg, 82%) as a yellow oil, R_F (75:25 hexane-EtOAc) 0.44; IR (ATR) 1732 (C=O, CO$_2$Me), 1707 (C=O, Boc), 1682 (C=C), 1209, 847 cm^{-1}; ^{1}H NMR (400 MHz, CDCl$_3$) (55:45 mixture of rotamers) δ 4.78-4.70 (m, 0.55H, NC*H*Me), 4.67-4.57 (m, 0.45H, NC*H*Me), 4.48-4.37 (m, 1H, NCH), 4.32-4.23 (m, 1H, NCH), 3.82 (s, 3H, OMe), 1.49-1.40 (m, 12H, CMe$_3$, CH*Me*); ^{13}C NMR (100.6 MHz, CDCl$_3$) (rotamers) δ 160.7 (C=O, CO$_2$Me), 160.6 (C=O, CO$_2$Me), 153.4 (C=O, Boc or =CO), 151.3 (C=O, Boc or =CO), 150.7 (C=O, Boc or =CO), 118.43 (=C), 118.38 (q, J = 321 Hz, CF$_3$), 118.3 (=C), 81.1 (*C*Me$_3$), 80.9 (*C*Me$_3$), 58.5 (NCHMe), 58.4 (NCHMe), 52.4 (OMe), 50.1 (NCH$_2$), 49.6 (NCH$_2$), 28.5 (C*Me*$_3$), 18.4 (C*Me*), 17.7 (C*Me*); MS (ESI) *m/z* 412 [(M + Na)$^+$, 100]; HRMS (ESI) *m/z* calcd for C$_{13}$H$_{18}$F$_3$NO$_7$S (M + Na)$^+$ 412.0648, found 412.0637 (+2.8 ppm error).

Lab Book Reference: TD 2/49

4-Methyl 2-methylpyrrolidine-4-carboxylate 156•TfOH
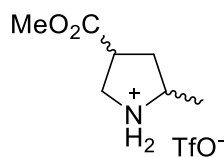
156•TfOH

Using general procedure **A**, dihydropyrrole **161** (490 mg, 1.37 mmol) and 10% Pd/C (49 mg, 0.05 mmol, 0.04 eq) in MeOH (25 mL) for 42 h gave the crude amine•TfOH salt **37•TfOH** (330 mg, 67%) as a yellow oil which contained a 65:35 mixture (by ^{1}H NMR spectroscopy) of pyrrolidines *trans*-**156** and *cis*-**156**, ^{1}H NMR (400 MHz, CDCl$_3$) δ 8.25 (br s, 1H, NH), 7.72 (br s, 1H, NH), 3.90-3.65 (m, 5H, OMe, NCH), 3.65-3.54 (m, 1H, NCH), 3.39-3.24 (m, 1H, C*H*CO$_2$Me), 2.57-2.48 (m, 0.35H, CH), 2.48-2.39 (m, 0.65H, CH) 2.07-1.97 (ddd, J = 13.5, 9.5, 9.5 Hz, 0.65H, CH), 1.97-1.88 (ddd, J = 13.5, 10.0, 10.0 Hz, 0.35H,

CH), 1.46 (br d, J = 6.5 Hz, 3H, CH*Me*). The crude amine•TfOH salt **37**•TfOH was sufficiently pure for use without further purification. To date, we have been unable to repeat this experiment and so full characterisation has not been possible.

Lab Book Reference: TD 2/51

1-Benzoyl-4-methyl 2-methylpyrrolidine-1,4-dicarboxylate 162

162
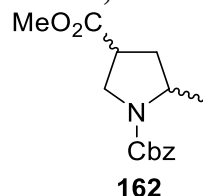
Procedure from pyrrolidines 156•TfOH

Et$_3$N (0.93 mL, 0.67 mmol, 3.0 eq) was added dropwise to a stirred solution of a 65:35 mixture of pyrrolidines *trans*-**156**•TfOH and *cis*-**156**•TfOH (65 mg, 0.22 mmol, 1.0 eq) in CH$_2$Cl$_2$ (3 mL) at 0 °C under Ar. The resulting solution was stirred at 0 °C for 30 min then benzyl chloroformate (0.35 mL, 0.24 mmol, 1.1 eq) and DMAP (3 mg, 0.02 mmol, 0.1 eq) were added. The resulting solution was allowed to warm to rt and was stirred at rt for 16 h. Then, H$_2$O (5 mL) was added and the two layers were separated. The aqueous layer was extracted with CH$_2$Cl$_2$ (3 x 10 mL) and the combined organic extracts were dried (Na$_2$SO$_4$) and evaporated under reduced pressure to give the crude product. Purification by flash column chromatography on silica with 80:20 hexane-EtOAc as eluent gave a 65:35 mixture (by ^{1}H NMR spectroscopy) of pyrrolidines *trans*-**162** and *cis*-**162** (43 mg, 70%) as a colourless oil, R_F (80:20 hexane-EtOAc) 0.20; IR (ATR) 1735 (C=O, CO$_2$Me), 1697 (C=O, Cbz), 1409 cm^{-1}; ^{1}H NMR (400 MHz, CDCl$_3$) δ 7.43-7.27 (m, 5H, Ph), 5.19-5.02 (m, 2H, OC*H*$_2$Ph), 4.16-4.03 (br m, 0.65H, NC*H*Me) 4.00-3.78 (m, 0.70H, NC*H*Me, NCH), 3.73-3.50 (m, 4.65H, OMe, NCH), 3.22-3.08 (br m, 0.65H, C*H*CO$_2$Me), 2.95 (dddd, J = 7.5, 7.5, 7.5, 7.5 Hz (apparent quintet), 0.35H, C*H*CO$_2$Me), 2.38 (ddd, J =13.0, 7.5, 7.5 Hz, 0.35H, CH), 2.32-2.17 (br m, 0.65H, CH), 1.92-1.80 (m, 1H, CH), 1.30-1.15 (m, 3H, CH*Me*); ^{13}C NMR (100.6 MHz, CDCl$_3$) δ (rotamers) 173.5 (C=O, CO$_2$Me), 173.44 (C=O, CO$_2$Me), 173.36 (C=O, *C*O$_2$Me), 154.72 (C=O, Cbz), 154.70 (C=O, Cbz), 154.5 (C=O, Cbz), 154.4 (C=O, Cbz), 136.9 (*ipso*-Ph), 136.8 (*ipso*-Ph) , 128.6 (Ph), 128.5 (Ph), 128.01 (Ph), 127.97 (Ph), 127.9 (Ph), 66.9 (O*C*H$_2$Ph), 66.7 (O*C*H$_2$Ph), 53.7 (N*C*HMe), 53.4 (N*C*HMe), 52.8 (N*C*HMe), 52.2 (OMe), 48.73 (N*C*H$_2$), 48.65 (N*C*H$_2$), 48.2 (N*C*H$_2$), 42.1 (*C*HCO$_2$Me), 41.4 (*C*HCO$_2$Me), 40.7 (*C*HCO$_2$Me), 37.3 (*C*H$_2$), 36.7 (*C*H$_2$), 36.5 (*C*H$_2$), 35.7 (*C*H$_2$), 21.0 (CH*Me*), 20.3 (CH*Me*), 20.1 (CH*Me*); MS (ESI) *m/z* 300 [(M + Na)$^+$, 100]; HRMS (ESI) *m/z* calcd for C$_{15}$H$_{19}$NO$_4$ (M + Na)$^+$ 300.1206, found 300.1216 (–3.2 ppm error).

Lab Book Reference TD 2/56

Procedure from ketonitrile 165

PtO_2 (20 mg, 0.09 mmol, 0.05 eq) was added to a stirred solution of nitrile **165** (276 mg, 1.78 mmol, 1.0 eq) in AcOH (10 mL) at rt. The reaction flask was evacuated under reduced pressure and back-filled with Ar three times. Then, the reaction flask was evacuated under reduced pressure and back-filled with H_2 three times. After the final evacuation, H_2 was charged and the reaction mixture was stirred vigorously under a H_2 balloon at rt for 16 h. Then, the solids were removed by filtration through Celite. The solvent was evaporated under reduced pressure to give the crude product which contained an 80:20 mixture (by ^{1}H NMR spectroscopy) of pyrrolidines **156** (as an 85:15 mixture of *cis*-**156** and *trans*-**156**) and pyrrole **175**. Et_3N (0.93 mL, 0.67 mmol, 3.0 eq) was added dropwise to a stirred solution of the crude product in CH_2Cl_2 (10 mL) at 0 °C under Ar. The resulting solution was stirred at 0 °C for 30 min. Then, benzyl chloroformate (0.28 mL, 1.95 mmol, 1.1 eq) and DMAP (21 mg, 0.17 mmol, 0.1 eq) were added. The resulting solution was allowed to warm to rt and was stirred at rt for 16 h. Then, H_2O (10 mL) was added and the two layers were separated. The aqueous layer was extracted with CH_2Cl_2 (3 x 10 mL) and the combined organic extracts were dried (Na_2SO_4) and evaporated under reduced pressure to give the crude product. Purification by flash column chromatography on silica with 80:20 hexane-EtOAc as eluent gave an 85:15 mixture (by ^{1}H NMR spectroscopy) of pyrrolidines *cis*-**162** and *trans*-**162** (91 mg, 18%) as a colourless oil.

Lab Book Ref: TD 3/47

1-*tert*-Butyl-4-methyl 2-methylpyrrolidine-1,4-dicarboxylate 152
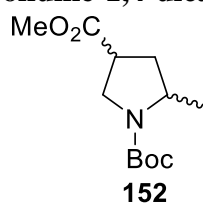
Hydrogenation of Alkene 157

Using general procedure **A**, dihydropyrroles **157** (171 mg, 0.71 mmol, 1.0 eq) and 10% $Pd(OH)_2$/C (100 mg, 0.071 mmol, 0.1 eq) in MeOH (10 mL) for 1 h gave the crude product. Purification by flash column chromatography on silica with 80:20 hexane-EtOAc as eluent gave a 55:45 mixture (by ^{1}H NMR spectroscopy) of pyrrolidines *cis*-**152** and *trans*-**152** (168 mg, 97%) as a colourless oil, R_F (80:20 hexane-EtOAc) 0.19; IR (ATR) 1736 (C=O, CO_2Me), 1691 (C=O, Boc), 1393, 1365, 1166 cm^{-1}; ^{1}H NMR (400 MHz, $CDCl_3$) (major diastereomer exists as a mixture of rotamers) δ 4.10-3.90 (br m, 0.55 H, NC*H*Me), 3.91-

3.71 (m, 1H, NCH), 3.694 (s, 1.35H, OMe), 3.688 (s, 1.65H, OMe), 3.63-3.51 (br m, 1H, NCH), 3.46 (dd, J = 11.0, 8.5 Hz, 0.45H, NCH), 3.20-3.04 (m, 0.55H C*H*CO₂Me), 2.92 (apparent quintet, J = 8.5 Hz, 0.45H C*H*CO₂Me), 2.36 (ddd, J = 13.0, 7.5, 7.5 Hz, 0.45H, CH), 2.22 (br s, 0.55H, CH), 1.88-1.77 (m, 1H, CH), 1.44 (s, 9H, C*Me₃*), 1.23 (br d, J = 6.0 Hz, 1.35H, CH*Me*) 1.16 (d, J = 6.0 Hz, 1.65H, CH*Me*); ¹³C NMR (100.6 MHz, CDCl₃) (rotamers) δ 173.8 (C=O, CO₂Me), 173.6 (C=O, CO₂Me), 154.2 (C=O, Boc), 79.5 (*C*Me₃), 79.4 (*C*Me₃), 53.1 (N*C*HMe), 52.8 (N*C*HMe), 52.1 (OMe), 48.4 (N*C*H₂), 42.0 (*C*HCO₂Me), 41.7 (*C*HCO₂Me), 41.4 (*C*HCO₂Me), 40.8 (*C*HCO₂Me), 37.4 (CH₂), 36.5 (CH₂), 35.8 (CH₂), 28.6 (C*Me₃*), 21.2 (CH*Me*), 20.9 (CH*Me*), 20.4 (CH*Me*), 20.3 (CH*Me*); MS (ESI) *m/z* 266 [(M + Na)⁺, 100]; HRMS (ESI) *m/z* calcd for C₁₂H₂₁NO₄ (M + Na)⁺ 266.1363, found 266.1359 (+1.3 ppm error).

Lab Book Ref: TD 2/81

Boc Protection of Pyrrolidines 156•TfOH

Et₃N (0.93 mL, 0.66 mmol, 3.0 eq) was added dropwise to a stirred solution of a 65:35 mixture of pyrrolidines *trans*-**156**•TfOH and *cis*-**156**•TfOH (65 mg, 0.22 mmol, 1.0 eq) in CH₂Cl₂ at 0 °C under Ar. The resulting mixture was stirred at 0 °C for 30 min. Then, di-*tert*-butyl dicarbonate (53 mg, 0.24 mmol, 1.1 eq) and DMAP (3 mg, 0.02 mmol, 0.1 eq) were added at 0 °C. The resulting mixture was allowed to warm to rt and stirred at rt for 64 h. Saturated NaHCO₃₍aq₎ (10 mL) was added and the aqueous layer was extracted with CH₂Cl₂ (3 x 10 mL). The combined organic extracts were dried (Na₂SO₄) and evaporated under reduced pressure to give the crude product. Purification by flash column chromatography on silica with 80:20 hexane-EtOAc as eluent gave a 65:35 mixture (by ¹H NMR spectroscopy) of pyrrolidines *cis*-**152** and *trans*-**152** (28 mg, 52%) as a colourless oil

Lab Book Ref: TD 2/57

Hydrogenation of Enol Triflate 161

10% Pd/C (29 mg, 0.03 mmol, 0.05 eq) was added to a stirred solution of dihydropyrrole **161** (200 mg, 0.56 mmol, 1.0 eq) and K₂CO₃ (85 mg, 0.61 mmol, 1.1 eq) in MeOH (10 mL) at rt. The reaction flask was evacuated under reduced pressure and back-filled with Ar three times. Then, the reaction flask was evacuated under reduced pressure and back-filled with H₂ three times. After the final evacuation, H₂ was charged and the reaction mixture was stirred vigorously under a H₂ balloon at rt for 16 h. Then, the solids were removed by filtration through Celite. The solvent was evaporated under reduced pressure to give the crude product. Purification by flash column chromatography on silica with 80:20 hexane-EtOAc as eluent gave pyrrolidine *cis*-**152** (15 mg, 8%) as a colourless oil.

Lab Book Ref: TD 2/64

4-Methyl 1,2-dimethylpyrrolidine-4-carboxylate 37•AcOH

37•AcOH
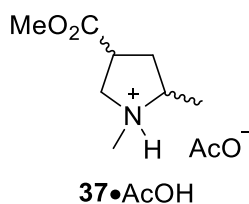
37% aqueous formaldehyde (0.507 mL, 6.82 mmol, 10.0 eq) was added dropwise to a stirred suspension of a 65:35 mixture of pyrrolidines *cis*-**156**•TfOH and *trans*-**156**•TfOH (200 mg, 0.682 mmol, 1.0 eq), NaBH(OAc)$_3$ (434 mg, 2.05 mmol, 3.0 eq) and MgSO$_4$ (507 mg, 4.21 mmol, 6.18 eq) in 3:1 CH$_2$Cl$_2$–AcOH (12 mL) at rt under Ar. The resulting mixture was stirred at rt for 1 h. The solids were removed by filtration and saturated NaHCO$_{3(aq)}$ was added to the filtrate until pH 9 was reached. The mixture was extracted with CH$_2$Cl$_2$ (3 x 10 mL) and the combined organic extracts were washed with brine (10 mL) and dried (Na$_2$SO$_4$). Then, AcOH (0.04 mL, 0.68 mmol, 1.0 eq) was added dropwise to the filtrate which was stirred at rt for 30 min. The solvent was evaporated under reduced pressure to give a 75:25 mixture (by ^{1}H NMR spectroscopy) of AcOH and pyrrolidines **37**•AcOH (65:35 mixture of *cis*-**37**•AcOH and *trans*-**37**•AcOH) (63 mg, 34 mg (23%) of pyrrolidines **37**•AcOH) as a yellow oil, IR (ATR) 1729 (C=O), 1392, 1212 cm^{-1}; ^{1}H NMR (400 MHz, d$_4$-MeOH) δ 3.94-3.88 (m, 0.35H, NCH), 3.84-3.77 (m, 0.65H, NCH), 3.73-3.67 (m, 3H, OMe), 3.41-3.23 (m, 3H, NCH, NC*H*Me, CHCO$_2$Me), 2.81-2.75 (m, 3H, NMe), 2.62-2.51 (m, 0.35H, CH), 2.49-2.41 (m, 0.65H, CH), 2.10-1.88 (m, 4H, CH, MeCO$_2^-$), 1.38-1.34 (m, 3H, CH*Me*); ^{13}C NMR (100.6 MHz, d$_4$-MeOH) δ 175.7 (C=O, MeCO$_2^-$) 173.2 (C=O, CO$_2$Me), 172.8 (C=O, CO$_2$Me), 64.4 (N*C*HMe), 63.4 (N*C*HMe), 55.8 (NCH$_2$), 55.6 (NCH$_2$), 51.7 (OMe), 39.3 (*C*HCO$_2$Me), 39.2 (*C*HCO$_2$Me), 37.43 (NMe), 37.36 (NMe), 35.1 (CH$_2$), 34.9 (CH$_2$), 20.6 (*Me*CO$_2^-$), 13.7 (CH*Me*); MS (ESI) *m/z* 158 [M$^+$, 100]; HRMS (ESI) *m/z* calcd for C$_8$H$_{16}$NO$_2$ M$^+$ 158.1019, found 158.1016 (–1.7 ppm error).

Lab Book Reference: TD 2/52

1-*tert*-Butyl-4-methyl 2-methyl-2,5-dihydro-1H-pyrrole-1,4-dicarboxylate 157

157
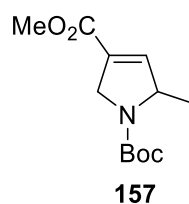
Detriflation with Triethylsilane and Pd(PPh₃)₄

Triethylsilane (0.446 mL, 2.79 mmol, 2.0 eq) was added dropwise to a stirred solution of enol triflate **161** (500 mg, 1.40 mmol, 1.0 eq), tetrakis(triphenylphosphine)palladium (162 mg, 0.1 eq, 0.14 mmol) and Et₃N (0.777 mL, 5.58 mmol, 4.0 eq) in DMF (15 mL) at rt under Ar. The resulting mixture was stirred and heated at 75 °C for 2 h then allowed to cool to rt. Saturated NaHCO₃₍aq₎ and then H₂O (20 mL) were added and the aqueous layer was extracted with Et₂O (3 x 20 mL). The combined organic extracts were washed with H₂O (5 x 20 mL), dried (Na₂SO₄) and evaporated under reduced pressure to give the crude product. Purification by flash column chromatography on silica with 80:20 hexane-EtOAc as eluent gave an 85:15 mixture of dihydropyrrole **157** and triethylsilane (190 mg, 56% of dihydropyrrole **157**) as a yellow oil, R_F (80:20 hexane-EtOAc) 0.33; IR (ATR) 2975, 1726 (C=O, CO₂Me), 1701 (C=O, Boc), 1394, 1284 cm⁻¹; ¹H NMR (400 MHz, CDCl₃) (55:45 mixture of rotamers) δ 6.64-6.61 (m, 0.55H, =CH) 6.61-6.58 (m, 0.45H, =CH), 4.78-4.69 (m, 0.55H, NC*H*Me), 4.67-4.59 (m, 0.45H, NC*H*Me), 4.37 (ddd, *J* = 15.5, 2.0, 2.0 Hz, 0.45H, NCH), 4.31 (ddd, *J* = 15.5, 2.0, 2.0 Hz, 0.55H, NCH), 4.24 (m, 0.55H, NCH), 4.20 (0.45H, m, NCH), 3.76 (s, 1.65H, OMe), 3.75 (s, 1.35H, OMe), 1.465 (s, 4.05H, CMe₃), 1.456 (s, 4.95H, CMe₃), 1.33 (d, *J* = 6.5 Hz, 1.65H, CH*Me*) 1.29 (d, *J* = 6.5 Hz, 1.35H, CH*Me*); ¹³C NMR (100.6 MHz, CDCl₃) δ 163.6 (C=O, CO₂Me), 154.0 (C=O, Boc), 142.5 (=CH), 142.3 (=CH), 130.4 (=C), 130.2 (=C), 79.9 (*C*Me₃), 79.7 (*C*Me₃), 60.8 (*C*Me), 60.6 (*C*Me), 52.2 (NCH₂), 51.9 (NCH₂), 51.9 (OMe), 28.6 (C*Me₃*), 20.1 (CH*Me*), 19.3 (CH*Me*); MS (ESI) *m/z* 264 [(M + Na)⁺, 100]; HRMS (ESI) *m/z* calcd for C₁₂H₁₉NO₄ (M + Na)⁺ 264.1206, found 264.1209 (–0.9 ppm error).

Lab Book Reference: TD 2/68

Hydrogenation of Enol Triflate 161 with added Et₃N

10% Pd/C (90 mg, 0.08 mmol) was added to a stirred solution of enol triflate **161** (900 mg, 2.51 mmol, 1 eq) and Et₃N (0.39 mL, 2.76 mmol, 1.1 eq) in MeOH (25 mL) at rt. The reaction flask was evacuated under reduced pressure and back-filled with Ar three times, then with H₂ three times. After the final evacuation, H₂ was charged and the reaction mixture

was stirred vigorously under a H$_2$ balloon at rt for 16 h. Then, the solids were removed by filtration through Celite. The solvent was evaporated under reduced pressure to give the crude product. Purification by flash column chromatography on silica with 80:20 hexane-EtOAc as eluent gave dihydropyrrole **157** (105 mg, 17%) as a yellow oil.

Lab Book Reference: TD 2/60

Methyl 1-benzyl-2-methylpyrrolidine-4-carboxylate 163

163
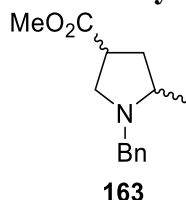
Epimerisation of pyrrolidines 163

K$_2$CO$_3$ (36 mg, 0.26 mmol, 1.2 eq) was added to a stirred solution of an 85:15 mixture of diastereomeric pyrrolidines *cis*-**163** and *trans*-**163** (50 mg, 0.21 mmol, 1.0 eq) in dry MeOH (2.5 mL) at rt under Ar. The resulting solution was stirred at rt for 16 h. Then, saturated NH$_4$Cl$_{(aq)}$ (5 mL) was added and the mixture was extracted with EtOAc (3 x 10 mL). The combined organic extracts were dried (Na$_2$SO$_4$) and evaporated under reduced pressure to give an 85:15 mixture of diastereomeric pyrrolidines *cis*-**163** and *trans*-**163** (50 mg, quant.) as a yellow oil, R_F (80:20 hexane-EtOAc) 0.16; IR (ATR) 1734 (C=O), 1194, 1174, 737, 698 cm^{-1}; ^{1}H NMR (400 MHz, CDCl$_3$) δ 7.35-7.19 (m, 5H, Ph), 4.02 (d, J = 13.0 Hz, 0.15H, NCHPh), 4.01 (d, J = 13.5 Hz, 0.85H, NCHPh), 3.64 (s, 2.55H, OMe), 3.63 (s, 0.45H, OMe), 3.22-3.10 (m, 2H, NCH, NCHPh), 2.99-2.92 (m, 0.15 H, C*H*CO$_2$Me), 2.85 (dddd, J = 9.5, 7.5, 6.5, 3.5 Hz, 0.85H, C*H*CO$_2$Me), 2.58-2.44 (m, 1H, NC*H*Me), 2.36 (dd, J = 10.0, 9.5 Hz, 0.85H, NCH), 2.32-2.15 (m, 1.15H, NCH, CH), 1.81 (ddd, J = 13.0, 9.5, 7.5 Hz, 0.85H, CH), 1.73 (ddd, J = 13.0, 11.0, 9.0 Hz, 0.15H, CH), 1.19-1.17 (m, 3H, CH*Me*); ^{13}C NMR (100.6 MHz, CDCl$_3$) δ 175.7 (C=O), 138.9 (*ipso*-Ph), 128.8 (Ph), 128.3 (Ph), 128.2 (Ph), 127.1 (Ph), 126.9 (Ph), 59.4 (N*C*HMe), 58.0 (N*C*HMe), 57.2 (N*C*H$_2$Ph), 57.0 (N*C*H$_2$Ph), 55.9 (N*C*H$_2$), 51.93 (OMe), 51.86 (OMe), 40.0 (*C*HCO$_2$Me), 36.6 (CH$_2$), 36.4 (CH$_2$), 18.9 (CH*Me*), 18.4 (CH*Me*); MS (ESI) *m/z* 234 [(M + H)$^+$, 100]; HRMS (ESI) *m/z* calcd for C$_{14}$H$_{19}$NO$_2$ (M + H)$^+$ 234.1489, found 234.1478 (–4.4 ppm error).

Lab Book Reference: TD 3/26

Boc Deprotection and Benzylaton of pyrrolidines 152

TFA (0.165 mL, 2.16 mmol, 6.25 eq) was added dropwise to a stirred solution of a 60:40 mixture of pyrrolidines *cis*-**152** and *trans*-**152** (84 mg, 0.345 mmol, 1.0 eq) in CH$_2$Cl$_2$ at rt under Ar. The resulting solution was stirred at rt for 4 h. Then, the solvent was evaporated

under reduced pressure to give the crude amine•TFA salt. NaBH(OAc)₃ (136 mg, 0.64 mmol, 2.0 eq) was added to a stirred solution of the crude amine•TFA salt, benzaldehyde (0.04 mL, 0.35 mmol, 1.1 eq) and AcOH (0.004 mL, 0.06 mmol, 0.2 eq) in dichloroethane (5 mL) at rt under Ar. The resulting solution was stirred at rt for 16 h. Then, saturated NaHCO₃(aq) (10 mL) was added and the mixture was extracted with CH₂Cl₂ (3 x 10 mL). The combined organic extracts were dried (Na₂SO₄) and evaporated under reduced pressure to give the crude product. Purification by flash column chromatography on silica with 80:20 hexane-EtOAc as eluent, with ¹H NMR spectroscopy being performed on individual fractions to identify the fractions containing pure *cis*-**163**, gave *N*-benzyl pyrrolidine *cis*-**163** (8 mg, 10%) as a yellow oil and a 55:45 mixture (by ¹H NMR spectroscopy) of pyrrolidines *trans*-**163** and *cis*-**163** (23 mg, 31%) as a yellow oil.

Lab Book Reference: TD 2/82, 2/83

K₂CO₃ (36 mg, 0.26 mmol, 1.2 eq) was added to a stirred solution of an 85:15 mixture of pyrrolidines *cis*-**163** and *trans*-**163** (50 mg, 0.21 mmol, 1.0 eq) in dry MeOH (2.5 mL) at rt under Ar. The resulting solution was stirred and heated at 60 °C for 16 h. Then, saturated NH₄Cl(aq) (5 mL) was added and the mixture was extracted with EtOAc (3 x 10 mL). The combined organic extracts were dried (Na₂SO₄) and evaporated under reduced pressure to give a 50:50 mixture of pyrrolidines *cis*-**163** and *trans*-**163** (11 mg, 22%) as a yellow oil.

Lab Book Reference: TD 3/27

4-Methyl *N*-(2-nitrophenyl)sulfonyl-2-methylpyrrolidine-4-carboxylate 164

164

TFA (0.33 mL, 4.31 mmol, 6.25 eq) was added dropwise to a stirred solution of a 60:40 mixture of pyrrolidines *cis*-**152** and *trans*-**152** (168 mg, 0.69 mmol, 1.0 eq) in CH₂Cl₂ (1.65 mL) at rt under Ar. The resulting solution was stirred at rt for 4 h. Then, the solvent was evaporated under reduced pressure to give the crude amine•TFA salt. 2-Nosyl chloride (78 mg, 0.35 mmol, 1.1 eq) was then added portionwise to a stirred solution of half of the crude amine•TFA salt (82 mg, 0.32 mmol, 1.0 eq) and Et₃N (0.11 mL, 0.80 mmol, 2.5 eq) in CH₂Cl₂ (3 mL) at 0 °C under Ar. The resulting solution was allowed to warm to rt and stirred at rt for 16 h. Then, saturated NaHCO₃(aq) (10 mL) was added and the two layers were separated. The aqueous layer was extracted with CH₂Cl₂ (3 x 10 mL) and the combined

organic extracts were dried (Na$_2$SO$_4$) and evaporated under reduced pressure to give the crude product. Purification by flash column chromatography on silica with 50:50 hexane-EtOAc as eluent gave a 60:40 mixture (by ^{1}H NMR spectroscopy) of pyrrolidines *cis*-**164** and *trans*-**164** (23 mg, 20%) as a yellow oil, R_F (50:50 hexane-EtOAc) 0.27; IR (ATR) 1732 (C=O), 1542, 1162 cm^{-1}; ^{1}H NMR (400 MHz, CDCl$_3$) δ 8.05-7.98 (m, 1H, Ar), 7.73-7.55 (m, 3H, Ar), 4.22-4.13 (m, 0.4H, NC*H*Me), 4.09-3.99 (ddq, J = 7.0, 6.5, 6.5 Hz, 0.6H, NC*H*Me), 3.88 (dd, J = 11.0, 8.0 Hz, 0.6H, NCH), 3.71 (dd, J = 10.5 Hz, 7.5 Hz, 0.4H, NCH), 3.68 (s, 1.8H, OMe) 3.66-3.60 (m, 1H, NCH), 3.59 (s, 1.2H, OMe), 3.17 (dddd, J = 7.5, 7.5, 7.5, 7.5 Hz (apparent quintet), 0.4H, C*H*CO$_2$Me), 2.97-2.87 (m, 0.6H, C*H*CO$_2$Me), 2.40 (ddd, J = 13.0, 7.5, 7.0 Hz, 0.6H, CH), 2.28-2.19 (ddd, J = 13.0, 8.0, 8.0 Hz, 0.4H, CH) 1.91-1.81 (m, 1H, CH) 1.26 (d, J = 6.5 Hz, 3H, CH*Me*); ^{13}C NMR (100.6 MHz, CDCl$_3$) δ 172.7 (C=O), 172.5 (C=O), 148.4 (*ipso*-Ar), 148.3 (*ipso*-Ar), 133.8 (Ar), 133.7 (Ar), 133.0 (Ar), 132.2 (Ar), 131.8 (Ar), 131.6 (Ar), 131.0 (Ar), 130.9 (Ar), 124.2 (Ar), 124.1 (Ar), 56.6 (N*C*HMe), 56.4 (N*C*HMe), 52.31 (OMe), 52.28 (OMe), 50.6 (NCH$_2$), 50.4 (NCH$_2$), 42.4 (*C*HCO$_2$Me), 41.5 (*C*HCO$_2$Me), 37.5 (CH$_2$), 36.9 (CH$_2$), 22.2 (CH*Me*), 21.7 (CH*Me*); MS (ESI) *m/z* 351 [(M + Na)$^+$, 100], 329 [(M + H)$^+$, 4%]; HRMS (ESI) *m/z* calcd for C$_{13}$H$_{16}$N$_2$O$_6$S (M + Na)$^+$ 351.0621, found 351.0604 (+4.9 ppm error).

Lab Book Reference: TD 2/82, 2/84

Methyl 2-cyano-5-oxopentanoate 165
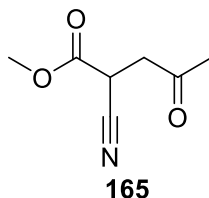
NaOMe (1.635 g, 30.27 mmol, 1.0 eq) was added to a stirred solution of methyl cyanoacetate (2.68 mL, 30.27 mmol, 1.0 eq) in MeOH (30 mL) at 0 °C under Ar. The resulting solution was stirred at 0 °C for 10 min. Then, chloroacetone (2.41 mL, 30.27 mmol, 1 eq) was added dropwise. The resulting solution was allowed to warm to rt and stirred at rt for 5 h. Saturated NH$_4$Cl$_{(aq)}$ (20 mL) was added and the aqueous layer was extracted with EtOAc (3 x 20 mL). The combined organic extracts were dried (Na$_2$SO$_4$) and evaporated under reduced pressure to give the crude product. Purification by flash column chromatography on silica with 80:20 hexane-EtOAc as eluent gave keto nitrile **165** (2.91 g, 62%) as a brown oil, R_F (50:50 hexane-EtOAc) 0.33; IR 2255 (C≡N), 1746 (C=O, CO$_2$Me), 1716 (C=O, ketone), 1267, 1167 cm^{-1}; ^{1}H NMR (400 MHz, CDCl$_3$) δ 3.95 (dd, J = 7.0, 5.5 Hz, 1H, CHCN), 3.82 (s, 3H, OMe), 3.20 (dd, J = 18.5, 7.0 Hz, 1H, C*H*C(O)Me), 3.00 (dd, J = 18.5, 5.5 Hz, 1H,

C*H*C(O)Me), 2.24 (s, 3H, C(O)Me); ^{13}C NMR (100.6 MHz, CDCl$_3$) δ 202.5 (C=O, ketone), 165.9 (C=O, CO$_2$Me), 116.0 (C≡N), 54.0 (OMe), 42.1 (CH$_2$), 31.3 (CH), 29.5 (C(O)*Me*); MS (ESI) *m/z* 156 [(M + H)$^+$, 100]; HRMS (ESI) *m/z* calcd for C$_7$H$_9$NO$_3$ (M + H)$^+$ 156.0655, found 156.0654 (–1.0 ppm error).

Lab Book Reference: TD 2/99

1-Benzoyl-4-methyl 2-methylpyrrolidine-1,4-dicarboxylate 176

176
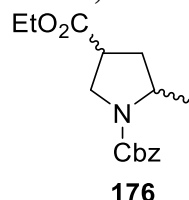
LiOH (22 mg, 1.08 mmol, 3.0 eq) was added to a stirred solution of an 85:15 mixture of pyrrolidines *cis*-**162** and *trans*-**162** in 4:1:1 THF-H$_2$O-MeOH (6 mL) at rt under Ar. The resulting solution was stirred at rt for 16 h. Then, 2 M HCl$_{(aq)}$ (10 mL) was added and the mixture was extracted with CH$_2$Cl$_2$ (3 x 10 mL). The combined organic extracts were basified to pH 9 with saturated NaHCO$_{3(aq)}$ and the mixture was washed with CH$_2$Cl$_2$ (2 x 10 mL). The mixture was then acidified to pH 3 with 2 M HCl$_{(aq)}$ and extracted with CH$_2$Cl$_2$ (3 x 10 mL). The combined organic extracts were dried (Na$_2$SO$_4$) and evaporated under reduced pressure to give the crude acid intermeditae. Thionyl chloride (0.044 mL, 0.605 mmol, 1.75 eq) was added to a stirred solution of the acid intermediate (91 mg, 1.0 eq) in EtOH (10 mL) at rt under Ar. The resulting mixture was stirred at rt for 16 h and then the solvent was evaporated under reduced pressure. The residue was dissolved in CH$_2$Cl$_2$ (10 mL) and washed with saturated NaHCO$_{3(aq)}$ (2 x 10 mL). The organic layer was dried (Na$_2$SO$_4$) and evaporated under reduced pressure to give the crude product. Purification by flash column chromatography on silica with 80:20 hexane-EtOAc as eluent gave an 85:15 mixture of pyrrolidines *cis*-**176** and *trans*-**176** (44 mg, 46%) as a colourless oil, R_F (80:20 hexane-EtOAc) 0.17; ^{1}H NMR (400 MHz, CDCl$_3$) δ 7.38-7.24 (m, 5H, Ph), 5.18-5.03 (m, 2H, OCH$_2$Ph), 4.18-4.10 (m, 2H, OC*H*$_2$Me), 4.00-3.75 (m, 1.85H, NC*H*Me, NCH), 3.70-3.60 (m, 0.3H, NCH), 3.56 (dd, *J* = 11.0, 8.5 Hz, 0.85H, NCH) 3.19-3.08 (m, 0.15 H, C*H*CO$_2$Me), 2.94 (dddd, *J* = 8.5, 8.5, 8.5, 8.5 Hz, 0.85H, C*H*CO$_2$Me), 2.38 (ddd, *J* = 13.0, 8.5, 8.5 Hz, 0.85H, CH), 2.31-2.19 (m, 0.15H, CH), 1.93-1.77 (m, 1H, CH), 1.32-1.19 (m, 6H, CH*Me*, OCH$_2$*Me*); ^{13}C NMR (100.6 MHz, CDCl$_3$) 174.5 (C=O, CO$_2$CH$_2$), 154.6 (C=O, Cbz) 139.4 (*ipso*-Ar), 128.7 (Ar), 128.2 (Ar), 126.8 (Ar), 80.2 (OC*H$_2$*Ph), 59.4 (CO$_2$*C*H$_2$), 57.2 (N*C*HMe), 56.1 (NCH), 41.3 (*C*HCO$_2$), 36.6 (CH$_2$), 28.1 (CH*Me*), 18.60 (CH$_2$*Me*). Spectroscopic data for *cis*-**176** are consistent with those reported in the literature.[92]

Lab Book Reference: TD 3/48, TD 3/49

Methyl 1-benzyl-2-methylpyrrolidine-4-carboxylate *cis*-163

cis-**163**
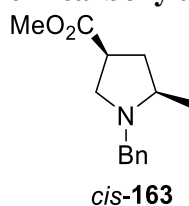
PtO$_2$ (14 mg, 0.06 mmol, 0.05 eq) was added to a stirred solution of nitrile **165** (191 mg, 1.23 mmol, 1.0 eq) in AcOH (5 mL) at rt. The reaction flask was evacuated under reduced pressure and back-filled with Ar three times. Then, the reaction flask was evacuated under reduced pressure and back-filled with H$_2$ three times. After the final evacuation, H$_2$ was charged and the reaction mixture was stirred vigorously under a H$_2$ balloon at rt for 16 h. Then, the solids were removed by filtration through Celite. The solvent was evaporated under reduced pressure and the residue dissolved in dichloroethane (10 mL). NaBH(OAc)$_3$ (0.52 g, 2.46 mmol, 2.0 eq), benzaldehyde (0.14 mL, 1.36 mmol, 1.1 eq) and AcOH (0.015 mL, 0.25 mmol, 0.2 eq) were added at rt under Ar. The resulting solution was stirred at rt for 16 h. Then, saturated NaHCO$_{3(aq)}$ (25 mL) was added and the mixture was extracted with CH$_2$Cl$_2$ (3 x 25 mL). The combined organic extracts were dried (Na$_2$SO$_4$) and evaporated under reduced pressure to give the crude product. Purification by flash column chromatography on silica with 80:20 hexane-EtOAc as eluent, with ^{1}H NMR spectroscopy being performed on individual fractions to identify the fractions containing pure *cis*-**163**, gave *N*-benzyl pyrrolidine *cis*-**163** (61 mg, 21%) as a yellow oil, R_F (80:20 hexane-EtOAc) 0.16; IR (ATR) 1733 (C=O), 1194, 1174, 737 cm^{-1}; ^{1}H NMR (400 MHz, CDCl$_3$) δ 7.35-7.19 (m, 5H, Ph), 4.01 (d, J = 13.5 Hz, 1H, NC*H*Ph), 3.64 (s, 3H, OMe), 3.19 (dd, J = 10.0, 3.5 Hz, 1H, NCH), 3.19 (d, J = 13.5 Hz, 1H, NC*H*Ph), 2.85 (dddd, J = 9.5, 7.5, 6.5, 3.5 Hz, 1H, C*H*CO$_2$Me), 2.49 (ddq, J = 9.5, 9.5, 6.0 Hz, 1H, NC*H*Me), 2.36 (dd, J = 10.0, 9.5 Hz, 1H, NCH), 2.20 (ddd, J = 13.0, 9.5, 6.5 Hz, 1H, CH), 1.81 (ddd, J = 13.0, 9.5, 7.5 Hz, 1H, CH), 1.18 (d, J = 6.0 Hz, 3H, CH*Me*); ^{13}C NMR (100.6 MHz, CDCl$_3$) δ 175.7 (C=O), 139.0 (*ipso*-Ph), 128.8 (Ph), 128.2 (Ph), 126.9 (Ph), 59.4 (N*C*HMe), 57.3 (N*C*H$_2$Ph), 55.9 (NCH$_2$), 51.9 (OMe), 40.1 (*C*HCO$_2$Me), 36.6 (CH$_2$), 18.4 (CH*Me*); MS (ESI) *m/z* 234 [(M + H)$^+$, 100]; HRMS (ESI) *m/z* calcd for C$_{14}$H$_{19}$NO$_2$ (M + H)$^+$ 234.1489, found 234.1478 (–4.4 ppm error) and an 80:20 mixture (by ^{1}H NMR spectroscopy) of diastereomeric pyrrolidines *cis*-**163** and *trans*-**163** (106 mg, 37%) as a yellow oil.

Lab Book Reference: TD 2/92

Methyl 1-benzyl-2-methylpyrrolidine-4-carboxylate *cis*-163, Methyl 1-benzyl-2-methylpyrrolidine-4-carboxylate *trans*-163 and *tert*-Butyl 1-benzyl-2-methylpyrrolidine-4-carboxylate *cis*-182

| MeO$_2$C | MeO$_2$C | tBuO$_2$C |
| *cis*-**163** | *trans*-**163** | *cis*-**182** |
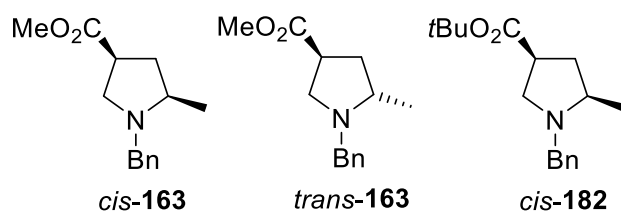
t-BuOK (29 mg, 0.26 mmol, 1.2 eq) was added to a stirred solution of an 85:15 mixture of pyrrolidines *cis*-**163** and *trans*-**163** (50 mg, 0.21 mmol, 1.0 eq) in THF (2.5 mL) at –78 °C under Ar. The resulting solution was stirred at –78 °C for 2 h. Then, H$_2$O (5 mL) was added and the mixture was extracted with EtOAc (3 x 10 mL). The combined organic extracts were dried (Na$_2$SO$_4$) and evaporated under reduced pressure to give a 40:50:10 mixture of pyrrolidines *cis*-**163,** *trans*-**163** and *cis*-**182** (48 mg, 98%) as a yellow oil.

Lab Book Reference: TD 3/29

1-*tert*-Butyl-4-methyl 2-methylpyrrolidine-1,4-dicarboxylate 152

152
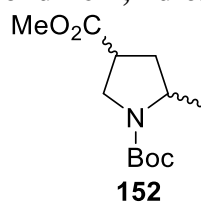
Preparation from ketonitrile 165

PtO$_2$ (36 mg, 0.16 mmol, 0.05 eq) was added to a stirred solution of nitrile **165** (500 mg, 3.23 mmol, 1.0 eq) in AcOH (30 mL) at rt. The reaction flask was evacuated under reduced pressure and back-filled with Ar three times. Then, the reaction flask was evacuated under reduced pressure and back-filled with H$_2$ three times. After the final evacuation, H$_2$ was charged and the reaction mixture was stirred vigorously under a H$_2$ balloon at rt for 16 h. Then, the solids were removed by filtration through Celite. The solvent was evaporated under reduced pressure and the residue dissolved in CH$_2$Cl$_2$ (40 mL) at 0 °C under Ar. Et$_3$N (2.25 mL, 16.15 mmol, 5.0 eq) was added dropwise to the stirred solution. The resulting mixture was stirred at 0 °C for 30 min. Then, di-*tert*-butyl dicarbonate (775 mg, 3.55 mmol, 1.1 eq) and DMAP (20 mg, 0.16 mmol, 0.1 eq) were added at 0 °C. The resulting mixture was allowed to warm to rt and stirred at rt for 64 h. Saturated NaHCO$_{3(aq)}$ (50 mL) was added and the aqueous layer was extracted with CH$_2$Cl$_2$ (3 x 50 mL). The combined organic extracts were dried (Na$_2$SO$_4$) and evaporated under reduced pressure to give the crude product. Purification by flash column chromatography on silica with 80:20 hexane-EtOAc

as eluent gave a 90:10 mixture (by ^{1}H NMR spectroscopy) of pyrrolidines *cis*-**152** and *trans*-**152** (377 mg, 48%) as a colourless oil

Lab Book Ref: TD 3/35

Epimerisation of pyrrolidines 152

NaOMe (14 mg, 0.25 mmol, 1.2 eq) was added to a stirred solution of a 90:10 mixture of pyrrolidines *cis*-**152** and *trans*-**152** (50 mg, 0.21 mmol, 1.0 eq) in dry MeOH (2.5 mL) at rt under Ar. The resulting solution was stirred at rt for 16 h. Then, saturated NH$_4$Cl$_{(aq)}$ (5 mL) was added and the mixture was extracted with EtOAc (3 x 10 mL). The combined organic extracts were dried (Na$_2$SO$_4$) and evaporated under reduced pressure to give a 50:50 mixture of pyrrolidines *cis*-**152** and *trans*-**152** (50 mg, 100%) as a yellow oil.

Lab Book Reference: TD 3/38

tert-**Butyl-2-cyano-5-oxopentanoate 183**

183
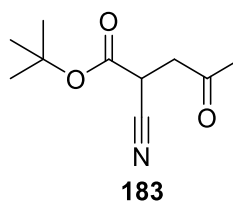
Procedure in *t*-BuOH as solvent

t-BuOK (500 mg, 3.54 mmol, 1.0 eq) was added to a stirred solution of *tert*-butyl cyanoacetate (0.506 mL, 3.54 mmol, 1.0 eq) in *t*-BuOH (30 mL) heated at 40 °C under Ar. The resulting solution was stirred and heated at 40 °C for 10 min. Then, chloroacetone (2.41 mL, 30.27 mmol, 1 eq) was added dropwise under Ar. The resulting solution was stirred and heated at 40 °C for 5 h. Saturated NH$_4$Cl$_{(aq)}$ (20 mL) was added and the aqueous layer was extracted with EtOAc (3 x 20 mL). The combined organic extracts were dried (Na$_2$SO$_4$) and evaporated under reduced pressure to give the crude product. Purification by flash column chromatography on silica with 80:20 hexane-EtOAc as eluent gave keto nitrile **183** (530 mg, 76%) as a brown oil, R_F (50:50 hexane-EtOAc) 0.51; IR (ATR) 2982, 2253 (C≡N), 1740 (C=O, ketone), 1722 (C=O, CO$_2$*t*-Bu), 1370, 1151 cm^{-1}; ^{1}H NMR (400 MHz, CDCl$_3$) δ 3.87-3.83 (m, 1H, CHCN), 3.14 (dd, J = 18.0, 7.5 Hz, 1H, C*H*C(O)Me), 2.92 (dd, J = 18.0, 5.0 Hz, 1H, CHCO), 2.22 (s, 3H, CHC(O)*Me*), 1.48 (s, 9H, C*Me$_3$*); ^{13}C NMR (100.6 MHz, CDCl$_3$) δ 202.7 (C=O, ketone), 164.1 (C=O, CO$_2$*t*-Bu), 116.6 (C≡N), 84.6 (*C*Me$_3$), 42.1 (CH$_2$), 32.5 (CH), 29.6 (C(O)*Me*), 27.8 (C*Me$_3$*); MS (ESI) *m/z* 220 [(M + Na)$^+$, 100]; HRMS (ESI) *m/z* calcd for C$_{10}$H$_{15}$NO$_3$ (M + Na)$^+$ 220.0944, found 220.0947 (–1.5 ppm error).

Lab Book Reference: TD 3/18

Procedure in THF as solvent

t-BuOK (500 mg, 3.54 mmol, 1.0 eq) was added to a stirred solution of *tert*-butyl cyanoacetate (0.506 mL, 3.54 mmol, 1.0 eq) in THF (30 mL) at 0 °C under Ar. The resulting solution was stirred at 0 °C for 10 min. Then, chloroacetone (2.41 mL, 30.27 mmol, 1 eq) was added dropwise. The resulting solution was allowed to warm to rt and stirred at rt for 5 h. Saturated $NH_4Cl_{(aq)}$ (20 mL) was added and the aqueous layer was extracted with EtOAc (3 x 20 mL). The combined organic extracts were dried (Na_2SO_4) and evaporated under reduced pressure to give the crude product. Purification by flash column chromatography on silica with 80:20 hexane-EtOAc as eluent gave keto nitrile **183** (437 mg, 63%) as a brown oil.

Lab Book Reference: TD 3/19

tert-Butyl 1-benzyl-2-methylpyrrolidine-4-carboxylate *cis*-182

cis-**182**
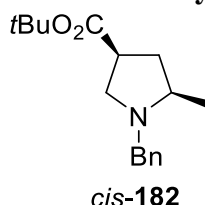
PtO_2 (103 mg, 0.45 mmol, 0.05 eq) was added to a stirred solution of nitrile **183** (1.79 g, 9.05 mmol, 1.0 eq) in AcOH (40 mL) at rt. The reaction flask was evacuated under reduced pressure and back-filled with Ar three times. Then, the reaction flask was evacuated under reduced pressure and back-filled with H_2 three times. After the final evacuation, H_2 was charged and the reaction mixture was stirred vigorously under a H_2 balloon at rt for 16 h. Then, the solids were removed by filtration through Celite. The solvent was evaporated under reduced pressure to give the crude product which contained an 80:20 mixture (by ^{1}H NMR spectroscopy) of pyrrolidine *cis*-**45** and pyrrole **184**. NaBH(OAc)$_3$ (3.84 g, 18.1 mmol, 2.0 eq) was added to a stirred solution of the crude mixture of pyrrolidines *cis*-**45**•AcOH and pyrrole **184**, benzaldehyde (1.02 mL, 9.96 mmol, 1.1 eq) and AcOH (0.10 mL, 1.81 mmol, 0.2 eq) in dichloroethane (100 mL) at rt under Ar. The resulting solution was stirred at rt for 16 h. Then, saturated NaHCO$_{3(aq)}$ (100 mL) was added and the mixture was extracted with CH_2Cl_2 (3 x 100 mL). The combined organic extracts were dried (Na_2SO_4) and evaporated under reduced pressure to give the crude product. Purification by flash column chromatography on silica with 90:10 hexane-EtOAc as eluent gave *N*-benzyl pyrrolidine *cis*-**182** (756 mg, 30%) as a yellow oil, R_F (90:10 hexane-EtOAc) 0.21; IR (ATR) 2971, 1728 (C=O), 1367, 1150 cm^{-1}; ^{1}H NMR (400 MHz, CDCl$_3$) δ 7.34-7.18 (m, 5H, Ph), 4.00 (d, *J* =

13.5 Hz, 1H, NCHPh), 3.16 (d, J = 13.5 Hz, 1H, NCHPh), 3.14 (dd, J = 10.0, 3.5 Hz, 1H, NCH), 2.74 (dddd, J = 9.0, 7.0, 6.5, 3.5 Hz, 1H, CHCO$_2$), 2.48 (ddq, J = 9.0, 9.0, 6.0 Hz, 1H, NC*H*Me), 2.30 (dd, J = 10.0, 9.0 Hz, 1H, NCH), 2.14 (ddd, J = 13.0, 9.0, 6.5 Hz, 1H, CH), 1.77 (ddd, J = 13.0, 9.0, 7.0 Hz, 1H, CH), 1.40 (s, 9H, CMe$_3$) 1.18 (d, J = 6.0 Hz, 3H, CH*Me*); ^{13}C NMR (100.6 MHz, CDCl$_3$) δ 174.5 (C=O), 139.4 (*ipso*-Ph), 128.7 (Ph), 128.2 (Ph), 126.8 (Ph), 80.2 (*C*Me$_3$) 59.4 (N*C*HMe), 57.2 (N*C*H$_2$Ph), 56.1 (N*C*H$_2$), 41.3 (*C*HCO$_2$), 36.6 (*C*H$_2$), 28.1 (C*Me*$_3$), 18.6 (CH*Me*); MS (ESI) m/z 276 [(M + H)$^+$, 100]; HRMS (ESI) m/z calcd for C$_{17}$H$_{25}$NO$_2$ (M + H)$^+$ 276.1958, found 276.1957 (0.2 ppm error).

Lab Book Reference: TD 3/59

tert-Butyl 2-methylpyrrolidine-4-carboxylate *cis*-45•AcOH

cis-**45**•AcOH
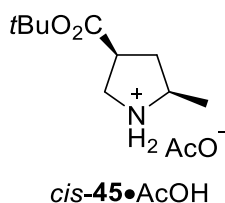
10% Pd(OH)$_2$/C (10 mg, 0.007 mmol, 0.01 eq) was added to a stirred solution of pyrrolidine *cis*-**182** (200 mg, 0.73 mmol, 1 eq) and ammonium formate (229 mg, 3.63 mmol, 5 eq) in MeOH (10 mL) at rt under Ar. The resulting solution was stirred and heated to 60 °C for 2 h. After being allowed to cool to rt, the solids were removed by filtration through Celite. AcOH (0.087 mL, 1.46 mmol, 2.0 eq) was added dropwise to the filtrate which was stirred at rt for 30 min. The solvent was evaporated under reduced pressure. Then, the residue was dissolved in CH$_2$Cl$_2$ and the solids were removed by filtration. The filtrate was evaporated under reduced pressure to give a 65:35 mixture (by ^{1}H NMR spectroscopy) of AcOH and pyrrolidine *cis*-**45**•AcOH (198 mg (141 mg, 79% of pyrrolidines *cis*-**45**•AcOH) as a brown oil, IR (ATR) 2979, 1724 (C=O), 1367, 1153 cm^{-1}; ^{1}H NMR (400 MHz, CDCl$_3$) δ 3.72-3.62 (m, 1H, NC*H*Me), 3.49-3.37 (m, 2H, NCH), 3.13 (dddd, J = 8.5, 8.5, 8.5, 8.5 Hz (apparent quintet), 1H, C*H*CO$_2$), 2.40 (ddd, 13.5, 8.5, 6.5 Hz, 1H, CH), 2.03 (s, 9H, MeCO$_2^-$), 1.81 (ddd, J = 13.5, 8.5, 8.5 Hz, 1H, CH), 1.43 (s, 9H, CMe$_3$), 1.38 (d, J = 6.5 Hz, CH*Me*); ^{13}C NMR (100.6 MHz, CDCl$_3$) δ 177.0 (C=O, Me*C*O$_2^-$), 171.3 (C=O, *C*O$_2$CMe$_3$), 82.1 (*C*Me$_3$), 55.5 (*C*HMe), 46.2 (NCH), 43.3 (*C*HCO$_2$), 36.2 (*C*H$_2$), 28.0 (C*Me*$_3$), 21.7 (*Me*CO$_2^-$), 17.5 (CH*Me*); MS (ESI) m/z 186 [M$^+$, 100]; HRMS (ESI) m/z calcd for C$_{10}$H$_{21}$NO$_2$ M$^+$ 186.1489, found 186.1491 (–1.6 ppm error).

Lab Book Reference: TD 3/67

tert-Butyl 1,2-dimethylpyrrolidine-4-carboxylate *cis*-46•AcOH
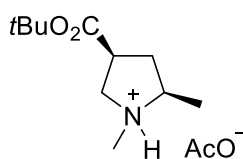
cis-**46**•AcOH

37% aqueous formaldehyde (1.52 mL, 20.4 mmol, 10.0 eq) was added dropwise to a stirred suspension of pyrrolidine *cis*-**45**•AcOH (500 mg, 2.04 mmol, 1.0 eq), NaBH(OAc)$_3$ (1.30 g, 6.12 mmol, 3.0 eq) and MgSO$_4$ (1.52 g, 12.6 mmol, 6.18 eq) in 3:1 CH$_2$Cl$_2$–AcOH (20 mL) at rt under Ar. The resulting mixture was stirred at rt for 1 h. The solids were removed by filtration and NaHCO$_{3(aq)}$ was added to the filtrate until pH 9 was reached. The mixture was extracted with CH$_2$Cl$_2$ (3 x 20 mL) and the combined organic extracts were washed with brine (20 mL) and dried (Na$_2$SO$_4$). AcOH (0.12 mL, 2.04 mmol, 1.0 eq) was added dropwise to the filtrate which was stirred at rt for 30 min. The solvent was evaporated under reduced pressure to give a 65:35 mixture (by ^{1}H NMR spectroscopy) of AcOH and pyrrolidine *cis*-**46**•AcOH (124 mg, 85 mg (16%) of pyrrolidine *cis*-**46**•AcOH) as a yellow oil, IR (ATR) 2977, 1726 (C=O), 1368, 1252, 1155 cm^{-1}; ^{1}H NMR (400 MHz, CDCl$_3$) δ 3.53 (dd, J = 10.5, 5.0 Hz, 1H, NCH), 3.20-3.01 (m, 3H, NCH, NC*H*Me, CHCO$_2$C), 2.56 (s, 3H, NMe), 2.38 (ddd, J = 13.5, 9.5, 6.5 Hz, 1H, CH), 2.02 (br s, 9H, MeCO$_2^-$), 1.95 (ddd, J = 13.5, 9.0, 7.5 Hz, 1H, CH), 1.43 (s, 9H, CMe$_3$), 1.27 (d, J = 6.5 Hz, 3H, CMe); ^{13}C NMR (100.6 MHz, CDCl$_3$) δ 176.4 (C=O, MeCO$_2^-$) 172.0 (C=O, CO$_2$CMe$_3$), 81.8 (*C*Me$_3$), 61.8 (NCHMe), 56.0 (NCH), 41.0 (*C*HCO$_2$), 37.7 (NMe), 35.5 (CH$_2$), 28.0 (C*Me*$_3$) 21.6 (*Me*CO$_2^-$), 15.2 (CH*Me*); MS (ESI) *m/z* 200 [M$^+$, 100]; HRMS (ESI) *m/z* calcd for C$_{11}$H$_{23}$NO$_2$ M$^+$ 200.1646, found 200.1645 (–0.6 ppm error).

Lab Book Reference: TD 3/52

tert-Butyl 1-acetyl-2-methylpyrrolidine-4-carboxylate *cis*-48
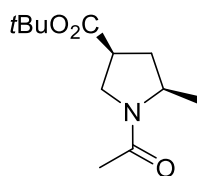
cis-**48**

Methanesulfonyl chloride (0.474 mL, 3.0 eq, 6.12 mmol) was added dropwise to a stirred solution of pyrrolidine salt *cis*-**45**•AcOH (500 mg, 1.0 eq, 2.04 mmol) and Et$_3$N (1.135 mL, 4.0 eq, 8.16 mmol) in CH$_2$Cl$_2$ (20 mL) at rt. The resulting solution was stirred at rt for 3 h. Saturated NaHCO$_{3(aq)}$ (20 mL) was added and the aqueous layer was extracted with CH$_2$Cl$_2$

(3 x 20 mL). The combined organic extracts were dried (Na₂SO₄) and evaporated under reduced pressure to give the crude product. Purification by flash column chromatography on silica with 50:50 hexane-EtOAc, then EtOAc and then 80:20 EtOAc-MeOH as eluent gave pyrrolidine *cis*-**48** (242 mg, 52%) as a red oil, R_F (50:50 hexane-EtOAc) 0.16; IR (ATR) 1724 (C=O, CO₂CMe₃), 1631 (C=O, NC(O)Me), 1418, 1368, 1154 cm^{-1}; ^{1}H NMR (400 MHz, CDCl₃) (65:35 mixture of rotamers) δ 4.10 (ddq, J = 6.5, 6.5, 6.5 Hz, 0.65H, NC*H*Me), 4.00 (dd, J = 12.5, 8.5 Hz, 0.35H, NCH), 3.97-3.90 (m, 0.35H, NC*H*Me), 3.70 (dd, J = 10.5, 7.5 Hz, 0.65H, NCH), 3.60 (dd, J = 10.5, 8.0 Hz, 0.65H, NCH), 3.52 (dd, J = 12.5, 7.0 Hz, 0.35H, NCH), 2.96-2.84 (m, 1H, C*H*CO₂Me), 2.44-2.29 (m, 1H, CH), 2.05 (s, 1.05H, NC(O)Me), 2.03 (s, 1.95H, NC(O)Me), 2.00-1.94 (m, 0.35H, CH), 1.82 (ddd, J = 13.5, 7.5, 6.0 Hz, 0.65H, CH), 1.44 (s, 5.85H, CMe₃), 1.43 (s, 3.15H, CMe₃), 1.22 (d, J = 6.5 Hz, 3H, CHMe); ^{13}C NMR (100.6 MHz, CDCl₃) (rotamers) 172.5 (C=O, NC(O)Me), 172.2 (C=O, NC(O)Me), 169.08 (C=O, CO₂CMe₃), 169.05 (C=O, CO₂CMe₃), 81.5 (*C*Me₃), 81.3 (*C*Me₃), 53.8 (N*C*HMe), 52.9 (N*C*HMe), 49.3 (NCH₂), 47.2 (NCH₂), 43.5 (*C*HCO₂), 42.2 (*C*HCO₂), 36.7 (CH₂), 36.2 (CH₂), 28.1 (C*Me*₃), 23.2 (NC(O)*Me*), 21.8 (Me), 21.7 (Me), 20.0 (C*Me*); MS (ESI) *m/z* 228 [(M + H)$^+$, 15], 250 [(M + Na)$^+$, 100]; HRMS (ESI) *m/z* calcd for C₁₂H₂₁NO₃ (M + Na)$^+$ 250.1414, found 250.1425 (–4.5 ppm error).

Lab Book Reference: TD 3/53

***tert*-Butyl 1-methanesulfonyl-2-methylpyrrolidine-4-carboxylate *cis*-47**

cis-**47**
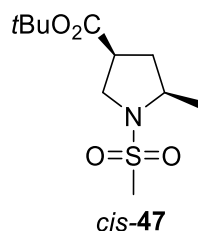
Methanesulfonyl chloride (0.032 mL, 1.0 eq, 0.40 mmol) was added dropwise to a stirred solution of pyrrolidine salt *cis*-**45**•AcOH (100 mg, 1.0 eq, 0.40 mmol) in pyridine (10 mL) at 0 °C. The resulting solution was stirred at 0 °C for 1 h then allowed to warm to rt and stirred at rt for 16 h. The resulting mixture was evaporated under reduced pressure to give the crude product. Purification by flash column chromatography on silica with 50:50 hexane-EtOAc as eluent gave pyrrolidine *cis*-**47** (89 mg, 83%) as a red oil, R_F (50:50 hexane-EtOAc) 0.32; IR (ATR) 1725 (C=O), 1332, 1150 cm^{-1}; ^{1}H NMR (400 MHz, CDCl₃) δ 3.90 (ddq, J = 6.5, 6.5, 6.5 Hz, 1H, NC*H*Me), 3.70 (dd, J = 11.0, 8.0 Hz, 1H, NCH), 3.54 (dd, J = 11.0, 8.5 Hz, 1H, NCH), 2.97-2.88 (m, 1H, CHCO₂), 2.87 (s, 3H, SO₂Me), 2.41 (ddd, J = 13.0, 7.5, 6.5 Hz, 1H, CH), 1.88 (ddd, J = 13.0, 9.0, 6.5 Hz, 1H, CH), 1.46 (s, 9H, CMe₃), 1.36 (d,

J = 6.5 Hz, 3H, CH*Me*); ^{13}C NMR (100.6 MHz, CDCl$_3$) δ 171.4 (C=O), 81.7 (*C*Me$_3$), 56.2 (N*C*HMe), 50.2 (N*C*H$_2$), 43.7 (*C*HCO$_2$), 37.8 (SO$_2$Me), 37.6 (CH$_2$), 28.1 (C*Me*$_3$), 22.0 (CH*Me*); MS (ESI) *m/z* 286 [(M + Na)$^+$, 100]; HRMS (ESI) *m/z* calcd for C$_{11}$H$_{21}$NO$_4$S (M + Na)$^+$ 286.1083, found 286.1085 (–0.5 ppm error).

Lab Book Reference: TD 3/55
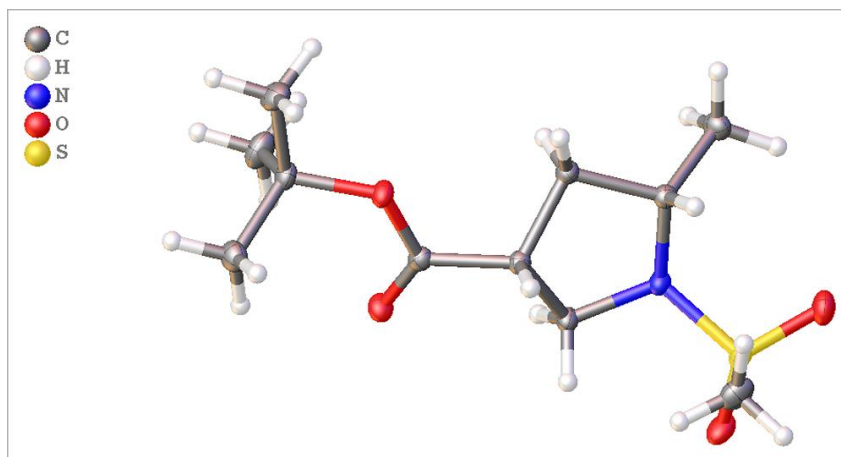
Table 5.1 Crystal data and structure refinement for *cis*-47.

Identification code	paob1913
Empirical formula	$C_{11}H_{21}NO_4S$
Formula weight	263.35
Temperature/K	110.00(10)
Crystal system	monoclinic
Space group	$P2_1/c$
a/Å	5.95574(9)
b/Å	9.69965(14)
c/Å	23.4296(3)
α/°	90
β/°	96.7003(13)
γ/°	90
Volume/Å^3	1344.25(3)
Z	4
ρ_{calc}g/cm^3	1.301
μ/mm^{-1}	0.244
F(000)	568.0
Crystal size/mm^3	$0.364 \times 0.126 \times 0.042$
Radiation	MoKα (λ = 0.71073)
2Θ range for data collection/°	6.726 to 59.15
Index ranges	-8 ≤ h ≤ 8, -13 ≤ k ≤ 13, -32 ≤ l ≤ 32
Reflections collected	15370
Independent reflections	3778 [R_{int} = 0.0278, R_{sigma} = 0.0248]
Data/restraints/parameters	3778/0/159
Goodness-of-fit on F^2	1.047
Final R indexes [I>=2σ (I)]	R_1 = 0.0328, wR_2 = 0.0812
Final R indexes [all data]	R_1 = 0.0392, wR_2 = 0.0853
Largest diff. peak/hole / e Å^{-3}	0.36/-0.40

5.2.3 Synthetic Procedures for Chapter 3

Methyl 2-trifluoromethylsulfonylcyclopent-1-ene-1-carboxylate 197
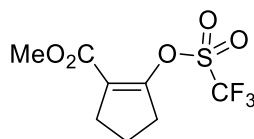
197

Using general procedure **B**, *i*Pr$_2$NEt (12.9 mL, 73.9 mmol, 5.0 eq), ester **193** (2.01 g, 14.8 mmol, 1.0 eq) and trifluoromethanesulfonic anhydride (2.98 mL, 17.7 mmol, 1.2 eq) in CH$_2$Cl$_2$ (100 mL) gave the crude product. Purification by flash column chromatography with 70:30 hexane-Et$_2$O as eluent gave enol triflate **197** (3.55 g, 92%) as an orange oil, R_F (70:30 hexane-Et$_2$O) 0.24; ^{1}H NMR (400 MHz, CDCl$_3$) δ 3.78 (s, 3H, OMe), 2.77-2.66 (m, 4H, CH$_2$), 2.01 (tt, J = 7.5, 7.5 Hz, 2H, CH$_2$); ^{13}C NMR (100.6 MHz, CDCl$_3$) δ 162.8 (C=O), 154.1 (=CO), 123.1 (=*C*CO$_2$Me), 118.4 (q, J = 320.0 Hz, CF$_3$), 51.9 (OMe), 32.8 (CH$_2$), 29.2 (CH$_2$), 18.9 (CH$_2$). Spectroscopic data are consistent with those reported in the literature.[81]

Lab Book Reference: TD 4/36

1-*tert*-Butyl-3-methyl 4-hydroxy-1,2,5,6-tetrahydropyridine-1,3-dicarboxylate 196a
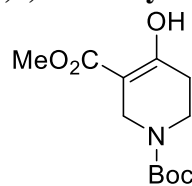
196a

Et$_3$N (6.33 mL, 45.5 mmol, 2.0 eq) was added dropwise to a stirred solution of methyl 4-oxopiperidine-3-carboxylate hydrochloride (4.40 g, 22.72 mmol, 1.0 eq) in THF (100 mL) at rt under Ar. The resulting solution was stirred at rt for 10 min. Then, di-*tert*-butyl dicarbonate (5.46 g, 25.0 mmol, 1.1 eq) was added to the stirred solution at rt under Ar. The resulting solution was stirred at rt for 16 h and then the solvent was evaporated under reduced pressure. The residue was dissolved in CH$_2$Cl$_2$ (100 mL) and washed with H$_2$O (2 x 100 mL). The organic layer was dried (Na$_2$SO$_4$) and evaporated under reduced pressure to give the crude product. Purification by flash column chromatography on silica with 80:20 hexane-EtOAc as eluent gave tetrahydropyridine **196a** (5.57 g, 95%) as a white solid, mp 46-50 °C; R_F (EtOAc) 0.67; ^{1}H NMR (400 MHz, CDCl$_3$) δ 11.97 (s, 1H, OH), 4.05 (br s, 2H, NCH$_2$), 3.78 (s, 3H, OMe), 3.56 (t, J = 6.0 Hz, 2H, NCH$_2$), 2.37 (t, J = 6.0 Hz, 2H, CH$_2$), 1.47 (s, 9H, CMe$_3$); ^{13}C NMR (100.6 Hz, CDCl$_3$) δ 171.4 (C=O, CO$_2$Me), 169.8 (=COH), 154.4 (C=O, Boc), 96.1 (=C), 80.1 (*C*Me$_3$), 51.6 (OMe), 40.4 (NCH$_2$), 39.2 (NCH$_2$), 28.9 (CH$_2$),

28.5 (C*Me*₃). The crude material was sufficiently pure for use without further purification. Spectroscopic data are consistent with those reported in the literature.[116]

1-*tert*-Butyl-3-methyl 4-trifluoromethylsulfonyl-1,2,5,6-tetyrahydropyridine-1,3-dicarboxylate 200

200
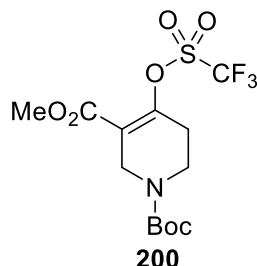
Using general procedure **B**, *i*Pr₂NEt (18.9 mL, 108.2 mmol, 5.0 eq), ester **196** (5.57 g, 21.6 mmol, 1.0 eq) and trifluoromethanesulfonic anhydride (4.37 mL, 26.0 mmol, 1.2 eq) in CH₂Cl₂ (200 mL) gave the crude product. Purification by flash column chromatography with 80:20 hexane-EtOAc as eluent gave enol triflate **200** (7.57 g, 90%) as a yellow solid, mp 42-45 °C; R_F (80:20 hexane-EtOAc) 0.27; IR (ATR) 1722 (C=O, CO₂Me), 1701 (C=O, Boc), 1609 (C=C), 1421, 1207 cm⁻¹; ¹H NMR (400 MHz, CDCl₃) δ 4.26 (br s, 2H, NCH₂), 3.82 (s, 3H, OMe), 3.61 (t, *J* = 5.5 Hz, 2H, NCH₂), 2.50 (tt, *J* = 5.5, 2.5 Hz, 2H, CH₂), 1.46 (s, 9H, C*Me*₃); ¹³C NMR (100.6 MHz, CDCl₃) δ 162.9 (C=O, CO₂Me), 154.1 (C=O, Boc), 150.9 (=CO), 120.5 (=C), 118.3 (q, *J* = 320 Hz, CF₃), 81.1 (*C*Me₃), 52.5 (OMe), 43.1 (NCH₂), 39.4 (NCH₂), 29.0 (CH₂), 28.4 (C*Me*₃); MS (ESI) *m/z* 412 [(M + Na)⁺, 100]; HRMS (ESI) *m/z* calcd for C₁₃H₁₈F₃NO₇S (M + Na)⁺ 412.0648, found 412.0648 (+0.2 ppm error).

Lab Book Reference: TD 3/99

1-*tert*-Butyl 4-methyl 3-phenyl-2,5-dihydro-1H-pyrrole-1,4-dicarboxylate 210

210
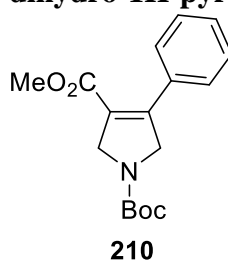
Procedure with THF as solvent

K₂CO₃ (1.84 g, 13.3 mmol, 2.5 eq) was added portionwise to a stirred mixture of enol triflate **99** (2.00 g, 5.33 mmol, 1.0 eq) and phenylboronic acid (975 mg, 7.99 mmol, 1.5 eq) in THF (50 mL) at rt. The reaction flask was evacuated under reduced pressure and back-filled with Ar three times. Then, Pd(PPh₃)₄ (616 mg, 0.53 mmol, 0.1 eq, 10 mol%) was added and the resulting mixture was stirred and heated at 65 °C for 40 h. The mixture was allowed to cool to rt and H₂O (100 mL) was added. The aqueous layer was extracted with EtOAc (3 x 100

mL). The combined organic extracts were dried (Na_2SO_4) and evaporated under reduced pressure to give the crude product. Purification by flash column chromatography on silica with 90:10 hexane-EtOAc as eluent gave dihydropyrrole **210** (528 mg, 33%) as a white solid, mp 119-122 °C; R_F (80:20 hexane-EtOAc) 0.28; IR (ATR) 1712 (C=O, CO_2Me), 1693 (C=O, Boc), 1646 (C=C), 1404, 1122 cm^{-1}; ^{1}H NMR (400 MHz, CDCl$_3$) (55:45 mixture of rotamers) δ 7.38-7.35 (m, 5H, Ph), 4.60-4.48 (m, 4H, NCH), 3.66 (s, 3H, OMe), 1.49 (s, 4.95H, CMe$_3$), 1.47 (s, 4.05H, CMe$_3$); ^{13}C NMR (100.6 MHz, CDCl$_3$) (rotamers) δ 174.0 (C=O, CO_2Me), 173.9 (C=O, CO_2Me), 153.8 (C=O, Boc), 148.5 (=CPh), 132.9 (*ipso*-Ph), 132.8 (*ipso*-Ph), 129.3 (Ph), 129.2 (Ph), 128.2 (Ph), 128.0 (Ph), 123.5 (=CCO$_2$Me), 80.1 (*C*Me$_3$), 80.0 (*C*Me$_3$), 58.4 (NCH$_2$), 58.1 (NCH$_2$), 54.8 (NCH$_2$), 54.6 (NCH$_2$), 51.7 (OMe), 51.6 (OMe), 29.8 (C*Me*$_3$), 28.6 (C*Me*$_3$); MS (ESI) *m/z* 326 [(M + Na)$^+$, 100]; HRMS (ESI) *m/z* calcd for C$_{17}$H$_{21}$NO$_4$ (M + Na)$^+$ 326.1363, found 326.1369 (–1.2 ppm error).

Lab Book Reference: TD 3/68

Procedure using 4:1 THF–H$_2$O as solvent

Using general procedure **C**, enol triflate **99** (1.00 g, 2.66 mmol, 1.0 eq), phenylboronic acid (488 mg, 4.00 mmol, 1.5 eq), Pd(PPh$_3$)$_4$ (308 mg, 0.266 mmol, 0.1 eq) and K$_2$CO$_3$ (920 mg, 6.66 mmol, 2.5 eq) in THF (80 mL) and H$_2$O (20 mL) gave the crude product. Purification by flash column chromatography with 90:10 hexane-EtOAc gave ester **210** (666 mg, 83%) as a white solid.

Lab Book Reference: TD 3/86

1-*tert*-Butyl-4-methyl 3-(2-furyl)-2,5-dihydro-1H-pyrrole-1,4-dicarboxylate 211
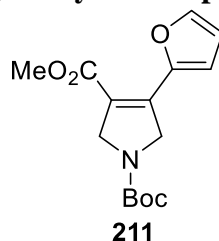
Using general procedure **C**, enol triflate **99** (1.74 g, 4.62 mmol, 1.0 eq), 2-furylboronic acid (776 mg, 6.93 mmol, 1.5 eq), Pd(PPh$_3$)$_4$ (534 mg, 0.462 mmol, 0.1 eq) and K$_2$CO$_3$ (1.60 g, 11.6 mmol, 2.5 eq) in THF (80 mL) and H$_2$O (20 mL) gave the crude product. Purification by flash column chromatography with 90:10 hexane-EtOAc gave ester **211** (980 mg, 72%) as a white solid, mp 135-138 °C; R_F 0.16 (90:10 hexane-EtOAc); IR (ATR) 1701 (C=O, Boc, CO$_2$Me), 1623 (C=C), 1406, 1245; ^{1}H NMR (400 MHz, CDCl$_3$) (50:50 mixture of rotamers) δ 7.78 (d, *J* = 3.5 Hz, 0.5H, Ar), 7.72 (d, *J* = 3.5 Hz, 0.5H, Ar), 7.49 (br s, 1H, Ar), 6.56-6.52 (m, 1H, Ar), 4.78-4.74 (m, 1H, NCH$_2$), 4.73-4.69 (m, 1H, NCH$_2$), 4.54-4.50 (m,

1H, NCH$_2$), 4.49-4.45 (m, 1H, NCH$_2$), 3.81 (s, 1.5H, OMe), 3.80 (s, 1.5H, OMe), 1.514 (s, 4.5H, CMe_3), 1.510 (s, 4.5H, CMe_3); ^{13}C NMR (100.6 MHz, CDCl$_3$) (rotamers) δ 163.50 (C=O, CO$_2$Me), 163.46 (C=O, CO$_2$Me), 153.9 (C=O, Boc), 153.8 (C=O, Boc), 147.6 (*ipso*-Ar), 144.0 (Ar), 143.7 (Ar), 136.6 (=CAr), 119.1 (=CCO$_2$Me), 118.8 (=CCO$_2$Me), 116.9 (Ar), 112.5 (Ar), 112.4 (Ar), 80.0 (CMe$_3$), 55.2 (NCH$_2$), 54.4 (NCH$_2$), 54.3 (NCH$_2$), 51.7 (OMe), 51.6 (OMe), 28.6 (CMe_3); MS (ESI) *m/z* 316 [(M + Na), 100]; HRMS (ESI) *m/z* calcd for C$_{15}$H$_{19}$NO$_5$ (M + Na)$^+$ 316.1155, found 316.1150 (+1.2 ppm error).

Lab Book Reference: TD 4/66

1-*tert*-Butyl-4-methyl 3-(2-fluorophenyl)-2,5-dihydro-1H-pyrrole-1,4-dicarboxylate 212

212
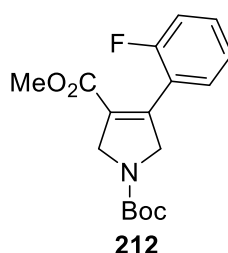
Using general procedure **C**, enol triflate **99** (709 g, 1.97 mmol, 1 eq.), 2-fluorophenylboronic acid (414 mg, 2.96 mmol, 1.5 eq), Pd(PPh$_3$)$_4$ (228 mg, 0.20 mmol, 0.1 eq) and K$_2$CO$_3$ (681 mg, 4.93 mmol, 2.5 eq) in THF (16 mL) and H$_2$O (4 mL) gave the crude product. Purification by flash column chromatography on silica with 80:20 hexane-EtOAc as solvent gave ester **212** (363 mg, 57%) as a yellow solid, mp 121-124 °C; R_F (80:20 hexane-EtOAc) 0.24; IR (ATR) 1715 (C=O, CO$_2$Me), 1692 (C=O, Boc), 1653 (C=C), 1408, 1123 cm^{-1}; ^{1}H NMR (400 MHz, CDCl$_3$) (50:50 mixture of rotamers) δ 7.37-7.30 (m, 1H, Ar), 7.27-7.20 (m, 1H, Ar), 7.17-7.11 (m, 1H, Ar), 7.11-7.05 (m, 1H, Ar), 4.57-4.46 (m, 4H, NCH$_2$), 3.64 (s, 3H, OMe), 1.49 (s, 4.5H, CMe_3), 1.45 (s, 4.5H, CMe_3); ^{13}C NMR (100.6 MHz, CDCl$_3$) (rotamers) δ 163.2 (C=O, CO$_2$Me), 163.1 (C=O, CO$_2$Me), 159.4 (d, J = 249.0 Hz, CF), 154.0 (C=O, Boc), 153.8 (C=O, Boc), 142.7 (=CAr), 142.52 (=CAr), 130.71 (d, J = 8.5 Hz, Ar), 130.68 (d, J = 8.5 Hz, Ar), 129.7 (d, J = 2.5 Hz, Ar), 129.5 (d, J = 2.5 Hz, Ar), 126.94 (=CCO$_2$Me), 126.85 (=CCO$_2$Me), 123.9 (br s, Ar), 121.2 (d, J = 15.5 Hz, *ipso*-Ar), 115.8 (d, J = 22.0 Hz, Ar), 80.1 (CMe$_3$), 80.0 (CMe$_3$), 57.8 (d, J = 1.5 Hz, NCH$_2$), 57.6 (d, J = 1.5 Hz, NCH$_2$), 54.2 (NCH$_2$), 53.9 (NCH$_2$), 51.7 (OMe), 28.5 (CMe_3); MS (ESI) *m/z* 344 [(M + Na), 100]; HRMS (ESI) *m/z* calcd for C$_{17}$H$_{20}$FNO$_4$ (M + Na)$^+$ 344.1269, found 344.1271 (–0.8 ppm error).

Lab Book Reference: TD 5/23

Methyl 2-(3-pyridyl)-cyclopent-1-enecarboxylate 213
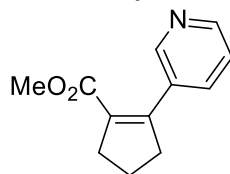
213

Using general procedure **C**, enol triflate **197** (100 mg, 0.37 mmol, 1.0 eq), 3-pyridyl boronic acid (67 mg, 0.55 mmol, 1.5 eq), Pd(PPh₃)₄ (42 mg, 0.037 mmol, 0.1 eq) and K₂CO₃ (126 mg, 0.91 mmol, 2.5 eq) in THF (4 mL) and H₂O (1 mL) gave the crude product. Purification by flash column chromatography with 50:50 hexane-EtOAc gave ester **213** (26 mg, 35%) as a yellow oil, R_F (50:50 hexane-EtOAc) 0.18; IR (ATR) 2950, 1709 (C=O), 1632 (C=C), 1434, 1234 cm⁻¹; ¹H NMR (400 MHz, CDCl₃) δ 8.55 (br s, 1H, Ar), 8.51 (br d, J = 4.5 Hz, 1H, Ar), 7.67 (ddd, J = 8.0, 2.0, 2.0 Hz, 1H, Ar), 7.26 (dd, 8.0, 4.5 Hz, 1H, Ar), 3.63 (s, 3H, OMe), 2.86 (m, 4H, =CCH₂), 2.02 (tt, J = 8.0, 8.0 Hz, 2H, CH₂); ¹³C NMR (400 MHz, CDCl₃) δ 166.0 (C=O), 150.4 (=*C*Ar), 148.9 (Ar), 148.7 (Ar), 135.3 (Ar), 132.9 (*ipso*-Ar), 130.9 (=*C*CO₂Me), 122.7 (Ar), 51.4 (OMe), 40.0 (=C*C*H₂), 35.1 (=C*C*H₂), 21.9 (CH₂); MS (ESI) *m/z* 204 [(M + H), 100]; HRMS (ESI) *m/z* calcd for C₁₂H₁₃NO₂ (M + H)⁺ 204.1019, found 204.1022 (–1.3 ppm error).

Methyl 2-(5-pyrimidyl)-cyclopent-1-enecarboxylate 214
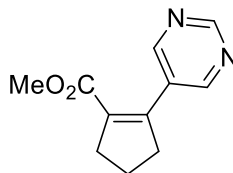
214

Using general procedure **C**, triflate **197** (200 mg, 0.73 mmol, 1.0 eq), pyrimidine-5-boronic acid (136 mg, 1.09 mmol, 1.5 eq), Pd(PPh₃)₄ (84 mg, 0.073 mmol, 0.1 eq) and K₂CO₃ (252 mg, 1.83 mmol, 2.5 eq) in THF (8 mL) and H₂O (2 mL) gave the crude product. Purification by flash column chromatography with 50:50 hexane-EtOAc gave ester **214** (122 mg, 81%) as a white solid, mp 79-82 °C; R_F (50:50 hexane-EtOAc) 0.17; IR (ATR) 1708 (C=O), 1630 (C=C), 1416, 1254 cm⁻¹; ¹H NMR (400 MHz, CDCl₃) δ 9.13 (s, 1H, Ar), 8.72 (s, 2H, Ar), 3.66 (s, 3H, OMe), 2.88 (m, 4H, =CCH₂), 2.06 (tt, J = 7.5, 7.5 Hz, 2H, CH₂); ¹³C NMR (100.6 MHz, CDCl₃) δ 165.5 (C=O), 157.8 (Ar), 155.6 (Ar), 146.8 (=*C*Ar), 132.9 (=*C*CO₂Me), 131.0 (*ipso*-Ar), 51.6 (OMe), 39.7 (=C*C*H₂), 35.0 (=C*C*H₂), 21.9 (CH₂); MS (ESI) *m/z* 205 [(M + H), 100]; HRMS (ESI) *m/z* calcd for C₁₁H₁₂N₂O₂ (M + H)⁺ 205.0972, found 205.0974 (–0.3 ppm error).

Lab Book Ref.: TD 4/38

Lab Book Reference: TD 4/41

Methyl 2-(3-*N*-methylpyrazole)-cyclopent-1-enecarboxylate 215

215
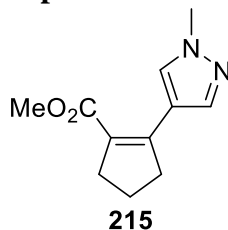
Using general procedure **C**, enol triflate **197** (100 mg, 0.37 mmol, 1.0 eq), 3-(*N*-methylpyrazole)boronic acid (69 mg, 0.55 mmol, 1.5 eq), Pd(PPh₃)₄ (42 mg, 0.037 mmol, 0.1 eq) and K₂CO₃ (126 mg, 0.91 mmol, 2.5 eq) in THF (4 mL) and H₂O (1 mL) gave the crude product. Purification by flash column chromatography with 50:50 hexane-EtOAc gave ester **215** (66 mg, 88%) as an orange oil, R_F (50:50 hexane-EtOAc) 0.19; IR (ATR) 2950, 1708 (C=O), 1631 (C=C), 1234 cm^{-1}; ^{1}H NMR (400 MHz, CDCl₃) δ 8.37 (s, 1H, Ar), 7.74 (s, 1H, Ar), 3.91 (s, 3H, NMe), 3.75 (s, 3H, OMe), 2.89 (tt, J = 8.0 Hz, 2.0 Hz, 2H, =CCH₂), 2.77 (tt, J = 8.0 Hz, 2.0 Hz, 2H, =CCH₂), 1.91 (tt, J = 8.0, 8.0 Hz, 2H, CH₂); ^{13}C NMR (100.6 MHz, CDCl₃) δ 166.8 (C=O), 145.2 (=*C*Ar), 140.5 (Ar), 132.4 (Ar), 123.7 (=*C*CO₂Me), 117.2 (*ipso*-Ar), 51.2 (OMe), 39.1 (NMe), 38.5 (=CCH₂), 34.9 (=CCH₂), 21.6 (CH₂); MS (ESI) *m/z* 207 [(M + H), 100], 229 [(M + Na), 66]; HRMS (ESI) *m/z* calcd for C₁₁H₁₄N₂O₂ (M + H)$^+$ 207.1128, found 207.1126 (+0.8 ppm error).

Lab Book Ref.: TD 4/42

Methyl 2-(3-thiophenyl)cyclopent-2-enecarboxylate 216

216
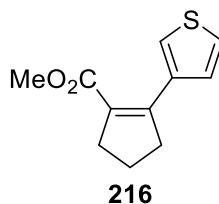
Using general procedure **C**, enol triflate **197** (2.00 g, 7.29 mmol, 1 eq.), 3-thiopheneboronic acid (1.40 g, 10.94 mmol, 1.5 eq), Pd(PPh₃)₄ (842 mg, 0.73 mmol, 0.1 eq) and K₂CO₃ (2.52 g, 18.23 mmol, 2.5 eq) in THF (0 mL) and H₂O (10 mL) gave the crude product. Purification by flash column chromatography on silica with 90:10 hexane–Et₂O as eluent gave ester **216** (1.23 g, 81%) as a yellow oil, R_F (90:10 hexane–Et₂O) 0.22; IR (ATR) 2948, 1711 (C=O), 1196 cm^{-1}; ^{1}H NMR (400 MHz, CDCl₃) δ 7.65 (dd, J = 3.0, 1.5 Hz, 1H, Ar), 7.36 (dd, J = 5.0, 1.5 Hz, 1H, Ar), 7.24 (dd, J = 5.0, 3.0 Hz, 1H, Ar), 3.71 (s, 3H, OMe), 2.89 (tt, J = 7.5, 2.0 Hz, 2H, =CCH₂), 2.80 (tt, J = 7.5, 2.0 Hz, 2H, =CCH₂), 1.93 (tt, J = 7.5, 7.5 Hz, 2H, CH₂); ^{13}C NMR (100.6 MHz, CDCl₃) δ 167.0 (C=O), 146.6 (=*C*Ar), 136.7 (*ipso*-Ar), 128.4

(Ar), 127.4 (=CCO$_2$Me), 125.9 (Ar), 124.4 (Ar), 51.4 (OMe), 39.6 (=CCH$_2$), 35.6 (=CCH$_2$), 21.8 (CH$_2$); MS (ESI) *m/z* 231 [(M + Na)$^+$, 100]; HRMS (ESI) *m/z* calcd for C$_{11}$H$_{12}$SO$_2$ (M + Na)$^+$ 231.0450, found 231.0448 (+0.8 ppm error).

Lab Book Reference: TD 4/81

1-*tert*-Butyl-4-methyl 3-phenyl-1,2,3,6-tetrahydropyridine-1,4-dicarboxylate 201
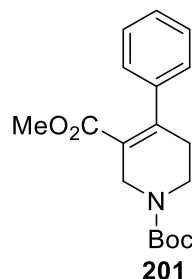
Using general procedure **C**, enol triflate **200** (200 mg, 0.51 mmol, 1 eq.), phenylboronic acid (94 mg, 0.77 mmol, 1.5 eq), Pd(PPh$_3$)$_4$ (59 mg, 0.05 mmol, 0.1 eq) and K$_2$CO$_3$ (178 mg, 1.29 mmol, 2.5 eq) in THF (10 mL) and H$_2$O (2.5 mL) gave the crude product. Purification by flash column chromatography on silica with 80:20 hexane–EtOAc as eluent gave ester **201** (140 g, 86%) as an orange oil, R_F (70:30 hexane-EtOAc) 0.19; IR (ATR) 1705 (C=O, CO$_2$Me), 1696 (C=O, Boc) 1628 (C=C) cm^{-1}; ^{1}H NMR (400 MHz, CDCl$_3$) (rotamers) δ 7.35-7.29 (m, 3H, Ph), 7.14-7.10 (m, 2H, Ph), 4.24 (br s, 2H, NCH$_2$), 3.60 (br t, J = 5.5 Hz, 2H, NCH_2CH$_2$), 3.47 (s, 3H, OMe), 2.53-2.46 (m, 2H, CH$_2$), 1.49 (m, 9H, CMe_3); ^{13}C NMR (100.6 MHz, CDCl$_3$) (rotamers) δ 167.2 (C=O, CO$_2$Me), 154.8 (C=O, Boc) , 146.7 (=CAr), 141.8 (*ipso*-Ar), 129.7 (Ar), 128.32 (Ar), 128.25 (Ar), 127.7 (Ar), 126.7 (Ar), 120.7 (Ar), 115.4 (=CCO$_2$Me), 80.3 (CMe$_3$), 51.5 (OMe), 44.0 (NCH$_2$), 43.8 (NCH$_2$), 38.88 (NCH$_2$CH$_2$), 38.85 (NCH$_2$CH$_2$), 32.9 (CH$_2$), 32.8 (CH$_2$), 28.6 (CMe_3); MS (ESI) *m/z* 318 [(M + H)$^+$, 5], 340 [(M + Na)$^+$, 100]; HRMS (ESI) *m/z* calcd for C$_{18}$H$_{23}$NO$_4$ (M + Na)$^+$ 340.1519, found 340.1520 (+0.1 ppm error).

Lab Book Reference: TD 4/2

1-*tert*-Butyl-4-methyl 3-(5-pyrimidyl)-1,2,3,6-tetrahydropyridine-1,4-dicarboxylate 217

217
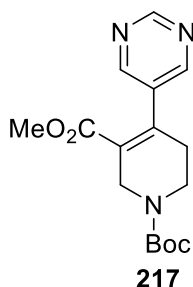
KHCO$_3$ (1.07 g, 10.7 mmol, 2.5 eq) was added portionwise to a stirred mixture of enol triflate **200** (2.00 g, 5.36 mmol, 1.0 eq) and 5-pyrimidylboronic acid (790 mg, 6.43 mmol, 1.5 eq) in THF (75 mL) and H$_2$O (25 mL) at rt. The reaction flask was evacuated under reduced pressure and back-filled with Ar three times. Then, Pd(dppf)Cl$_2$ (198 mg, 0.27 mmol, 0.05 eq) was added and the resulting mixture was stirred and heated at 65 °C for 2 h. The mixture was allowed to cool to rt and the solids were removed by filtration through Celite. H$_2$O (100 mL) was added and the aqueous layer was extracted with EtOAc (3 x 100 mL). The combined organic extracts were dried (Na$_2$SO$_4$) and evaporated under reduced pressure to give the crude product. Purification by flash column chromatography on silica that had been washed with 99:1 EtOAc–Et$_3$N with EtOAc as eluent gave ester **217** (976 mg, 57%) as a brown oil, R_F (EtOAc) 0.26; IR (ATR) 1710 (C=O, CO$_2$Me), 1694 (C=O, Boc), 1625 (C=C); ^{1}H NMR (400 MHz, CDCl$_3$) (rotamers) δ 9.14 (s, 1H, Ar), 8.52 (s, 2H, Ar), 4.29 (br s, 2H, NCH$_2$), 3.63 (br t, J = 5.5 Hz, 2H, NC*H*$_2$CH$_2$), 3.55 (s, 3H, OMe), 2.53-2.45 (m, 2H, CH$_2$), 1.49 (m, 9H, C*Me*$_3$); ^{13}C NMR (100.6 MHz, CDCl$_3$) (rotamers) δ 167.5 (C=O, CO$_2$Me), 158.8 (Ar), 158.4 (Ar), 157.8 (=*C*Ar), 155.6 (=*C*Ar), 155.2 (Ar), 154.6 (Ar), 140.1 (*ipso*-Ar), 139.3 (*ipso*-Ar), 125.2 (=*C*CO$_2$Me), 84.0 (*C*Me$_3$), 53.0 (NCH$_2$), 52.7 (NCH$_2$), 51.8 (OMe), 37.8 (NCH$_2$), 28.4 (CH$_2$), 28.1 (C*Me*$_3$); MS (ESI) *m/z* 319 [(M + H)$^+$, 100]; HRMS (ESI) *m/z* calcd for C$_{16}$H$_{21}$N$_3$O$_4$ (M + Na)$^+$ 319.1532, found 319.1529 (–0.9 ppm error).

Lab Book Reference: TD 4/51

Methyl 3-(4-fluorophenyl)-2,5-dihydrofuran-4-carboxylate 219

219
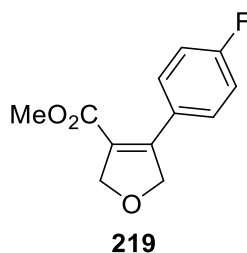
Using general procedure **B**, β-ketoester **194** (203 mg, 1.41 mmol, 1 eq), iPr$_2$NEt (1.23 mL, 7.05 mmol, 5 eq) and trifluoromethanesulfonic anhydride (0.285 mL, 1.69 mmol, 1.2 eq) in CH$_2$Cl$_2$ (25 mL) gave the crude product. Purification by flash column chromatography with 80:20 hexane–EtOAc as eluent gave enol triflate **204** (331 mg) as a brown oil, ^{1}H NMR (400 MHz, CDCl$_3$) for enol triflate **204**: δ 4.89 (t, J = 5.0 Hz, 2H, OCH$_2$), 4.77 (t, J =5.0 Hz, 2H, OCH$_2$), 3.81 (s, 3H, OMe). Using general procedure **C**, enol triflate **204** (331 mg, 1.20 mmol, 1 eq), 4-fluorophenylboronic acid (252 mg, 1.80 mmol, 1.5 eq), Pd(PPh$_3$)$_4$ (138 mg, 0.12 mmol, 0.1 eq) and K$_2$CO$_3$ (414 mg, 3.00 mmol, 2.5 eq) in THF (16 mL) and H$_2$O (4 mL) gave the crude product. Purification by flash column chromatography on silica with 90:10 hexane-EtOAc as eluent gave ester **219** (168 g, 53% over two steps) as a white solid, mp 68-70 °C, R_F (90:10 hexane-EtOAc) 0.18; IR (ATR) 1725 (C=O), 1645 (C=C), 830 cm^{-1}; ^{1}H NMR (400 MHz, CDCl$_3$) δ 7.53-7.45 (m, 2H, Ar), 7.09-7.03 (m, 2H, Ar), 5.05-4.99 (m, 4H OCH$_2$), 3.70 (s, 3H, OMe); ^{13}C NMR (100.6 MHz, CDCl$_3$) δ 163.3 (C=O), 163.2 (d, J = 250 Hz, CF), 148.3 (=CAr), 130.5 (d, J = 8.5 Hz, Ar), 127.4 (d, J = 3.5 Hz, $ipso$-Ar), 124.3 (=CCO$_2$Me), 115.3 (d, J = 21.5 Hz, Ar), 79.8 (OCH$_2$), 77.5 (OCH$_2$), 51.7 (OMe); MS (ESI) m/z 245 [(M + Na)$^+$, 100]; HRMS (ESI) m/z calcd for C$_{12}$H$_{11}$O$_3$F (M + Na)$^+$ 245.0584, found 245.0580 (+1.9 ppm error).

Lab Book Reference: TD 4/50

Methyl 3-(2-tolyl)-2,5-dihydrofuran-4-carboxylate 220
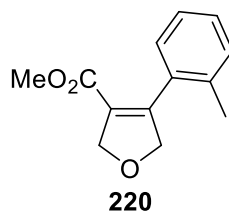
220

Using general procedure **B**, β-ketoester **194** (522 mg, 3.62 mmol, 1 eq), iPr$_2$NEt (3.15 mL, 18.1 mmol, 5 eq) and trifluoromethanesulfonic anhydride (0.731 mL, 4.34 mmol, 1.2 eq) in CH$_2$Cl$_2$ (50 mL) gave the crude product. Purification by flash column chromatography with 80:20 hexane–EtOAc as eluent gave enol triflate **204** (831 mg) as a brown oil. Using general

procedure **C**, enol triflate **204** (831 mg, 3.01 mmol, 1 eq), 2-tolylboronic acid (613 mg, 4.51 mmol, 1.5 eq), Pd(PPh$_3$)$_4$ (347 mg, 0.30 mmol, 0.1 eq) and K$_2$CO$_3$ (1.04 g, 7.52 mmol, 2.5 eq) in THF (40 mL) and H$_2$O (10 mL) gave the crude product. Purification by flash column chromatography on silica with 80:20 hexane-EtOAc as eluent gave a 60:40 mixture (by ^{1}H NMR spectroscopy) of ester **220** and 4-fluorophenyl boronic acid (312 mg, i.e. 220 mg (28%) of ester **220** over 2 steps) and ester **220** (128 g, 16% over 2 steps) as an orange oil, R_F (80:20 hexane-EtOAc) 0.10; IR (ATR) 1712 (C=O), 1648 (C=C), 1140 cm^{-1}; ^{1}H NMR (400 MHz, CDCl$_3$) δ 7.25-7.15 (m, 3H, Ar), 7.08-7.04 (m, 1H, Ar), 5.04 (d, J = 5.0 Hz, 1H, OCH), 5.03 (d, J = 5.0 Hz, 1H, OCH), 4.91 (d, J = 5.0 Hz, 1H, OCH), 4.89 (d, J = 5.0 Hz 1H, OCH), 3.59 (s, 3H, OMe), 2.25 (s, 3H, CMe); ^{13}C NMR (100.6 MHz, CDCl$_3$) δ 162.8 (C=O), 151.3 (=CAr), 135.4 (*ipso*-Ar), 132.1 (*ipso*-Ar), 130.1 (Ar), 128.4 (Ar), 127.2 (Ar), 126.4 (=CCO$_2$Me), 125.6 (Ar), 80.5 (OCH$_2$), 76.5 (OCH$_2$), 51.5 (OMe), 19.6 (CMe); MS (ESI) m/z 219 [(M + H)$^+$, 3], 241 [(M + Na)$^+$, 100]; HRMS (ESI) m/z calcd for C$_{13}$H$_{14}$O$_3$ (M + Na)$^+$ 241.0835, found 241.0832 (+1.2 ppm error).

Lab Book Reference: TD 4/91

Methyl 3-(3-pyridyl)-2,5-dihydrofuran-4-carboxylate 221
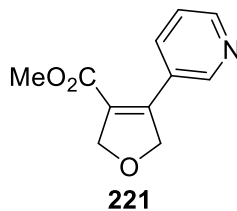
221

Using general procedure **B**, β-ketoester **194** (522 mg, 3.62 mmol, 1 eq), iPr$_2$NEt (3.15 mL, 18.1 mmol, 5 eq) and trifluoromethanesulfonic anhydride (0.731 mL, 4.34 mmol, 1.2 eq) in CH$_2$Cl$_2$ (50 mL) gave the crude product. Purification by flash column chromatography with 80:20 hexane–EtOAc as eluent gave enol triflate **204** (847 mg) as a brown oil. Using general procedure **C**, enol triflate **204** (847 mg, 3.07 mmol, 1 eq), 3-pyridylboronic acid (566 mg, 4.60 mmol, 1.5 eq), Pd(PPh$_3$)$_4$ (354 mg, 0.30 mmol, 0.1 eq) and K$_2$CO$_3$ (1.06 g, 0.30 mmol, 2.5 eq) in THF (40 mL) and H$_2$O (10 mL) gave the crude product. Purification by flash column chromatography on silica with 50:50 hexane-EtOAc as eluent gave ester **221** (184 mg, 23%) as an orange oil, R_F (50:50 hexane-EtOAc) 0.14; IR (ATR) 1718 (C=O), 1638 (C=C), 1223; ^{1}H NMR (400 MHz, CDCl$_3$) δ 8.62 (ddd, J = 2.0, 1.5, 1.5 Hz, 1H, Ar), 8.57 (ddd, J = 5.0, 1.5, 1.5 Hz, 1H, Ar), 7.85 (ddd, J = 8.0, 2.0, 1.5 Hz, Ar), 7.32 (ddd, J = 8.0, 5.0, 1.5 Hz, 1H, Ar), 5.09-5.05 (m, 2H, OCH$_2$), 5.04-5.01 (m, 2H, OCH$_2$), 3.69 (s, 3H, OMe); ^{13}C NMR (100.6 MHz, CDCl$_3$) δ 162.9 (C=O), 150.1 (Ar), 148.8 (Ar), 146.0 (=CAr), 136.1

(Ar), 127.7 (*ipso*-Ar or =CCO$_2$Me), 126.5 (*ipso*-Ar or =CCO$_2$Me), 123.1 (Ar), 79.5 (OCH$_2$), 77.4 (OCH$_2$), 51.8 (OMe); MS (ESI) *m/z* 206 [(M + H)$^+$, 100]; HRMS (ESI) *m/z* calcd for C$_{11}$H$_{11}$NO$_3$ (M + H)$^+$ 206.0812, found 206.0813 (–0.7 ppm error).

Lab Book Reference: TD 4/92

Methyl 4-(3-fluorophenyl)-5,6-dihydro-2*H*-tetrahydropyran-3-carboxylate 223

223
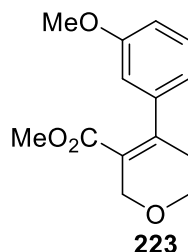
Using general procedure **B**, *β*-ketoester **195** (546 mg, 3.45 mmol, 1 eq), *i*Pr$_2$NEt (3.00 mL, 17.3 mmol, 5 eq) and trifluoromethanesulfonic anhydride (0.696 mL, 4.14 mmol, 1.2 eq) in CH$_2$Cl$_2$ (50 mL) gave the crude product. Purification by flash column chromatography with 80:20 hexane–EtOAc as eluent gave enol triflate **218** (812 mg) as a brown oil, ^{1}H NMR (400 MHz, CDCl$_3$) for enol triflate **218**: *δ* 4.43 (t, *J* = 2.5 Hz, 2H, OCH$_2$), 3.87 (t, *J* = 5.5 Hz, OCH$_2$), 3.80 (s, 3H, OMe), 2.52 (tt, *J* = 5.0, 2.5 Hz, 2H, CH$_2$). Using general procedure **C**, enol triflate **218** (812 mg, 2.80 mmol, 1 eq.), 3-methoxyphenylboronic acid (637 mg, 4.20 mmol, 1.5 eq), Pd(PPh$_3$)$_4$ (243 mg, 0.21 mmol, 0.05 eq) and K$_2$CO$_3$ (966 mg, 7.00 mmol, 2.5 eq) in THF (40 mL) and H$_2$O (10 mL) gave the crude product. Purification by flash column chromatography on silica with 80:20 hexane-EtOAc as eluent gave ester **223** (447 mg, 52%) as a yellow oil, R_F (80:20 hexane-EtOAc) 0.15; IR (ATR) 1711 (C=O), 1642 (C=C), 1413 ^{1}H NMR (400 MHz, CDCl$_3$) *δ* 7.25 (dd, *J* = 8.0, 8.0 Hz, 1H, Ar), 6.83 (ddd, *J* = 8.0, 2.5, 1.0 Hz, 1H, Ar), 6.74-6.71 (m, 1H, Ar), 6.68 (dd, *J* = 2.5, 1.5 Hz, 1H, Ar), 4.43 (t, *J* = 2.5 Hz, 2H, OCH$_2$), 3.88 (t, *J* = 5.5 Hz, 2H, OCH_2CH$_2$), 3.79 (s, 3H, ArOMe), 3.49 (s, 3H, CO$_2$Me), 2.49 (tt, *J* = 5.5, 2.5 Hz, 2H, CH$_2$); ^{13}C NMR (100.6 MHz, CDCl$_3$) *δ* 166.6 (C=O), 159.4 (*ipso*-Ar), 146.0 (=CAr), 142.9 (*ipso*-Ar), 129.3 (Ar), 126.08 (=CCO$_2$Me), 119.3 (Ar), 113.0 (Ar), 112.5 (Ar), 65.8 (OCH$_2$CH$_2$), 64.2 (OCH$_2$), 55.3 (ArOMe), 51.5 (CO$_2$$Me$), 32.4 (CH$_2$); MS (ESI) *m/z* 271 [(M + Na)$^+$, 100]; HRMS (ESI) *m/z* calcd for C$_{14}$H$_{16}$O$_4$ (M + Na)$^+$ 271.0941, found 271.0941 (+0.1 ppm error).

Lab Book Reference: TD 5/14

1-*tert*-Butyl 4-methyl 3-phenylpyrrolidine-1,4-dicarboxylate *cis*-224
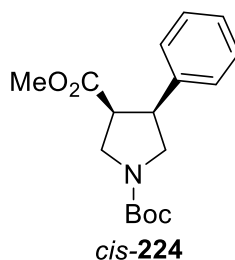
cis-**224**

Using general procedure **A**, dihydropyrrole **210** (258 mg, 0.84 mmol) and 10% Pd/C (26 mg, 0.02 mmol, 0.03 eq) in MeOH (10 mL) for 16 h gave pyrrolidine *cis*-**224** (260 mg, 97%) as a yellow oil, R_F (80:20 hexane-EtOAc) 0.27; IR (ATR) 1735 (C=O, CO_2Me), 1691 (C=O, Boc), 1398, 1161 cm^{-1}; ^{1}H NMR (400 MHz, CDCl$_3$) (50:50 mixture of rotamers) δ 7.33-7.27 (m, 2H, Ph), 7.26-7.22 (m, 1H, Ph), 7.20-7.14 (m, 2H, Ph), 3.85-3.62 (m, 5H, NCH, C*H*Ph), 3.45-3.36 (m, 4H, OMe, C*H*CO$_2$Me), 1.51 (s, 4.5H, CMe$_3$), 1.50 (s, 4.5H, CMe$_3$); ^{13}C NMR (100.6 MHz, CDCl$_3$) (rotamers) δ 171.8 (C=O, CO_2Me), 171.7 (C=O, CO_2Me), 154.4 (C=O, Boc), 138.6 (*ipso*-Ph), 138.4 (*ipso*-Ph), 128.6 (Ph), 127.6 (Ph), 127.4 (Ph), 79.84 (*C*Me$_3$), 79.80 (*C*Me$_3$), 51.6 (OMe), 50.4 (NCH$_2$), 50.3 (NCH$_2$), 48.9 (*C*HCO$_2$Me), 48.0 (*C*HCO$_2$Me), 47.1 (NCH$_2$), 47.0 (NCH$_2$), 46.5 (*C*HPh), 45.5 (*C*HPh), 28.6 (C*Me*$_3$); MS (ESI) *m/z* 328 [(M + Na)$^+$, 100]; HRMS (ESI) *m/z* calcd for C$_{17}$H$_{23}$NO$_4$ (M + Na)$^+$ 328.1519, found 328.1520 (–0.6 ppm error).

Lab Book Reference: TD 3/69

1-*tert*-Butyl-3-methyl 4-phenylpiperidine-1,3-dicarboxylate *cis*-225
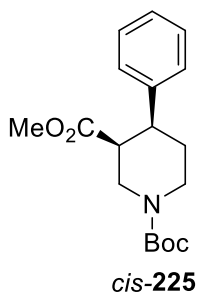
cis-**225**

Using general procedure **A**, tetrahydropyridine **201** (85 mg, 0.27 mmol) and 10% Pd(OH)$_2$/C (9 mg, 0.006 mmol, 0.02 eq) in MeOH (10 mL) for 16 h gave piperidine *cis*-**225** (85 mg, quant.) as a yellow oil, IR (ATR) 1731 (C=O, CO_2Me), 1693 (C=O, Boc), 1423, 761 cm^{-1}; ^{1}H NMR (400 MHz, CDCl$_3$) δ 7.30-7.24 (m, 2H, Ph), 7.23-7.16 (m, 3H, Ph), 4.56-4.16 (m, 2H, NCH), 3.45 (s, 3H, OMe), 3.25-3.05 (m, 1H, NCH), 2.97 (ddd, *J* = 12.5, 4.0, 4.0 Hz, 1H, C*H*Ph), 2.93-2.78 (m, 2H, NCH, C*H*CO$_2$Me), 2.70-2.57 (m, 1H, CH), 1.76-1.67 (m, 1H, CH), 1.44 (s, 9H, CMe$_3$); ^{13}C NMR (100.6 MHz, CDCl$_3$) (rotamers) δ 172.1 (C=O, CO_2Me), 155.0 (C=O, Boc), 154.9 (C=O, Boc) 137.43 (*ipso*-Ph), 137.37 (*ipso*-Ph), 128.8 (Ph), 127.6

(Ph), 127.5 (Ph), 127.0 (Ph), 79.7 (CMe$_3$), 52.0 (OMe), 46.1 (NCH$_2$), 45.9 (NCH$_2$), 44.7 (NCH$_2$), 43.2 (CHCO$_2$Me), 37.6 (CHPh), 28.1 (CMe_3), 25.0 (CH$_2$); MS (ESI) m/z 320 [(M + H)$^+$, 6], 342 [(M + Na)$^+$, 100]; HRMS (ESI) m/z calcd for C$_{18}$H$_{25}$NO$_4$ (M + Na)$^+$ 342.1676, found 342.1678 (–0.7 ppm error).

Lab Book Reference: TD 4/47
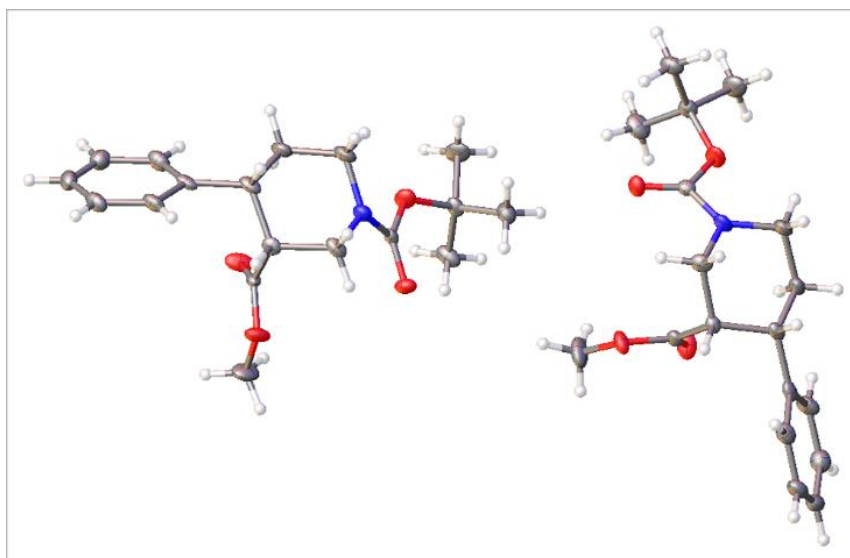
Table 4.2 Crystal data and structure refinement for *cis*-225.

Identification code	TD 4/47
Empirical formula	$C_{18}H_{25}NO_4$
Formula weight	319.39
Temperature/K	110.00(10)
Crystal system	orthorhombic
Space group	$Pca2_1$
a/Å	19.7482(5)
b/Å	5.66608(19)
c/Å	30.5147(11)
α/°	90
β/°	90
γ/°	90
Volume/Å^3	3414.43(19)
Z	8
ρ_{calc}g/cm^3	1.243
μ/mm^{-1}	0.708
F(000)	1376.0
Crystal size/mm^3	$0.339 \times 0.048 \times 0.015$
Radiation	CuKα (λ = 1.54184)
2Θ range for data collection/°	8.956 to 134.144
Index ranges	$-23 \leq h \leq 17, -6 \leq k \leq 6, -35 \leq l \leq 36$
Reflections collected	11627
Independent reflections	5473 [R_{int} = 0.0390, R_{sigma} = 0.0472]
Data/restraints/parameters	5473/1/423
Goodness-of-fit on F^2	1.076
Final R indexes [I>=2σ (I)]	R_1 = 0.0863, wR_2 = 0.2119
Final R indexes [all data]	R_1 = 0.0942, wR_2 = 0.2244
Largest diff. peak/hole / e Å^{-3}	1.07/-0.30
Flack parameter	0.1(3)

3-Methyl-1-*tert*-butyl 4-(5-pyrimidyl)piperidine-1,3-dicarboxylate *cis*-226
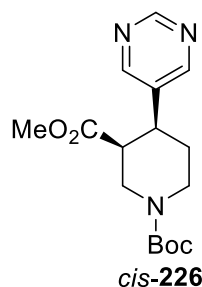
cis-**226**

Using general procedure **A**, tetrahydropyridine **217** (1.94 g, 6.07 mmol) and 10% Pd/C (46 mg, 0.04 mmol, 0.01 eq) in MeOH (50 mL) for 40 h gave piperidine *cis*-**226** (1.93 g, 99%) as a yellow oil, IR (ATR) 1733 (C=O, CO$_2$Me), 1687 (C=O, Boc), 1415, 1156 cm^{-1}; ^{1}H NMR (400 MHz, CDCl$_3$) δ 9.07 (s, 1H, Ar), 8.64 (s, 2H, Ar) 4.67-4.16 (m, 2H, NCH), 3.52 (s, 3H, OMe), 3.27-3.05 (m, 1H, NCH), 3.27-3.05 (m, 1H, NCH), 2.98 (ddd, J = 12.5, 4.0, 4.0 Hz, 1H, C*H*Ar), 2.94-2.77 (m, 2H, NCH, C*H*CO$_2$Me), 2.77-2.60 (m, 1H, CH), 1.76-1.68 (m, 1H, CH), 1.44 (s, 9H, CMe$_3$); ^{13}C NMR (100.6 MHz, CDCl$_3$) δ 171.4 (C=O, CO$_2$Me), 157.3 (Ar), 156.4 (Ar), 155.3 (C=O, Boc), 135.7 (*ipso*-Ar), 80.1 (*C*Me$_3$), 51.8 (OMe), 46.8 (NCH$_2$), 45.0 (NCH$_2$ or *C*HCO$_2$Me) , 44.7 (NCH$_2$ or *C*HCO$_2$Me), 39.4 (*C*HAr), 28.4 (C*Me*$_3$), 24.8 (CH$_2$); MS (ESI) *m/z* 322 [(M + H)$^+$, 12], 344 [(M + Na)$^+$, 100]; HRMS (ESI) *m/z* calcd for C$_{16}$H$_{23}$N$_3$O$_4$ (M + Na)$^+$ 344.1581, found 344.1573 (+2.1 ppm error).

Lab Book Reference: TD 5/25

Methyl 1-acetyl-3-phenylpyrrolidine-4-carboxylate *cis*-227
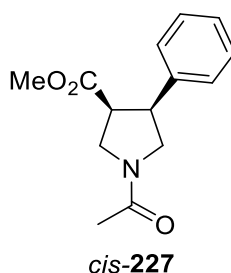
cis-**227**

TFA (2.0 mL, 26.1 mmol, 32.0 eq) was added dropwise to a stirred solution of pyrrolidine *cis*-**224** (253 mg, 0.83 mmol, 1.0 eq) in CH$_2$Cl$_2$ (10 mL) at rt under Ar. The resulting solution was stirred at rt for 16 h. Then, the solvent was evaporated under reduced pressure to give the crude amine•TFA salt. Et$_3$N (1.16 mL, 8.29 mmol, 10.0 eq) was then added dropwise to a stirred solution of the crude amine•TFA salt in CH$_2$Cl$_2$ (10 mL) at rt under Ar. The resulting solution was stirred at rt for 10 min. Then, acetyl chloride (0.18 mL, 2.49 mmol, 3.0 eq) was added dropwise and the resulting solution was stirred at rt for 16 h. Then, the solvent was evaporated under reduced pressure to give the crude product. Purification by flash column chromatography on silica with EtOAc and then 80:20 EtOAc-MeOH as eluent gave

pyrrolidine *cis*-**227** (101 mg, 49%) as a colourless oil, R_F (EtOAc) 0.10; IR (ATR) 1731 (C=O, CO$_2$Me), 1639 (C=O, NC(O)Me), 1420, 1209 cm^{-1}; ^{1}H NMR (400 MHz, CDCl$_3$) (50:50 mixture of rotamers) δ 7.33-7.20 (m, 3H, Ph), 7.17-7.08 (m, 2H, Ph), 3.99-3.83 (m, 3H, NCH or C*H*Ph), 3.79-3.67 (m, 2H, NCH or C*H*Ph), 3.50 (ddd, J = 7.5, 7.5, 7.5 Hz, 0.5 H, C*H*CO$_2$Me), 3.43-3.36 (m, 3.5H, C*H*CO$_2$Me, CO$_2$Me), 2.13 (s, 1.5H, NC(O)Me), 2.12 (s, 1.5H, NC(O)Me); ^{13}C NMR (100.6 MHz, CDCl$_3$) (rotamers) 171.8 (C=O, NC(O)Me), 171.2 (C=O, NC(O)Me), 169.42 (C=O, CO$_2$Me), 169.38 (C=O, CO$_2$Me), 138.2 (*ipso*-Ph), 137.6 (*ipso*-Ph), 128.72 (Ph), 128.66 (Ph), 127.7 (Ph), 127.6 (Ph), 127.42 (Ph), 127.39 (Ph), 51.73 (OMe), 51.65 (OMe), 51.4 (NCH$_2$), 50.2 (NCH$_2$), 49.1 (*C*HCO$_2$Me), 48.0 (NCH$_2$), 47.6 (*C*HCO$_2$Me), 47.4 (NCH$_2$), 46.7 (*C*HPh), 44.9 (*C*HPh), 22.6 (NC(O)*Me*), 22.50 (NC(O)*Me*); MS (ESI) *m/z* 248 [(M + H)$^+$, 14], 270 [(M + Na)$^+$, 100]; HRMS (ESI) *m/z* calcd for C$_{14}$H$_{17}$NO$_3$ (M + Na)$^+$ 270.1101, found 270.1103 (–1.1 ppm error).

Lab Book Reference: TD 3/72

1-Ethyl-4-hydroxymethyl-3-phenylpyrrolidine *cis*-231
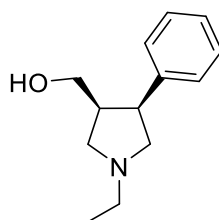
cis-**231**

A suspension of LiAlH$_4$ (22 mg, 0.57 mmol, 2.0 eq.) in THF (2 mL) was added dropwise to a stirred solution of ester *cis*-**227** (70 mg, 0.28 mmol, 1.0 eq.) in THF (5 mL) at 0 °C under Ar. The resulting mixture was stirred at 0 °C for 2 h. Then, H$_2$O (0.1 mL), 2 M NaOH$_{(aq)}$ (0.2 mL) and H$_2$O (0.1 mL) were added sequentially. The solids were removed by filtration through Celite and the filtrate was dried (MgSO$_4$) and evaporated under reduced pressure to give a mixture of products containing alcohol *cis*-**231** (28 mg). Diagnostic signals for *cis*-**231**: ^{1}H NMR (400 MHz, CDCl$_3$) δ 7.35-7.26 (m, 4H, Ph), 7.22-7.17 (m, 1H, Ph), 3.56 (ddd, J = 8.5, 8.5, 8.5 Hz, 1H, C*H*Ph), 3.39 (br s, 1H, OH), 3.37 (dd, J = 10.5, 5.5 Hz, 1H, HOC*H*), 3.20 (dd, J = 10.5, 5.5 Hz, 1H, HOC*H*), 2.96-2.89 (m, 3H, NCH), 2.68 (dd, J = 11.0, 5.5 Hz, 1H, NCH$_2$) 2.57 (q, J = 7.0 Hz, 2H, NC*H*$_2$Me), 2.56-2.48 (m, 1H, C*H*Ph), 1.13 (t, J = 7.0 Hz, 3H, NCH$_2$*Me*).

Lab Book Reference: TD 4/4

1-Acetyl-4-hydroxymethyl-3-phenylpyrrolidine *cis*-228
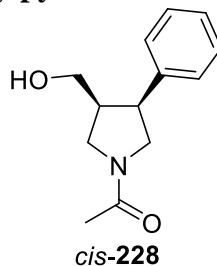
cis-**228**

LiBH$_4$ (1.21 mL of a 4 M solution in THF, 4.85 mmol, 4.0 eq.) was added dropwise to a stirred solution of ester *cis*-**227** (300 mg, 1.21 mmol, 1.0 eq) in THF (5 mL) at 0 °C under Ar. The solution was allowed to warm to rt and then stirred at rt for 16 h. Then, H$_2$O (0.3 mL) and 2 M NaOH$_{(aq)}$ (0.6 mL) were added sequentially and the mixture was evaporated under reduced pressure. The residue was dissolved in EtOAc (10 mL) and then washed with H$_2$O (2 x 10 mL), dried (Na$_2$SO$_4$) and evaporated under reduced pressure to give the crude product. Purification by flash column chromatography on silica with 50:50 hexane-EtOAc as eluent gave alcohol *cis*-**228** (97 mg, 37%) as an orange oil, R_F (50:50 hexane-EtOAc) 0.16; IR (ATR) 3371 (OH), 2936, 1621 (C=O), 1456, 1423 cm^{-1}; ^{1}H NMR (400 MHz, CDCl$_3$) (50:50 mixture of rotamers) δ 7.37-7.27 (m, 3H, Ph), 7.20-7.14 (m, 2H, Ph), 3.89-3.85 (m, 1H, NCH), 3.82-3.62 (m, 2H, NCH), 3.62-3.47 (m, 1.5H, C*H*Ph, NCH), 3.47-3.40 (m, 1H, NCH, C*H*HO), 3.33-3.29 (m, 1H, HOC*H*), 3.27-3.21 (m, 0.5H, HOC*H*), 2.78 (ddddd, *J* = 7.0, 7.0, 7.0, 7.0, 7.0 Hz, 0.5H, C*H*CH$_2$OH), 2.70 (ddddd, *J* = 7.0, 7.0, 7.0, 7.0, 7.0 Hz, 0.5H, C*H*CH$_2$OH), 2.14 (s, 1.5 H, NC(O)Me), 2.13 (s, 1.5 H, NC(O)Me); ^{13}C NMR (100.6 MHz, CDCl$_3$) (rotamers) δ 169.8 (C=O), 169.7 (C=O), 139.1 (*ipso*-Ph), 138.9 (*ipso*-Ph), 128.9 (Ph), 128.8 (Ph), 127.8 (Ph), 127.7 (Ph), 127.3 (Ph), 127.2 (Ph), 61.6 (HOCH$_2$), 61.4 (HOCH$_2$), 52.9 (NCH$_2$), 50.2 (NCH$_2$), 49.2 (NCH$_2$), 47.5 (NCH$_2$), 45.7 (*C*HCH$_2$OH), 45.5 (*C*HCH$_2$OH), 44.1 (*C*HPh), 44.0 (*C*HPh), 22.5 (NC(O)*Me*); MS (ESI) *m/z* 220 [(M + H)$^+$, 15], 242 [(M + Na)$^+$, 100], 258 [(M + K)$^+$, 9]; HRMS (ESI) *m/z* calcd for C$_{13}$H$_{17}$NO$_2$ (M + Na)$^+$ 242.1151, found 242.1152 (–0.2 ppm error).

Lab Book Reference: TD 4/40

1-Acetyl-3-phenylpyrrolidine-4-carboxylic acid *trans*-229 and *cis*-229

trans-**229**   *cis*-**229**
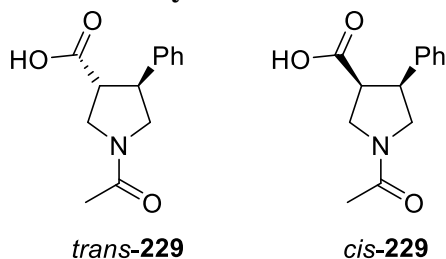
LiOH (12 mg, 0.61 mmol, 3.0 eq) was added portionwise to a stirred solution of ester *cis*-**227** (50 mg, 0.20 mmol, 1 eq) in 4:1:1 THF–H_2O–MeOH (3 mL) at rt under Ar. The resulting mixture was stirred at rt for 16 h. Then, the solvent was evaporated under reduced pressure and H_2O (5 mL) was added. The mixture was washed with CH_2Cl_2 (5 mL) and then 1 M $HCl_{(aq)}$ (5 mL) was added. The mixture was extracted with CH_2Cl_2 (2 x 10 mL) and the combined organic extracts were dried (Na_2SO_4) and evaporated under reduced pressure to give a mixture of products containing a 85:15 mixture by ^{1}H NMR spectroscopy of pyrrolidines *trans*-**229** and *cis*-**229** (13 mg) as a yellow oil. Diagnostic signals for 85:15 mixture of *trans*-**229** and *cis*-**229**, ^{1}H NMR (400 MHz, CDCl$_3$) (55:45 mixture of rotamers for *trans*-**229**, 50:50 mixture of rotamers for *cis*-**229**) δ 7.35-7.19 (m, 5H, Ar), 4.05-3.67 (m, 3.55H, NCH, C*H*Ph), 3.64 (ddd, J = 7.5, 7.5, 7.5 Hz, 0.45H, C*H*Ph), 3.55-3.48 (m, 1H, NCH), 3.40 (ddd, J = 7.5, 7.5, 5.0 Hz, 0.15H, C*H*CO$_2$H), 3.25 (ddd, J = 8.5, 8.5, 8.5 Hz, 0.40H, C*H*CO$_2$H), 3.18 (ddd, J = 8.5, 8.5, 8.5 Hz, 0.45H, C*H*CO$_2$H), 2.11 (s, 0.22H, NC(O)Me), 2.10 (s, 0.23H, NC(O)Me), 2.07 (s, 1.2H, NC(O)Me), 2.04 (s, 1.35H, NC(O)Me). Spectroscopic data for *trans*-**229** were consistent with a sample independently synthesised by another group member.[83]

Lab Book reference: TD 3/73

LiOH (12 mg, 0.58 mmol, 3.0 eq) was added portionwise to a stirred solution of ester *cis*-**227** (48 mg, 0.19 mmol, 1 eq) in 4:1:1 THF–H_2O–MeOH (3 mL) at rt under Ar. The resulting mixture was stirred at rt for 2 h. Then, the solvent was evaporated under reduced pressure and H_2O (5 mL) was added. The mixture was washed with CH_2Cl_2 (5 mL) and then 1M $HCl_{(aq)}$ (5 mL) was added. The mixture was extracted with CH_2Cl_2 (2 x 10 mL) and the combined organic extracts were dried (Na_2SO_4) and evaporated under reduced pressure to give a mixture of products containing a 75:25 mixture (by ^{1}H NMR spectroscopy) of pyrrolidines *trans*-**229** and *cis*-**229** (39 mg) as a yellow oil.

Lab Book Reference: TD 4/3

Methyl 2-(3-*N*-methylpyrazole)cyclopentane-1-carboxylate *cis*-254
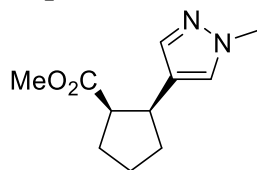
cis-**254**

Using general procedure **A**, cyclopentene **215** (830 mg, 4.02 mmol, 1.0 eq) and 10% Pd/C (83 mg, 0.08 mmol, 0.02 eq) in MeOH (50 mL) for 112 h gave cyclopentane *cis*-**254** (775 mg, 92%) as an orange oil, IR (ATR) 2949, 1727 (C=O), 1167 cm^{-1}; ^{1}H NMR (400 MHz, CDCl$_3$) δ 7.28 (s, 1H, Ar), 7.14 (s, 1H, Ar), 3.83 (s, 3H, NMe), 3.43 (s, 3H, OMe), 3.33 (ddd, *J* = 7.5, 7.5, 7.5 Hz, 1H, C*H*Ar), 3.04 (ddd, *J* = 7.5, 7.5, 7.5 Hz, 1H, C*H*CO$_2$Me), 2.10-1.85 (m, 5H, CH), 1.76-1.66 (m, 1H, CH); ^{13}C NMR (100.6 MHz, CDCl$_3$) δ 175.2 (C=O), 138.5 (Ar), 128.2 (Ar), 121.9 (*ipso*-Ar), 51.2 (OMe), 49.5 (*C*HCO$_2$Me), 39.4 (*C*HAr), 38.9 (NMe), 32.7 (*C*H$_2$CH), 27.9 (*C*H$_2$CH), 24.2 (CH$_2$*C*H$_2$CH$_2$); MS (ESI) *m/z* 209 [(M + H)$^+$, 100], 231 [(M + Na)$^+$, 46]; HRMS (ESI) *m/z* calcd for C$_{11}$H$_{16}$N$_2$O$_2$ (M + H)$^+$ 209.1285, found 209.1285 (–0.2 ppm error).

Lab Book Reference: TD 4/59

1-Hydroxymethyl-2-(3-*N*-methylpyrazole)cyclopentane *cis*-252
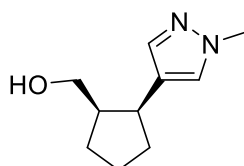
cis-**252**

A suspension of LiAlH$_4$ (219 mg, 5.76 mmol, 2.0 eq.) in THF (5 mL) was added dropwise to a stirred solution of ester *cis*-**254** (600 mg, 2.88 mmol, 1.0 eq.) in THF (10 mL) at 0 °C under Ar. The resulting mixture was stirred at 0 °C for 2 h. Then, H$_2$O (0.6 mL), 2 M NaOH$_{(aq)}$ (1.2 mL) and H$_2$O (0.6 mL) were added sequentially. The solids were removed by filtration through Celite and the filtrate was dried (MgSO$_4$) and evaporated under reduced pressure to give alcohol *cis*-**252** (503 mg, 98%) as a colourless oil, IR (ATR) 3342 (br, OH), 2946, 2871, 1401 cm^{-1}; ^{1}H NMR (400 MHz, CDCl$_3$) δ 7.32 (s, 1H, Ar), 7.16 (s, 1H, Ar), 3.86 (s, 3H, NMe), 3.41-3.32 (m, 2H, HOC*H*), 3.20 (ddd, *J* = 7.0, 7.0, 7.0 Hz, C*H*Ar), 2.26 (ddddd, *J* = 7.0, 7.0, 7.0, 7.0, 7.0 Hz, 1H, C*H*CH$_2$OH), 2.05-1.96 (m, 1H, CH), 1.88-1.78 (m, 2H, CH), 1.77-1.65 (m, 2H, CH), 1.48-1.37 (m, 1H, CH), 1.33 (br s, 1H, OH); ^{13}C NMR (100.6 MHz, CDCl$_3$) δ 138.7 (Ar), 128.4 (Ar), 122.4 (*ipso*-Ar), 64.3 (HOCH$_2$), 45.9 (*C*HCH$_2$OH), 38.9 (NMe), 37.2 (*C*HAr), 32.6 (*C*H$_2$CH), 27.7 (*C*H$_2$CH), 23.5

(CH$_2$CH$_2$CH$_2$); MS (ESI) *m/z* 181 [(M + H)$^+$, 100], 203 [(M + Na)$^+$, 18]; HRMS (ESI) *m/z* calcd for C$_{10}$H$_{16}$N$_2$O (M + H)$^+$ 181.1335, found 181.134 (+0.7 ppm error).

Lab Book Reference: TD 4/61

1-Fluoromethyl-2-(3-*N*-methylpyrazole)cyclopentane *cis*-253
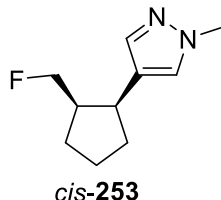
cis-**253**

PyFluor (249 mg, 1.54 mmol, 1.1 eq) was added portionwise to a stirred solution of alcohol *cis*-**252** (253 mg, 1.40 mmol, 1.0 eq) and DBU (0.418 mL, 2.80 mmol, 2.0 eq) in toluene (2 mL) at rt under Ar. The resulting solution was stirred and heated at 70 °C for 64 h. The mixture was then allowed to cool to rt and CH$_2$Cl$_2$ (2 mL) was added. Purification by flash column chromatography on silica with 50:50 hexane-EtOAc as eluent gave cyclopentane *cis*-**253** (57 mg, 22%) as a colourless oil, R_F (50:50 hexane-EtOAc) 0.30; IR (ATR) 2953, 1444, 1399, 986 cm^{-1}; ^{1}H NMR (400 MHz, CDCl$_3$) δ 7.25 (s, 1H, Ar), 7.11 (s, 1H, Ar), 4.13 (ddd, *J* = 47.5, 9.0, 6.5 Hz, 1H, CHF), 4.09 (ddd, *J* = 47.5, 9.0, 7.0 Hz, 1H, CHF), 3.82 (s, 3H, NMe), 3.18 (ddd, *J* = 7.0, 7.0, 7.0 Hz, 1H, C*H*Ar), 2.42-2.47 (m, 1H, C*H*CH$_2$F), 2.03-1.92 (m, 1H, CH), 1.87-1.64 (m, 4H, CH), 1.53-1.42 (m, 1H, CH); ^{13}C NMR (100.6 MHz, CDCl$_3$) δ 138.7 (Ar), 128.6 (Ar), 121.6 (*ipso*-Ar), 85.3 (d, *J* = 165.5 Hz, CH$_2$F), 43.7 (d, *J* = 18.0 Hz, *C*HCH$_2$F), 38.8 (NMe), 37.1 (d, *J* = 4.5 Hz, *C*HAr), 32.5 (CH$_2$), 26.7 (d, *J* = 4.5 Hz, CH$_2$), 23.3 (CH$_2$); MS (ESI) *m/z* 183 [(M + H)$^+$, 100], 205 [(M + Na)$^+$, 7]; HRMS (ESI) *m/z* calcd for C$_{10}$H$_{15}$N$_2$F (M + H)$^+$ 183.1292, found 183.1291 (+0.8 ppm error).

Lab Book Reference: TD 4/87

Methyl 2-(3-pyridyl)cyclopentanecarboxylate *cis*-250
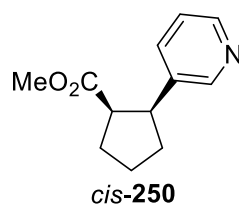
cis-**250**

Using general procedure **A**, cyclopentene **213** (197 mg, 0.97 mmol, 1.0 eq) and 10% Pd/C (20 mg, 0.02 mmol, 0.02 eq) in MeOH (10 mL) for 40 h gave cyclopentane *cis*-**250** (130 mg, 63%) as a yellow oil, R_F (50:50 hexane-EtOAc) 0.33; IR (ATR) 2951, 1728 (C=O), 1197, 1169 cm^{-1}; ^{1}H NMR (400 MHz, CDCl$_3$) δ 8.45-8.38 (m, 2H, Ar), 7.49 (ddd, J = 8.0, 4.0, 2.0 Hz, 1H, Ar), 7.20-7.15 (m, 1H, Ar), 3.43-3.34 (m, 1H, C*H*Ar), 3.23 (s, 3H, OMe), 3.20-3.13 (m, 1H, C*H*CO$_2$Me), 2.14-1.94 (m, 5H, CH), 1.78-1.66 (m, 1H, CH); ^{13}C NMR (100.6 MHz, CDCl$_3$) δ 174.7 (C=O), 149.9 (Ar), 147.9 (Ar), 137.2 (*ipso*-Ar), 135.1 (Ar), 123.0 (Ar), 51.2 (OMe), 49.6 (*C*HCO$_2$Me), 46.5 (*C*HAr), 31.1 (CH$_2$), 28.7 (CH$_2$), 24.8 (CH$_2$); MS (ESI) *m/z* 206 [(M + H)$^+$, 100]; HRMS (ESI) *m/z* calcd for C$_{12}$H$_{15}$NO$_2$ (M + H)$^+$ 206.1176, found 206.1172 (+1.6 ppm error).

Lab Book Reference: TD 5/1

1-Hydroxymethyl-2-(3-pyridyl)cyclopentane *cis*-249

cis-**249**
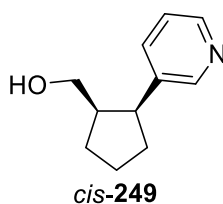
A suspension of LiAlH$_4$ (37 mg, 0.97 mmol, 2.0 eq.) in THF (2 mL) was added dropwise to a stirred solution of ester *cis*-**250** (100 mg, 0.487 mmol, 1.0 eq.) in THF (3 mL) at 0 °C under Ar. The resulting mixture was stirred at 0 °C for 2 h. Then, H$_2$O (0.1 mL), 2 M NaOH$_{(aq)}$ (0.2 mL) and H$_2$O (0.1 mL) were added sequentially. The solids were removed by filtration through Celite and the filtrate was dried (MgSO$_4$) and evaporated under reduced pressure to give alcohol *cis*-**249** (72 mg, 83%) as a colourless oil, IR (ATR) 3269 (OH), 2950, 2871, 1425 cm^{-1}; ^{1}H NMR (400 MHz, CDCl$_3$) δ 8.42 (br s, 1H, Ar), 8.37 (br s, 1H, Ar), 7.50 (d, J = 8.0 Hz, 1H, Ar), 7.23-7.15 (m, 1H, Ar), 3.28 (ddd, J = 7.5, 7.5, 7.5 Hz, 1H, C*H*Ar), 3.22 (dd, J = 10.5, 7.5 Hz, 1H, HOC*H*), 3.17 (dd, J = 10.5, 7.5 Hz, 1H, HOC*H*), 2.39 (ddddd, J = 7.5, 7.5, 7.5, 7.5, 7.5 Hz, 1H, C*H*CH$_2$OH), 2.14 (br s, 1H, OH), 2.11-2.02 (m, 1H, CH), 1.97-1.83 (m, 3H, CH), 1.79-1.68 (m, 1H, CH), 1.60-1.50 (m, 1H, CH); ^{13}C NMR (100.6 MHz, CDCl$_3$) δ 149.8 (Ar), 147.3 (Ar), 138.4 (*ipso*-Ar), 135.9 (Ar), 123.2 (Ar), 63.5 (HOCH$_2$), 46.3 (*C*HCH$_2$OH), 44.7 (*C*HAr), 31.0 (CH$_2$), 28.2 (CH$_2$), 23.9 (CH$_2$); MS (ESI)

m/z 178 [(M + H)⁺, 100]; HRMS (ESI) *m/z* calcd for $C_{11}H_{15}NO$ (M + H)⁺ 178.1226, found 178.1226 (+0.4 ppm error).

Lab Book Reference: TD 5/9

**1-Fluoromethyl-2-(3-pyridyl)cyclopentane *cis*-248**
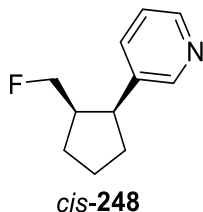
cis-**248**

PyFluor (68 mg, 0.31 mmol, 1.1 eq) was added portionwise to a stirred solution of alcohol *cis*-**249** (68 mg, 0.282 mmol, 1.0 eq) and DBU (0.115 mL, 0.564 mmol, 2.0 eq) in toluene (1 mL) at rt under Ar. The resulting solution was stirred and heated at 50 °C for 40 h. The mixture was then allowed to cool to rt and CH_2Cl_2 (2 mL) was added. Purification by flash column chromatography on silica with 50:50 hexane-EtOAc as eluent gave cyclopentane *cis*-**248** (18 mg, 36%) as a colourless oil, R_F (70:30 EtOAc-hexane) 0.46; IR (ATR) 2956, 2873, 1424 cm⁻¹; ¹H NMR (400 MHz, CDCl₃) δ 8.50-8.40 (m, 2H, Ar, Ar), 7.54-7.50 (m, 1H, Ar), 7.22 (dd, *J* = 8.0, 5.0 Hz, 1H, Ar), 4.06 (ddd, *J* = 47.5, 9.5, 6.0 Hz, 1H, CHF), 4.00 (ddd, *J* = 47.5, 9.5, 6.0 Hz, 1H, CHF), 3.30 (ddd, *J* = 8.0, 8.0, 8.0 Hz, 1H, C*H*Ar), 2.61-2.46 (m, 1H, C*H*CH₂F), 2.12-2.02 (m, 1H, CH), 2.02-1.86 (m, 2H, CH), 1.80-1.70 (m, 2H, CH), 1.68-1.58 (m, 1H, CH); ¹³C NMR (100.6 MHz, CDCl₃) δ 150.0 (Ar), 147.8 (Ar), 137.3 (*ipso*-Ar), 135.8 (Ar), 123.2 (Ar), 84.7 (d, *J* = 167.5 Hz, CH₂F), 44.8 (d, *J* = 4.0 Hz, *C*HAr), 44.2 (d, *J* = 18.0 Hz, *C*HCH₂F), 31.0 (CH₂), 27.4 (d, *J* = 5.5 Hz, CH₂), 24.1 (CH₂); MS (ESI) *m/z* 180 [(M + H)⁺, 100]; HRMS (ESI) *m/z* calcd for $C_{11}H_{14}NF$ (M + H)⁺ 180.1183, found 180.1183 (+0.3 ppm error).

Lab Book Reference: TD 5/12

Methyl 2-(3-pyridyl)tetrahydrofurancarboxylate *cis*-259
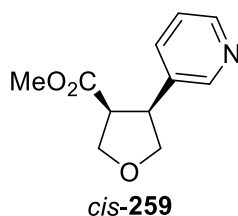
cis-**259**

Using general procedure **A**, dihydrofuran **222** (184 mg, 0.89 mmol, 1.0 eq) and 10% Pd/C (18 mg, 0.02 mmol, 0.02 eq) in MeOH (10 mL) for 40 h gave tetrahydrofuran *cis*-**259** (177 mg, 96%) as an orange oil, IR (ATR) 2952, 2880, 1730 (C=O), 1200, 1173 cm⁻¹; ¹H NMR (400 MHz, CDCl₃) δ 8.46 (br s, 2H, Ar), 7.63-7.58 (m, 1H, Ar), 7.25-7.21 (m, 1H, Ar), 4.29 (dd, *J* = 9.0, 7.0 Hz, 1H, OCH), 4.17-4.07 (m, 3H, OCH), 3.74-3.68 (m, 1H, C*H*Ar), 3.55

(ddd, J = 8.5, 8.5, 7.0 Hz, 1H, C*H*CO2Me), 3.31 (s, 3H, OMe); ^{13}C NMR (100.6 MHz, CDCl3) δ 171.4 (C=O), 149.6 (Ar), 148.5 (Ar), 135.5 (Ar), 134.9 (*ipso*-Ar), 123.5 (Ar), 73.5 (OCH2), 69.0 (OCH2), 51.7 (OMe), 49.8 (*C*HCO2Me), 45.6 (*C*HAr); MS (ESI) *m/z* 208 [(M + H)$^+$, 100], 230 [(M + Na)$^+$, 11]; HRMS (ESI) *m/z* calcd for C11H13NO3 (M + H)$^+$ 208.0968, found 208.0969 (–0.5 ppm error).

Lab Book Reference: TD 5/2

Methyl 2-(2-tolyl)tetrahydrofurancarboxylate *cis*-258
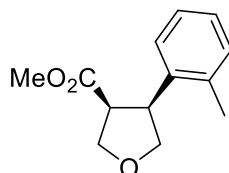
cis-**258**

Using general procedure **A**, dihydrofuran **221** (69 mg, 0.32 mmol, 1.0 eq) and 10% Pd/C (7 mg, 0.006 mmol, 0.02 eq) in MeOH (5 mL) for 64 h gave tetrahydrofuran *cis*-**258** (45 mg, 64%) as an orange oil, IR (ATR) 2950, 1734 (C=O), 1200, 1173 cm^{-1}; ^{1}H NMR (400 MHz, CDCl3) δ 7.20-7.08 (m, 4H, Ar), 4.33 (dd, J = 9.5, 6.0 Hz, 1H, OCH), 4.20-4.09 (m, 3H, OCH), 3.93-3.86 (m, 1H, C*H*Ar), 3.53 (ddd, J = 9.5, 8.0, 6.0, 1H, C*H*CO2Me), 3.17 (s, 3H, OMe), 2.37 (s, 3H, CMe); ^{13}C NMR (100.6 MHz, CDCl3) δ 172.4 (C=O), 136.9 (*ipso*-Ar), 136.4 (*ipso*-Ar), 130.2 (Ar), 127.0 (Ar), 126.5 (Ar), 126.1 (Ar), 72.6 (OCH2), 70.0 (OCH2), 51.3 (OMe), 48.6 (*C*HCO2Me), 44.2 (*C*HAr), 20.0 (C*Me*); MS (ESI) *m/z* 243 [(M + Na)$^+$, 100]; HRMS (ESI) *m/z* calcd for C13H16O3 (M + Na)$^+$ 243.0992, found 243.0991 (–0.1 ppm error).

Lab Book Reference: TD 5/5

3-Hydroxymethyl-4-(2-fluorophenyl)tetrahydrofuran *cis*-257
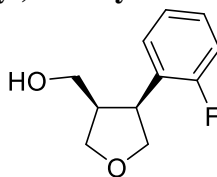
cis-**257**

Using general procedure **B**, β-ketoester **194** (3.00 g, 20.8 mmol, 1 eq), *i*Pr2NEt (18.1 mL, 104 mmol, 5 eq) and trifluoromethanesulfonic anhydride (4.20 mL, 25.0 mmol, 1.2 eq) in CH2Cl2 (200 mL) gave the crude product. Purification by flash column chromatography with 80:20 hexane–EtOAc as eluent gave enol triflate **204** (3.10 g) as a brown oil. Using general procedure **C**, triflate **204** (3.10 g, 11.2 mmol, 1 eq), 2-fluorophenylboronic acid (2.36 mg, 16.9 mmol, 1.5 eq), Pd(PPh3)4 (1.30 mg, 1.12 mmol, 0.1 eq) and K2CO3 (3.88 g, 28.1 mmol, 2.5 eq) in THF (160 mL) and H2O (40 mL) gave the crude product. Purification by flash

column chromatography on silica with 80:20 hexane-EtOAc as eluent gave a 60:40 mixture (by ^{1}H NMR spectroscopy) of alkene **220** and 2-fluorophenylboronic acid (2.13 g (i.e. 1.31 g (28%) over 2 steps) of alkene **220**). ^{1}H NMR (400 MHz, CDCl$_3$) of alkene **220**: δ 7.38-7.27 (m, 2H, Ar), 7.18-7.12 (m, 1H, Ar), 7.12-7.06 (m, 1H, Ar), 5.02-5.00 (m, 4H, OCH$_2$), 3.66 (s, 3H, OMe). Using general procedure **A**, the 60:40 mixture of alkene **220** (2.13 g i.e. 1.31 g (5.90 mmol) of alkene **220**) and 10% Pd(OH)$_2$/C (65 mg, 0.04 mmol, 0.01 eq) in MeOH (50 mL) for 40 h gave the crude product. Purification by flash column chromatography with 80:20 hexane-EtOAc as eluent gave a 60:40 mixture (by ^{1}H NMR spectroscopy) of ester *cis*-**264** and 2-fluorophenylboronic acid (1.42 g (i.e. 870 mg (66%) of ester *cis*-**264**)). ^{1}H NMR of ester *cis*-**264**: δ 7.26-7.17 (m, 2H, Ar), 7.10-7.04 (m, 1H, Ar), 7.04-6.98 (m, 1H, Ar), 4.29 (dd, $J = 9.0, 6.0$ Hz, 1H, OCH), 4.15-4.09 (m, 3H, OCH$_2$), 4.06-3.99 (m, 1H, C*H*Ar), 3.59-3.52 (m, 1H, C*H*CO$_2$Me), 3.28 (s, 3H, OMe). A stirred solution of the 60:40 mixture of ester *cis*-**264** and 2-fluoroboronic acid (1.42 g (i.e. 870 mg (3.88 mmol, 1.0 eq) of ester *cis*-**264**) in THF (10 mL) at 0 °C was added dropwise to a stirred suspension of LiAlH$_4$ (295 mg, 7.76 mmol, 2.0 eq) in THF (10 mL) at 0 °C under Ar. The resulting mixture was stirred at 0 °C for 2 h. Then, H$_2$O (0.2 mL), 2 M NaOH$_{(aq)}$ (0.4 mL), and H$_2$O (0.2 mL) were added dropwise sequentially. The solids were removed by filtration through Celite and the filtrate was dried (MgSO$_4$) and evaporated under reduced pressure to give the crude product. Purification by flash column chromatography with 50:50 hexane-EtOAc as eluent gave alcohol *cis*-**257** (598 mg, 79%, 15% over 4 steps) as a colourless oil, R_F (50:50 hexane-EtOAc) 0.20; IR (ATR) 3393 (br, OH), 1491, 759 cm^{-1}; ^{1}H NMR (400 MHz, CDCl$_3$) δ 7.36-7.32 (m, 1H, Ar), 7.26-7.21 (m, 1H, Ar), 7.16-7.11 (m, 1H, Ar), 7.09-7.02 (m, 1H, Ar), 4.17-4.08 (m, 3H, OCH), 3.89-3.82 (m, 1H, C*H*Ar), 3.78 (dd, $J = 8.5, 7.5$ Hz, 1H, OCH), 3.44-3.36 (m, 1H, HOC*H*), 3.33-3.24 (m, 1H, HOC*H*), 2.87 (ddddd, $J = 7.5, 7.5, 7.5, 7.5, 7.5$ Hz, 1H, C*H*CH$_2$OH), 1.44 (br s, 1H, OH); ^{13}C NMR (100.6 MHz, CDCl$_3$) δ 160.9 (d, $J = 244.0$ Hz, CF), 129.0 (d, $J = 4.0$ Hz, Ar), 128.5, (d, $J = 8.0$ Hz, Ar), 126.6 (d, $J = 14.5$ Hz, *ipso*-Ar), 124.6 (d, $J = 3.5$ Hz, Ar), 115.2 (d, $J = 23.0$ Hz, Ar), 73.0 (OCH$_2$), 70.3 (OCH$_2$), 62.0 (HOCH$_2$), 45.6 (*C*HCH$_2$OH), 38.8 (*C*HAr); MS (ESI) m/z 219 [(M + Na)$^+$, 100]; HRMS (ESI) m/z calcd for C$_{11}$H$_{13}$O$_2$F (M + Na)$^+$ 219.0792, found 219.0790 (+0.8 ppm error).

Lab Book Reference: TD 5/32

3-(*O*-Methanesulfonyl)hydroxymethyl-4-(2-fluorophenyl)tetrahydrofuran *cis*-265
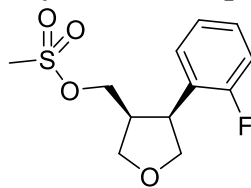
cis-265

Methanesulfonyl chloride (0.265 mL, 3.43 mmol, 1.2 eq) was added dropwise to a stirred solution of alcohol *cis*-**257** (560 mg, 2.85 mmol, 1.0 eq) and Et₃N (0.796 mL, 5.71 mmol, 2.0 eq) in CH₂Cl₂ (10 mL) at rt. The resulting solution was stirred at rt for 16 h. Then, H₂O (10 mL) was added and the aqueous layer was extracted with CH₂Cl₂ (2 x 10 mL). The combined organic extracts were dried (Na₂SO₄) and evaporated under reduced pressure to give mesylate *cis*-**265** (492 mg, 63%) as a yellow oil, R_F (50:50 hexane-EtOAc) 0.30; IR (ATR) 1491, 1355 (S=O), 1174 (S=O) cm⁻¹; ¹H NMR (400 MHz, CDCl₃) δ 7.34-7.29 (m, 1H, Ar), 7.29-7.24 (m, 1H, Ar), 7.15 (dddd, *J* = 7.5, 7.5, 1.0, 1.0 Hz, 1H, Ar), 7.10-7.04 (m, 1H, Ar), 4.20-4.12 (m, 3H, OCH), 3.96 (dd, *J* = 10.0, 6.0 Hz, 1H, OCH), 3.91 (m, 1H, C*H*Ar), 3.87-3.79 (m, 2H, OCH), 3.09 (ddddd, *J* = 7.5, 7.5, 7.5, 7.5, 7.5 Hz, C*H*CH₂OS), 2.84 (s, 3H, SO₂Me); ¹³C NMR (100.6 MHz, CDCl₃) δ 160.8 (d, *J* = 245.0 Hz, CF), 129.1-128.9 (m, Ar), 125.4 (d, *J* = 14.5 Hz, *ipso*-Ar), 124.8 (d, *J* = 3.5 Hz, Ar), 115.5 (d, *J* = 22.5 Hz, Ar), 72.8 (OCH₂), 70.1 (OCH₂), 68.6 (OCH₂), 42.2 (*C*HCH₂OS), 38.8 (*C*HAr), 37.1 (SO₂Me); MS (ESI) *m/z* 275 [(M + H)⁺, 5], 297 [(M + Na)⁺, 100], 313 [(M + K)⁺, 6]; HRMS (ESI) *m/z* calcd for C₁₂H₁₅O₄SF (M + Na)⁺ 297.0567, found 297.0565 (+0.8 ppm error).

Lab Book Reference: TD 5/33

3-Azidomethyl-4-(2-fluorophenyl)tetrahydrofuran *cis*-266
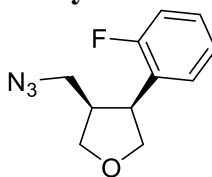
cis-266

Sodium azide (350 mg, 5.38 mmol, 3.0 eq) was added portionwise to a stirred solution of mesylate *cis*-**265** (492 mg, 1.79 mmol, 1.0 eq) in DMF (5 mL) at rt under Ar. The resulting mixture was stirred at rt for 10 min and then stirred and heated at 120 °C for 16 h. The solution was allowed to cool to rt. Then, H₂O (25 mL) and Et₂O (25 mL) were added and the two layers were separated. The aqueous layer was extracted with Et₂O (2 x 25 mL) and the combined organic extracts were washed with brine (25 mL), dried (MgSO₄) and evaporated under reduced pressure to give azide *cis*-**266** (336 mg, 89%) as a colourless oil, R_F (50:50 hexane-EtOAc) 0.47; IR (ATR) 2097 (N₃), 1490, 758 cm⁻¹; ¹H NMR (400 MHz,

CDCl$_3$) δ 7.33-7.23 (m, 2H, Ar), 7.15 (ddd, J = 7.5, 7.5, 1.5 Hz, 1H, Ar), 7.10-7.04 (m, 1H, Ar), 4.19-4.11 (m, 3H, OCH), 3.89-3.82 (m, 1H, CHAr), 3.75 (dd, J = 9.0, 6.5 Hz, 1H, OCH), 3.17 (br dd, J = 9.0, 6.5 Hz, 1H, CHN$_3$), 2.93-2.81 (m, 2H, CHN$_3$, CHCH$_2$N$_3$); ^{13}C NMR (100.6 MHz, CDCl$_3$) δ 160.8 (d, J = 245.0 Hz, CF), 128.9 (d, J = 4.0 Hz, Ar), 124.7 (d, J = 8.0 Hz, Ar), 125.9 (d, J = 14.5 Hz, *ipso*-Ar), 124.7 (d, J = 3.5 Hz, Ar), 115.4 (d, J = 22.5 Hz, Ar), 72.7 (OCH$_2$), 71.0 (OCH$_2$), 51.3 (CH$_2$N$_3$), 42.7 (CHCH$_2$N$_3$), 39.3 (d, J = 3.0 Hz, CHAr); MS (ESI) *m/z* 244 [(M + Na)$^+$, 100]; HRMS (ESI) *m/z* calcd for C$_{11}$H$_{12}$ON$_3$F (M + Na)$^+$ 244.0857, found 244.0856 (+0.2 ppm error).

Lab Book Reference TD 5/34

4-(2-Fluorophenyl)-3-aminomethyltetrahydrofuran *cis*-256

cis-**256**
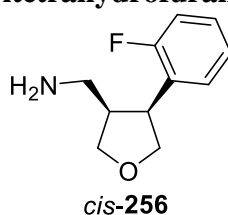
Triphenylphosphine (832 mg, 3.17 mmol, 2.0 eq) was added portionwise to a stirred solution of azide *cis*-**266** (335 mg, 1.59 mmol, 1.0 eq) in 5:1 THF-H$_2$O (10 mL) at rt under Ar. The solution was stirred and heated at 65 °C for 16 h. Then, the mixture was allowed to cool to rt and the solvent was evaporated under reduced pressure to give the crude product. Purification by flash column chromatography on silica with 50:50 hexane-EtOAc and then 80:20 EtOAc-MeOH as eluent gave amine *cis*-**256** (270 mg, 87%) as a yellow oil, R_F (90:10 EtOAc-MeOH) 0.17; IR (ATR) 2937 (NH), 2868 (NH), 1490, 759 cm^{-1}; 7.32 (ddd, J = 7.5, 7.5, 2.0 Hz, 1H, Ar), 7.23 (dddd, J = 8.0, 7.5, 5.5, 2.0 Hz, 1H, Ar), 7.13 (ddd, J = 7.5, 7.5, 1.5 Hz, 1H, Ar), 7.04 (ddd, J = 10.5, 8.0, 1.5 Hz, 1H, Ar), 4.19-4.09 (m, 3H, OCH), 3.87-3.81 (m, 1H, CHAr), 3.68 (dd, J = 8.5, 8.5 Hz, 1H, OCH), 2.72 (ddddd, J = 8.0, 8.0, 8.0, 8.0, 8.0 Hz, 1H, CHCH$_2$NH$_2$), 2.49 (dd, J = 12.5, 8.0 Hz, 1H, CHNH$_2$), 2.35 (dd, J = 12.5, 8.0 Hz, 1H, CHNH$_2$), 2.13 (br s, 2H, NH$_2$); ^{13}C NMR (100.6 MHz, CDCl$_3$) δ 160.8 (d, J = 244 Hz, CF) , 129.2 (d, J = 4.0 Hz, Ar), 128.4 (d, J = 8.5 Hz, Ar), 127.0 (d, J = 14.5 Hz, *ipso*-Ar), 124.6 (d, J = 3.5 Hz, Ar), 115.2 (d, J = 23.0 Hz, Ar), 73.4 (OCH$_2$), 70.9 (OCH$_2$), 46.6 (CHCH$_2$NH$_2$), 41.0 (CH$_2$NH$_2$), 39.0 (d, J = 3.0 Hz, CHAr); MS (ESI) *m/z* 196 [(M + H)$^+$, 100], 218 [(M + Na)$^+$, 5]; HRMS (ESI) *m/z* calcd for C$_{11}$H$_{14}$ONF (M + H)$^+$ 196.1132, found 196.1128 (+2.0 ppm error).

Lab Book Reference: 5/37

Methyl 4-(3-pyrimidyl)-piperidine-3-carboxylate hydrochloride *cis*-244•HCl

cis-**244**•HCl
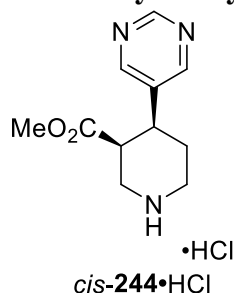
HCl (1.90 mL of a 2 M solution in Et$_2$O, 3.80 mmol, 10.0 eq) was added dropwise to a stirred solution of piperidine *cis*-**226** (122 mg, 0.38 mmol, 1.0 eq) in Et$_2$O (5 mL) at rt under Ar. The resulting solution was stirred at rt for 16 h. Then, the solvent was evaporated under reduced pressure to give piperidine *cis*-**244**•HCl (90 mg, 92%) as a yellow oil, IR (ATR) 2951, 1729 (C=O), 1494, 1219 cm^{-1}; ^{1}H NMR (400 MHz, CD$_3$OD) δ 9.39 (br s, 1H, Ar), 9.16 (br s, 2H, Ar), 3.85-3.78 (m, 1H, C*H*Ar), 3.69-3.59 (m, 2H, NCH), 3.57 (s, 3H, OMe), 3.54-3.42 (m, 3H, NCH, C*H*CO$_2$Me), 2.54-2.40 (m, 1H, CH), 2.26-2.16 (m, 1H, CH); ^{13}C NMR (100.6 MHz, CD$_3$OD) δ 170.7 (C=O), 155.9 (Ar), 151.9 (Ar), 136.7 (*ipso*-Ar), 51.1 (OMe), 44.3 (NCH$_2$), 43.1 (NCH$_2$), 41.6 (C*H*Ar), 35.6 (C*H*CO$_2$Me), 21.3 (NCH$_2$*C*H$_2$); MS (ESI) *m/z* 222 [M$^+$, 100]; HRMS (ESI) *m/z* calcd for C$_{11}$H$_{16}$N$_3$O$_2$ M$^+$ 222.1237, found 222.1236 (+0.6 ppm error).

Lab Book Reference: TD 5/39

1-*tert*-Butyl-3-methyl 4-(2-fluorophenyl)pyrrolidine-1,3-dicarboxylate *cis*-268
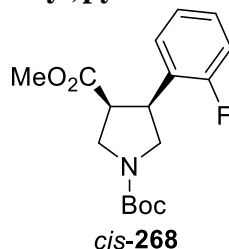
cis-**268**

Using general procedure **A**, ester **220** (338 mg, 1.04 mmol, 1.0 eq.) and 10% Pd/C (34 mg, 0.03 mmol, 0.03 eq.) in MeOH (10 mL) for 40 h gave ester *cis*-**268** (339 mg, quant.) as a white solid, mp 96–100 °C; IR (ATR) 1736 (C=O, CO$_2$Me), 1693 (C=O, Boc), 1401, 1165 cm^{-1}; ^{1}H NMR (400 MHz, CDCl$_3$) δ 7.23-7.18 (m, 1H, Ar), 7.17-7.11 (m, 1H, Ar), 7.05 (ddd, *J* = 7.5, 7.5, 1.0 Hz, 1H, Ar), 7.00 (br dd, *J* = 9.5, 9.5 Hz, 1H, Ar), 3.95 (ddd, *J* = 7.5, 7.5, 7.5 Hz, 1H, C*H*Ar or C*H*CO$_2$Me), 3.83-3.60 (m, 4H, NCH, C*H*Ar or C*H*CO$_2$Me), 3.49-3.42 (m, 1H, NCH), 3.34 (s, 3H, OMe), 1.47 (br s, 9H, CMe$_3$); ^{13}C NMR (100.6 MHz, CDCl$_3$) (rotamers) δ 172.13 (C=O, *C*O$_2$Me) 172.04 (C=O, *C*O$_2$Me), 160.9 (d, *J* = 247 Hz, CF), 154.4 (C=O, Boc), 128.9 (d, *J* = 8.5 Hz, Ar), 127.7 (d, *J* = 4.0 Hz, Ar), 125.2 (d, *J* = 14.5 Hz, *ipso*-Ar), 125.0 (d, *J* = 14.5 Hz, *ipso*-Ar), 124.3 (d, *J* = 2.5 Hz, Ar), 124.2 (d, *J* =

2.5 Hz, Ar), 115.3 (d, J = 5.5 Hz, Ar), 115.1 (d, J = 5.5 Hz, Ar), 79.8 (*C*Me$_3$) 51.5 (OMe), 48.8 (N*C*H$_2$), 48.6 (N*C*H$_2$), 47.7 (N*C*H$_2$), 47.5 (*C*HCO$_2$Me), 46.6 (*C*HCO$_2$Me), 39.1 (*C*HAr), 38.3 (*C*HAr), 28.5 (C*Me*$_3$); MS (ESI) *m/z* 346 [(M + Na), 100]; HRMS (ESI) *m/z* calcd for C$_{17}$H$_{22}$FNO$_4$ (M + Na)$^+$ 346.1425, found 346.1425 (–0.1 ppm error).

Lab Book Reference: TD 5/27

Methyl 3-(2-fluorophenyl)-pyrrolidine-4-carboxylate hydrochloride *cis*-246•HCl
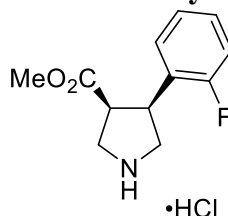
cis-**246**•HCl

HCl (2.03 mL of a 2 M solution in Et$_2$O, 4.05 mmol, 10.0 eq) was added dropwise to a stirred solution of pyrrolidine *cis*-**268** (131 mg, 0.405 mmol, 1.0 eq) in Et$_2$O (5 mL) at rt under Ar. The resulting solution was stirred at rt for 16 h. Then, the solvent was evaporated under reduced pressure to give pyrrolidine *cis*-**246**•HCl (105 mg, quant.) as a white solid, mp 81-83 °C; IR (ATR) 1723 (C=O), 1626, 1433 cm^{-1}; ^{1}H NMR (400 MHz, CD$_3$OD) δ 7.39-7.30 (m, 1H, Ar), 7.25-7.05 (m, 3H, Ar), 4.20-4.06 (m, 1H, C*H*Ar), 3.92-3.60 (m, 5H, NCH, C*H*CO$_2$Me), 3.28 (s, 3H, OMe); ^{13}C NMR (100.6 MHz, CD$_3$OD) δ 171.3 (C=O) 160.7 (d, J = 246.0 Hz, CF), 129.3 (d, J = 8.5 Hz, Ar), 127.0 (d, J = 3.5 Hz, Ar), 123.7 (d, J = 3.0 Hz, Ar), 121.4 (d, J = 14.5 Hz, *ipso*-Ar), 114.6 (d, J = 22.0 Hz, Ar), 50.6 (OMe), 46.02 (NCH$_2$), 45.95 (NCH$_2$), 39.3 (*C*HAr), 35.0 (*C*HCO$_2$Me); MS (ESI) *m/z* 224 [M$^+$, 100]; HRMS (ESI) *m/z* calcd for C$_{12}$H$_{15}$FNO$_2$ M$^+$ 224.1081, found 224.1081 (+0.3 ppm error).

Lab Book Reference: TD 5/38

***tert*-Butyl 3-(2-fluorophenyl)-4-hydroxymethylpyrrolidine-1-carboxylate *cis*-269**
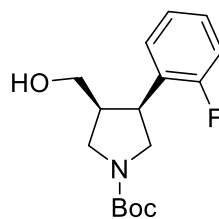
cis-**269**

A suspension of LiAlH$_4$ (55 mg, 1.44 mmol, 2.0 eq.) in THF (5 mL) at 0 °C was added dropwise to a stirred solution of ester *cis*-**268** (233 mg, 0.72 mmol, 1.0 eq.) in THF (5 mL) at 0 °C under Ar. The resulting mixture was stirred at 0 °C for 2 h. Then, H$_2$O (0.1 mL), 2 M NaOH$_{(aq)}$ (0.2 mL) and H$_2$O (0.1 mL) were added sequentially. The solids were removed by filtration through Celite and the filtrate was dried (MgSO$_4$) and evaporated under reduced

pressure to give alcohol *cis*-**269** (166 mg, 56%) as a yellow oil, IR (ATR) 3280 (OH), 1696 (C=O), 871 cm^{-1}; ^{1}H NMR (400 MHz, CDCl$_3$) δ 7.27-7.20 (m, 1H, Ar), 7.16-7.10 (m, 2H, Ar), 7.07-7.00 (m, 1H, Ar), 3.85-3.57 (m, 4H, NCH), 3.45-3.35 (m, 1H, HOC*H*), 3.33-3.20 (m, 2H, C*H*Ar, HOC*H*), 2.83-2.70 (m, 1H, C*H*CH$_2$OH), 1.49 (s, 9H, CMe$_3$); ^{13}C NMR (100.6 MHz, CDCl$_3$) (rotamers) δ 161.0 (d, J = 236 Hz, CF), 156.2 (C=O, Boc), 129.9 (d, J = 8.5 Hz, Ar), 128.6 (d, J = 8.5 Hz, Ar), 128.3 (d, J = 4.5 Hz, Ar), 127.6 (d, J = 5.0 Hz *ipso*-Ar), 126.4 (d, J = 5.0 Hz, Ar), 124.74 (d, J = 4.1 Hz, Ar), 124.70 (d, J = 3.9 Hz, Ar), 115.4 (d, J = 25.4 Hz, Ar), 79.7 (*C*Me$_3$), 61.9 (HOCH$_2$), 50.0 (NCH$_2$), 48.0 (NCH$_2$), 47.5 (NCH$_2$), 44.7 (*C*HCH$_2$OH), 44.0 (*C*HCH$_2$OH), 36.99 (*C*HAr), 36.96 (*C*HAr), 28.6 (C*Me*$_3$); MS (ESI) *m/z* 295 [(M + H), 100]; HRMS (ESI) *m/z* calcd for C$_{16}$H$_{22}$FNO$_3$ (M + H)$^+$ 295.1584, found 295.1580 (–1.0 ppm error).

Lab Book Reference: TD 5/30

4-Hydroxymethyl-3-(2-fluorophenyl)-pyrrolidine hydrochloride *cis*-247•HCl
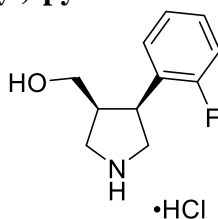

cis-**247**•HCl

HCl (2.30 mL of a 2 M solution in Et$_2$O, 4.60 mmol, 10.0 eq) was added dropwise to a stirred solution of pyrrolidine *cis*-**269** (136 mg, 0.46 mmol, 1.0 eq) in Et$_2$O (50 mL) at rt under Ar. The resulting solution was stirred at rt for 16 h. Then, the solvent was evaporated under reduced pressure to give pyrrolidine *cis*-**247**•HCl (106 mg, 97%) as a white solid, mp 53-55 °C; IR (ATR) 3359 (OH or NH), 2925, 1493, 757 cm^{-1}; ^{1}H NMR (400 MHz, CD$_3$OD) δ 7.40-7.28 (m, 2H, Ar), 7.18 (dd, J = 7.5, 7.5 Hz, 1H, Ar), 7.11 (dd, J = 10.5, 8.5 Hz, 1H, Ar), 4.00-3.90 (m, 1H, NCH), 3.78 (dd, J = 11.0, 11.0 Hz, 1H, NCH), 3.67-3.50 (m, 3H, C*H*Ar, NCH), 3.37 (dd, J = 10.5, 4.0 Hz, 1H, HOC*H*), 3.19 (dd, J = 10.5, 5.5 Hz, 1H, HOC*H*), 2.78 (br s, 1H, C*H*CH$_2$OH); ^{13}C NMR (100.6 MHz, CD$_3$OD) δ 162.5 (d, J = 244.5 Hz, CF), 130.6 (d, J = 8.5 Hz, Ar), 130.1 (d, J = 4.0 Hz, Ar), 125.7 (d, J = 3.5 Hz, Ar), 124.4 (d, J = 14.5 Hz, *ipso*-Ar), 116.6 (d, J = 22.5 Hz, Ar), 61.5 (HOCH$_2$), 49.6 (NCH$_2$), 49.2 (NCH$_2$), 43.6 (*C*HCH$_2$OH), 40.5 (d, J = 2.0 Hz, *C*HAr); MS (ESI) *m/z* 196 [M$^+$, 100]; HRMS (ESI) *m/z* calcd for C$_{11}$H$_{15}$FNO M$^+$ 196.1132, found 196.1131 (+0.8 ppm error).

Lab Book Reference: TD 5/35

Methyl 4-(3-methoxyphenyl)tetrahydropyran-3-carboxylate *cis*-255
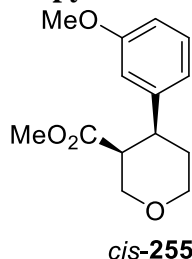
cis-**255**

Using general procedure **A**, dihydropyran **223** (57 mg, 0.23 mmol, 1.0 eq) and 10% Pd/C (6 mg, 0.006 mmol, 0.02 eq) in MeOH (5 mL) for 16 h gave tetrahydropyran *cis*-**255** (47 mg, 82%) as an orange oil, IR (ATR) 2955, 2841, 1738 (C=O), 1165 cm^{-1}; ^{1}H NMR (400 MHz, CDCl$_3$) δ 7.21 (dd, J = 8.0, 8.0 Hz, 1H, Ar), 6.87-6.83 (m, 1H, Ar), 6.82-6.79 (m, 1H, Ar), 6.74 (dd, J = 8.0, 2.5 Hz, 1H, Ar), 4.27 (br d, J = 11.5 Hz, 1H, OCH), 4.18 (ddd, J = 11.5, 4.0, 1.5 Hz, 1H, OCH), 3.78 (s, 3H, ArO*Me*), 3.75 (dd, J = 11.5, 3.0 Hz, 1H, OCH), 3.55 (ddd, J = 11.5, 11.5, 2.5 Hz, 1H, OCH), 3.51 (s, 3H, CO$_2$Me), 3.05 (ddd, J = 12.5, 4.0, 4.0 Hz, 1H, C*H*Ar), 2.90 (br s, 1H, C*H*CO$_2$Me), 2.72 (dddd, 1H, J = 12.5, 12.5, 11.5, 4.0 Hz, 1H, OCH$_2$C*H*), 1.71 (br dd, 1H, J = 12.5, 1.5 Hz, OCH$_2$C*H*); ^{13}C NMR (100.6 MHz, CDCl$_3$) 172.3 (C=O), 159.6 (*ipso*-Ar), 144.3 (*ipso*-Ar), 129.3 (Ar), 119.7 (Ar), 113.5 (Ar), 111.6 (Ar), 69.8 (O*C*H$_2$CH), 68.6 (O*C*H$_2$CH$_2$), 55.2 (ArO*Me*), 51.5 (CO$_2$*Me*), 46.5 (*C*HCO$_2$Me), 41.7 (*C*HAr), 26.7 (OCH$_2$*C*H$_2$); MS (ESI) *m/z* 251 [(M + H)$^+$, 11] 273 [(M + Na)$^+$, 100]; HRMS (ESI) *m/z* calcd for C$_{14}$H$_{18}$O$_4$ (M + Na)$^+$ 273.1097, found 273.1084 (+4.7 ppm error).

Lab Book Reference: TD 5/18

Methyl 2-(3-thiophenyl)cyclopentanecarboxylate *cis*-251
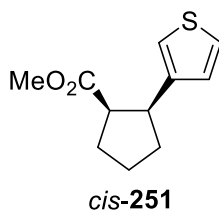
cis-**251**

Using general procedure **A**, cyclopentene **216** (100 mg, 0.48 mmol, 1.0 eq) and 10% Pd/C (10 mg, 0.009 mmol, 0.02 eq) in MeOH (10 mL) for 40 h gave cyclopentane *cis*-**251** (70 mg, 69%) as an orange oil, IR (ATR) 2949, 1730 (C=O), 1196, 1169 cm^{-1}; ^{1}H NMR (400 MHz, CDCl$_3$) δ 7.22 (dd, J = 5.0, 3.0 Hz, 1H, Ar), 6.99-6.97 (m, 1H, Ar), 6.94 (dd, J = 5.0, 1.5 Hz, 1H, Ar), 3.49 (ddd, J = 8.0, 8.0, 8.0 Hz, 1H, C*H*Ar), 3.33 (s, 3H, OMe), 3.16-3.09 (m, 1H, C*H*CO$_2$Me), 2.17-1.91 (m, 5H, CH), 1.76-1.64 (m, 1H, CH), ^{13}C NMR (100.6 MHz, CDCl$_3$) 175.2 (C=O), 142.5 (*ipso*-Ar), 128.0 (Ar), 124.8 (Ar), 120.6 (Ar), 51.2 (OMe), 49.5 (*C*HCO$_2$Me), 44.7 (*C*HAr), 32.0 (CH$_2$), 28.3 (CH$_2$), 24.6 (CH$_2$); MS (ESI) *m/z* 233 [(M +

Na)$^+$, 100]; HRMS (ESI) *m/z* calcd for C$_{11}$H$_{14}$O$_2$S (M + Na)$^+$ 233.0607, found 233.0604 (+1.0 ppm error).

Lab Book Reference: TD 4/94

2-(3-Thiophenyl)cyclopent-1-enecarboxylic acid 282

282
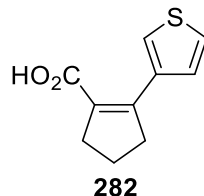
2 M NaOH$_{(aq)}$ (3 mL) was added dropwise to a stirred solution of ester **201** (150 mg, 0.72 mmol, 1 eq) in MeOH (3mL) and THF (3 mL) at rt under Ar. The resulting mixture was stirred and heated at 70 °C for 1 h. The mixture was then allowed to cool to rt and H$_2$O (15 mL) was added. The mixture was washed with CH$_2$Cl$_2$ (10 mL) and 1 M HCl$_{(aq)}$ (10 mL) was added. The mixture was extracted with CH$_2$Cl$_2$ (2 x 50 mL) and the combined organic extracts were dried (Na$_2$SO$_4$) and evaporated under reduced pressure to give acid **282** (115 mg, 84%) as a white solid, mp 116-119 °C; IR (ATR) 2942, 1669 (C=O), 1648 (C=C), 1594, 1268 cm^{-1}; ^{1}H NMR (400 MHz, CDCl$_3$) δ 7.71 (dd, *J* = 3.0, 1.0 Hz, 1H, Ar), 7.41 (dd, *J* = 5.0, 1.0 Hz), 7.24 (dd, *J* = 5.0, 3.0 Hz, 1H, Ar), 2.93 (tt, *J* = 7.5, 2.0 Hz, 2H, =CCH$_2$), 2.91 (tt, *J* = 7.5, 2.0 Hz, 2H, =CCH$_2$), 1.94 (tt, *J* = 7.5, 7.5 Hz, 2H, CH$_2$); ^{13}C NMR (100.6 MHz, CDCl$_3$) δ 171.3 (C=O), 149.7 (=*C*Ar), 136.4 (*ipso*-Ar), 128.7 (Ar), 126.8 (Ar), 126.7 (=*C*CO$_2$H), 124.4 (Ar), 40.4 (=C*C*H$_2$), 35.5 (=C*C*H$_2$), 21.6 (CH$_2$); MS (ESI) *m/z* 195 [(M + H)$^+$, 23], 217 [(M + Na)$^+$, 100]; HRMS (ESI) *m/z* calcd for C$_{10}$H$_{10}$O$_2$S (M + Na)$^+$ 217.0294, found 217.0292 (+1.0 ppm error).

Lab Book Reference: TD 4/93

2-(3-Thiophenyl)cyclopentanecarboxylic acid *cis*-276
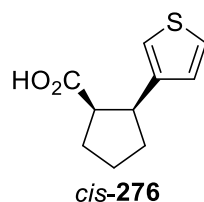
cis-**276**

Using general procedure **A**, cyclopentene **282** (200 mg, 1.03 mmol, 1.0 eq) and 10% Pd/C (20 mg, 0.014 mmol, 0.01 eq) in MeOH (10 mL) for 40 h gave cyclopentane *cis*-**276** (188 mg, 93%) as a white solid, mp 75-77 °C; IR (ATR) 2953 (br, OH), 1699 (C=O), 1233, 787 cm^{-1}; ^{1}H NMR (400 MHz, CDCl$_3$) δ 7.19 (dd, *J* = 5.0, 3.0 Hz, 1H, Ar), 6.99-6.96 (m, 1H, Ar), 6.93 (dd, *J* = 5.0, 1.0 Hz, 1H, Ar), 3.48 (ddd, *J* = 8.0, 8.0, 8.0 Hz, 1H, C*H*Ar), 3.08 (ddd, *J* = 8.0, 8.0, 6.0 Hz, 1H, C*H*CO$_2$H), 2.08-1.90 (m, 5H, CH), 1.76-1.66 (m, 1H, CH); ^{13}C

NMR (100.6 MHz, CDCl$_3$) δ 180.1 (C=O), 142.0 (*ipso*-Ar), 127.9 (Ar), 125.1 (Ar), 120.8 (Ar), 49.3 (*C*HCO$_2$H), 44.6 (*C*HAr), 31.8 (CH$_2$), 28.3 (CH$_2$), 24.1 (CH$_2$); MS (ESI) *m/z* 219 [(M + Na)$^+$, 100]; HRMS (ESI) *m/z* calcd for C$_{10}$H$_{12}$O$_2$S (M + Na)$^+$ 219.0450, found 219.0449 (+0.6 ppm error).

Lab Book Reference: TD 4/98
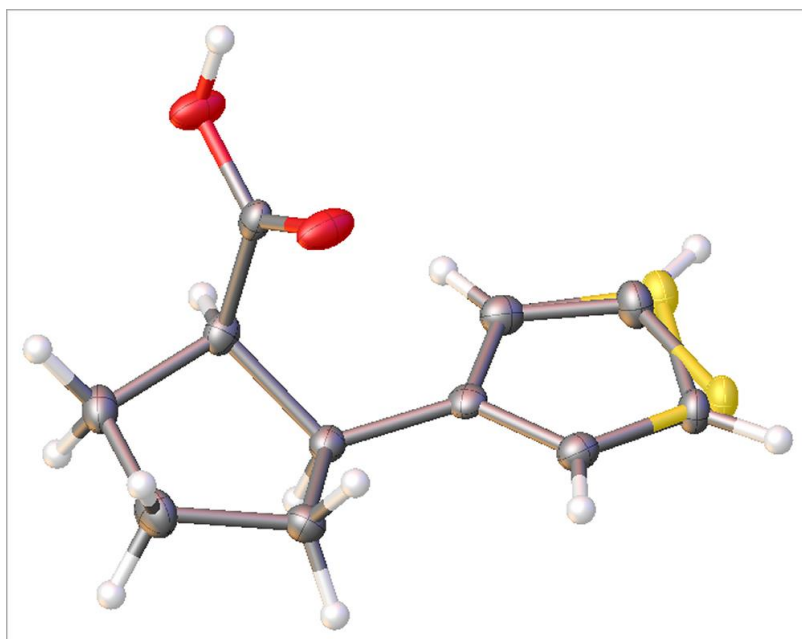
Table 5.3 Crystal data and structure refinement for *cis*-276.

Identification code	TD 4/98
Empirical formula	$C_{10}H_{12}O_2S$
Formula weight	196.26
Temperature/K	109.95(10)
Crystal system	monoclinic
Space group	$P2_1/c$
a/Å	5.3862(2)
b/Å	6.8010(3)
c/Å	24.9772(13)
α/°	90
β/°	91.998(4)
γ/°	90
Volume/Å^3	914.40(8)
Z	4
ρ_{calc}g/cm^3	1.426
μ/mm^{-1}	2.837
F(000)	416.0
Crystal size/mm^3	$0.279 \times 0.116 \times 0.022$
Radiation	CuKα (λ = 1.54184)
2Θ range for data collection/°	7.082 to 134.092
Index ranges	$-6 \leq h \leq 6$, $-6 \leq k \leq 8$, $-25 \leq l \leq 29$
Reflections collected	2995
Independent reflections	1636 [$R_{int} = 0.0172$, $R_{sigma} = 0.0253$]
Data/restraints/parameters	1636/0/173
Goodness-of-fit on F^2	1.032
Final R indexes [I>=2σ (I)]	$R_1 = 0.0306$, $wR_2 = 0.0731$
Final R indexes [all data]	$R_1 = 0.0361$, $wR_2 = 0.0781$
Largest diff. peak/hole / e Å^{-3}	0.32/-0.20

2-(3-Thiophenyl)cyclopentanecarboxamide *cis*-275
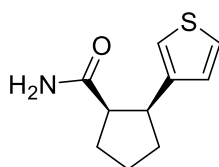
cis-**275**

Ammonia (0.04 mL of a 35% solution in H_2O, 0.765 mmol, 3.0 eq) was added to a stirred solution of acid *cis*-**276** (50 mg, 0.255 mmol, 1.0 eq), T3P (0.243 mL of a 50% solution in EtOAc, 0.382 mmol, 1.5 eq) and iPr$_2$NEt (0.133 mL, 0.765 mmol, 3.0 eq) in CH_2Cl_2 (3 mL) at rt under Ar. The resulting solution was stirred at rt for 18 h. Then, 2 M HCl$_{(aq)}$ (5 mL) was added and the mixture was extracted with CH_2Cl_2 (2 x 5 mL). The combined organic extracts were washed with NaHCO$_{3(aq)}$ (2 x 10 mL), dried (Na$_2$SO$_4$) and evaporated under reduced pressure to give amide *cis*-**275** (24 mg, 48%) as a white solid, mp 107-110 °C; IR (ATR) 3322 (NH), 3189 (NH), 2952, 1653 (C=O) cm^{-1}; ^{1}H NMR (400 MHz, CDCl$_3$) δ 7.23 (dd, J = 5.0, 3.0 Hz, 1H, Ar), 7.04-7.01 (m, 1H, Ar), 6.98 (dd, J = 5.0, 1.5 Hz, 1H, Ar), 5.16 (br s, 1H, NH), 4.96 (br s, 1H, NH), 3.42 (ddd, J = 8.0, 8.0, 8.0 Hz, 1H, CHAr), 2.88 (ddd, J = 8.0, 8.0, 5.5 Hz, 1HMS (ESI) m/z 196 [(M + H)$^+$, 5], 218 [(M + Na)$^+$, 100]; HRMS (ESI) m/z calcd for C$_{10}$H$_{13}$ONS (M + Na)$^+$ 218.0610, found 218.0608 (+0.8 ppm error).

Lab Book Reference: TD 4/100

4-(3-Methoxyphenyl)-2,3-2*H*-dihydropyran-3-carboxylic acid 284
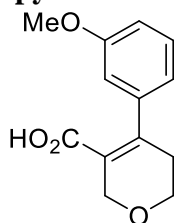
284

2 M NaOH$_{(aq)}$ (12 mL) was added dropwise to a stirred solution of ester **223** (590 mg, 2.38 mmol, 1 eq) in MeOH (12 mL) and THF (12 mL) at rt under Ar. The resulting mixture was stirred and heated at 70 °C for 1 h. The mixture was then allowed to cool to rt and H_2O (25 mL) was added. The mixture was washed with CH_2Cl_2 (25 mL) and then 1 M HCl$_{(aq)}$ (50 mL) was added. The mixture was extracted with CH_2Cl_2 (2 x 50 mL) and the combined organic extracts were dried (Na$_2$SO$_4$) and evaporated under reduced pressure to give acid **284** (481 mg, 86%) as a white solid, mp 101-103 °C; IR (ATR) 1675 (C=O), 1446 (C=C), 832 cm^{-1} ^{1}H NMR (400 MHz, CDCl$_3$) δ 7.23 (dd, J = 8.0, 8.0 Hz, 1H, Ar), 6.82 (ddd, J = 8.0, 2.5, 1.0 Hz), 6.72 (ddd, J = 8.0, 1.5, 1.0 Hz, 1H, Ar), 6.67 (ddd, J = 2.5, 1.5 Hz), 4.40 (t, J = 2.5 Hz, 2H, OCH$_2$), 3.85 (t, J = 5.5 Hz, 2H, OCH_2CH$_2$), 3.77 (s, 3H, OMe), 2.48 (tt,

$J = 5.5, 2.5$ Hz, 2H, CH$_2$); ^{13}C NMR (100.6 MHz, CDCl$_3$) δ 170.3 (C=O), 159.4 (*ipso*-Ar), 149.2 (=*C*Ar), 142.5 (*ipso*-Ar), 129.4 (Ar), 125.0 (=*C*CO$_2$H), 119.2 (Ar), 113.2 (Ar), 112.6 (Ar), 65.6 (OCH$_2$), 64.0 (OCH$_2$CH$_2$), 55.3 (OMe), 33.1 (CH$_2$); MS (ESI) *m/z* 257 [(M + Na)$^+$, 100]; HRMS (ESI) *m/z* calcd for C$_{13}$H$_{14}$O$_4$ (M + Na)$^+$ 257.0784, found 257.0783 (+0.3 ppm error).

Lab Book Reference: TD 5/17

4-(3-Methoxylphenyl)tetrahydropyran-3-carboxylic acid *cis*-280
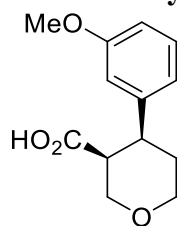
cis-**280**

Using general procedure **A**, dihydropyran **284** (460 mg, 1.94 mmol, 1.0 eq) and 10% Pd(OH)$_2$/C (46 mg, 0.03 mmol, 0.02 eq) in MeOH (50 mL) for 64 h gave tetrahydropyran *cis*-**280** (449 mg, 98%) as a white solid, mp 111-113 °C; IR (ATR) 2965 (br, OH), 2930, 1703 (C=O), 1165 cm^{-1}; ^{1}H NMR (400 MHz, CDCl$_3$) δ 9.45 (br s, 1H, CO$_2$H), 7.20 (dd, $J = 8.0, 8.0$ Hz, 1H, Ar), 6.86-6.82 (m, 1H, Ar), 6.82-6.79 (m, 1H, Ar), 6.77-6.73 (m, 1H, Ar), 4.32 (br dd, $J = 12.0, 1.5$ Hz, 1H, OCH), 4.17 (ddd, $J = 11.5, 4.5, 1.5$ Hz, 1H, OCH), 3.77-3.72 (m, 4H,rOMe, OCH), 3.55 (ddd, $J = 11.5, 11.5, 2.5$ Hz, 1H, OCH), 3.04 (ddd, $J = 12.0, 4.0, 4.0$ Hz, 1H, C*H*Ar), 2.92-2.88 (m, 1H, C*H*CO$_2$H), 2.66 (dddd, 1H, $J = 12.5, 12.0, 11.5, 4.0$ Hz, 1H, OCH$_2$C*H*), 1.70 (m, 1H, OCH$_2$C*H*); ^{13}C NMR (100.6 MHz, CDCl$_3$) δ 177.6 (C=O), 159.5 (*ipso*-Ar), 143.8 (*ipso*-Ar), 129.3 (Ar), 119.7 (Ar), 113.4 (Ar), 111.7 (Ar), 69.7 (O*C*H$_2$CH), 68.5 (O*C*H$_2$CH$_2$), 55.1 (OMe), 46.2 (*C*HCO$_2$H), 41.3 (*C*HAr), 26.4 (OCH$_2$*C*H$_2$); MS (ESI) *m/z* 235 [(M − H)$^-$, 11]; HRMS (ESI) *m/z* calcd for C$_{13}$H$_{16}$O$_4$ (M − H)$^-$ 235.0976, found 235.0975 (+0.4 ppm error).

Lab Book Reference: TD 5/26

4-(3-Methoxylphenyl)tetrahydropyran-3-carboxamide *cis*-279
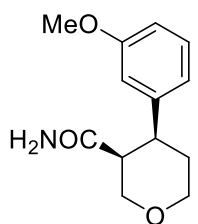
*cis-*279

Ammonia (0.06 mL of a 35% solution in H_2O, 1.27 mmol, 3.0 eq) was added to a stirred solution of acid *cis-*280 (100 mg, 0.42 mmol, 1.0 eq), T3P (0.404 mL of a 50% solution in EtOAc, 0.635 mmol, 1.5 eq) and *i*Pr$_2$NEt (0.221 mL, 1.27 mmol, 3.0 eq) in CH_2Cl_2 (5 mL) at rt under Ar. The resulting solution was stirred at rt for 18 h. Then, 2 M HCl$_{(aq)}$ (5 mL) was added and the mixture was extracted with CH_2Cl_2 (2 x 5 mL). The combined organic extracts were washed with NaHCO$_{3(aq)}$ (2 x 10 mL), dried (Na$_2$SO$_4$) and evaporated under reduced pressure to give amide *cis-*279 (40 mg, 41%) as a white solid, mp 71-73 °C; IR (ATR) 2980 (NH), 1736 (C=O), 1180 cm^{-1}; ^{1}H NMR (400 MHz, CDCl$_3$) δ 7.25-7.20 (m, 1H, Ar), 6.84-6.81 (m, 1H, Ar), 6.82-6.79 (m, 1H, Ar), 6.78-6.73 (m, 1H, Ar), 6.55 (br s, 1H, NH), 5.65 (br s, 1H, NH), 4.25 (br d, J = 12.0 Hz, 1H, OCH), 4.21 (br dd, J = 12.0, 4.5 Hz, 1H, OCH), 3.77 (s, 3H, OMe), 3.68 (dd, J = 12.0, 3.0 Hz, OCH), 3.58 (ddd, J = 12.0, 12.0, 2.5 Hz, 1H, OCH), 3.15-3.08 (m, 1H, C*H*Ar), 2.64 (br s, 1H, C*H*CONH$_2$), 2.42 (dddd, 1H, J = 13.0, 12.0, 12.0, 4.5 Hz, 1H, OCH$_2$C*H*), 1.76-1.68 (m, 1H, OCH$_2$C*H*); ^{13}C NMR (100.6 MHz, CDCl$_3$) δ 174.3 (C=O), 159.6 (*ipso*-Ar), 143.5 (*ipso*-Ar), 129.5 (Ar), 119.6 (Ar), 113.6 (Ar), 111.9 (Ar), 69.4 (O*C*H$_2$CH), 68.6 (O*C*H$_2$CH$_2$), 55.2 (OMe), 48.2 (*C*HCONH$_2$), 42.6 (*C*HAr), 27.1 (OCH$_2$*C*H$_2$); MS (ESI) *m/z* 236 [(M + H)$^+$, 25], 258 [(M + Na)$^+$, 100]; HRMS (ESI) *m/z* calcd for C$_{13}$H$_{17}$O$_3$N (M + Na)$^+$ 258.1101, found 258.1096 (+1.9 ppm error).

Lab Book Reference: TD 5/28

4-(3-Methoxyphenyl)-3-(*N*-benzyloxycarbonyl)aminotetrahydropyran *cis-*285
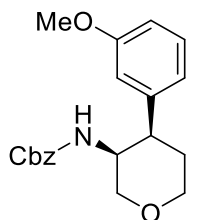
*cis-*285

Diphenylphosphorylazide (0.161 mL, 0.745 mmol, 1.1 eq) was added dropwise to a stirred solution of acid *cis-*280 (160 mg, 0.677 mol, 1 eq) and Et$_3$N (0.189 mL, 1.35 mmol, 2 eq) in benzyl alcohol (2 mL) at rt under Ar. The resulting solution was stirred at rt for 1 h and then stirred and heated at 85 °C for 16 h. The resulting solution was allowed to cool to rt and the

solids were removed by filtration through Celite. The filtrate was evaporated under reduced pressure to give the crude product. Purification by flash column chromatography with 50:50 hexane-EtOAc as eluent gave Cbz-protected amine *cis*-**285** (144 mg, 62%) as a colourless oil, R_F 0.33 (50:50 hexane-EtOAc); IR (ATR) 2954 (NH), 1709 (C=O), 1234, 696 cm^{-1}; ^{1}H NMR (400 MHz, CDCl$_3$) (80:20 mixture of rotamers) δ 7.35-7.15 (m, 5.6H, Ar), 6.97 (br s, 0.4H, Ar), 6.84-6.72 (m, 3H, Ar), 5.26 (br d, J = 9.0 Hz, 1H, NH), 4.94 (d, J = 12.5 Hz, 0.8H, OC*H*Ph), 4.90 (d, J = 12.5 Hz, 0.8H, OC*H*Ph), 4.85 (d, J = 12.5 Hz, 0.2H, OC*H*Ph), 4.42 (d, J = 12.5 Hz, 0.2H, OC*H*Ph)**,** 4.15-4.03 (m, 1.8H, OC*H*$_2$CH$_2$, C*H*NH), 4.00 (d, J = 11.5 Hz, 0.8H, OC*H*$_2$CH), 3.97-3.85 (m, 0.4H, OC*H*$_2$CH$_2$, C*H*NH), 3.76 (s, 2.4H, OMe), 3.73 (s, 0.6H, OMe), 3.66 (br d, J = 11.5 Hz, 1H, OC*H*$_2$CH), 3.54 (br dd, J = 12.5, 12.5 Hz, 1H, C*H*NH), 3.11-3.02 (m, 1H, C*H*Ar), 3.02-2.93 (m, 1H, C*H*Ar), 2.26-2.12 (m, 0.2H, CH), 2.05 (dddd, J = 12.5, 12.5, 12.5, 4.5 Hz, 0.8H, CH), 1.78-1.67 (m, 0.8H, CH), 1.63-1.57 (m, 0.2H, CH); ^{13}C NMR (100.6 MHz, CDCl$_3$) δ 159.7 (*ipso*-Ar), 155.8 (C=O), 142.9 (*ipso*-Ar), 136.6 (*ipso*- Ar), 129.4 (Ar), 128.5 (Ar), 128.04 (Ar), 127.97 (Ar), 119.8 (Ar), 113.3 (Ar), 112.0 (Ar), 72.4 (O*C*H$_2$CH), 68.2 (O*C*H$_2$CH$_2$), 66.6 (O*C*H$_2$Ph), 55.2 (OMe), 50.8 (CHNH), 43.3 (*C*HAr), 26.1 (CH$_2$). MS (ESI) *m/z* 342 [(M + H)$^+$, 10], 364 [(M + Na)$^+$, 100]; HRMS (ESI) *m/z* calcd for C$_{20}$H$_{23}$O$_4$N (M + Na)$^+$ 364.1519, found 364.1516 (+1.0 ppm error).

Lab Book Reference: TD 5/29

4-(3-Methoxyphenyl)-3-aminotetrahydropyran *cis*-278
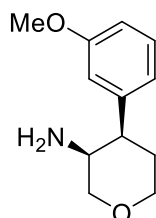
Using general procedure **A**, Cbz-protected amine *cis*-**285** (144 mg, 0.42 mmol, 1.0 eq) and 10% Pd(OH)$_2$/C (14 mg, 0.01 mmol, 0.02 eq) in MeOH (10 mL) for 16 h gave amine *cis*-**278** as a yellow oil (89 mg, quant.), IR (ATR) 3362 (NH$_2$), 3290 (NH$_2$), 1600, 1583, 725 cm^{-1}; ^{1}H NMR (400 MHz, CDCl$_3$) δ 7.26-7.21 (m, 1H, Ar), 6.82-6.74 (m, 3H, Ar), 4.18-4.02 (m, 4H, OCH, NH$_2$), 3.78 (s, 3H, OMe), 3.62 (br d, J = 12.0 Hz, 1H, OC*H*$_2$CH), 3.47-3.39 (m, 1H, OCH), 3.18 (br s, 1H, C*H*NH$_2$), 3.05-2.99 (m, 1H, C*H*Ar), 2.42 (dddd, J = 13.0, 13.0, 13.0, 4.5 Hz, 1H, OCH$_2$C*H*), 1.58 (br d, J = 13.0 Hz, 1H, OCH$_2$C*H*$_2$); ^{13}C NMR (100.6 MHz, CDCl$_3$) δ 160.0 (*ipso*-Ar), 142.6 (*ipso*-Ar) , 129.9 (Ar), 119.8 (Ar), 113.4 (Ar), 112.4 (Ar), 71.5 (O*C*H$_2$CH), 68.3 (O*C*H$_2$CH$_2$), 55.3 (OMe), 51.7 (CHNH$_2$), 43.5 (*C*HAr), 24.2

(OCH₂*C*H₂); MS (ESI) *m/z* 208 [(M + H)⁺, 100], 230 [(M + Na)⁺, 6], ; HRMS (ESI) *m/z* calcd for $C_{12}H_{17}NO_2$ (M + H)⁺ 208.1332, found 208.1329 (+1.2 ppm error).

Lab Book Reference: TD 5/36

3-(4-Fluorophenyl)-2,5-dihydrofuran-4-carboxylic acid 286

286
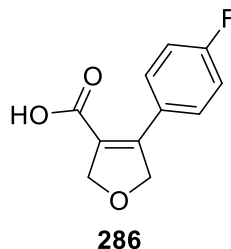
LiOH (41 mg, 2.03 mmol, 3.0 eq) was added portionwise to a stirred solution of ester **219** (150 mg, 0.68 mmol, 1 eq) in 4:1:1 THF–H_2O–MeOH (36 mL) at rt under Ar. The mixture stirred at rt for 2 h. Then, the solvent was evaporated under reduced pressure and H_2O (10 mL) was added. The mixture was washed with CH_2Cl_2 (10 mL) and 1 M $HCl_{(aq)}$ (10 mL) was added. The mixture was extracted with CH_2Cl_2 (2 x 20 mL) and the combined organic extracts were dried (Na_2SO_4) and evaporated under reduced pressure to give acid **286** (110 mg, 78%) as a yellow oil, IR (ATR) 1678 (C=O), 1439 (C=C), 1220, 751 cm⁻¹; ¹H NMR (400 MHz, CDCl₃) δ 7.48-7.43 (m, 2H, Ar), 7.10-7.03 (m, 2H, Ar), 5.08-5.00 (m, 4H, OCH₂); ¹³C NMR (100.6 MHz, CDCl₃) δ 167.7 (C=O), 163.4 (d, *J* = 250 Hz, CF), 151.0 (=*C*Ar), 130.6 (d, *J* = 8.5 Hz, Ar), 127.0 (d, *J* = 3.5 Hz, *ipso*-Ar), 123.7 (=*C*CO₂H), 115.5 (d, *J* = 22.0 Hz, Ar), 80.2 (OCH₂), 77.4 (OCH₂); MS (ESI) *m/z* 207 [(M − H)⁻, 100]; HRMS (ESI) *m/z* calcd for $C_{11}H_8FO_3$ (M − H)⁻ 207.0463, found 207.0466 (−1.4 ppm error).

Lab Book Reference: TD 4/57

3-(4-Fluorophenyl)tetrahydrofuran-4-carboxylic acid *cis*-277, 3-(4-Fluorophenyl)-2,3-dihydrofuran-4-carboxylic acid 287 and 3-(4-Fluorophenyl)furan-4-carboxylic acid 288

cis-**277**   **287**   **288**
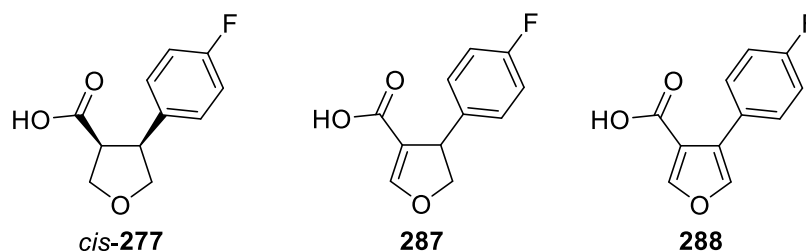
Using general procedure **A**, dihydrofuran **286** (102 mg, 0.49 mmol, 1.0 eq) and 10% Pd/C (11 mg, 0.01 mmol, 0.02 eq) in MeOH (10 mL) for 16 h gave the crude product. Purification by flash column chromatography on silica with 69:30:1 hexane-EtOAc-AcOH as eluent gave tetrahydrofuran *cis*-**277** (60 mg, 58%) as a white solid, mp 65-67 °C; *R*F (69:30:1 hexane-

EtOAc-AcOH) 0.11; IR (ATR) 2959 (br, OH), 2890, 1731 (C=O), 1709, 1511, 1224 cm^{-1}; ^{1}H NMR (400 MHz, CDCl$_3$) δ 7.22-7.16 (m, 2H, Ar), 7.00-6.92 (m, 2H, Ar), 4.20 (dd, J = 7.5, 7.5 Hz, 1H, OCH), 4.17-4.05 (m, 3H, OCH), 3.74-3.67 (m, 1H, C*H*Ar), 3.47 (ddd, J = 7.5, 7.5, 7.5 Hz, 1H, C*H*CO$_2$H); ^{13}C NMR (100.6 MHz, CDCl$_3$) δ 176.4 (C=O), 162.0 (d, J = 246.0 Hz, CF), 134.1 (d, J = 3.0 Hz, *ipso*-Ar), 129.8 (d, J = 8.0 Hz, Ar), 115.3 (d, J = 21.0 Hz, Ar), 73.7 (OCH$_2$), 68.9 (OCH$_2$), 49.7 (*C*HAr), 47.3 (*C*HCO$_2$H); MS (ESI) *m/z* 209 [(M – H)$^-$, 100]; HRMS (ESI) *m/z* calcd for C$_{11}$H$_{10}$FO$_3$ (M – H)$^-$ 209.0619, found 209.0618 (+0.7 ppm error) and an 85:15 mixture (by ^{1}H NMR spectroscopy) of dihydrofuran **287** and furan **288** (9 mg, i.e. 8 mg (8%) of dihydrofuran **287** and 1 mg (1%) of furan **288**) as a yellow oil, ^{1}H NMR (400 MHz, CDCl$_3$) δ 8.12 (d, J = 2.0 Hz, 0.15H, OCH), 7.51 (d, J = 1.5 Hz, 0.85H, OCH), 7.44 (d, J = 2.0 Hz, 0.15H, OCH), 7.43-7.37 (m, 0.3H, Ar), 7.19-7.13 (m, 1.7H, Ar), 7.07-7.01 (m, 0.3H, Ar), 7.01-6.94 (m, 1.7H, Ar), 4.88 (dd, J = 10.0, 10.0 Hz, 0.85H, OCH), 4.45 (dd, J = 10.0, 5.0 Hz, 0.85H, OCH), 4.26 (ddd, J = 10.0, 5.0, 1.0 Hz, 0.85H, C*H*Ar).

Lab Book Reference: TD 4/64
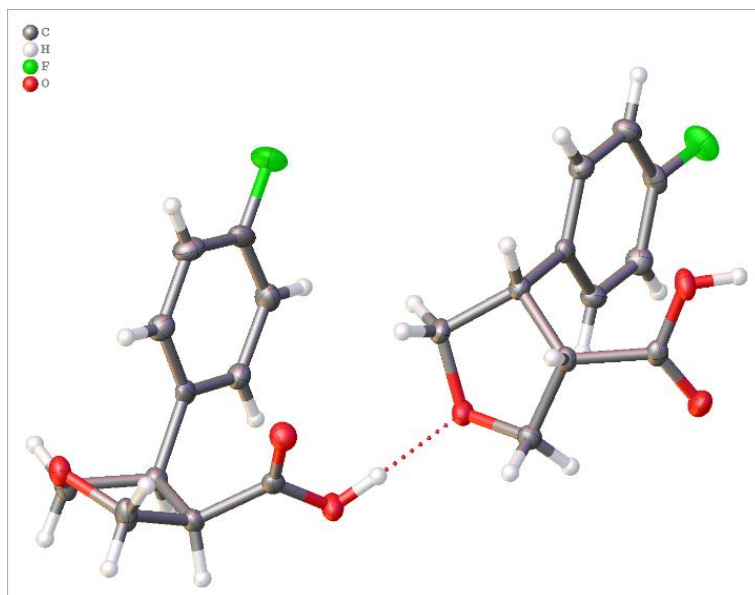
Table 5.4 Crystal data and structure refinement for *cis*-277.

Identification code	TD 4/64
Empirical formula	$C_{11}H_{11}O_3F$
Formula weight	210.20
Temperature/K	110.00(10)
Crystal system	triclinic
Space group	P-1
a/Å	5.6368(5)
b/Å	11.7599(8)
c/Å	15.6467(12)
α/°	68.397(7)
β/°	86.839(7)
γ/°	87.855(6)
Volume/Å^3	962.71(13)
Z	4
ρ_{calc}g/cm^3	1.450
μ/mm^{-1}	1.000
F(000)	440.0
Crystal size/mm^3	$0.189 \times 0.146 \times 0.096$
Radiation	CuKα (λ = 1.54184)
2Θ range for data collection/°	8.088 to 142.106
Index ranges	-6 ≤ h ≤ 6, -14 ≤ k ≤ 11, -19 ≤ l ≤ 17
Reflections collected	6094
Independent reflections	3610 [R_{int} = 0.0221, R_{sigma} = 0.0383]
Data/restraints/parameters	3610/0/279
Goodness-of-fit on F^2	1.035
Final R indexes [I>=2σ (I)]	R_1 = 0.0400, wR_2 = 0.0969
Final R indexes [all data]	R_1 = 0.0517, wR_2 = 0.1046
Largest diff. peak/hole / e Å^{-3}	0.24/-0.23

Methyl 4-(2-methylphenyl)-2,5-dihydrofuran-3-carboxylate 289

289
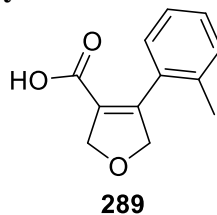
2 M NaOH$_{(aq)}$ (1 mL) was added dropwise to a stirred solution of a 60:40 mixture of ester **221** and 2-tolylboronic acid (72 mg, i.e. 50 mg (0.23 mmol, 1 eq) of ester **221**) in MeOH (1 mL) and THF (1 mL) at rt under Ar. The mixture was stirred and heated at 70 °C for 1 h. The mixture was then allowed to cool to rt and H$_2$O (10 mL) was added. The mixture was washed with CH$_2$Cl$_2$ (5 ml) and 1 M HCl$_{(aq)}$ (5 mL) was added. The mixture was extracted with CH$_2$Cl$_2$ (2 x 20 mL) and the combined organic extracts were dried (Na$_2$SO$_4$) and evaporated under reduced pressure to give acid **289** (36 mg, 78%) as a yellow oil, IR (ATR) 2861 (br, OH), 1685 (C=O), 1272, 754 cm^{-1}; ^{1}H NMR (400 MHz, CDCl$_3$) δ 9.09 (br s, 1H, CO$_2$H) 7.26-7.14 (m, 3H, Ar), 7.04 (d, J = 7.5 Hz, 1H, Ar), 5.01 (t, J = 5.0 Hz, 2H, OCH$_2$), 4.90 (t, J = 5.0 Hz, 2H, OCH$_2$), 2.24 (s, 3H, C*Me*); ^{13}C NMR (100.6 MHz, CDCl$_3$) δ 167.4 (C=O), 153.5 (=*C*CO$_2$H), 135.3 (*ipso*-Ar or *C*Me), 131.6 (*ipso*-Ar or *C*Me), 130.3 (Ar), 128.6 (Ar), 127.1 (Ar), 126.0 (=*C*Ar), 125.7 (Ar), 80.9 (OCH$_2$), 76.4 (OCH$_2$), 19.6 (C*Me*); MS (ESI) *m/z* 195 [(M – H)$^-$, 100]; HRMS (ESI) *m/z* calcd for C$_{12}$H$_{12}$O$_3$ (M – H)$^-$ 203.0714, found 203.0709 (+2.3 ppm error).

Lab Book Reference: TD 5/3

2-(2-Tolyl)tetrahydrofurancarboxylic acid *cis*-281

cis-**281**
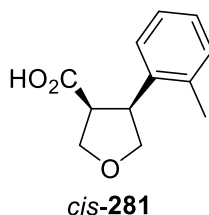
Using general procedure **A**, dihydrofuran **289** (189 mg, 0.925 mmol, 1.0 eq) and 10% Pd(OH)$_2$/C (19 mg, 0.02 mmol, 0.02 eq) in MeOH (10 mL) for 112 h gave the crude product. Purification by flash column chromatography with 79:20:1 hexane-EtOAc-AcOH as eluent gave tetrahydrofuran *cis*-**281** (122 mg, 46%) as an orange oil, R_F (80:20:1 hexane-EtOAc-AcOH) 0.09; IR (ATR) 2980 (br, OH), 1736 (C=O), 1180 cm^{-1}; ^{1}H NMR (400 MHz, CDCl$_3$) δ 7.17-7.06 (m, 4H, Ar), 4.25 (dd, J = 9.0, 6.0 Hz, 1H, OCH), 4.17-4.07 (m, 3H, OCH), 3.92-3.85 (m, 1H, C*H*Ar), 3.52-3.45 (m, 1H, C*H*CO$_2$Me), 2.35 (s, 3H, CMe); ^{13}C NMR (100.6 MHz, CDCl$_3$) δ 177.1 (C=O), 136.9 (*ipso*-Ar), 135.8 (*ipso*-Ar), 130.4 (Ar), 127.2 (Ar), 126.6 (Ar), 126.2 (Ar), 72.7 (OCH$_2$), 69.9 (OCH$_2$), 48.2 (*C*HCO$_2$Me), 44.2 (*C*HAr), 20.0 (C*Me*);

MS (ESI) *m/z* 205 [(M – H)⁻, 100]; HRMS (ESI) *m/z* calcd for $C_{12}H_{14}O_3$ (M – H)⁻ 205.0870, found 205.0878 (–3.9 ppm error).

Lab Book Reference: TD 5/19

REFERENCES

(1)   Jencks, W. P. *Proc. Natl. Acad. Sci.* **1981**, *78*, 4046–4050.

(2)   Shuker, S. B.; Hajduk, P. J.; Meadows, R. P.; Fesik, S. W. *Science.* **1996**, *274* (5292), 1531–1534.

(3)   Bollag, G.; Tsai, J.; Zhang, J.; Zhang, C.; Ibrahim, P.; Nolop, K.; Hirth, P. *Nat Rev Drug Discov* **2012**, *11*, 873–886.

(4)   Souers, A. J.; Leverson, J. D.; Boghaert, E. R.; Ackler, S. L.; Catron, N. D.; Chen, J.; Dayton, B. D.; Ding, H.; Enschede, S. H.; Fairbrother, W. J.; Huang, D. C. S.; Hymowitz, S. G.; Jin, S.; Khaw, S. L.; Kovar, P. J.; Lam, L. T.; Lee, J.; Maecker, H. L.; Marsh, K. C.; Mason, K. D.; Mitten, M. J.; Nimmer, P. M.; Oleksijew, A.; Park, C. H.; Park, C.-M.; Phillips, D. C.; Roberts, A. W.; Sampath, D.; Seymour, J. F.; Smith, M. L.; Sullivan, G. M.; Tahir, S. K.; Tse, C.; Wendt, M. D.; Xiao, Y.; Xue, J. C.; Zhang, H.; Humerickhouse, R. A.; Rosenberg, S. H.; Elmore, S. W. *Nat Med* **2013**, *19* (2), 202–208.

(5)   BALVERSA^TM (erdafitinib) Receives U.S. FDA Approval for the Treatment of Patients with Locally Advanced or Metastatic Urothelial Carcinoma with Certain FGFR Genetic Alterations https://www.jnj.com/balversa-erdafitinib-receives-u-s-fda-approval-for-the-treatment-of-patients-with-locally-advanced-or-metastatic-urothelial-carcinoma-with-certain-fgfr-genetic-alterations (accessed May 10, 2019).

(6)   English, A. C.; Done, S. H.; Caves, L. S. D.; Groom, C. R.; Hubbard, R. E. *Proteins Struct. Funct. Bioinforma.* **1999**, *37*, 628–640.

(7)   Ringe, D.; Mattos, C. *Location of binding sites on proteins by the multiple solvent crystal structure method*; Wiley Online Library, 2006; Vol. 34.

(8)   Nienaber, V. L.; Richardson, P. L.; Klighofer, V.; Bouska, J. J.; Giranda, V. L.; Greer, J. *Nat Biotech* **2000**, *18*, 1105–1108.

(9)   Duong-Thi, M.-D.; Meiby, E.; Bergstroem, M.; Fex, T.; Isaksson, R.; Ohlson, S. *Anal. Biochem.* **2011**, *414*, 138–146.

(10)   Neumann, T.; Junker, H.-D.; Sekul, K. S. and R. *Current Topics in Medicinal Chemistry.* **2007**, 1630–1642.

(11)   Ladbury, J. E.; Klebe, G.; Freire, E. *Nat. Rev. Drug Discov.* **2009**, *9*, 23.

(12)   Congreve, M.; Carr, R.; Murray, C.; Jhoti, H. *Drug Disc. Today* **2003**, *8*, 876–877.

(13)   Lipinski, C. A.; Lombardo, F.; Dominy, B. W.; Feeney, P. J. *Adv. Drug Deliv. Rev.* **2001**, *46*, 3–26.

(14)   Mortenson, P. N.; Erlanson, D. A.; de Esch, I. J. P.; Jahnke, W.; Johnson, C. N. *J. Med. Chem.* **2019**, *62*, 3857–3872.

(15)   Fink, T.; Reymond, J.-L. *J. Chem. Inf. Model.* **2007**, *47*, 342–353.

(16)   Reymond, J.-L. *Acc. Chem. Res.* **2015**, *48*, 722–730.

(17)   Nadin, A.; Hattotuwagama, C.; Churcher, I. *Angew. Chem. Int. Ed.* **2012**, *51*, 1114–1122.

(18)   Leeson, P. D.; Springthorpe, B. *Nat. Rev. Drug Discov.* **2007**, *6*, 881.

(19)   Young, R. J.; Green, D. V. S.; Luscombe, C. N.; Hill, A. P. *Drug Discov. Today* **2011**, *16*, 822–830.

(20)   Erlanson, D. A.; Fesik, S. W.; Hubbard, R. E.; Jahnke, W.; Jhoti, H. *Nat Rev Drug Discov* **2016**, *15*, 605–619.

(21)   Lovering, F.; Bikker, J.; Humblet, C. *J. Med. Chem.* **2009**, *52*, 6752–6756.

(22)   Firth, N. C.; Brown, N.; Blagg, J. *J. Chem. Inf. Model.* **2012**, *52*, 2516–2525.

(23)   Meyer, A. Y. *J. Comput. Chem.* **1986**, *7*, 144–152.

(24)   Timmermans, J. *Nature* **1954**, *174*, 235–235.

(25)   Sauer, W. H. B.; Schwarz, M. K. *J. Chem. Inf. Model.* **2003**, *43*, 987–1003.

(26)   Hung, A. W.; Ramek, A.; Wang, Y.; Kaya, T.; Wilson, J. A.; Clemons, P. A.;

Young, D. W. *Proc. Natl. Acad. Sci. U. S. A.* **2011**, *108*, 6799–6804, S6799/1-S6799/41.

(27) Hajduk, P. J.; Galloway, W. R. J. D.; Spring, D. R. *Nature* **2011**, *470*, 42–43.

(28) Mateu, N.; Kidd, S. L.; Kalash, L.; Sore, H. F.; Madin, A.; Bender, A.; Spring, D. R. *Chem. – A Eur. J.* **2018**, *24*, 13681–13687.

(29) Sveiczer, A.; North, A. J. P.; Mateu, N.; Kidd, S. L.; Sore, H. F.; Spring, D. R. *Org. Lett.* **2019**, *21*, 4600–4604.

(30) Morley, A. D.; Pugliese, A.; Birchall, K.; Bower, J.; Brennan, P.; Brown, N.; Chapman, T.; Drysdale, M.; Gilbert, I. H.; Hoelder, S.; Jordan, A.; Ley, S. V; Merritt, A.; Miller, D.; Swarbrick, M. E.; Wyatt, P. G. *Drug Discov. Today* **2013**, *18*, 1221–1227.

(31) Zhang, R.; McIntyre, P. J.; Collins, P. M.; Foley, D. J.; Arter, C.; von Delft, F.; Bayliss, R.; Warriner, S.; Nelson, A. *Chem. – A Eur. J.* **2019**, *25* (27), 6831–6839.

(32) Foley, D. J.; Doveston, R. G.; Churcher, I.; Nelson, A.; Marsden, S. P. *Chem. Commun.* **2015**, *51*, 11174–11177.

(33) Newman, D. J.; Cragg, G. M. *J. Nat. Prod.* **2016**, *79* (3), 629–661.

(34) Over, B.; Wetzel, S.; Gruetter, C.; Nakai, Y.; Renner, S.; Rauh, D.; Waldmann, H. *Nat. Chem.* **2013**, *5*, 21–28.

(35) Köster, H.; Craan, T.; Brass, S.; Herhaus, C.; Zentgraf, M.; Neumann, L.; Heine, A.; Klebe, G. *J. Med. Chem.* **2011**, *54*, 7784–7796.

(36) Prescher, H.; Koch, G.; Schuhmann, T.; Ertl, P.; Bussenault, A.; Glick, M.; Dix, I.; Petersen, F.; Lizos, D. E. *Bioorg. Med. Chem.* **2017**, *25*, 921–925.

(37) Morgan, K. F.; Hollingsworth, I. A.; Bull, J. A. *Chem. Commun.* **2014**, *50*, 5203–5205.

(38) Chawner, S. J.; Cases-Thomas, M. J.; Bull, J. A. *Eur. J. Org. Chem.* **2017**, *2017*, 5015–5024.

(39) Twigg, D. G.; Kondo, N.; Mitchell, S. L.; Galloway, W. R. J. D.; Sore, H. F.; Madin, A.; Spring, D. R. *Angew. Chem. Int. Ed.* **2016**, *55*, 12479–12483.

(40) Guimond, N.; Gorelsky, S. I.; Fagnou, K. *J. Am. Chem. Soc.* **2011**, *133*, 6449–6457.

(41) Murray, C. W.; Rees, D. C. *Angew. Chem. Int. Ed.* **2016**, *55*, 488–492.

(42) Tran, N. C.; Dhondt, H.; Flipo, M.; Deprez, B.; Willand, N. *Tetrahedron Lett.* **2015**, *56*, 4119–4123.

(43) Prevet, H.; Flipo, M.; Roussel, P.; Deprez, B.; Willand, N. *Tetrahedron Lett.* **2016**, *57*, 2888–2894.

(44) Sarges, R.; Schnur, R. C.; Belletire, J. L.; Peterson, M. J. *J. Med. Chem.* **1988**, *31*, 230–243.

(45) Chalyk, B. A.; Isakov, A. A.; Butko, M. V; Hrebeniuk, K. V; Savych, O. V; Kucher, O. V; Gavrilenko, K. S.; Druzhenko, T. V; Yarmolchuk, V. S.; Zozulya, S.; Mykhailiuk, P. K. *Eur. J. Org. Chem.* **2017**, *2017*, 4530–4542.

(46) Terao, Y.; Kotaki, H.; Imai, N.; Achiwa, K. *Chem. Pharm. Bull.* **1985**, *33*, 2762–2766.

(47) Garner, P.; Cox, P. B.; Rathnayake, U.; Holloran, N.; Erdman, P. *ACS Med. Chem. Lett.* **2019**, *10*, 811–815.

(48) Hassan, H.; Marsden, S. P.; Nelson, A. *Bioorg. Med. Chem.* **2018**, *26*, 3030–3033.

(49) Grainger, R.; Heightman, T. D.; Ley, S. V.; Lima, F.; Johnson, C. N. *Chem. Sci.* **2019**, *10*, 2264–2271.

(50) Fuller, N.; Spadola, L.; Cowen, S.; Patel, J.; Schönherr, H.; Cao, Q.; McKenzie, A.; Edfeldt, F.; Rabow, A.; Goodnow, R. *Drug Discov. Today* **2016**, *21*, 1272–1283.

(51) Taylor, R. D.; MacCoss, M.; Lawson, A. D. G. *J. Med. Chem.* **2014**, *57*, 5845–5859.

(52) Stead, D.; O'Brien, P.; Sanderson, A. *J. Org. Lett.* **2005**, *7*, 4459–4462.

(53) Bilke, J. L.; Moore, S. P.; O'Brien, P.; Gilday, J. *Org. Lett.* **2009**, *11*, 1935–1938.

(54) Stead, D.; Carbone, G.; O'Brien, P.; Campos, K. R.; Coldham, I.; Sanderson, A. *J. Am. Chem. Soc.* **2010**, *132*, 7260–7261.

(55) Barker, G.; McGrath, J. L.; Klapars, A.; Stead, D.; Zhou, G.; Campos, K. R.; O'Brien, P. *J. Org. Chem.* **2011**, *76*, 5936–5953.

(56) Sheikh, N. S.; Leonori, D.; Barker, G.; Firth, J. D.; Campos, K. R.; Meijer, A. J. H. M.; O'Brien, P.; Coldham, I. *J. Am. Chem. Soc.* **2012**, *134*, 5300–5308.

(57) Rayner, P. J.; O'Brien, P.; Horan, R. A. J. *J. Am. Chem. Soc.* **2013**, *135*, 8071–8077.

(58) Sieburth, S. M.; Somers, J. J.; O'Hare, H. K. *Tetrahedron* **1996**, *52*, 5669–5682.

(59) Hamilton, G. L.; Backes, B. J. *Tetrahedron Lett.* **2006**, *47*, 2229–2231.

(60) Padwa, A.; Dent, W. *J. Org. Chem.* **1987**, *52*, 235–244.

(61) Pandiancherri, S.; Ryan, S. J.; Lupton, D. W. *Org. Biomol. Chem.* **2012**, *10*, 7903–7911.

(62) Miller, W. H.; Axten, J. M.; Seefeld, M. A. Antibacterial Agents. WO2006/2047, 2006.

(63) Belmessieri, D.; Cordes, D. B.; Slawin, A. M. Z.; Smith, A. D. *Org. Lett.* **2013**, *15*, 3472–3475.

(64) Dees, F.; Perez-Luna, A.; Chemla, F. *J. Org. Chem.* **2007**, *72*, 398–406.

(65) Galeazzi, R.; Martelli, G.; Mobbili, G.; Orena, M.; Rinaldi, S. *Tetrahedron: Asymmetry* **2003**, *14*, 3353–3358.

(66) Delker, S. L.; Ji, H.; Li, H.; Jamal, J.; Fang, J.; Xue, F.; Silverman, R. B.; Poulos, T. L. *J. Am. Chem. Soc.* **2010**, *132*, 5437–5442.

(67) Devita, R. J.; Mills, S. G.; Young, J. R.; Lin, P. Phenyl Pyrrolidine Ether Tachykinin Receptor Antagonists. WO2005/32464, 2005.

(68) Hulin, B.; Piotrowski, D. Therapeutic compounds. US2005/256310, 2005.

(69) Abrams, T.; Barsanti, P. A.; Ding, Y.; Duhl, D.; Han, W.; Hu, C.; Pan, Y. Triazole Compounds As KSP Inhibitors. US2011/256128, 2011.

(70) Wang, X.; Espinosa, J. F.; Gellman, S. H. *J. Am. Chem. Soc.* **2000**, *122*, 4821–4822.

(71) Rodríguez-Rodríguez, J. A.; Brieva, R.; Gotor, V. *Tetrahedron* **2010**, *66*, 6789–6796.

(72) Antermite, D.; Affron, D. P.; Bull, J. A. *Org. Lett.* **2018**, *20*, 3948–3952.

(73) Atobe, M. *Unpubl. results,* University of York, **2015**.

(74) Kurkin, A. V; Sumtsova, E. A.; Yurovskaya, M. A. *Chem. Heterocycl. Compd.* **2007**, *43*, 34–40.

(75) Karlsson, S.; Hogberg, H.-E. *J. Chem. Soc. Perkin Trans. 1* **2002**, No. 8, 1076–1082.

(76) Bentley, J. M.; Brookings, D. C.; Brown, J. A.; Cain, T. P.; Chovatia, P. T.; Foley, A. M.; Gallimore, E. O.; Gleave, L. J.; Heifetz, A.; Horsley, H. T.; Hutchings, M. C.; Jackson, V. E.; Johnson, J. A.; Johnstone, C.; Kroeplien, B.; Lecomte, F. C.; Leigh, D.; Lowe, M. A.; Madden, J.; Porter, J. R.; Quincey, J. R.; Reed, L. C.; Reuberson, J. T.; Richardson, A. J.; Richardson, S. E.; Selby, M. D.; Shaw, M. A.; Zhu, Z. Imidazopyridine Derivatives As Modulators Of TNF Activity, 2014.

(77) Lüthy, M.; Wheldon, M. C.; Haji-Cheteh, C.; Atobe, M.; Bond, P. S.; O'Brien, P.; Hubbard, R. E.; Fairlamb, I. J. S. *Bioorg. Med. Chem.* **2015**, *23*, 2680–2694.

(78) Wommack, A. J.; Kingsbury, J. S. *J. Org. Chem.* **2013**, *78*, 10573–10587.

(79) Christoffers, J.; Sluiter, J.; Schmidt, J. *Synthesis* **2011**, 895–900.

(80) Akue-Gedu, R.; Gautret, P.; Lelieur, J.-P.; Rigo, B. *Synthesis* **2007**, 3319–3322.

(81) Logan, A. W. J.; Parker, J. S.; Hallside, M. S.; Burton, J. W. *Org. Lett.* **2012**, *14*, 2940–2943.

(82) Jolit, A.; Vazquez-Rodriguez, S.; Yap, G. P. A.; Tius, M. A. *Angew. Chemie Int. Ed.*

2013, *52*, 11102–11105.

(83) Firth, J. D. *Unpubl. results,* University of York, **2018**.

(84) Aversa, R. J.; Burger, M. T.; Dillon, M. P.; Dineen Jr, T. A.; Karki, R.; Ramurthy, S.; Rauniyar, V.; Robinson, R.; Sarver, P. J. Tricyclic Compounds and Compositions as Kinase Inhibitors. WO2017103824 (A1), 2017.

(85) Mitsumori, S.; Zhang, H.; Ha-Yeon Cheong, P.; Houk, K. N.; Tanaka, F.; Barbas, C. F. *J. Am. Chem. Soc.* **2006**, *128*, 1040–1041.

(86) Corporation, I.; Li, Y.-L.; Burns, D. M.; Feng, H.; Huang, T.; Mei, S.; Pan, J.; Vechorkin, O.; Ye, H.-F.; Zhu, W.; Rafalski, M.; Wang, A.; Xue, C.-B. Furo- And Thieno-Pyridine Carboxamide Compounds Useful As PIM Kinase Inhibitors. US2005/256310, 2015.

(87) Coudert, E.; Acher, F.; Azerad, R. *Synthesis* **1997**, *8*, 863–865.

(88) Gómez-Vidal, J. A.; Silverman, R. B. *Org. Lett.* **2001**, *3*, 2481–2484.

(89) Gopalan, B.; Ravi, D.; Rasheed, M.; Sreedhara, S.; Keshavapura, H.; Ishtiyaque, A. Novel Dipeptidyl Peptidase Inhibitors And Processes For Their Preparation And Pharmaceutical Compositions Containing Them. WO2007/113634, 2007.

(90) Atamanyuk, D.; Chevreueil, F.; Faivre, F.; Gerusz, V.; Gold, J.; Moreau, F.; Simon, C. 3H-Thieno[3,4]Pyrimidin-4-one and Pyrrolopyrimid-4-one as Gram-Positive Antibacterial Agents. WO2015/128334, 2015.

(91) Yan, L.; Budhu, R.; Huo, P.; Lynch, C. L.; Hale, J. J.; Mills, S. G.; Hajdu, R.; Keohane, C. A.; Rosenbach, M. J.; Milligan, J. A.; Shei, G.-J.; Chrebet, G.; Bergstrom, J.; Card, D.; Mandala, S. M. *Bioorg. Med. Chem. Lett.* **2006**, *16*, 3564–3568.

(92) Yin, F.; Garifullina, A.; Tanaka, F. *Org. Biomol. Chem.* **2017**, *15* (29), 6089–6092.

(93) Takigawa, Y.; Ito, H.; Omodera, K.; Koura, M.; Kai, Y.; Yoshida, E.; Taguchi, T. *Synthesis* **2005**, *12*, 2046–2054.

(94) Axten, M. J.; Blackledge, W. C.; Brady, P. G.; Feng, G. Y.; Grant, W. S.; Medina, R. J.; Miller, H. W.; Romeril, P. S. CHEMICAL COMPOUNDS. WO2010/59658, 2010.

(95) Park, Y.; Lee, Y. J.; Hong, S.; Kim, M.; Lee, M.; Kim, T.-S.; Lee, J. K.; Jew, S.; Park, H. *Adv. Synth. Catal.* **2011**, *353*, 3313–3318.

(96) Yoshimitsu, T.; Atsumi, C.; Iimori, E.; Nagaoka, H.; Tanaka, T. *Tetrahedron Lett.* **2008**, *49*, 4473–4475.

(97) Takeda, K.; Toyota, M. *Tetrahedron* **2011**, *67*, 9909–9921.

(98) Bogle, K. M.; Hirst, D. J.; Dixon, D. J. *Tetrahedron* **2010**, *66*, 6399–6410.

(99) Magnus, P.; Fielding, M. R.; Wells, C.; Lynch, V. *Tetrahedron Lett.* **2002**, *43*, 947–950.

(100) Moody, C. L.; Franckevičius, V.; Drouhin, P.; Klein, J. E. M. N.; Taylor, R. J. K. *Tetrahedron Lett.* **2012**, *53*, 1897–1899.

(101) Abels, F.; Lindemann, C.; Koch, E.; Schneider, C. *Org. Lett.* **2012**, *14*, 5972–5975.

(102) Mruk, R.; Zentel, R. *Macromolecules* **2002**, *35*, 185–192.

(103) Jones, S. P. *PhD Thesis*, University of York, **2019**.

(104) Khatri, B. B.; Sieburth, S. M. *Org. Lett.* **2015**, *17*, 4360–4363.

(105) Korte, F.; Trautner, K. *Chem. Ber.* **1962**, *95*, 307–318.

(106) Jang, K. P.; Kim, C. H.; Na, S. W.; Jang, D. S.; Kim, H.; Kang, H.; Lee, E. *Bioorganic Med. Chem. Lett.* **2010**, *20*, 2156–2158.

(107) Menear, K. A.; Javaid, M. H.; Gomez, S.; Hummersone, M. G.; Lence, C. F.; Martin, N. M. B.; Rudge, D. A.; Roberts, C. A.; Blades, K. Phthalazinone Derivatives. US2009/192156, 2009.

(108) Hauske, J. R. Multimediator Transporter Inhibitors For Use In Treatment Of Central

Nervous System Disorders. US20100093706A1, 2010.

(109) Jana, N.; Zhou, F.; Driver, T. G. *J. Am. Chem. Soc.* **2015**, *137*, 6738–6741.

(110) Dowd, P.; Choi, S.-C. *Tetrahedron* **1991**, *47*, 4847–4860.

(111) Cai, J.; Crespo, A.; Du, X.; Dubois, B. G.; Liu, P.; Liu, R.; Quan, W.; Sinz, C.; Wang, L. Inhibitors of the HIF Prolyl Hydroxylase. WO/2016/049100, 2016.

(112) Wolkerstorfer, A.; Szolar, O.; Handler, N.; Buschmann, H.; Cusack, S.; Smith, M.; So, S.-S.; Hawley, R. C.; Sidduri, A.; Zhang, Z. Pyrimidone Derivatives And Their Use In The Treatment, Amelioration Or Prevention Of A Viral Disease. US2014194431, 2014.

(113) Christensen, J. A.; Squires, R. F. 4-Phenylpiperidine compounds. US4007196A, 1973.

(114) Fusano, A.; Kobayashi, T.; Saito, Y.; Kanai, T. Nitrogen-Containing Saturated Heterocyclic Compound. US2016/221948, 2016.

(115) Tran, J. A.; Chen, C. W.; Tucci, F. C.; Jiang, W.; Fleck, B. A.; Chen, C. *Bioorg. Med. Chem. Lett.* **2008**, *18*, 1124–1130.

(116) Glaxo Group Limited. Azabicyclic Compounds As Inhibitors Of Monoamines Reputake, 2008.

(117) Lennox, A. J. J.; Lloyd-Jones, G. C. *Chem. Soc. Rev.* **2014**, *43*, 412–443.

(118) Metcalf, B. W.; Li, Z. Compounds and uses thereof for the modulation of hemoglobin, 2014.

(119) Novak, A.; Humphreys, L. D.; Walker, M. D.; Woodward, S. *Tetrahedron Lett.* **2006**, *47*, 5767–5769.

(120) Middleton, W. J. *J. Org. Chem.* **1975**, *40*, 574–578.

(121) L'heureux, A.; Beaulieu, F.; Bennett, C.; Bill, D. R.; Clayton, S.; Laflamme, F.; Mirmehrabi, M.; Tadayon, S.; Tovell, D.; Couturier, M. *J. Org. Chem.* **2010**, *75*, 3401–3411.

(122) Nielsen, M. K.; Ugaz, C. R.; Li, W.; Doyle, A. G. *J. Am. Chem. Soc.* **2015**, *137*, 9571–9574.

(123) Murray, C. W.; Rees, D. C. *Angew. Chem. Int. Ed.* **2015**, *55*, 488–492.

(124) Hall, R. J.; Mortenson, P. N.; Murray, C. W. *Prog. Biophys. Mol. Biol.* **2014**, *116*, 82–91.

(125) Vo, C.-V. T.; Luescher, M. U.; Bode, J. W. *Nat. Chem.* **2014**, *6*, 310.

(126) Luescher, M. U.; Vo, C.-V. T.; Bode, J. W. *Org. Lett.* **2014**, *16*, 1236–1239.

(127) Terao, Y.; Kotaki, H.; Imai, N.; Achiwa, K. *Chem. Pharm. Bull.* **1985**, *33*, 2762–2766.

(128) Pandiancherri, S.; Ryan, S. J.; Lupton, D. W. *Org. Biomol. Chem.* **2012**, *10*, 7903–7911.

(129) Vargas-Caporali, J.; Cruz-Hernandez, C.; Juaristi, E. *Heterocycles* **2012**, *86*, 1275–1300.

(130) Shendage, D. M.; Fröhlich, R.; Haufe, G. *Org. Lett.* **2004**, *6*, 3675–3678.

(131) C. G. Biagini, S.; E. Gibson Thomas, S.; P. Keen, S. *J. Chem. Soc., Perkin Trans. 1* **1998**, *16*, 2485–2500.

(132) Maldaner, A. O.; Pilli, R. A. *Tetrahedron* **1999**, *55*, 13321–13332.

(133) Kobayashi, K.; Narumi, T.; Oishi, S.; Ohno, H.; Fujii, N. *J. Org. Chem.* **2009**, *74*, 4626–4629.